SPHINGOLIPIDS IN HUMAN NEUROLOGICAL DISEASES

PHD THESIS

Anne Sofie Braun Olsen

July 2017

Supervisor: Professor Nils J. Færgeman

Department of Biochemistry and Molecular Biology
Faculty of Science
University of Southern Denmark

SDU

Author

Anne Sofie Braun Olsen

Department of Biochemistry and Molecular Biology
University of Southern Denmark

Supervisor

Professor Nils J. Færgeman, PhD

Department of Biochemistry and Molecular Biology
University of Southern Denmark

Assessment Committee

Professor Brage S. Andersen, PhD (Assessment chair)

Department of Biochemistry and Molecular Biology
University of Southern Denmark

Professor Thierry Levade, MD, PhD

Department of Biochemistry and Molecular Biology
Toulouse-Rangueil Medical School, France

Professor Thorsten Hornemann, PhD

Institute for Clinical Chemistry
University Hospital Zürich, Switzerland

Front page image designed by Harryarts/Freepik.

Preface

The work presented in this PhD thesis was performed in the Lipid group at the Department of Biochemistry and Molecular Biology at the University of Southern Denmark under the supervision of Professor Nils J. Færgeman. The project was financed by the Lundbeck Foundation and the Danish Council for Independent Research, Natural Sciences.

The success of this thesis has depended on several people to whom I am grateful and would like to acknowledge.

First of all I would like to thank my supervisor Nils J. Færgeman for giving me the opportunity to work with this exciting project. Thank you for your guidance and encouragement throughout the project, and for allowing me to work very independently. A big thank you to the Spanish lipidomics-ladies Sandra Fernández Gallego and Marta Moreno Torres for performing the MS lipid work on my project. I am grateful to Ditte Ness for her support and input whenever it was needed. I would also like to thank former and present members of the Lipid group for their contributions to the project in one way or the other, and for creating a great working environment with crazy and sarcastic humor.

I would like to thank Associate Professor Diana Bautista from the Department of Molecular & Cell Biology at the University of California, Berkely, USA for allowing me to conduct my environmental exchange under her guidance during my stay at the Marine Biological Laboratory (MBL), Woods Hole, USA.

A warm thank you to Mai-Britt Mosbech and my sister Louise Cathrine Braun Elmelund-Præstekær for constructive proofreading of this thesis. Louise you have read almost everything I have produced during my education, and I am very grateful for that you have always taken your time to provide me with constructive criticism.

Last, but not least, I would like to thank my family and friends for their continuous support throughout my education. A special thank you to my boyfriend Søren for his love and encouragement through the ups and downs and for always keeping me grounded, and to my daughter Gry, who has been a constant reminder of that there is more to life than work – I love you both from the bottom of my heart.

In loving memory of my father, John Gerner Olsen.

July 2017, Odense

Anne Sofie Braun Olsen

Summary

Sphingolipids are essential components of cellular membranes where they are involved in a range of processes through their ability to regulate membrane organization. They constitute an intricate metabolic network centered around ceramide, which consists of sphingoid long-chain base attached to a fatty acid. Ceramide constitutes a building block from which more complex sphingolipids can be synthesized. Deciphering the roles of sphingolipids in cellular processes is not straightforward. Numerous sphingolipid species exist, and it is becoming evident that function of each species relies on its specific structure as well as its cellular localization. Sphingolipids are particularly abundant in the nervous system, and aberrations in the sphingolipid homeostasis have been associated with a vast number of neurological diseases. This PhD thesis is based on a review, a research paper, and unpublished results, which all revolve around understanding how perturbation of the sphingolipid network contributes to the development of neurological disorders, particularly epilepsy.

Sphingolipids have proven to be important for the development of the human brain as well as maintaining neurological functions, which is reviewed in *Supplement I*. Moreover, *Supplement I* discusses how sphingolipids, through their ability to compartmentalize the plasma membrane, are involved in many neurological processes, including neuronal differentiation, polarization, synapse formation, synaptic transmission, glial-neural interactions, and myelin stability. Lastly, *Supplement I* discusses how disturbances of the sphingolipid metabolism can lead to plasma membrane rearrangements, which has been linked to the development of several neurological diseases.

Deficiency of several enzymes in the sphingolipid network has been associated with the development of epilepsy. Here we have for the first time described a patient diagnosed with progressive myoclonic epilepsy linked to a heterozygous deletion of the gene encoding ceramide synthase 2 (*Supplement II*). Characterization of patient skin fibroblasts shows that the patient indeed has only one functional *CERS2* allele, which leads to alterations in the membrane lipid composition, particular in regards to sphingolipids and glycerophospholipids (*Supplement II* and *III*). These changes may disturb processes relying on plasma membrane compartmentalization and the dynamics hereof, as indicated by preliminary data suggesting that patient fibroblasts are more insulin sensitive. Thus, deregulation of plasma membrane composition and organization may contribute to the development of progressive myoclonic epilepsy.

The unpublished results addresses the role of sphingolipids in regulating proteins residing in the plasma membrane by investigating how perturbation of the sphingolipid metabolism affects properties of the late-rectifier potassium ion channel Kv2.1. Kv2.1 is, by its dynamic modulation of phosphorylation and localization in clusters in the plasma membrane, involved in regulating the intrinsic excitability of neurons. We find that sphingolipid metabolism is important for Kv2.1 cluster size, but not constitutive phosphorylation, in human embryonic kidney cells during a “resting” state. Future research is needed to determine if similar regulation is present during an “active” state and if Kv2.1 kinetics rely on intact sphingolipid homeostasis. This is pivotal for determining if disruption of the sphingolipid network affects the intrinsic excitability of neurons regulated by Kv2.1.

Collectively, this thesis emphasizes the importance of investigating sphingolipid metabolism in relation to neurobiology. By understanding the role of sphingolipids in the normal functioning brain, we are more able to deduce how dysfunctions in the sphingolipid network can lead to the development of neurological diseases, and ultimately develop efficient therapeutic treatments for these disorders.

Dansk Resumé

Sphingolipider er vigtige komponenter i cellulære membraner, hvor de er involveret i en række processer gennem deres evne til at regulere membranorganiseringen. De udgør et komplekst metabolisk netværk centreret omkring ceramid, der består af en langkædet sphingoid base koblet til en fedtsyre. Ceramid udgør fundamentet for syntese af mere komplekse sphingolipider. Udredning af sphingolipiders rolle i cellulære processer er ikke ligetil. Der findes mange sphingolipidarter, og det tyder på at hver arts funktion er afhængig af dens specifikke struktur såvel som dens cellulære lokalisering. Sphingolipider er særligt beriget i nervesystemet, og forstyrrelser i sphingolipidhomeostasen er forbundet med et stort antal af neurologiske sygdomme. Denne ph.d.-afhandling er baseret på et review, en forskningsartikel og upublicerede resultater, som alle handler om at forstå, hvordan forstyrrelse af sphingolipidnetværket bidrager til udviklingen af neurologiske lidelser, især epilepsi.

Sphingolipider har vist sig at være vigtige for udviklingen af hjernen samt opretholdelse af neurologiske funktioner i mennesker, hvilket belyses i *Supplement I*. Desuden diskuteres det i *Supplement I* hvordan sphingolipider, gennem deres evne til at samles i særlige områder af plasmamembranen, er involveret i mange neurologiske processer, herunder neuronal differentiering, polarisering, dannelse af synapser, synaptisk transmission, glial-neurale interaktioner og myelinstabilitet. Endeligt beskriver *Supplement I*, hvordan ændringer i sphingolipidmetabolismen kan føre til omgrupperinger i plasmamembranen, hvilket er blevet associeret med udviklingen af flere neurologiske sygdomme.

Flere enzymdefekter i sphingolipidnetværket er blevet sat i forbindelse med udvikling af epilepsi. Her har vi for første gang beskrevet en patient diagnosticeret med progressiv myoklonisk epilepsi forbundet med en heterozygot deletion af genet kodende for ceramidsynthase 2 (CERS2) (*Supplement II*). Karakterisering af patientens hudfibroblaster viser at patienten kun har en funktionel *CERS2*-allel, hvilket fører til ændringer i sammensætningen af membranlipider, især med hensyn til sphingolipider og glycerophospholipider (*Supplement II* og *III*). Disse ændringer kan forstyrre processer som er afhængige af plasmamembranens opdeling i særlige områder, og disses dynamik, hvilket foreløbige data tyder på, idet patientens hudfibroblaster er mere insulinsensitive. Det kan derfor tænkes at deregulering af plasmamembranens sammensætning og organisering kan bidrage til udviklingen af progressiv myoklonisk epilepsi.

De upublicerede resultater adresserer sphingolipiders rolle i reguleringen af proteiner som befinder sig i plasmamembranen ved at undersøge hvordan forstyrrelse af sphingolipidmetabolismen påvirker egenskaber for kalium ionkanalen Kv2.1. Kv2.1 er, ved sin dynamiske modulering af fosforylering og lokalisering i klynger i plasmamembranen, involveret i regulering af neuronal excitabilitet. Vi finder at sphingolipidmetabolisme er vigtig for Kv2.1-klyngestørrelse, men ikke konstitutiv fosforylering, i humane embryonale nyreceller under en "hvilende" tilstand. Fremtidig forskning er nødvendig for at afgøre om lignende regulering er til stede under en "aktiv" tilstand, og om hvorvidt Kv2.1's kinetik afhænger af intakt sphingolipidhomeostase. Dette er afgørende for at bestemme, om forstyrrelser af sphingolipidnetværket påvirker den iboende excitabilitet af neuroner reguleret af Kv2.1.

Samlet set understreger denne afhandling vigtigheden af at undersøge sphingolipidmetabolisme i relation til neurobiologi. Ved at forstå sphingolipiders rolle i den normalt fungerende hjerne, er vi bedre rustet til at udlede hvordan dysfunktioner i sphingolipidnetværket kan føre til udvikling af neurologiske sygdomme, og i sidste ende udvikle effektive terapeutiske behandlinger for disse lidelser.

List of Publications

This thesis is based on the following publications/manuscripts:

Supplement I

Olsen ASB & Færgeman NJ: ”*Sphingolipids: membrane microdomains in brain development, function and neurological diseases*” OPEN BIOLOGY, 31 May 2017.DOI: 10.1098/rsob.170069

Supplement II

Mosbech MB[a], **Olsen AS[a]**, Neess D, Ben-David O, Klitten LL, Larsen J, Sabers A, Vissing J, Nielsen JE, Hasholt L, Klein AD, Tsoory MM, Hjalgrim H, Tommerup, N, Futerman AH, Møller RS, Færgeman NJ: ”*Reduced ceramide synthase 2 activity causes progressive myoclonic epilepsy*.” Ann Clin Transl Neurol, 2014 Feb;1(2):88-98

[a]Shared 1st author.

Supplement III

Global lipidomics analysis of human ceramide synthase 2-deficient fibroblasts reveals alterations in membrane lipid composition.
Sandra F. Gallego, **Anne S. B. Olsen**, Christer S. Ejsing, and Nils J. Færgeman

Manuscript in Preparation

In addition, unpublished results are presented and discussed. During my PhD I have contributed to the following publication, which is not formally included in this thesis:

Harvald EB, **Olsen AS**, Færgeman NJ (2015): ”*Autophagy in the light of sphingolipid metabolism*.” Apoptosis 2015 May;20(5)

Morita T, McClain SP, Batia LM, Pellegrino M, Wilson SR, Kienzler MA, Lyman K, **Olsen AS**, Wong JF, Stucky CL, Brem RB, Bautista DM: “*HTR7 mediates serotonergic acute and chronic itch.*” Neuron. 2015 Jul 1;87(1):124-38.

Contents

Abbreviations

3-KSph	3-ketodihydrosphingosine
ABCA1	ATP-binding cassette receptor A1
ABCG1	ATP-binding cassette receptor G1
aCDase	Acid ceramidse
AMPA	α-amino-3-hydroxy-5-methyl-4-isoxazolepropionic acid
AP	Alkaline phosphatase
ASD	Autism spectrum disorder
aSMase	Acid sphingomyelinase
C1P	Ceramide-1-phosphate
CAMKII	Ca^{2+}-calmodulin kinase II
CE	Cholesteryl ester
CERK	Ceramide kinase
CERS	Ceramide synthase
CERT	Ceramide transfer protein
CDase	Ceramidases
CGT	Ceramide galactosyltransferase
CKII	Casein kinase II
CST	Cerebroside sulfotransferase
DeoxyMSa	1-deoxymethylsphinganine
DeoxySa	1-deoxysphinganine
DMSO	Dimethyl sulfoxide
EET	Enzyme enhancement therapy
ELOVL1	Elongation of very long chain fatty acids protein 1
ERT	Enzyme replacement therapy
FA	Fatty acid
FAPP2	Phosphatidylinositol-4-phosphate adaptor protein 2
FB1	Fumonisin B1
GalCer	Galactosylceramide
GCase	Glucosylceramidase
GluCer	Glucosylceramide
GSL	Glycosphingolipid
HexCer	Hexosylceramide
Hox	Homeobox
HPCD	2-hydroxypropyl-β-cyclodextrin
HSAN	Hereditary sensory and autonomic neuropathy type
LacCer	Lactosylceramide
LAG1	Longevity-assurance gene 1
LCB	Long-chain base
LSD	Lysosomal storage disorder
LC-MS	Liquid chromatography-mass spectrometry
MAG	Myelin-associated glycoprotein
MRI	Magnetic resonance imaging
nCDase	Neutral ceramidase
NMDA	*N*-methyl-D-aspartate
NPC	Niemann Pick type C
nSMase	Neutral sphingomyelinase
PC	Phosphatidylcholine
PDMP	D-*threo*-1-phenyl-2-decanoylamino-3 morpholino-1-propanol
PKC	Protein kinase C
PME	Progressive myoclonic epilepsy
PP1	Protein phosphatase 1
PP2A	Protein phosphatase 2A
PRC	Proximal restriction and clustering
PS	Phosphatidylserine
ROS	Reactive oxygen species
S1P	Sphingosine-1-phosphate
Sa	Sphinganine
SIMS	High-resolution secondary ion mass spectrometry
SK	Sphingosine kinase
SL	Sphingolipid
SM	Sphingomyelin
SMA-PME	Spinal muscular atrophy with progressive myoclonic epilepsy
SMS	Sphingomyelin synthase
SMase	Sphingomyelinase
SNP	Single nucleotide polymorphism
SPT	Serine palmitoyltransferase
SREBP	Sterol regulatory element binding protein 2
SRT	Substrate reduction therapy
TLC	TRAM-LAG1-CLN8
UOG1	Upstream of growth and differentiation factor 1

Chapter 1

INTRODUCTION

1.1 Motivation to Study Sphingolipid-related Neurological Diseases

There is more to the cell membrane than just providing a physical barrier between the cellular and extracellular milieu. The plasma membrane is a very heterogeneous, complex environment composed of hundreds of different lipids important for orchestrating a vast number of cellular processes. One of the key lipid classes contributing to this complexity is sphingolipids (SLs). SLs were initially discovered in the 1880s by J. L. W. Thudichum while studying the lipid composition of the brain [1]. They were named after the Greek mythological creature, the Sphinx, due to their enigmatic nature. Since then, comprehensive research has revealed that this lipid class constitutes a diverse group of lipids, both in structure and in function. Central to the SL metabolism is ceramide composed of a sphingoid long-chain base (LCB) to which a fatty acid is attached. Ceramide can function as a precursor for the synthesis of more complex SLs. SL synthesis and degradation constitute a dynamic network, whose interconnected metabolism and subcellular compartmentalization, as well as regulation hereof, are central to SL functions.

SLs are particularly enriched in the nervous system and have proven to be essential in a number of processes necessary for central nervous functions, including neuronal differentiation, polarization, synapse formation, synaptic transmission, glial-neural interactions, and myelin stability (reviewed in [2-5]). Compartmentalization of the plasma membrane is involved in each of these processes, to which SLs provide the framework. Not surprisingly, perturbations of the SL network have been associated with development of several neurological diseases, including several types of epilepsy, hereditary sensory and autonomic neuropathy (HSAN), Krabbe, Gaucher, Alzheimer's, and Parkinson's diseases among others. Understanding how the SL network is integrated and regulated in cellular processes, as well as how disruption of SL homeostasis leads to neuropathological disorders, is essential for developing targeted therapeutic strategies needed in the treatment of these disorders.

In the following sections a general introduction to topics relevant for the work presented in this thesis will be given. First, the structure of SLs and their synthesis as well as metabolism will be described in order to provide a basic understanding of this very diverse group of lipids along with their interchangeable nature. Next, the role of SLs in neurophysiology will be addressed (*Supplement I*) to provide a foundation for understanding how defects in the SL network leads to the development of neurological disorders. Lastly, examples on how disturbances of the SL homeostasis have been linked to a number of neurological diseases are provided, and some of the therapeutic strategies used in the treatment of these diseases are briefly touched upon.

1.2 Ceramide and Sphingolipids

SLs comprise an interconnected network with common synthetic and catabolic pathways, which is centered around the intermediate ceramide (reviewed in [6, 7]). Attachment of different molecules to ceramide creates a variety of SLs within the classes of sphingomyelin (SM), glycosphingolipids (GSLs), and sulfatides. Previously, the functionality of SLs was very simplistically thought to depend only on the SL class, however it is becoming evident that specific SL species within each SL class have unique roles of their own [8]. Thus, in order to understand how SLs are implicated in biological functions, we need to pay close attention to their precise structure.

1.2.1. Structure

The name SL is derived from the simplest form of SLs, namely the sphingoid LCB, which forms the structural base for all SLs. The most common mammalian LCBs are sphingosine and dihydrosphingosine (also known as sphinganine, Sa), while 1-deoxysphinganine (deoxySa) is less abundant (Figure 1) [9-11]. The dominating length of LCBs in mammals is 18 carbons (C18), while C20 LCBs are the second most common variant found especially in GSLs in the brain [11]. Furthermore, LCBs also vary in number, position, and stereochemistry of double bonds and hydroxyl groups [11].

Ceramide is produced by attachment of a fatty acid to the LCB via an amide bond at the C2 position (Figure 1). The chain length, degree of saturation as well as hydroxylation of the fatty acid can vary, which will be addressed in more detail later. Ceramide functions as the foundation for the synthesis of more complex SLs, which are generated by attaching various head groups at the C1 position of ceramide (Figure 1). Attachment of phosphocholine to ceramide yields SM, while sequential transfer of sugars such as glucose, galactose, fucose, N-acetylglucosamine, N-acetylgalactosamine, and sialic acid gives rise to more than 500 different GSLs, constituting the apex of SL complexity [12].

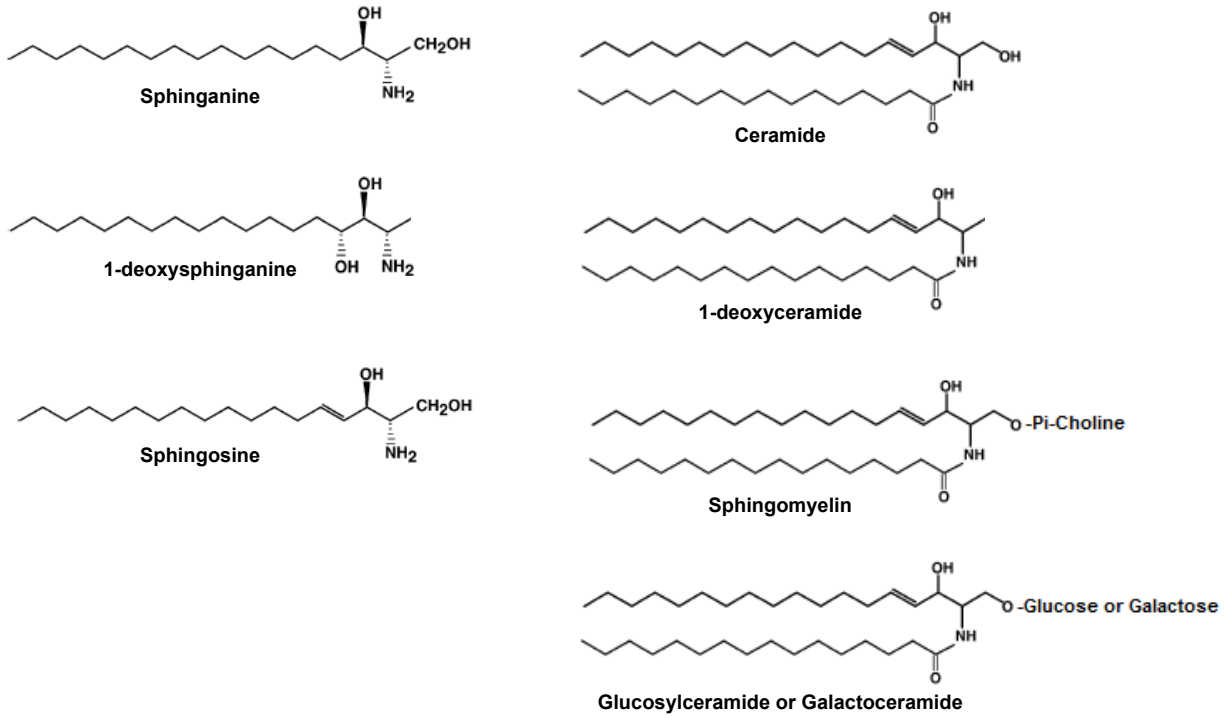

Figure 1: Overview of SL structures. *Left*) Structures of the three sphingoid long-chain bases sphinganine, 1-deoxysphinganine, and sphingosine. *Right*) Structure of ceramide, the central intermediate in the sphingolipid network. Structure of the non-metabolizable 1-deoxyceramide is also shown. Attachment of phosphocholine, glucose, or galactose to ceramide at the C1 position generates the more complex sphingolipids sphingomyelin, glucosylceramide, and galactosylceramide, respectively. Figure adapted from [9].

1.1.2 The Sphingolipid Network

Comprehensive research during the last decades has led to significant advances within the characterization of the SL network, of which many enzymes involved in the SL biosynthesis and further metabolism have been identified and well described (reviewed in [6, 12, 13]). In order to fully understand the role of each SL component in this network, one must also pay close attention to their subcellular localization. Figure 2 provides an overview of the SL biosynthesis and metabolism pathways, which are outlined in the next sections.

1.2.2.1 *De Novo* Synthesis of Sphingolipids

The first steps of *de novo* SL biosynthesis take place at the cytosolic leaflet of the endoplasmic reticulum (ER), where ceramide is generated in a four-step process [14-17]. The initial step, which is also the rate-limiting step, is catalyzed by the serine palmitoyltransferase (SPT), which condensates serine and palmitoyl-CoA to 3-ketodihydrosphingosine (3-KSph) [9]. In the second step, 3-KSph is rapidly reduced to Sa by the 3-KSph reductase before the ceramide synthase (CERS), in the third step, acylates Sa, resulting in the formation of dihydroceramide. In the final step, a 4,5-*trans* double bond is introduced into dihydroceramide by the dihydroceramide desaturase thereby producing ceramide. SPT is also able to use alanine and glycine

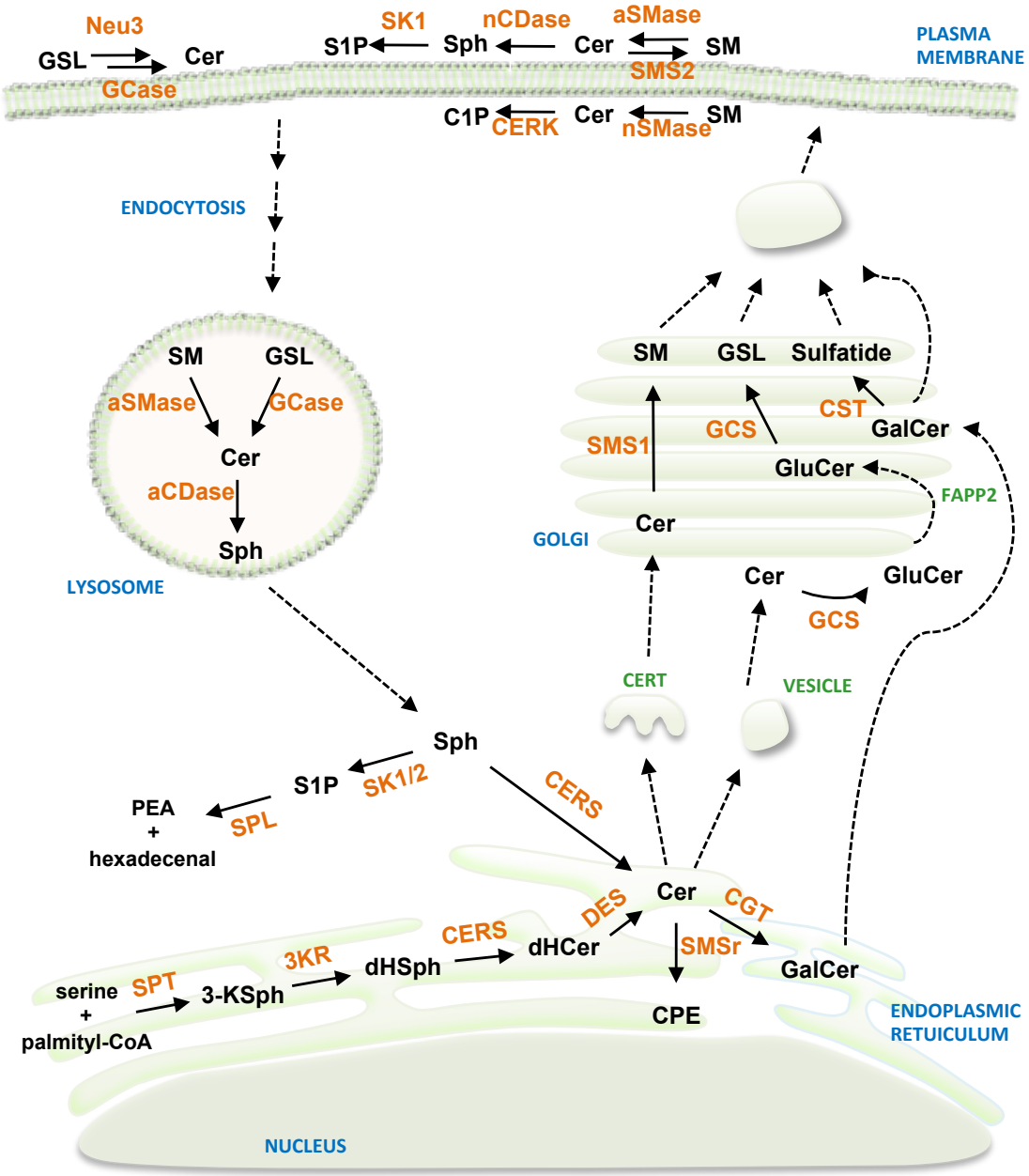

Figure 2: Overview of the sphingolipid pathways. *De novo* synthesis of ceramide (Cer) occurs at the cytosolic leaflet of the endoplasmic reticulum where it can be further metabolized or alternatively be transported to the Golgi apparatus for the synthesis of more complex sphingolipids. From the Golgi, sphingolipids are transported to other compartments, including the plasma membrane. While residing in the plasma membrane, sphingolipids can be metabolized according to cellular demands. Degradation of complex sphingolipids occurs through the endolysosomal pathway where they are broken down to sphingosine (Sph), which can either reenter the sphingolipid pathway by being acylated by a ceramide synthase (CERS) thereby forming Cer, or it can be further degraded. For further details, see main text. Other abbreviations: 3-ketodihydrosphingosine (3-KSph), 3-KSph reductase (3KR), acid ceramidase (aCDase), acid sphingomyelinase (aSMase), Cer galactosyltransferase (CGT), Cer-1-phosphate (C1P), Cer kinase (CERK), Cer phosphoethanolamine (CPE), Cer transport protein (CERT), cerebroside sulfotransferase (CST), dihydroCer (dHCer), dHCer 4-desaturase (DES), dihydrosphingosine (dHSph), galactosylCer (GalCer), glucosylCer (GluCer), GluCer synthase (GluCerS), glycosidases (GCase), glycosphingolipids (GSL), GSL synthases (GCSs), neutral CDase (nCDase), neutral SMase (nSMase), phosphatidylinositol-4-phosphate adaptor protein 2 (FAPP2), phosphoethanolamine (PEA), serine palmitoyltransferase (SPT), sphingomyelin (SM), SM synthase (SMS), SMS-related protein (SMSr), Sph-1-phosphate (S1P), Sph kinase (SK). Adapted from [18].

instead of serine, leading to the formation of deoxySa, and ultimately deoxyceramide, as well as 1-deoxymethylsphinganine (deoxyMSa), which cannot enter the complex SL synthesis pathways nor be degraded [10].

Once formed, ceramide can be processed through different pathways needed for the synthesis of complex SLs. In the ER lumen, the ceramide galactosyltransferase (CGT) catalyzes the transfer of galactose from UDP-galactose to ceramide thereby forming galactosylceramide (GalCer), while the SM synthase-related protein converts ceramide into ceramide phosphoethanolamine [19, 20]. Ceramide can also be transported to the Golgi apparatus where the synthesis of SM and the majority of GSLs occurs. However, trafficking of ceramide to the Golgi depends on which of the two synthesis pathways ceramide is utilized in. Vesicular transport mediates the delivery of ceramide used in the synthesis of GSLs, whereas a ceramide transfer protein (CERT) has been identified as being responsible for the trafficking of ceramide used in SM synthesis [12, 21]. Synthesis of SM takes place at the luminal leaflet of the Golgi, where SM synthase 1 (SMS1) catalyzes the transfer of phosphocholine from phosphatidylcholine (PC) to ceramide producing diacylglycerol as a by-product [22, 23]. The GSL synthesis initiates on the cytosolic leaflet of the Golgi where glucose is attached to ceramide by the glucosylceramide synthase thereby generating glucosylceramide (GluCer) [24]. Additional transfer of sugars onto GluCer takes place in the Golgi lumen, which requires translocation of GluCer facilitated by the phosphatidylinositol-4-phosphate adaptor protein 2 (FAPP2) [25]. FAPP2 has been shown to transport GluCer by vesicular and non-vesicular trafficking, thereby channeling GluCer through two distinct glycosylation tracks located at the Golgi cisternae and the *trans*-Golgi, respectively [25]. This channeling is thought to direct the branching of GluCer and in turn the SL glycosylation pattern. Inside the Golgi, GluCer is converted into lactosylceramide (LacCer) by the attachment of galactose by the action of galactosyltransferase I [6]. Structurally, LacCer serves as a branching point for the synthesis of higher GSLs, which is conducted by sequential transfer of sugars by GSL synthases, including galactosyltransferases, sialyltransferases, and N-acetylgalactosamine transferases, all residing in the Golgi apparatus [12]. Moreover, the Golgi also serves at the site for the synthesis of sulfatides from GalCer made at the ER by the action of cerebroside sulfotransferase (CST) [26].

After synthesis is complete, vesicular transport facilitates the transfer of SM and GSLs from the Golgi to the plasma membrane. As the synthesis of complex SLs occurs on the luminal side of the Golgi, the SLs reside in the extracellular leaflet of the plasma membrane after vesicle fusion. In the plasma membrane the SLs are involved in several processes, including signal transduction and cell adhesion as well as being recognized as binding agents for growth factors and microbial toxins [12].

In addition to being the precursor of complex SLs, ceramide can also be directly phosphorylated by the ceramide kinase (CERK) in the Golgi, resulting in the formation of ceramide-1-phosphate (C1P). The trafficking route of ceramide used for the generation of C1P still needs to be fully elucidated, but trafficking

of C1P from the Golgi to the plasma membrane occurs similar as for GSLs and SM [27, 28]. C1P has proven to be a short-lived metabolite, pointing towards a role as a signaling molecule [27]. Indeed, C1P is regarded as a pro-survival molecule and an important mediator of chemotaxis in inflammatory responses [29].

1.2.2.2 Metabolism

Of the complex SLs, SM is the most abundant in mammalian cells, and its regulation is thought to be an essential part of membrane homeostasis. Moreover, SM constitutes a major resource of ceramide through its degradation into ceramide and phosphocholine catalyzed by a group of sphingomyelinases (SMases). Three different types of SMases exit, which have been classified according to the optimal pH for their activity: Acid SMase (aSMase), alkaline SMase, and neutral SMase (nSMase) [6, 30]. aSMase and nSMase are both ubiquitously expressed. aSMase is, as the name implies, located in lysosomes, but it can also be secreted. Several isoforms of nSMase exist of which nSMase2 is the best characterized [30]. nSMase2 localizes to the plasma membrane, while nSMase1 predominantly localizes to the ER, but is also found at the Golgi and in the nucleus. nSMase3 localizes to both the ER and *trans*-Golgi network, and finally the mitochondria-associated nSMase is found in the ER and mitochondria.

Ceramide produced by the SMases can be deacylated, thereby forming sphingosine and a free fatty acid, by a family of ceramidases (CDases) [31]. There are three types of mammalian CDases, which differ in their localization and, as for SMases, have also been classified according to their pH-dependent activity: Acid CDase (aCDase) found in lysosomes, neutral CDase (nCDase) associated with the plasma membrane; and three alkaline CDases located in the ER and/or Golgi apparatus. The degradation of ceramide is the only known source of intracellular sphingosine [32].

Sphingosine generated by the CDases can be phosphorylated by sphingosine kinases (SKs) resulting in the formation of sphingosine-1-phosphate (S1P). Two mammalian SKs have been identified, SK1 and SK2, which differ in their localization [33]. SK1 is primarily cytosolic, whereas SK2 localizes to the nucleus.

SLs residing in the plasma membrane can undergo remodeling according to cellular demands. SM can be degraded by either nSMase or secreted aSMase thereby producing ceramide, which in turn can be phosphorylated by CERK or degraded further into sphingosine by the nCDase [31]. Sphingosine can subsequently be phosphorylated by SK1. The aforementioned ceramide can also be converted back into SM by SMS2. Moreover, gangliosides can be broken down into ceramide by the membrane-associated sialidase Neu3 in combination with glycosidases [34].

SM and GSLs can also contribute to the pool of ceramide through the endolysosomal pathway, also known as the salvage pathway. In this pathway, endosomes carrying GSLs and SM fuse with lysosomes containing the glycosidases and aSMase necessary for the degradation of the complex SLs into ceramide. Ceramide can

then be further degraded into sphingosine by aCDase. Sphingosine can either by reacylated by CERSs, thereby recycling sphingosine back into ceramide, which yet again can function as a precursor for more complex SLs, or alternatively sphingosine can be phosphorylated by SK1/2. S1P can be converted back into sphingosine by the action of S1P phosphatase, or be degraded to phosphoethanolamine and hexadecenal via the S1P lyase. These two metabolites cannot be recycled back into the SL pathway and thus represent the only known exit route from the SL pathway [35]. Instead, the hexadecanal and phosphoethanolamine can be used in the synthesis of glycerophospholipids [36]. The levels of ceramide and S1P are tightly regulated as these molecules have proven to control cell survival through their pro-apoptotic and pro-survival properties, respectively (reviewed in [12]).

The routes through the SL network are many. Hundreds of different SL species exists, each with their own specific structure, pathway, and subcellular localization, which is a consequence of the distinct localizations of the enzymes of the SL metabolism. Thus, SLs are thought to have very distinct compartmentalized functions besides being merely components of the membrane important for structural integrity [8]. The current challenge is to understand the regulation and integration of the SL metabolism in order to decipher how specific SLs are involved in specific cellular responses.

1.3 Ceramide Synthases

CERSs are key enzymes of the SL pathway as they are responsible for synthesizing the central precursor (dihydro)ceramide. The first gene responsible for the generation of ceramide was identified in a screen for longevity related genes in *Saccharomyces cerevisiae* [37]. Deletion of the longevity-assurance gene 1 (LAG1) promoted longer lifespan in yeast, but it was not until later that LAG1, along with its close homolog LAC1, were shown to be necessary for the synthesis of ceramide in yeast [38, 39]. The mammalian LAG1 homolog UOG1 (upstream of growth and differentiation factor 1) was found to functionally complement deletion of both LAG1 and LAC1 in yeast, but is was first later, when overexpression of UOG1 in mammalian cells was shown to increase ceramide synthesis, that this enzyme was denoted a CERS, namely CERS1 [40, 41]. Since then, bioinformatic analyses and functional studies have led to the identification of five additional mammalian CERSs (CERS2-6) [42].

1.3.1 Structure

All mammalian CERSs share the TLC (TRAM-LAG1-CLN8) domain, which consists of transmembrane α-helices. The TLC domain contains a highly conserved stretch of ~50 amino acid residues known as the Lag1p motif. The motif is involved in CERS activity, and six amino acid residues herein have proven to be essential for this [43]. Furthermore, all the mammalian CERSs, besides CERS1, also possesses an N-terminal homeobox (Hox)-like domain [44]. The Hox domain is primarily found in transcription factors, but as the Hox-like domain in CERS2-6 lacks key residues enabling DNA binding, it is not likely that this domain

facilitates transcription factor function.

1.3.2 Specificity and Tissue Distribution

As discussed, the term ceramide covers a range of ceramide species, which, among other variations, differ in the length of the acyl-chain linked to the LCB. This is due to the fact that the six mammalian CERSs each display a unique specificity towards the length of the fatty acyl-CoAs they use for ceramide synthesis [41, 46-51]. The specificity is summarized in Figure 3A. CERS1 predominantly uses C18- acyl-CoAs, while CERS2 and CERS3 attach longer acyl-CoAs, primarily C22-C24 and C26-C34 acyl-CoA, respectively. CERS4 utilizes C18-C20 acyl-CoAs, while CERS5 and CERS6 both display highest specificity towards shorter C14-C16 acyl-CoAs. The region defining the substrate specificity is still being elucidated, but a study using CERS chimeras has narrowed this region down to 150 residues within the TLC domain corresponding to 40% of the CERS sequence [52].

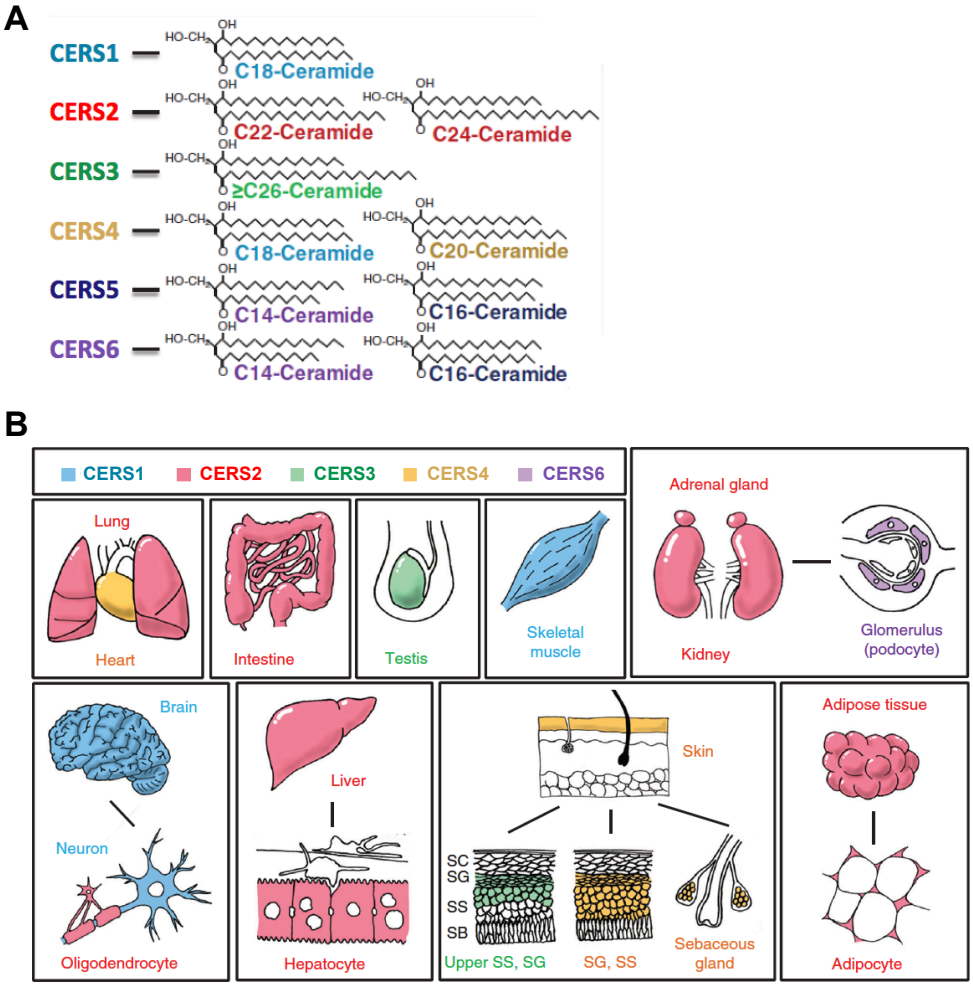

Figure 3: Substrate specificity and expression profiles of mammalian ceramide synthases. *A)* Each ceramide synthase (CERS) catalyzes the synthesis of ceramide using acyl-CoAs of defined lengths. *B)* Color-indicated distribution of the highest expressed CERSs at the transcriptional level [45]. Other abbreviations: SB, stratum basale; SC, stratum corneum; SG stratum granulosum; SS, stratum spinosum. Figures adapted from [45].

All mammalian CERSs are encoded by different genes located on different chromosomes, which enable a tight regulation of differential CERS expression. Along this line, each cell type and tissue display a unique CERS expression profile leading to distinct SL profiles. CERS tissue distribution is outlined in Figure 3B. Briefly, CERS1 is mainly expressed in neurons and skeletal muscles [46, 53]. CERS2 is more ubiquitously expressed and is in particular highly expressed in kidney, liver, and oligodendrocytes in the brain [46]. CERS3 is predominantly expressed in the skin and testis, whereas CERS4 displays a broad tissue distribution, but have highest expression in the skin, heart, liver, and leukocytes [46, 47, 51]. CERS5 and CERS6 are expressed in most tissues, yet the latter shows the highest expression in the kidneys and intestines [46].

Collectively, through their acyl-CoA specificity and tissue distribution, CERSs are highly responsible for the diverse SL profiles found in cells and tissues of the mammalian body. Remarkably, it has been found that the CERS mRNA expression does not always correlate with the SL profile in tissues, indicating that CERS activity is regulated by post-translational mechanisms [46]. These will be elaborated in the following section.

1.3.3 Regulation of Ceramide Synthases

In the light of the diversified roles of ceramide and SL species in physiological as well as pathophysiological processes, it is important to understand how CERSs are regulated. Years of research have shown that CERSs are regulated on multiple levels, including epigenetic, transcriptional, post-transcriptional, and post-translational levels (reviewed in [54]). Yet only few general mechanisms have been described.

Numerous studies have reported alterations in CERS mRNA expression in response to various stimuli and knockdown/knockout of non-targeted CERSs [54]. For instance, toxic stimuli have been associated with increase in *CerS1* expression [55, 56], while the expression of *CerS5* is elevated in the livers of *CerS2*$^{-/-}$ mice [57]. Systematic knockdown of CERSs in the MCF-7 human breast cancer cell line has revealed that down-regulation of each CERS leads to counter-regulation of non-targeted CERSs, which maintains the overall level of ceramide at the expense of profound changes in the SL profile [58].

Kinases may also be involved in the regulation of CERSs, as several CERSs have been found to be phosphorylated. A large-scale phosphorylation study on mice liver has identified phosphorylation of CERS2 and CERS5 at multiple sites in their C-terminals [59], which is in agreement with a recent study revealing phosphorylation of CERS2-6 at several sites in the C-terminal region in human embryonic kidneys cells [60]. It was found that CERS2 activity was heavily dependent on phosphorylation, while the activity of CERS3-6 was only mildly increased upon phosphorylation. Moreover, activation of protein kinase C (PKC) has been shown to mediate phosphorylation of CERS1, which in turn slows down the turnover of CERS1 [61]. PKC has also been shown to regulate translocation of CERS1 from ER to the Golgi during stress conditions, which probably is specific for CERS1, as neither CERS4 nor CERS5 translocate upon stress induction [62].

An increasing number of studies have shown that CERSs activity is modulated by interaction with other enzymes or lipids. S1P inhibits CERS2 activity *in vitro* via direct interaction with a S1P receptor-like motif found exclusively in CERS2 [46]. In addition to S1P, the elongation of very long chain fatty acids protein 1 (ELOVL1), which, as the name implies, catalyzes the synthesis of very long-chain fatty acids, also interacts with CERS2 [63]. The activity of ELOVL1 is regulated by CERS2, thereby efficiently coordinating the production of very long-chain fatty acids with their utilization for ceramide synthesis. Recently, CERS2 and CERS3 have been shown to interact with the acyl-coenzyme A-binding protein (ACBP), which enhances their activity more than 2-fold and 7-fold, respectively [64]. Lastly, CERSs themselves have also been shown to regulate CERS activity through homo- and hetero-dimerization [65].

Collectively, the acyl chain length of ceramides and subsequent complex SLs in specific tissues does not entirely depend on CERS expression patterns, but also rely on CERS regulation by phosphorylation and interaction partners, which are specific for each CERS. This aspect is important to keep in mind when trying to decipher SL-related diseases.

1.4 Neurophysiology Orchestrated by Sphingolipid Metabolism

SLs are essential components of the plasma membrane in all eukaryotic cells, and the cells of the nervous system are no exception. In fact the brain is particularly enriched in SLs [1, 3]. The nervous system contains two basic types of cells: Neurons and glial cells. Glial cells encompass, among other cell types, oligodendrocytes and astrocytes in the central nervous system as well as Schwann cells and satellite cells in the peripheral nervous system. Neurons and oligodendrocytes/Schwann cells are highly polarized cells that rely on distinct morphological and functional compartmentalization in order to uphold normal physiology (Figure 4). The role of SLs in plasma membranes extends beyond being merely structural elements as they are also recognized as important mediators of membrane organization through their ability to form microdomains. Along these lines, the nature of SLs provides a structured environment allowing for compartmentalization of cellular processes necessary for normal neurophysiological functions. Indeed, spatial and temporary regulation of SL metabolism is essential for maintaining the functional integrity of the nervous system, including neuronal differentiation, neuronal survival, synapse formation, synaptic transmission, neuron-glial interactions, as well as the formation and stability of myelin (reviewed in [3, 66, 67]). *Supplement I,* which should be considered as a part of this introduction, addresses the importance of SLs in brain development and function seen particularly in relation to SLs' importance for membrane organization [68].

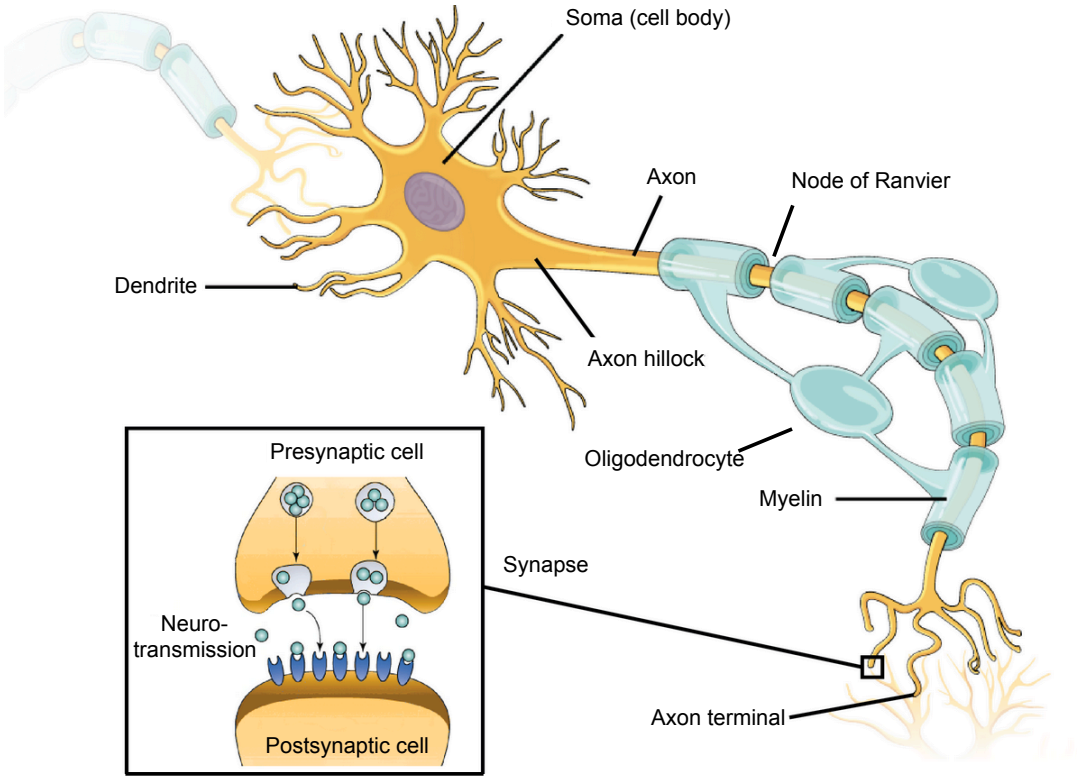

Figure 4: Neurons and oligodendrocytes are highly polarized cells. Both neurons and oligodendrocytes have specialized structures making them highly polarized cells. Neurons are composed of a soma from which dendrites and axon project. The axon terminal forms a synapse with the postsynaptic cell, which allows for signal transduction. Oligodendrocytes extend their membrane thereby forming myelin sheaths that wrap around the neuronal axon. Image adapted from [69].

1.5 Sphingolipids in Neurological Diseases

Multiple enzymes along the SL pathway have been associated with the development of neurological diseases. Deficiencies of these enzymes disturb the cellular SL homeostasis, leading to a range of neurological phenotypes. Neurological diseases linked to enzyme defects both in the synthesis and degradation of SLs, along with therapeutic approaches for the treatment of these diseases, are described in the following sections.

1.5.1 Synthesis Pathway

Even though the synthesis of SLs involves a range of enzymes, relatively few of these enzymes have been linked to the development of neurological disorders (summarized in Table 1).

SPT catalyzes the initial step in *de novo* synthesis of ceramide. A number of reports have identified mutations in the genes encoding the SPT subunits *SPTLC1* and *SPTLC2,* which are associated with the

development of HSAN [71-74, 77]. The mutations cause a permanent shift in the substrate preference from serine to alanine and glycine, leading to the generation of deoxySa, and subsequently deoxyceramides, along with deoxyMSa instead of Sa. Moreover, the localization of the different mutations has shown to correlate with the severity of the disease [78]. As deoxySa and deoxyMSa lack the C1 hydroxyl group of normal Sa, they cannot enter the SL biosynthesis pathway as normal LCBs, which hinder their metabolization [78]. Thus, both metabolites cannot be phosphorylated, thereby preventing their degradation, as they cannot enter the canonical catabolic pathway, which leads to accumulation of deoxySa and deoxyMSa (Figure 2). DeoxySa has proven to be toxic for a range of cells, including neurons [77, 87], and its apoptosis-inducing effect has been associated with deregulation of cytoskeletal structures [88]. Indeed, it is believed that it is the accumulation of these two neurotoxic deoxyLCBs that is responsible for the pathology of SPT-related development of HSAN [77, 78].

Table 1: Human neurological diseases linked to the biosynthesis of sphingolipids. Table updated and modified from [70].

Gene	Enzyme	SL effect	Disease, phenotypes	Ref.
SPTLC1/ SPTLC2	SPT	Increased *de novo* GluCer Accumulation of neurotoxic deoxySa and deoxyMSa Increased C20 LCBs	Hereditary sensory and autonomic neuropathy Distal sensory loss, atrophy and demyelination in the cauda equine, thinning of the sciatic and ulnar nerves, atrophy of the dorsal root ganglia, significant loss of myelinated fibers in several afferent peripheral nerves, sensorineural hearing loss	[71-78]
CERS1	CERS1	Not described for patient cells. *Probably reductions in C18 ceramide and more complex sphingolipids synthesized from C18 ceramide (particular gangliosides), and increase in LCBs [79].*	Progressive myoclonic epilepsy Myoclonus, generalized tonic-clonic seizures, and moderate to severe cognitive impairment	[80, 81]
CERS2	CERS2	Reduction in C24 and C26 ceramide and SM species Increase in C14, C16, and C18 glycosylceramide species.	Progressive myoclonic epilepsy Myoclonus, generalized tonic-clonic seizures, tremor, dysarthria, ataxia, developmental delay	[82]
SIAT9	GM3 synthase	Absence of a- and b-series gangliosides Increase in LacCer and other ganglioside series.	Refractory epilepsy Myoclonus, generalized tonic-clonic seizures, psychomotor delay, developmental stagnation, blindness, and deafness	[83, 84]
GALGT1	GM2/GD2 synthase	GM3 accumulation.	Hereditary spastic paraplegia Progressive weakness and spasticity, non-progressive cognitive impairment, seizure activity	[85, 86]

Deficiencies in CERS1, CERS2, and the GM3 synthase have all been associated with the development of epilepsy in humans [80-84], which is discussed in *Supplement I* [68].

Hereditary spastic paraplegia is a motor neuron disease, which has been associated with mutations in the gene encoding the GM2/GD2 synthase that catalyzes the second step in the synthesis of gangliosides [85]. Loss of the GM2/GD2 synthase in mice leads to elevated levels of the simple gangliosides GM3 and GD3 along with reduced levels of complex gangliosides downstream the action of the GM2/GD2 synthase [89]. These mice suffer from progressive neuropathy, impaired motor coordination, reduced conduction velocities in motor nerves, and diminished hind-limb reflexes [90]. The radical change in ganglioside composition causes abnormal organization of the nodes of Ranvier [91]. Moreover, the mice display decreased central myelination, which probably is due to neuronal lack of the complex gangliosides GD1a and GT1b normally interacting with myelin-associated protein (MAG), which is important for axon-myelin stability [90, 92, 93]. Thus, disturbances of nodes of Ranvier organization and the axon-myelin stability may drive the pathology linked to GM2/GD2 synthase deficiency observed in humans.

1.5.2 Degradation Pathway

Defects in the degradation of SLs have been associated with a vast number of human diseases, also known as lysosomal storage disorders (LSDs) as the catabolic enzymes are localized in late endosomes and lysosomes (reviewed in [70]). These are often complex, multi-system progressive diseases, where accumulation of lipids occurs in many cells and tissues of the human body simultaneously. This causes progressive cell and tissue damage along with impairment of function of multiple organs. Multiple LSDs involve the nervous system where neurodegeneration is a typical phenotype. The severity of the LSDs is often reflected at the level of residual activity of the catabolic enzyme in question [70, 94]. Table 2 summarizes SL-related LSDs associated with neurological hallmarks.

Mutations and deletions in the gene encoding aCDase have been associated with both spinal muscular atrophy with progressive myoclonic epilepsy (SMA-PME) and Farber disease, but the latter far outnumbers the former in occurrences. The pathology of Farber disease is more severe compared to SMA-PME, which is thought to be due to a higher residual aCDase activity in SMA-PME patients [95]. Interestingly, in most cases the aCDase-deficiency related to Farber disease does not result in the same neurological phenotypes as described for SMA-PME, pointing towards a more neuronal sensitive condition in the SMA-PME cases [70, 95]. Accumulation of ceramide is a recognized inducer of apoptosis in various cell types, and thus aCDase, by catalyzing the hydrolysis of ceramide to sphingosine and a fatty acid, is a key enzyme in controlling cell survival. In line with this, the pathology of aCDase-related SMA-PME is associated with neuronal cell death in the CNS as well as in motor neurons [95].

Table 2: Human neurological diseases linked to catabolic enzymes of the sphingolipid pathway. Table updated and modified from [70].

Gene	Enzyme	Major storage materials	Disease, phenotypes	Ref.
ASAH1	aCDase	Ceramide	Spinal muscular atrophy with progressive myoclonic epilepsy Progressive walking difficulties, frequent falls, tremor, muscle weakness, muscular atrophy, myoclonic seizures, generalized epileptic seizures, neurogenic atrophy, cognitive impairment of variable degree, sensorineural hearing loss	[96-99]
		Ceramide, hydroxyl ceramide	Farber disease Granulomas, lipid-laden macrophages in the CNS, mild or no neurological involvement, subcutaneous skin nodules near or over joints	[97, 100-105]
ASRA	Arylsulfatase A (cerebroside-3-sulfate 3-sulfo-hydrolase)	Sulfatide	Metachromatic leukodystrophy Difficulties walking, progressive peripheral neuropathies, muscle wasting/weakness, developmental delay, seizures, dementia	[106-109]
GALC	GalCer β-galactosidase	GalCer, galactosylsphingosine	Krabbe disease Progressive CNS and PNS involvement, hypertonicity/hyperactive reflexes, progressive flaccidity, peripheral neuropathy, severe developmental delay, blindness, spastic paraparesis, dementia, loss of vision, infiltration of characteristic "globoid cells"	[110-113]
GBA1	GCase	GluCer, GM1. GM2, GM3, GD3, glucosylsphingosine	Gaucher disease type 2 Progressive CNS and lung involvement, neural death/drop-out	[114, 115]
		GluCer	Gaucher disease type 3 Variable seizures, normal intelligence, short stature with splenomegaly, abnormal eye movements	[114, 115]
GLB1	GM1-β-galactosidase	GM1, GA1, GM2, GM3, GD1A, lyso-GM1, GluCer, LacCer, oligosaccharides, keratin sulfate	GM1 gangliosidosis Hepatosplenomegaly, localized skeletal involvement, CNS deterioration, seizures, mental regression, dystonia, gait disturbances, dysarthria.	[116, 117]
HEX A	Hexosaminidase A	GM2, GD1aGalNac, GA2, lyso-GM2	GM2 gangliosidosis, Tay-Sachs disease CNS disease, rapid mental and motor deterioration, exaggerated startle response, fine motor problems, visual problems, seizures, variable early dementia in adults	[117, 118]
HEX B	Hexosaminidase B	GM2, GD1aGalNac, globoside, oligosaccharides, lyso-GM2	GM2 gangliosidosis, Sandhoff disease Neurological symptoms begin within first year, facial dysmorphism, skeletal dysplasia, hepatosplenomegaly	[117-119]
SMPD1	aSMase	SM, cholesterol, Bis (monoacylglycero) phosphate, GluCer, LacCer, Gb3, GM2, GM3	Niemann-Pick (type A) Infantile onset of severe neurodegeneration with progressive psychomotor deterioration, neuronal cell loss in cerebral and cerebellar cortices, gliosis, demyelination and infiltration of foam cells, hepatosplenomegaly	[94, 120-123]

GalCer and sulfatide are the major GLSs in myelin and are made by oligodendrocytes and Schwann cells. Deficiencies in the enzymes responsible for GalCer and sulfatide degradation (GalCer β-galactosidase and arylsulfatase A, respectively) have both been associated with neurological diseases (reviewed in [113, 124]). This points towards an essential role of myelin turnover/remyelination for normal functioning oligodendrocytes and Schwann cells, which in turn is pivotal for the central and peripheral nervous system.

Delineating the pathological mechanisms of the SL-related LSDs is far from straight forward. The numerous gene variants, enzymatic consequence, and their clinical outcomes do only to some extent correlate with disease severity [70]. Moreover, deficiencies in several SL activator proteins have also been linked to the development of LSDs, thereby adding another layer of complexity [70]. As seen in Table 2, alterations in the degradation of both SM and GSLs are accompanied by accumulation of a range of SL species. The question still remains if the pathology is caused by direct accumulation of lipids in lysosomes, or by other effects such as accumulation of secondary lipids, secondary molecular defects in the cells, or inflammation. Inflammation is a general pathological event in SL-related LSDs [70]. The accumulation of lipids triggers a pro-inflammatory response, activating the microglial/macrophage system and resulting in damages in the central nervous system. Understanding the pathological mechanisms will be most beneficial in the development of therapeutic strategies for SL-related LSDs.

1.5.3 Therapeutic Treatments

Successful development of therapeutic treatments for SL-related neurological diseases relies on understanding the basic and initial mechanisms causing the disease, as well as the pathophysiological phenotypes of the disease. Several drugs for the treatment of GSL LSDs are already on the marked or in clinical trials [70, 125]. However, as many of these drugs cannot cross the blood-brain barrier, the treatment of neurological LSDs are lacking behind.

Several strategies have been developed for the treatment of SL-related LSDs: 1) Enzyme replacement therapy (ERT) where the needed enzymes is directly supplied; 2) Enzyme enhancement therapy (EET) where chemical chaperones stabilize the enzyme in question, thereby preventing its degradation; 3) Substrate reduction therapy (SRT) where accumulation of lipids are prevented by partial inhibition of their synthesis; 4) Gene therapy where the needed enzymes is indirectly delivered using virus or transplanted cells; 5) Administration of molecules affecting the synthesis of SLs. The latter strategy has proven difficult in most cases due to problems with passing the blood-brain barrier. However, a pilot study with patients diagnosed with HSAN has shown that L-serine supplementation reduces the level of the neurotoxic deoxySa, which is why L-serine administration is now in clinical trial for treatment of HSAN [126, 127]. The drug Miglustat, which inhibits GSL synthesis, is an example of SRT and is approved for the treatment of both Gaucher disease type 1 and Niemann Pick type C (NPC) [125]. In case of NPC, Miglustat has proven to slow down

the neurological progression of the disease [128]. Although NPC is not caused by a direct deficiency in an enzyme of the SL pathway, accumulation of GSLs, among other lipids, is the cause of this disease [70]. It is therefore possible that Miglustat, or derivatives thereof, may prove beneficial in the treatment of GSL LSDs.

Early diagnosis of SL-related neurological diseases is important for the success of the treatment, as the pathology for the majority of these diseases develop very early and are progressive. Moreover, it is pivotal that we are able to identify the manner in which the enzyme in question is affected, as this is crucial for determining the type of treatment needed. Hopefully, concurrently with our increasing knowledge of the pathogenic mechanisms underlying SL-related neurological diseases, efficient therapeutic treatments will be developed to help combat or at least slow down these devastating diseases.

Chapter 2

AIM OF PROJECT

Prior to my project, a collaboration was established with the Danish Filadelfia Epilepsy Hospital as they had identified a heterozygous deletion containing the *CERS2* gene in a patient diagnosed with progressive myoclonic epilepsy (PME). Based on this discovery, the overall aim of this thesis was to investigate how perturbation of the SL metabolism can contribute to the development of epilepsy or associated phenotypes.

More specifically, the aims were to:

i. Characterize human primary skin fibroblasts obtained from the patient diagnosed with PME linked to a heterozygous deletion of *CERS2*, and to further investigate cellular consequences caused by the deletion.

ii. Investigate the role of SLs in the function of the voltage-gated potassium channel Kv2.1, which, by its dynamic modulation of localization in clusters in the plasma membrane, is involved in regulating the intrinsic excitability of neurons.

Chapter 3

RESULTS AND DISCUSSION

3.1 *CERS2*$^{+/-}$ Patient

3.1.1 Supplement II - Reduced Ceramide Synthase 2 Activity Causes Progressive Myoclonic Epilepsy

Supplement II describes the identification of a *de novo* heterozygous 27 kb deletion on chromosome 1q21, harboring the entire *CERS2* gene, in a patient diagnosed with PME. Collectively, characterization of patient primary skin fibroblasts shows a 50% reduction on the level of CERS2 mRNA, protein, and activity compared to parental controls. The reduced level of CERS2 activity is reflected in the SL profile of the patient fibroblasts, which shows a reduction in ceramide and SM species containing the very long-chain fatty acids C24-26 and increased levels of ceramide, GluCer, and LacCer species containing the long-chain fatty acids C16-18. Additionally, cholera toxin B staining of the patient fibroblasts is strongly decreased indicating a reduction of the ganglioside GM1 in the plasma membrane and hence an altered lipid composition and possibly formation of membrane microdomains.

The 27 kb deletion on chromosome 1q21 found in our patient also includes the distal part of the gene encoding *SETDB1* (exon 15-22). Expression analysis of muscle biopsies from the patient and six unrelated controls shows normal levels of shorter *SETDB1* transcripts, while longer transcripts are reduced to ~50% in the patient, consistent with the identified deletion. The later was also observed on protein level in patient primary skin fibroblasts compared to parental controls (result not shown). SETDB1 is a histone H3 Lys9 methyltransferase, which is highly expressed in the early stages of mouse brain development, and ablation of SETDB1 in mice embryos results in peri-implantation lethality [129]. Conditional knockout of *Setdb1* in mice has shown that SETDB1 controls the expression of neural genes and suppresses the expression of non-neural genes during neurogenesis [130]. In the adult mouse brain increased *Setdb1* expression leads to repression of ionotropic glutamate receptor *N*-methyl-D-aspartate (NMDA) genes involved in controlling mood-related behavior [131]. Heterozygous mutations and intragenic deletions in *SETDB1* have been found in a genetic screen for autism spectrum disorders (ASDs) [132]. However, all the detected *SETDB1* variants

in the genetic screen were inherited from healthy parents, suggesting that reduced level of SETDB1 does not necessarily result in the development of ASD. In line with this, our patient has not shown any typical signs of ASD. Collectively, it is not likely that the partial deletion of *SETDB1* is the cause of the development of PME seen in our patient, but it cannot be ruled out that the partial deletion of *SETDB1* may contribute to the phenotypes observed in the patient.

In the central nervous system CERS2 is expressed in the white matter tracts of the cerebrum, cerebellum, and brainstem, which is consistent with its expression in myelin producing oligodendrocytes [133-135]. CERS2 is also expressed in Schwann cells, which are the myelinating cells of the peripheral nervous system [53]. Ablation of CERS2 in mice leads to the development of several brain phenotypes, including myelin degeneration and detachment, cerebellar degeneration, as well as abnormal motor behavior with generalized and symmetrical myoclonic jerks [134, 135]. These phenotypes correlate well with the clinical phenotypes described for our patient. No abnormalities were described in initial magnetic resonance imaging (MRI) scans of the patient's brain, however, cerebellar atrophy was found on the most recent MRI scan and indicates degeneration of the cerebellum. This correlates with progression of dysarthria and ataxia in the patient during recent years. EEG recordings show abnormal fast rhythmic activity that does not change during myoclonic events in both the patient and *CerS2*$^{-/-}$ mice [135]. This points towards abnormal subcortical functions being responsible for the motor dysfunctions, which correlates with astrogliosis and microglial activation in several subcortical regions observed in the *CerS2*$^{-/-}$ mice [135]. GalCer is the primary SL in myelin, and during normal development of the brain the level of GalCer increases proportional with the myelination process [136]. Pronounced reductions in C22-C24 GalCers are found in the brain of *CerS2*$^{-/-}$ mice, which is believed to cause the observed myelin sheath defects [135]. As human skin fibroblasts do not synthesize GalCer [137], it has not been possible to evaluate if having one functional *CERS2* allele affects the synthesis of this important myelin SL. The patient has been highly light sensitive, which is also observed for the *CerS2*$^{-/-}$ mice along with increased sensitivity towards audiogenic stimuli [82, 135]. This suggests that CERS2 is important for proper sensory perception. CERS2 is also highly expressed in the liver and kidney [46], and ablation of CERS2 in mice leads to the development of hepatocarcinomas and gaps in the renal parenchyma beyond seven months of age [134]. Yet, having one functional *CERS2* allele appears to be sufficient for maintaining normal liver functions in humans, as no liver pathologies in humans related to CERS2 has been reported to date. However, single nucleotide polymorphisms (SNPs) in the *CERS2* gene has been associated with accelerated increase in albuminuria in patients with diabetes [138]. Albuminuria is a pathological condition where the protein albumin is abnormally present in the urine, which is assign of early kidney disease. It is currently not know to which extent the SNPs affects the activity or stability of CERS2, but the they underline the importance of CERS2 for normal kidney function in humans. The study in which SNPs were described does not report the age of the patients used for the analysis. Thus, it is possible that *CERS2*$^{+/-}$ patient diagnosed with PME might develop kidney pathologies with age. It can only be speculated

why *CERS2* haploinsufficiency in one case is connected to the development of PME and in another case is associated with early kidney disease. It is possible that the genetic background of the patients is the deciding factor, which is in line with the fact that the two different *CerS2*$^{-/-}$ mice described do not display identical phenotypes [134, 139].

SLs are particularly abundant in the brain where they are pivotal for development as well as maintenance of the functional integrity of the nervous system [1, 3]. An increasing number of studies associate defects in both the SL biosynthesis and degradation pathway with the development of epilepsy and in particular development of PME. PME is a group of rare genetic disorders characterized by generalized tonic-clonic seizures, myoclonus, and progression of neurologic dysfunctions, including ataxia and cognitive deterioration [140]. Usually PME shows an autosomal recessive pattern of inheritance, but in the current case the PME appears to be caused by haploinsufficiency. We are awaiting whole genome sequencing analysis in order to exclude possible recessive mutations in the regulatory part of the functional *CERS2* allele. Recently, a homozygous mutation in the gene encoding CERS1 has been identified in a patient diagnosed with PME [81]. The mutation leads to a substitution of the conserved amino acid (H183Q) in the Lag1-motif, which is important for enzyme activity. While CERS2 is the primary CERS in oligodendrocytes, CERS1 is the predominant CERS in neurons [53]. Ablation of CERS1 in mice results in cerebellar ataxia, Purkinje cell degeneration, and accumulation of lipofuscin in several brain regions [141]. These phenotypes are all symptoms related to PME subtypes [140, 141]. The neuronal degeneration observed in CERS1-deficient mice can be explained by increased apoptosis [79], which possibly is a result of increased ER stress and induction of pro-apoptotic pathways as seen when downregulating *CERS1* in a neuroblastoma cell line [81]. SL analysis of the forebrain of CERS1-deficient mice displays reduced levels of C18-ceramide, hexosylceramide (HexCer) species, C18 SM, and gangliosides, while C16 and C22 ceramide levels were increased along with C18 LCBs [79]. A homozygous loss-of-function mutation in the GM3 synthase gene has been linked to the development of infantile-onset symptomatic epilepsy syndrome and refractory epilepsy [83, 84]. Analyses of blood plasma from the affected children show a complete lack of GM3 and its downstream derivatives, whereas gangliosides in the alternative ganglioside pathways are increased [83]. Yet this compensatory flux in gangliosides is not observed in patient-derived GM3 synthase-deficient skin fibroblasts where the total level of gangliosides is reduced to 7% of control skin fibroblasts [142]. Besides hearing loss, no obvious neurological phenotypes are observed in GM3 synthase-deficient mice [143], which highlights the fact that SL metabolism in mice might be more redundant compared to humans, as mice seems to be able to compensate more sufficiently upon disturbances in the SL metabolism. Further analysis of patient-derived GM3 synthase-deficient skin fibroblasts shows reduced mitochondrial membrane potential and increased apoptosis [84], which possibly causes the neurodegeneration and development of PME in the patients. Yet, whether the neurodegeneration is caused by lack of gangliosides, a possible increase in ceramide, something third, or a combination of perturbations remains to be elucidated. Lastly, several studies

have linked mutations in the gene encoding the aCDase with development of SMA-PME [96-99, 144]. Several of the studies report a pronounced reduction in aCDase activity rather than total ablation. Common traits in the reported cases are muscle weakness in line with muscle denervation, tremor, and myoclonic seizures [98]. aCDase deficiency in mice results in accumulation of ceramides, hydroxyl-ceramides, dihydroceramides, dihexoxylceramides, and GM3 in the brain, leading to several behavioral abnormalities, including reduced voluntary locomotion, impaired grip strength, and defects in motor coordination [145]. A study performed in zebrafish has shown that knockdown of the aCDase orthologue reduces motor neuron axonal branching and increases apoptosis in the spinal cord [96]. Collectively, SL-related development of epilepsy seems to revolve around increased susceptibility towards apoptosis. The molecular mechanisms leading to apoptosis may very well differ between the SL-related epilepsies as they have very different SL profiles. A recent study suggests that an increase in LCBs probably is the primary cause of neuronal death in CERS1-deficient mice [87]. Ectopic expression of *CerS2* in CERS1-deficient mice almost completely rescues neurodegeneration, which most likely is because of a reduction in LCBs as CERS2 produces C22- and C24-ceramides and not C18-ceramides. This is in line with induction of neurite fragmentation by LCBs in cultured neurons when administered in the elevated levels found in CERS1-deficient mice brains [87]. Future research will hopefully help clarify the molecular mechanisms governing each of the SL-related epilepsies.

As CERS2 has proven essential for maintaining proper myelination of neurons in the mouse brain, and the fact that CERS2 is not expressed in neurons, indicates that the development of PME seen in our patient might be caused by malfunctioning oligodendrocytes. Stability of myelin depends on lipid-lipid interactions between myelin sheaths as well as lipid-protein interactions between the neuronal axon and myelin sheaths. GalCer and its derivative sulfatide, which are both significantly reduced in *CerS2*$^{-/-}$ mice, form glycosynapses in between myelin sheaths important for long-term myelin stability [146, 147]. GalCer also controls the localization of major myelin proteins, including MAG [148], which is known to interact with the gangliosides GD1a and GT1b residing in axonal membranes [92, 93, 149]. Neurons require proper myelination in order to maintain axonal organization of proteins, including ion channels, and disturbances hereof compromise neuronal signal transduction [68]. Mice lacking the ability to synthesize GalCer and/or sulfatide have disrupted axon-glial interactions, leading to diffuse organization of the Nodes of Ranvier (unmyelinated regions along the axon, which are highly enriched in ion channels and responsible for action potential propagation), ultimately resulting in conduction defects and distinct tremor along with progressive ataxia [150-152]. As it has not been possible to assess the level of GalCer and sulfatide in the brain of the patient, it remains an open question to whether or not similar ultrastructural defects may cause the neurological phenotypes observed in the patient. The patient's disease progression involves neuronal degeneration, observed as cerebellar atrophy in latest MRI scans, which is consistent with cerebellar degeneration at 9 months of age in *CerS2*$^{-/-}$ mice [135]. The neuronal degeneration is most likely a secondary

effect of compromised myelin stability, as myelin not only serves to insulate axons, but also provides trophic support important for long-term axonal survival [153]. Indeed, axonal degeneration is observed in mice lacking individual key myelin proteins [154], and thus it is very likely that myelin defects can lead to axonal degeneration as well.

Several laboratory analyses have been performed on the patient, but only few abnormalities have been found, including lowered activity of complex I/citrate synthase ratio (0.18 compared to the normal range of 0.19-0.54) and an elevated level of cholesterol in the blood plasma (>10 mM compared to normal level of <5.2 mM). The latter will be discussed later in relation to unpublished patient data. The low activity of complex I of the respiratory chain indicates that mitochondrial function may be compromised in the patient. In line with this, it has been shown that ablation of CERS2 in mice liver leads to mitochondrial dysfunction displayed as reduced mitochondrial membrane potential and increased generation of reactive oxygen species (ROS) [155]. Ceramide can trigger ROS generation, but this ability is dependent on the FA chain length of the ceramide. *CerS2*$^{-/-}$ mice lack the ability to synthesize C22- and C24-ceramide, which is compensated for by an increased level of C16-ceramide [139]. Consistent with this, C16-ceramide, and not C24:0- or C24:1-ceramide, has been found to directly inhibit complex IV of the respiratory chain leading to increased generation of ROS [155]. As described, a similar compensatory mechanism is seen in patient fibroblasts compared to parental controls at the ceramide level. Thus, the low level of complex I in the patient might be due to increased levels of C16-18 ceramides. As generation of ROS and oxidative stress have been associated with the pathology of neurodegenerative diseases, such as Alzheimer's and Parkinson's diseases [156], it would be relevant to investigate if the low complex I activity is sufficient to increase ROS generation. As mentioned, CERS2 is highly expressed in oligodendrocytes, which are particularly susceptible to oxidative stress due to a low supply of the antioxidant glutathione and a high level of iron, of which the latter is important for the synthesis of cholesterol and as a co-factor of several enzymes involved in the myelination process [157, 158]. Increased oxidative stress can result in death of oligodendrocytes, and it has been shown that several ROS-promoting molecules and ROS itself can activate the nSMase, thereby producing ceramide and ultimately inducing apoptosis and cell death [159]. It can be speculated that increased ceramide/ROS production in the patient might contribute to progression of his disease through compromising oligodendrocyte function.

3.1.2 Supplement III - Global Lipidomics Analysis of Ceramide Synthase 2-Deficient Fibroblasts Reveals Alterations in Lipid Membrane Composition

Supplement III is an extension of *Supplement II* and describes the application of MS-based global lipidomics to elaborate the lipid profile of primary skin fibroblasts obtained from the *CERS2*$^{+/-}$ patient, which is compared to gender- and age-matched controls rather than parental controls as in *Supplement II*. The motive

behind this change in controls is discussed in the next sections. Surprisingly, the lipidomics analysis shows a reduction in practically all ceramide species detected (C16, C22, and C24) and not only in the ceramide species corresponding to the substrate specificity of CERS2. However, the decrease in C16 ceramide correlates with an increase in the level of C16 SM (assuming a LCB chain length of C18 in the analyzed SM species), which indicates a possible increased flux of C16 ceramide towards synthesis of SM. In contrast to the SL profile presented in *Supplement II*, no other significant SL changes were observed besides a marked reduction of approximately 50% in the ganglioside GM3 species containing C22-24 FAs (assuming a LCB chain length of C18 in the analyzed GM3 species) in patient skin fibroblasts compared to controls (Figure 5). Intriguingly, a clear reduction in cholesteryl esters (CE) was found in patient fibroblasts compared to controls, while a 2.5-fold increase was observed for phosphatidylserine (PS) species containing very long polyunsaturated FAs (C22:4 - C22:6).

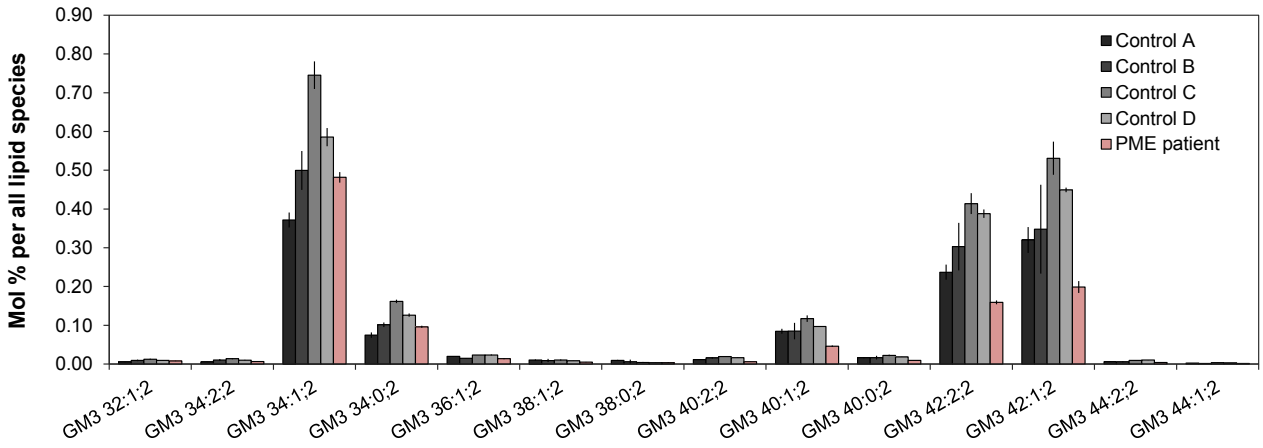

Figure 5: Very long-chain ganglioside GM3 species are reduced in patient skin fibroblasts. Global lipidomics analysis was performed on lipid extracts prepared from three independent skin fibroblast cultures from the patient (PME patient) and four gender- and age-matched controls and analyzed using Fourier Transform Mass Spectrometry. The results indicate a reduction in species containing very long-chain fatty acids (i.e. 40:1;2, 42:1;2, and 42:2;2) in patient fibroblasts compared to controls. Mean ± SD of n=3 fibroblast cultures per group is shown. The figure is extracted from Figure 2 in *Supplement III.*

Application of patient-derived cells and tissues is pivotal in the search for disease cause and effects. When performing such research, it is important to keep in mind the human variability, to which gender and age are contributing factors. In *Supplement II* we applied parental primary skin fibroblasts as controls, which lead to the conclusion that the SL profile of *CERS2*$^{+/-}$ patient skin fibroblasts is significantly changed on SM and GSLs levels. In *Supplement III* we have applied gender- and age-matched skin fibroblasts, which shows that the reduction in ceramides species does not affect the level of more complex SLs besides a considerable reduction in the ganglioside GM3. A probable cause of this disparity in SL profiles when employing the two different control groups is senescence, biological ageing. A study performed in human diploid fibroblasts has demonstrated that the level of ceramide increases significantly as these cells become senescent [160]. Further

investigations showed that the activity of nSMase was markedly increased in the fibroblasts correlating with an elevated ceramide level. Although these results relate to cellular senescence, it can be speculated that similar changes occur during normal biological ageing of the human body. In line with this, the level of ceramide has been reported to rise during normal ageing of the mouse brain [161]. As reported in *Supplement II*, cholera toxin B staining of patient fibroblasts showed a clear reduction of the ganglioside GM1 in plasma membrane compared to parental controls. The staining has not been repeated using the gender- and age-matched controls. However, the decrease of GM3 in the patient fibroblasts compared to the gender- and age-matched controls suggests that the GM1 reduction is real, as GM1 is downstream GM3 in the ganglioside synthesis pathway. Both GM1 and GM3 have been shown to form clusters in living cells [162], and hence the reductions of these gangliosides strongly suggests that the formation of membrane microdomains is compromised in patient skin fibroblasts.

When it comes to gangliosides, the primary focus is on neurons, rather than oligodendrocytes, as a hallmark of neurons is their particular enrichment in this group of GSLs. However, few gangliosides, including GM3, are also found in oligodendrocytes. It has been shown that GM3 enhances differentiation of oligodendrocytes in culture [163, 164], which suggests a role for gangliosides in oligodendrocyte biology. It is currently impossible to find out whether or not the changes in GM3 found in the patient fibroblasts reflect that of his oligodendrocytes, as the patient currently still alive and no brain biopsies have been performed. Moreover, if such a change is present in the oligodendrocytes, it can still only be speculated to what extend that will affect the functional aspects of oligodendrocyte biology.

As mentioned, laboratory analyses performed on the patient show reduced activity of the complex I of the respiratory chain. Based on the ceramide levels presented in *Supplement III*, it can be questioned whether or not the compromised mitochondrial function in the patient is caused by an increase in C16-18 ceramides as discussed above. Analysis of *CERS* mRNA levels in the human skin fibroblasts in *Supplement II* indicates that CERS2 and CERS5 are the major CERSs in these cells. Both CERSs are expressed in oligodendrocytes, but the role of CERS2 in white matter gets more prominent during development, seen by increases in C22-24 ceramides while C16-18 ceramides are reduced [53, 165]. It can be speculated that concurrently with the oligodendrial maturation and formation of the myelin sheath, having only one functional allele of *CERS2* is not sufficient to uphold normal levels of very long-chain ceramides. In the *CerS2*$^{-/-}$ mice, upregulation of CERS5 is observed as an attempt to compensate for the loss of CERS2, which leads to elevation of long-chain ceramides [57, 135, 166]. As discussed, such an increase in long chain ceramides could lead to mitochondrial dysfunction or other dysfunctions for that matter, ultimately compromising oligodendrocyte functions.

Initial blood work performed on the patient showed an increased level of cholesterol in the plasma. This is also seen in *CerS2*$^{-/-}$ mice [57] and heterozygous *CerS2* mice when kept on a high-fat diet [167]. Reduced

CERS2 activity does also affect the cholesterol pathway in the patient skin fibroblasts, where the level of cholesteryl esters is markedly reduced compared to gender- and age-matched skin fibroblasts. In an initial attempt to address the level of free cholesterol in patient skin fibroblasts, fibroblasts were fixated and stained with the fluorescent compound filipin, which is known to bind free cholesterol [168]. The filipin staining (Figure 6) indicates a minor reduction of free cholesterol in the patient skin fibroblasts compared to parental control 2. However, it has been reported that filipin is also able to bind to ganglioside GM1 [168], and therefore it is likely that the slight decrease in filipin staining reflects the observed reduction of GM1 staining reported in *Supplement II*. Moreover, analysis of free cholesterol was originally included in the global lipidomics analysis described in *Supplement III* and suggests that free cholesterol levels are similar in patient skin fibroblasts compared to gender- and age-matched controls, but the quality of the data does not allow for free cholesterol quantification (results not shown).

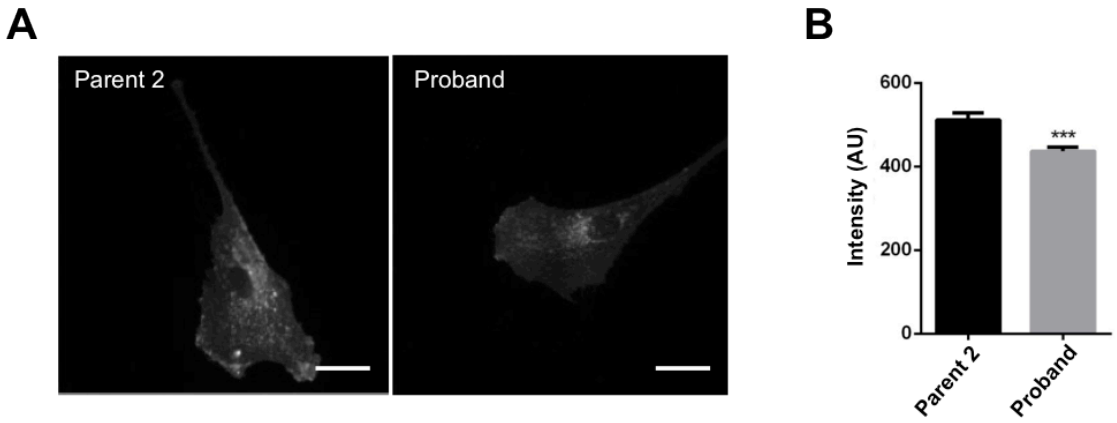

Figure 6: Filipin staining of cholesterol is slightly reduced in primary patient fibroblasts. Primary skin fibroblasts isolated from the patient and parental control 2 were stained with the cholesterol-binding compound filipin. Fibroblasts were fixated using 3% paraformaldehyde for 1 hour followed by filipin staining (50 µg/mL) for 2 hours. *A*) Representative fluorescence images of filipin-stained fibroblasts. *Scale bar*: 10 µm. *B*) Quantification of fluorescence intensity according to cell area was performed using ImageJ. Statistical analysis was performed using unpaired two-tailed t-test with Welch's correction using GraphPad Prism software. Error bars represent ±SEM. Experiment was performed twice; n(parent 2) = 38 and n(patient) = 49.

Several studies have shown that SL metabolism is involved in the regulation of cholesterol homeostasis [169, 170]. The molecular mechanisms behind this regulation are not clear, but manipulations of ceramide, SM, and GSLs levels have all been associated with the maturation and translocation of sterol regulatory element binding protein 2 (SREBP2), a key transcription factor activating genes responsible for cholesterol synthesis [169, 170]. Furthermore, SLs have been implicated in the regulation of plasma cholesterol by the ATP-binding cassette receptors A1 (ABCA1) and ABCG1, both regulators of cholesterol efflux [170]. Inhibition of *de novo* ceramide synthesis has been shown to increase ABCA1 expression in the plasma membrane leading to elevated cholesterol efflux [170]. Cholesterol is transported in the blood by LDL and HDL particles, which are able to deliver cholesterol to cells through receptor-mediated endocytosis [171, 172]. CERS2-derived SLs are emerging players in the regulation of protein trafficking, including endocytosis

[173, 174], and in a recent study the rate of LDL internalization was found to be reduced in astrocytes isolated from the *CerS2* KO mice. Thus, the elevated level of plasma cholesterol in the patient might be explained by elevated cholesterol efflux, impaired cellular cholesterol uptake, or a combination of both. More work is necessary in order to understand how reduced activity of CERS2 leads to hypercholesterolemia.

Besides the described changes in SL species, the global lipidomics analysis also showed a significant increase in several PS species containing very long polyunsaturated fatty acids in patient skin fibroblasts compared to gender- and age-matched controls. PS is considered to be the major acidic phospholipid in cellular membranes, and is particularly enriched in myelin in human brain [175]. PS supplementation has shown positive effects on multiple cognitive functions, including memory, ability to learn, concentration, and ability to communicate, and it also leads to beneficial support of locomotor functions [175]. The molecular mechanism leading to the observed increase in PS in patient fibroblasts remains to be elucidated along with the biological consequences, but as PS supplementation has shown many beneficial effects, the elevated level of PS does probably not add to the patient pathology.

3.1.3. Insulin Sensitivity (Unpublished Results)

Increasing evidence suggests that SLs are important regulators of insulin signaling as several SLs species has been associated with either development or prevention of insulin resistance. The insulin receptor localizes to membrane microdomains in the plasma membrane, and signaling through receptor has shown to depend on the lipid environment it resides in [176-179]. Ablation of CERS2 in mice has pronounced effect on the membrane SL composition, which results in altered biophysical membrane properties, including fluidity, curvature, and phases [57, 134, 135]. These changes may very well disturb the plasma membrane organization, which is in line with the inability of the insulin receptor to translocate into detergent-resistant membranes, thereby preventing phosphorylation of Akt in the liver of *CerS2*$^{-/-}$ mice, ultimately leading to hepatic insulin resistance [179]. Interestingly, *CerS2*$^{+/-}$ mice display enhanced phosphorylation of Akt upon insulin stimulation [167]. Thus, it was relevant to investigate if the reduced activity of CERS2 found in the patient skin fibroblasts affects insulin sensitivity. Patient and parental control skin fibroblasts were serum starved for 15 hours followed by stimulation with 10 nM or 100 nM insulin. Insulin sensitivity was evaluated by monitoring phosphorylation of the down-stream effector Akt at Ser473 by Western Blotting. As shown in Figure 7, patient skin fibroblasts display enhanced insulin sensitivity when treating with both 10 nM and 100 nM insulin, and as seen in the figure this is not due to an increase in Akt protein. This result supports the earlier observation that having one functional allele of *CERS2* seems to improve insulin signaling, while total ablation of CERS2 leads to insulin resistance. The reduced level of ganglioside GM3 in patient skin fibroblasts compared to gender- and age-matched controls presented in *Supplement III* may very well be the cause of the increased insulin sensitivity. This is supported by the observation that insulin sensitivity is

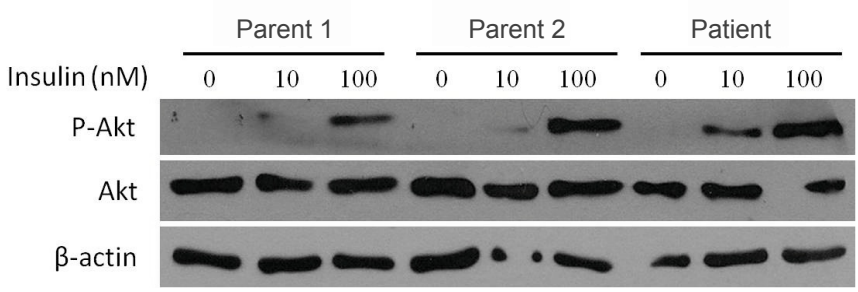

Figure 7: Increased insulin sensitivity in patient skin fibroblasts. Primary skin fibroblasts isolated from the patient and parental controls were serum starved for 15 hours after which the fibroblasts were stimulated with 0 nM, 10 nM, or 100 nM insulin for 10 min. Protein was extracted and used for detection of Akt and insulin-stimulated phosphorylation of Akt at Ser473 by Western Blotting. Equal amounts of protein (15 ug) were loaded in each lane. β–actin was used as loading control. Phosphorylation of Akt is more pronounced in patient fibroblasts after both 10 nM and 100 nM insulin stimulation compared to both parental controls indicating increased insulin sensitivity. The experiment was performed once in technical duplicate.

enhanced in mice lacking the GM3 synthase [180]. A mechanism of the GM3-mediated regulation of insulin signaling has been proposed in adipocytes [177, 178]. Here GM3 is thought to disturb the interaction between the insulin receptor and the protein caveolin-1, which keeps the receptor within the membrane microdomain caveolae necessary for signaling. Thus, having reduced level of GM3 might sustain the insulin receptor in microdomains to a higher extent than normal, thereby increasing signaling through it.

In order to test the hypothesis of increased insulin sensitivity caused by a reduction in GM3 in patient skin fibroblasts, the insulin stimulation experiment was repeated using gender- and age-matched skin fibroblasts and stimulation with 10 nM insulin with the intention to test if supplementation of GM3 could reduce insulin sensitivity to that of control gender- and age-matched controls. Unfortunately, none of the fibroblasts were responding the insulin stimulation as only a very faint band of phosphorylated Akt at Ser473 could be detected (*Appendix I*). The lacking phosphorylation can be explained by malfunctioning insulin or an inability of the fibroblasts to respond to the insulin. The fibroblasts used in the repetition of the insulin experiment were similar in passage number as the fibroblasts used in the initial experiment. Primary skin fibroblasts are very sensitive towards senescence and are only suitable for experiments in a limited number of passages before they go into growth arrest. Therefore, it was not possible to repeat the insulin stimulation experiment, as the fibroblasts would undergo too many passages before having enough material to perform the experiment, and unfortunately only a limited amount of fibroblasts has been available to us.

3.1.4. Summary and Comments

We have for the first time identified a patient diagnosed with PME linked to a heterozygous deletion of *CERS2*. We find that the patient has only one functional *CERS2* allele as levels of CERS2 mRNA, protein, and enzyme activity are reduced to approximately 50% of controls. The decrease in CERS2 activity leads to altered SL and glycerophospholipid composition, indicating a changes lipid composition of the plasma

membrane and possibly disturbance of membrane microdomain formation. We show that patient skin fibroblasts are more insulin sensitive, which we speculate is due to a reduction in the level of the ganglioside GM3. Further analyses are needed to validate this hypothesis.

Skin fibroblasts are easily obtainable from patients and are often used in initial investigations of disease pathology. However, as a cell type, skin fibroblasts are often remarkably different from the tissue/cell types in which the disease originates. Therefore, results or trends found in skin fibroblasts should only be considered as indications as enzymes are differentially expressed and regulated in different cells and tissues, which constitute the basis of development of the mammalian organism. Thus, it is possible that the haploinsufficiency of *CERS2* has a more pronounced effect on the SL metabolism in the brain, as the clinical phenotypes described for our patient are highly related to disturbances in the nervous system. Much more information is needed in order to pinpoint the molecular mechanism underlying the disease onset and progression in our patient. Moving future investigations into a cellular system where neurons and oligodendrocytes of human origin are co-cultured will most likely help unravel how dysfunctions in the SL network can lead to the development of PME as well as other SL-related neurological disorders.

3.2 Regulation of the Kv2.1 Ion Channel by Sphingolipids (Unpublished Data)

As discussed, deregulation of the SL metabolism has been associated with a vast number of neurological disorders, of which several are characterized by the occurrence of epileptic seizures. The presented case linking CERS2-deficiency to the development of PME is an example of such a disorder. In this case, reduced CERS2 activity causes subtle change in the SL profile of skin fibroblasts, which apparently is enough to affect microdomain formation and signaling events depending on this structural organization. This spurred us to investigate how changes in the SL metabolism can affect ion channels known to localize to membrane microdomains and whose deregulation can contribute to the development of epilepsy or associated phenotypes. More precisely, we aimed to investigate the role of SLs in the function of the voltage-gated potassium channel Kv2.1, which, by its dynamic modulation of phosphorylation and localization in clusters, is involved in regulating the intrinsic excitability of neurons.

Kv2.1 is expressed in excitatory as well as inhibitory neurons throughout the brain [181, 182]. It is a delayed rectifier K^+ channel, meaning that its activation is slow, and moreover it inactivates quite slowly over a period of seconds [183]. Thus, Kv2.1 is not involved in the repolarization process during single action potentials, but rather serves as a regulator of intrinsic excitability during periods of repetitive high-frequency firing [184, 185]. The distribution of Kv2.1 is highly restricted in neurons as it is only present in the soma, proximal dendrites, and the axon initial segment [186, 187]. In a resting state, Kv2.1 is localized in distinct high-density clusters, which are believed to be rich in cholesterol and SLs [183, 186-188]. Initially, a link between Kv2.1 function and membrane microdomain integrity was found when cholesterol depletion was

shown to induce a hyperpolarization shift in the Kv2.1 inactivation curve in Ltk- cells [183]. Later, cholesterol depletion was also found to affect Kv2.1 localization by increasing cluster size in HEK293 cells (hereafter referred to as HEK cells) [189]. It is becoming evident that SLs are important for Kv2.1 function as well. Cleavage of the positively charged choline group from SM by SMase D causes a hyperpolarization shift in the conductance-voltage curve for Kv2.1 in *Xenopus* oocytes, meaning that the ion channel will activate at more negative membrane potentials where it would otherwise have been low conducting [190, 191]. Moreover, removing the charged phosphodiester group along with the choline from SM by SMase C treatment profoundly inhibits Kv2.1 current, which is thought to be attributed to SM's role in counteracting charges in the voltage censor domain of Kv2.1 important for ion channel gating [192]. Thus, disturbances of microdomain integrity and direct interaction between Kv2.1 and SM have different outcomes in regard to Kv2.1 function, but this nevertheless shows that the lipid environment surrounding Kv2.1 is most important for maintaining its functional properties.

In resting neurons and HEK cells clustered Kv2.1 channels are highly phosphorylated [186, 193, 194]. More than 20% of the amino acids located in the cytoplasmic regions of Kv2.1 are serine, threonine, or tyrosine residues [193]. Phosphoproteomic analysis of recombinant Kv2.1 expressed in HEK cells has identified 16 phosphorylated sites primarily located on the cytoplasmic C-terminal tail [193]. Excitatory synaptic transmission is often mediated through the neurotransmitter glutamate, which binds to glutamate receptors, for instance the NMDA ion channel and the α-amino-3-hydroxy-5-methyl-4-isoxazolepropionic acid (AMPA) ion channel, in the postsynaptic membrane. This induces a influx of Ca^{2+} into the postsynaptic neuron. Several of the Kv2.1 phosphorylation sites have shown to be sensitive to Ca^{2+}-induced dephosphorylation [193]. Indeed, dephosphorylation of Kv2.1 upon neuronal activity or simulation hereof has been demonstrated in several studies [186, 193, 194]. The change in Kv2.1 phosphorylation induces lateral translocation of Kv2.1 from clusters to a more dispersed state, both *in vivo* and *in vitro,* by stimulation with glutamate [186]. In cultured hippocampal neurons the delocalization of Kv2.1 leads to a large hyperpolarizing shift in the voltage-dependence of activation, resulting in activation at membrane potentials of -55 to -50 mV instead of -25 to 20 mV when Kv2.1 is phosphorylated in clusters [186, 195]. Furthermore, in a study analyzing the importance of the Kv2.1 C-terminus in clustering of the ion channel, a 25 amino acid segment, termed the proximal restriction and clustering (PRC) signal, was found to be necessary and sufficient for clustering in MDCK cells [196]. The PRC signal contains four amino acid residues, which have proven particularly important for Kv2.1 localization in clusters. As three of these four residues in the PRC signal are serines, and thus potential phosphorylation sites, it suggests that the Kv2.1 clustering and phosphorylation state indeed are connected.

Several heterozygous *de novo* missense mutations in the gene encoding Kv2.1 have been associated with infantile epileptic encephalopathy [197-199]. The identified mutations are located within the pore forming

domain, and functional analyses of the mutations show loss of ion selectivity leading to gain of depolarization currents [197, 199]. This affects the neuron's ability to repolarize and leaves it more susceptible to excitability and repetitive firing. The function of the Kv2.1 as a suppressor of neuronal activity correlates with observed hyperactivity and hypersensitivity towards convulsants in mice lacking this ion channel [200]. Thus, both defects in the Kv2.1 channel resulting in a more depolarized membrane potential and total lack of the ion channel lead to phenotypes related to epilepsy. As discussed, neuronal activity dictates the dynamic regulation of Kv2.1 phosphorylation and localization in microdomains. Given SLs' prominent role in microdomain formation and several associations of derailed SL metabolism with epileptic seizure phenotypes [81-84, 96, 97], it is highly relevant to investigate the role of SLs in Kv2.1 localization as well as phosphorylation.

The HEK cell line is derived from human embryonic kidney and does not display the same sophisticated level of cellular architecture, organization, or biochemistry as *in vivo* or cultured neurons does. However, HEK cells have proven to be a valuable tool in the study of several aspects of neurobiology due to their easy handling and manipulation, as well as endogenous expression of several important neurophysiological receptors and proteins [201]. In regards to the Kv2.1 ion channel, HEK cells contain the machinery necessary for the formation of exogenous Kv2.1 clusters in the plasma membrane, as well as constitutive phosphorylation and voltage-gated activity of Kv2.1 as observed for endogenous Kv2.1 in neurons [193, 194]. Furthermore, Ca^{2+}-dependent regulation of Kv2.1 phosphorylation and localization has been shown to occur in HEK cells [185, 186, 193, 194]. Thus, the HEK cell line constitutes a simple, but relevant model system for the study of the Kv2.1 ion channel.

3.2.1 Sphingolipids in Kv2.1 Clustering

Initial investigations of the role of membrane microdomains in Kv2.1 localization have shown that cholesterol depletion dramatically alters the Kv2.1 cluster size from small discrete clusters to large patches in live HEK cells [189]. In order to confirm the applicability of our model system to study Kv2.1 clustering, HEK cells were transfected with EGFP-Kv2.1 (*The EGFP-Kv2.1 construct was kindly provided by Professor Michael Tamkun (Colorado State University, USA)*) followed by cholesterol depletion using 2% 2-hydroxypropyl-β-cyclodextrin (HPCD) for 1 hour at 37°C. Kv2.1 clusters on the basal surface of HEK cells were imaged using confocal microscopy with a pinhole size corresponding to 1 Airy Unit for optimal resolution of the clusters. Kv2.1 clusters localized on the basal surface of HEK cells have been found to be representative for the entire cell surface, and thus only the basal surface was imaged [202]. As expected, cholesterol depletion induced a significant change in the Kv2.1 clustering with an average cluster size of 1.73 ± 0.13 μm^2 for cholesterol-depleted cells compared to 0.75 ± 0.06 μm^2 for control cells (Figure 8). The Kv2.1 cluster size after cholesterol depletion is in fact an underestimation as the Kv2.1 tended to arrange into

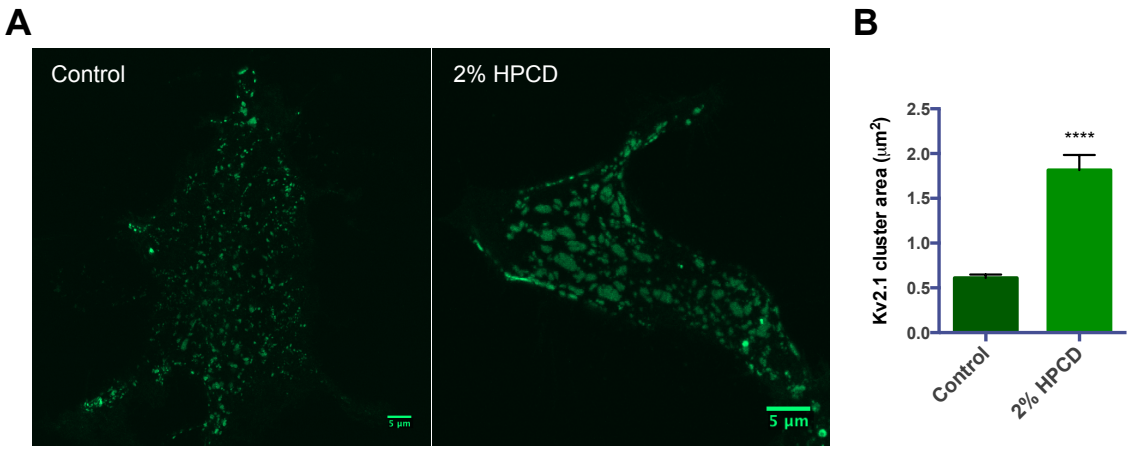

Figure 8: Cholesterol depletion leads to increased Kv2.1 cluster size in HEK293 cells. HEK293 cells transfected with EGFP-tagged Kv2.1 were cholesterol depleted using 2% 2-hydroxypropyl-β-cyclodextrin (HPCD) for 1 hour at 37°C. Within 1 hour, confocal imaging of the basal surface of the cells was performed in order to evaluate Kv2.1 cluster size. The laser power was adjusted manually for each image in order to avoid signal saturation. Cluster size analysis was performed using FIJI software with the LSM Toolbox plugin. Six representative clusters were measured per cell. A) Representative fluorescent images. *Scale bar*: 5 µm. B) Kv2.1 cluster area is shown as mean ±SEM. The average cluster area for control cells was 0.75 ± 0.06 µm^2 (n = 48) and 1.73 ± 0.13 µm^2 (n = 36) for cholesterol depleted cells. Statistical analysis was performed by unpaired t-test with Welch's correction using GraphPad Prism software. The data represent one of three independent replicates.

large plaques of whose boundaries were difficult to distinguish and thus analyze. Based on this result, our model system appears to be applicable to investigate Kv2.1 localization.

The investigation of how changes in the SL metabolism influence the clustering of Kv2.1 was initiated by examining how inhibition of ceramide synthesis by the CERS inhibitor fumonisin B1 (FB1) affects Kv2.1 cluster area. HEK cells were transfected with EGFP-Kv2.1 followed by incubation with 20 µM FB1 for 48 hours at 5% CO_2, 37°C. As shown in Figure 9, inhibition of ceramide synthesis significantly increased Kv2.1 cluster size with an average area of 1.22 ± 0.13 µm^2 compared to 0.45 ± 0.06 µm^2 for control cells.

Next, the question was which SL species, or the lack hereof, were responsible for the increased Kv2.1 cluster size. It is evident that when inhibiting ceramide synthesis, the synthesis of downstream complex SLs is also affected. To evaluate the effect of FB1 on the SL profile of HEK cells, a liquid chromatography-mass spectrometry (LC-MS) analysis of FB1-treated HEK cells was performed (Figure 10). As seen in Figure 10A-E, all the investigated SL species (ceramide, HexCer, SM, and gangliosides) were dramatically reduced by FB1. The metabolism of glycerolipids and SLs are connected through the degradation of SLs to hexadecenal, which can be turned into palmitoyl-CoA and then used in the synthesis of glycerolipids, including the major glycerophospholipid PC [36]. No marked changes were observed in PC species upon FB1 treatment, indicating that the glycerolipid pathway was not affected by inhibition of ceramide synthesis

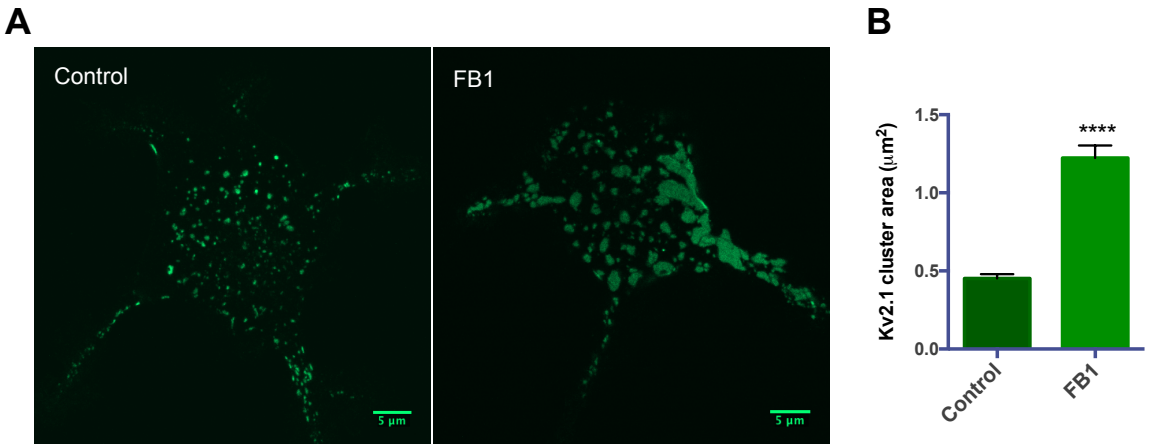

Figure 9: Inhibition of ceramide synthesis results in increased Kv2.1 cluster size in HEK293 cells. HEK293 cells transfected with EGFP-tagged Kv2.1 were treated with 20 µm fumonisin B1 (FB1) for 48 hours at 5% CO_2, 37°C in order to inhibit ceramide synthesis. Within 1 hour, confocal imaging of the basal surface of the cells was performed in order to evaluate Kv2.1 cluster size. The laser power was adjusted manually for each image in order to avoid signal saturation. Cluster size analysis was performed using FIJI software with the LSM Toolbox plugin. Six representative clusters were measured per cell. A) Representative fluorescent images. *Scale bar*: 5 µm. B) Kv2.1 cluster area is shown as mean ±SEM. The average cluster area for control cells was 0.45 ± 0.06 μm^2 (n = 42) and 1.22 ± 0.13 μm^2 (n = 41) for FB1 treated cells. Statistical analysis was performed by unpaired t-test with Welch's correction using GraphPad Prism software. The data represent one of three independent replicates.

(Figure 10F). This is contrary to observations in rat hepatocytes where FB1 has been found to increase the synthesis of PC [203], which indicates a cell type specific connection between glycerolipid and SL metabolism.

We then addressed the role of reduced complex SL synthesis in the FB1-mediated increase in Kv2.1 clustering. SMase from *Bacillus cereus* (hereafter referred to as SMase) is a homologue to the mammalian nSMase, which hydrolyzes SM to ceramide and phosphocholine [204]. In HeLa cells this SMase has been shown to hydrolyze plasma membrane SM completely using a concentration of 25 mU/mL for 10 min. with a concurrent rise in ceramide levels [205]. To investigate if reduced SM in the plasma membrane of HEK cells would enhance Kv2.1 clustering, HEK cells transfected with EGFP-Kv2.1 were subjected to SMase treatment at 25, 50, and 100 mU/mL for 10 min. at 37°C. Kv2.1 cluster area was increased for all treatments proportional with the increase in SMase concentration (Figure 11). An average cluster size of 0.68 ± 0.06 µm2 was found for control cells compared to 1.31 ± 0.05 µm2, 2.00 ± 0.23 µm2, and 2.43 ± 0.19 µm2 for cells incubated with 25, 50, and 100 mU/mL SMase, respectively. The observed effect could potentially be caused by two aspects of SL metabolism, either a decrease in SM or an increase in ceramide. To address the latter we transfected EGFP-Kv2.1 into a HEK cell line overexpressing CERS5 having increased level of C16 ceramide, as C16 SM constitutes the major SM in HEK cells (Figure 10D). No change in Kv2.1 clustering was observed (*Appendix II*), indicating that the increased Kv2.1 cluster size found upon SMase treatment indeed is due to a decrease in SM rather than an increase in ceramide. The FB1 treatment of the HEK cells

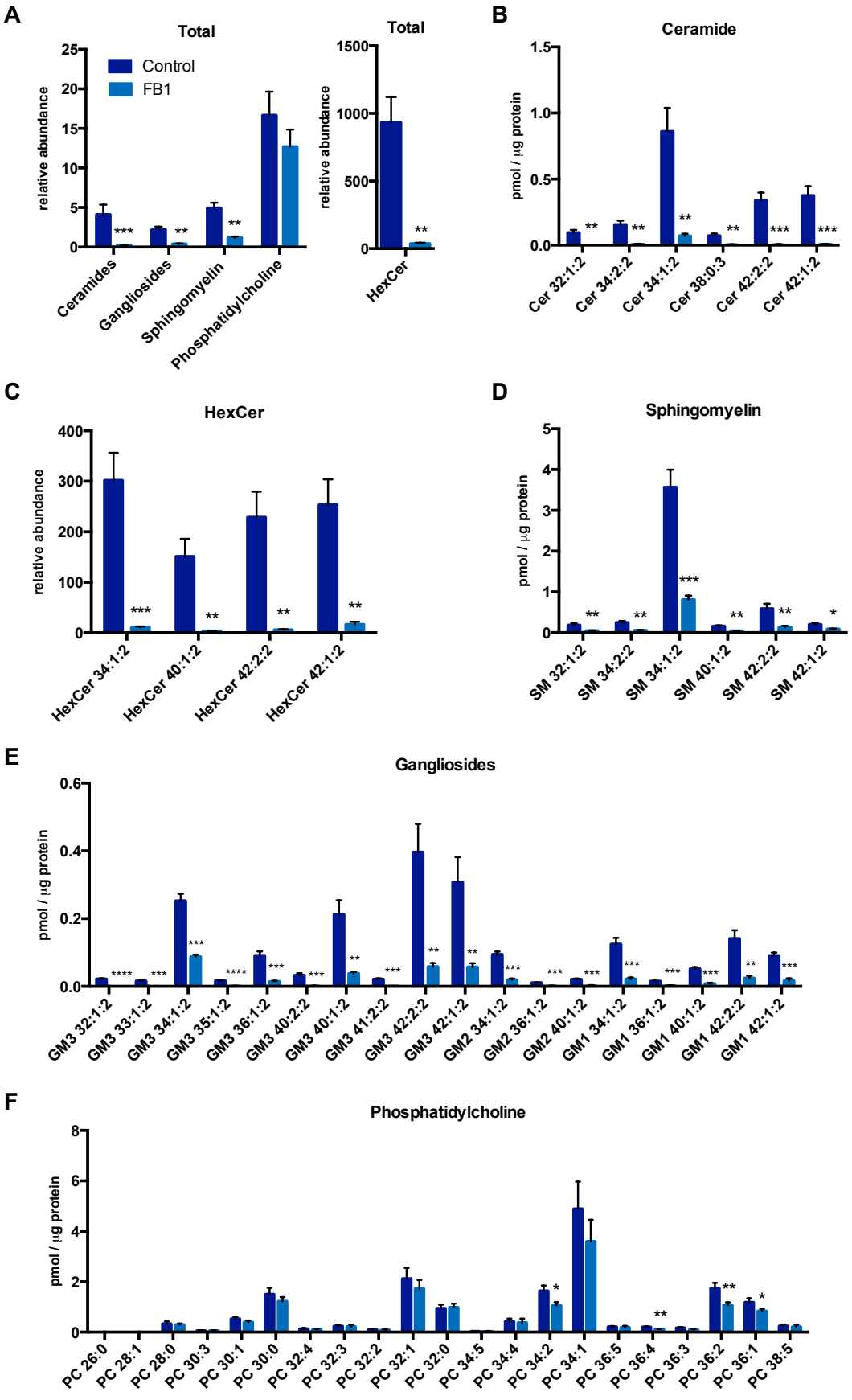
A
Total
Control
FB1
relative abundance
Ceramides
Gangliosides
Sphingomyelin
Phosphatidylcholine
Total
HexCer
B
Ceramide
pmol / µg protein
Cer 32:1;2
Cer 34:2;2
Cer 34:1;2
Cer 38:0;3
Cer 42:2;2
Cer 42:1;2
C
HexCer
HexCer 34:1;2
HexCer 40:1;2
HexCer 42:2;2
HexCer 42:1;2
D
Sphingomyelin
SM 32:1;2
SM 34:2;2
SM 34:1;2
SM 40:1;2
SM 42:2;2
SM 42:1;2
E
Gangliosides
GM3 32:1;2
GM3 33:1;2
GM3 34:1;2
GM3 35:1;2
GM3 36:1;2
GM3 40:2;2
GM3 40:1;2
GM3 41:2;2
GM3 42:2;2
GM3 42:1;2
GM2 34:1;2
GM2 36:1;2
GM2 40:1;2
GM1 34:1;2
GM1 36:1;2
GM1 40:1;2
GM1 42:2;2
GM1 42:1;2
F
Phosphatidylcholine
PC 26:0
PC 28:1
PC 28:0
PC 30:3
PC 30:1
PC 30:0
PC 32:4
PC 32:3
PC 32:2
PC 32:1
PC 32:0
PC 34:5
PC 34:4
PC 34:2
PC 34:1
PC 36:5
PC 36:4
PC 36:3
PC 36:2
PC 36:1
PC 38:5

Figure 10: Major changes in the sphingolipid profile upon inhibition of ceramide synthesis. Lipid extracts prepared from three independent HEK293 cell control cultures and cultures treated with 20 µM fumonisin B (FB1) for 48 hours at 5% CO_2, 37 °C were analyzed by LC-MS using appropriate internal standards. All lipid species besides hexosylceramides (HexCer) are presented as pmol/µg protein. Due to lack of internal standards, HexCer species are presented as relative abundance. Mean ± SD of n = 3 HEK293 cell cultures per group is shown. A) Total levels of analyzed lipid species. B) Ceramide, C) HexCer species. D) Sphingomyelin species E) Ganglioside species. F) Phosphatidylcholine species. Statistical analysis was performed by a multiple t-test using GraphPad Prism software. Lipid extraction and analysis were kindly performed by Marta Moreno Torres (Dept. Biochemistry and Molecular Biology, University of Southern Denmark).

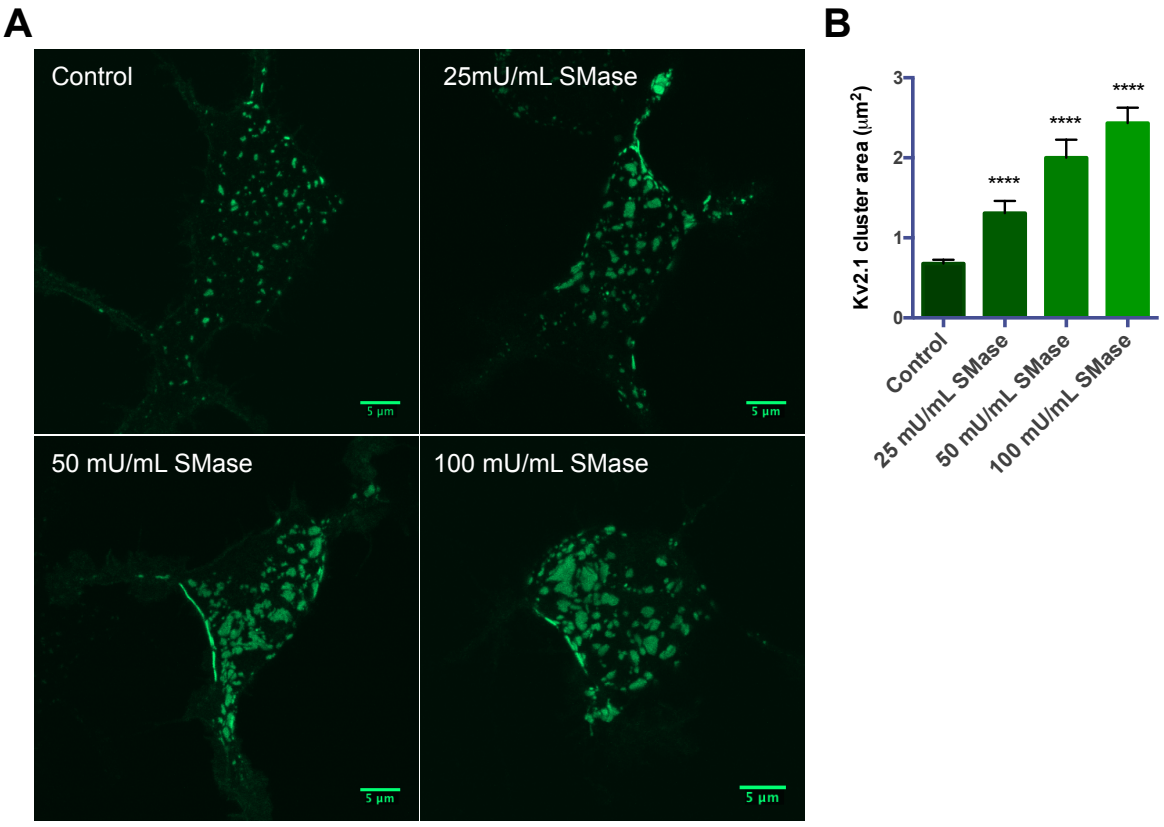

Figure 11: Hydrolysis of sphingomyelin in the plasma membrane leads to pronounced increase in Kv2.1 cluster size in HEK293 cells. HEK293 cells transfected with EGFP-tagged Kv2.1 were treated with 25, 50, or 100 mU/mL SMase for 10 min at 37°C in order to reduce the amount of sphingomyelin in the plasma membrane. Within 1 hour, confocal imaging of the basal surface of the cells was performed in order to evaluate Kv2.1 cluster size. The laser power was adjusted manually for each image in order to avoid signal saturation. Cluster size analysis was performed using FIJI software with the LSM Toolbox plugin. Six representative clusters were measured per cell. A) Representative fluorescent images. *Scale bar*: 5 µm. B) Kv2.1 cluster area is shown as mean ±SEM. The average cluster area for control cells was 0.68 ± 0.06 µm^2 (n = 48) and 1.31 ± 0.05 µm^2 (n = 36), 2.00 ± 0.23 µm^2 (n = 36), and 2.43 ± 0.19 µm^2 (n = 36) for cells treated with 25, 50, or 100 mU/mL SMase, respectively. Statistical analysis was performed by One-way ANOVA with Brown Forsythe and Bartlett's tests for correction of significantly different standard deviations using GraphPad Prism software. The data represent one of three independent replicates.

also lead to a pronounced reduction in GSLs (Figure 10A,C,E). To investigate the contribution of this in the enhanced Kv2.1 clustering, HEK cells transfected with EGFP-Kv2.1 were incubated with 10 µM D-*threo*-1-phenyl-2-decanoylamino-3-morpholino-1-propanol (PDMP) for 48 hours at 5% CO_2, 37°C. PDMP inhibits the GluCer synthase catalyzing the transfer of glucose to ceramide, which is the first step in GSL synthesis.

Lipid LC-MS analysis of PDMP-treated HEK cells showed that PDMP effectively inhibited the synthesis of HexCer and ganglioside species without markedly affecting other SLs species (*Appendix III*). In relation to Kv2.1 clustering, treatment with PDMP did not significantly change the cluster area given an average Kv2.1 cluster size of 0.53 ± 0.04 μm^2 for control cells compared to 0.67 ± 0.10 μm^2 for PDMP- treated cells (*Appendix II*). Collectively, these results indicate that a reduction in the level of SM in the plasma membrane, and not GSLs, is most likely contributing to the increased Kv2.1 cluster size observed in FB1-treated cells.

Several studies have shown that accumulation of ceramide precursors, such as Sa and deoxySa, occurs when ceramide synthesis is inhibited by FB1 [204-206]. Thus, we aimed to examine if increased levels of Sa and deoxySa could mediate an effect on Kv2.1 clustering. As these LCBs are known pro-apoptotic molecules, we first tested the toxicity of Sa and deoxySa at several concentrations in HEK cells. No obvious detachment or morphology changes where observed for HEK cells when treating with 1 μM Sa for 24 hours (results not shown). Increased levels of Sa and deoxySa have previously been found to be neurotoxic effectors in primary neurons in *CerS1*$^{-/-}$ mice [87]. In these neurons, the concentrations of Sa and deoxySa were calculated to be 15 μM and 0.15 μM, respectively. Our LC-MS setup did not allow us to detect LCBs, and therefore it was not possible to measure Sa and deoxySa levels induced by FB1 treatment of HEK cells. Thus, a 1:100 ratio in the concentrations between Sa and deoxySa was chosen for subsequent experiments. No obvious detachment or morphology changes were observed when treating HKE293 cells with 0.01 μM deoxySa. To analyze the effect of Sa and deoxySa on Kv2.1 clustering, HEK cells transfected with EGFP-Kv2.1 were incubated with 1 μM Sa or 0.01 μM deoxySa complexed with bovine serum albumin (mol 1:1) for 24 hours at 5% CO_2, 37°C. As shown in Figure 12, both LCB treatments increased Kv2.1 cluster area with an average cluster size of 1.02 ± 0.10 μm^2 for Sa-treated cells compared to 0.66 ± 0.06 μm^2 for control cells and 1.07 ± 0.06 μm^2 for deoxySa-treated cells compared to 0.53 ± 0.03 μm^2 for control cells. The results suggest that increased levels of LCBs upon inhibition of ceramide synthesis by FB1 may contribute to the increase size of Kv2.1 clusters in addition to the contribution from reduced SM in the plasma membrane. The question remains how the LCBs mechanistically adds to this effect, as LC-MS analyses of HEK cells incubated with 1 μM Sa and 0.01 μM deoxySa for 24 hours at 5% CO_2, 37°C do not reveal any pronounced changes in the SL profile (*Appendix IV*). Yet treatment with deoxySa did lead to an increase in several deoxyceramide species (Figure 13), suggesting that the effect can be mediated though elevation of either deoxySa directly or deoxyceramide, as the latter cannot be metabolized further.

To address whether inhibition of *de novo* ceramide synthesis contributes to the increased Kv2.1 cluster area observed for FB1 treatment, HEK cells transfected with EGFP-Kv2.1 were treated with 20 uM myriocin, a known inhibitor of SPT, which catalyzes the initial step in *de novo* ceramide synthesis. Unexpectedly, Kv2.1 clustering proved to be very sensitive towards the solvents, methanol and dimethyl sulfoxide (DMSO), in

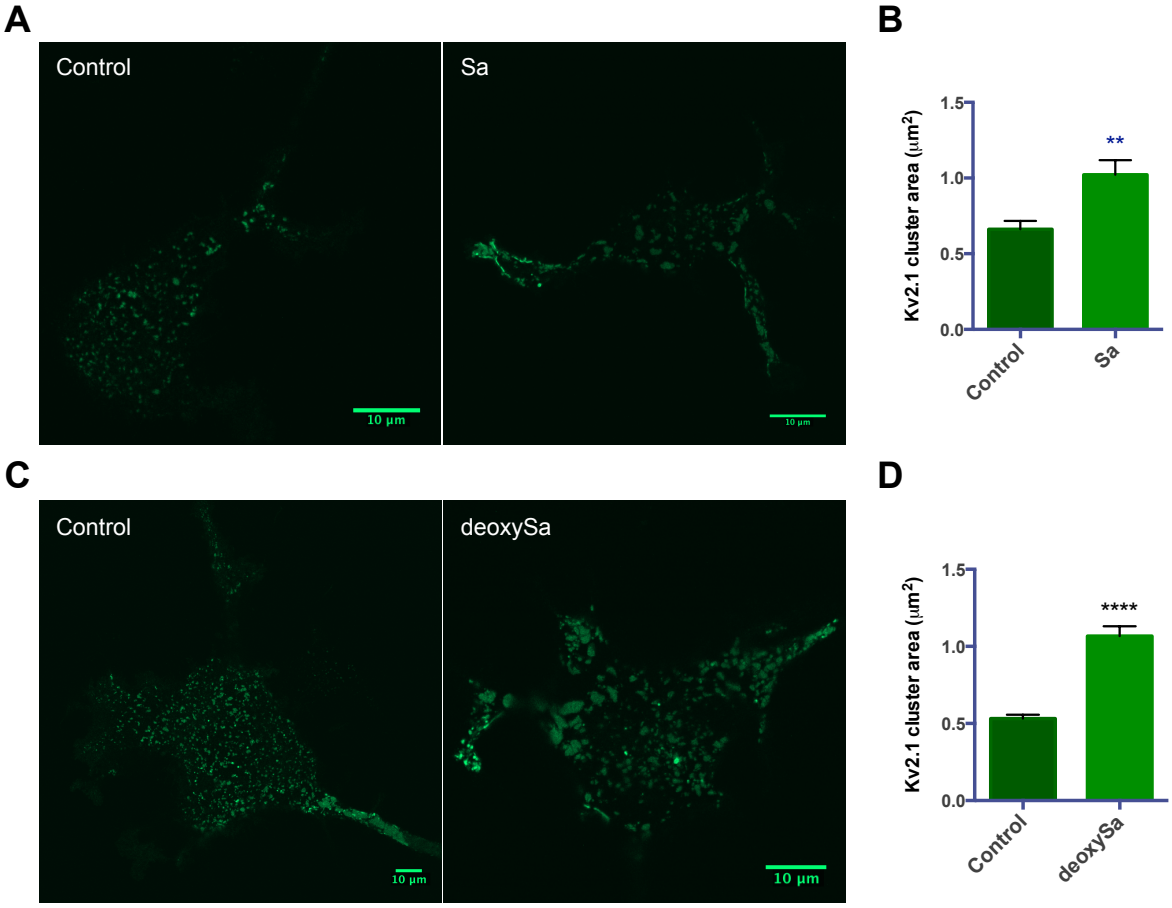

Figure 12: Stimulation with sphinganine and 1-deoxysphinganine increases Kv2.1 cluster size. HEK293 cells transfected with EGFP-tagged Kv2.1 were treated with 1 uM sphinganine (Sa) and 0.01 uM 1-deoxysphinganine (deoxySa) complexed with bovine serum albumin (mol 1:1) for 24 hour at 5% CO_2, 37°C. Within 1 hour, confocal imaging of the basal surface of the cells was performed in order to evaluate Kv2.1 cluster size. The laser power was adjusted manually for each image in order to avoid signal saturation. Cluster size analysis was performed using FIJI software with the LSM Toolbox plugin. Six representative clusters were measured per cell. A) Representative fluorescent images for cells treated with Sa. *Scale bar*: 10 µm. B) Kv2.1 cluster area is shown as mean ±SEM. The average cluster area for control cells was 0.66 ± 0.06 μm^2 (n = 36) and 1.02 ± 0.10 μm^2 (n = 36) for Sa treated cells. C) Representative fluorescent images for cells treated with deoxySa. *Scale bar*: 10 µm. D) Kv2.1 cluster area is shown as mean ±SEM. The average cluster area for control cells was 0.53 ± 0.03 μm^2 (n = 36) and 1.07 ± 0.06 μm^2 (n = 36) for deoxySa treated cells. Statistical analyses were performed by unpaired t-test with Welch's correction using GraphPad Prism software. For each treatment the data represent one of three independent replicates. Results were kindly provided by Cathrine Høyer Christensen (Dept. Biochemistry and Molecular Biology, University of Southern Denmark).

which the myriocin was dissolved (results not shown). Even at concentrations of 0.2% solvent, Kv2.1 clustering was significantly increased, making it impossible to achieve SPT inhibition and simultaneously investigate Kv2.1 clustering. In order to evaluate the role of *de novo* ceramide synthesis in Kv2.1 clustering, other inhibitors of SPT could be applied [207], or alternatively the experiment could be carried out in a HEK cell line having reduced SPT activity.

.

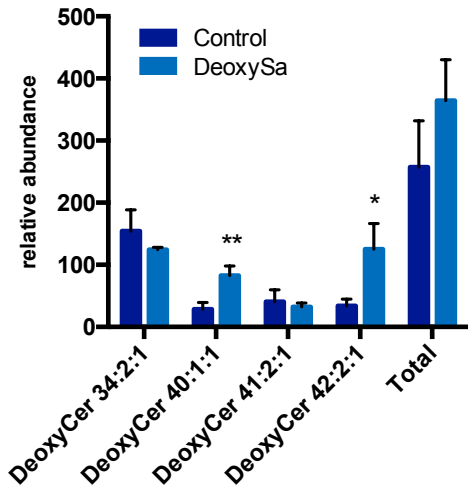

Figure 13: Deoxyceramide is synthesized upon treatment with 1-deoxysphinganine. Lipid extracts prepared from three independent HEK293 cell control cultures and cultures treated with 0.01 µM 1-deoxysphinganine (deoxySa) for 24 hours at 5% CO_2, 37 °C were analyzed by LC-MS. Due to lack of internal standards, deoxyceramides (DeoxyCer) are presented as relative abundance. Mean ± SD of n = 3 HEK293 cell cultures per group is shown. Statistical analysis was performed by multiple t-test using GraphPad Prism software. Lipid extraction and analysis were kindly performed by Marta Moreno Torres (Dept. Biochemistry and Molecular Biology, University of Southern Denmark).

Future experiments should encompass explorations of how specific steps in the SL metabolism are involved in the regulation of Kv2.1 localization. This could be obtained through investigations of Kv2.1 clustering in HEK cells lacking specific enzymes along the SL pathway. We tried to access the role of CERS2 in Kv2.1 clustering by transfecting EGFP-Kv2.1 into primary skin fibroblasts obtained from the *CERS2*$^{+/-}$ PME patient and gender- and age-matched controls. As seen in Figure 14, Kv2.1 does not cluster in human primary skin fibroblasts, making it impossible to use these cells in the investigation of Kv2.1 clustering.

Collectively, the described results show that reducing the amount of SM in the plasma membrane of HEK cells alongside increasing the concentrations of Sa and deoxySa promote accumulation of Kv2.1 in larger patches compared to small discrete clusters under control conditions. The molecular mechanisms causing the assembly of Kv2.1 into larger clusters remain to be elucidated. It could be postulated that increased Kv2.1 clustering upon SMase treatment is caused by elevated levels of ceramide in the plasma membrane, which through its ability to self-associate leads to the generation of larger microdomains [208]. Yet this mechanism is not likely to explain the increased Kv2.1 clustering upon treatment with FB1, as ceramide is practically absent in FB1-treated cells (Figure 10). Ablation of CERS2 has shown to strongly affect

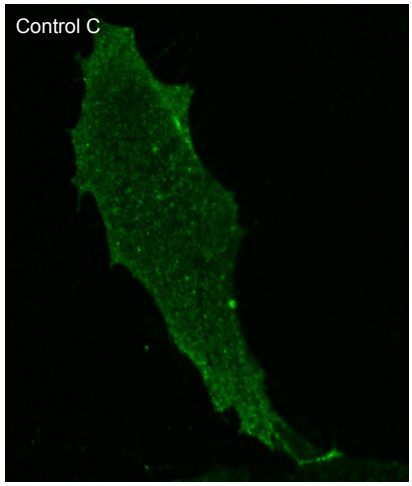

Figure 14: Kv2.1 clusters are not observed in human primary skin fibroblasts. EGFP-tagged Kv2.1 transfected into primary skin fibroblasts from the gender- and age-matched control C used in *Supplement III*. Image was obtained using a Nikon-Andor Spinning Disk setup.

biophysical properties of membranes from tissues where CERS2 is considered to be one of the primary CERSs [208]. Lack of CERS2 causes alterations in membrane curvature promoting vesicle adhesion and vesicle fusion in membranes isolated from mouse liver and brain. Therefore, it is possible that the changes observed in Kv2.1 localization upon FB1 treatment is causes by overall changes in membrane properties leading to accumulation of Kv2.1 in larger patches. As increased level of Sa has been found to induce apoptosis, a process to which the generation of ceramide platforms has been associated [209, 210], it can be speculated that the observed increase in Kv2.1 cluster size after treatment with Sa is a consequence of the discussed ceramide-mediated generation of larger microdomains. However, the fact that no marked changes were observed in the SL profile of Sa-treated HEK cells (*Appendix IV*) points towards that the increased level of Sa does not change the overall SL profile, which complicates the interpretation of Sa-mediated Kv2.1 clustering. In respect to deoxySa, a recent study has shown that treatment with an analog of deoxySa, alkyne-deoxySa, leads to morphological changes of the ER in mouse embryonic fibroblasts observed as enlarged and dense-appearing ER sheets compared to a net-like appearance [211]. Interestingly, clusters of Kv2.1 on the soma and proximal dendrites in pyramidal neurons have been found to lie over subsurface cisternae derived from the ER [184]. Thus, it can be speculated that the increase in Kv2.1 clustering in the plasma membrane of deoxySa-treated HEK cells is a secondary effect to disturbances in the ER morphology. Further investigations are necessary in order to address this aspect.

The presented results suggest that SL metabolism indeed is important for regulation of Kv2.1 localization in what corresponds to a ”resting” state. Future experiments should encompass how changes in the SL profile affect Kv2.1 clustering in an “active” state during which Kv2.1 channels are nonclustered. This could be achieved by raising the intracellular level of Ca^{2+} promoting dephosphorylation and declustering of Kv2.1 as seen in rat hippocampal neurons [186]. It can be hypothesized that treatment with FB1, SMase, Sa, or deoxySa prevents delocalization of Kv2.1 upon “activation” in HEK cells. This in turn could potentially affect the activation threshold of Kv2.1. Future experiments are necessary in order to determine if this indeed is the case.

Our intention was to extend the presented results with corresponding experiments performed in mouse hippocampal neuron, as HEK cells cannot replicate the full environment of neuronal proteins nor the complex regulation of these. In order to achieve this, a collaboration was set up with the laboratory of Associate Professor Nicole Schmitt, Section of Heart and Circulatory Research, University of Copenhagen, Denmark. Visualization of endogenous Kv2.1 in hippocampal neurons was attempted using immunohistochemistry, but unexpectedly Kv2.1 displayed a more diffuse localization with only few clusters (Figure 15). Several attempts to optimize Kv2.1 detection were performed without successful improvements. Instead we tried overexpression of Kv2.1 in the neurons, but the majority of the Kv2.1 clusters had donut-shapes with uneven fluorescence much different from other observations of Kv2.1 clustering in hippocampal

neurons (Figure 15) [186, 187]. Overexpression of Kv2.1 using different constructs was attempted without successful improvements. Thus, due to the time limiting nature of this project, we were not able to complement our results with equivalent experiments in neurons, but these will be most important in future experiments in order to address the role of SLs on Kv2.1 localization under more physiological relevant conditions.

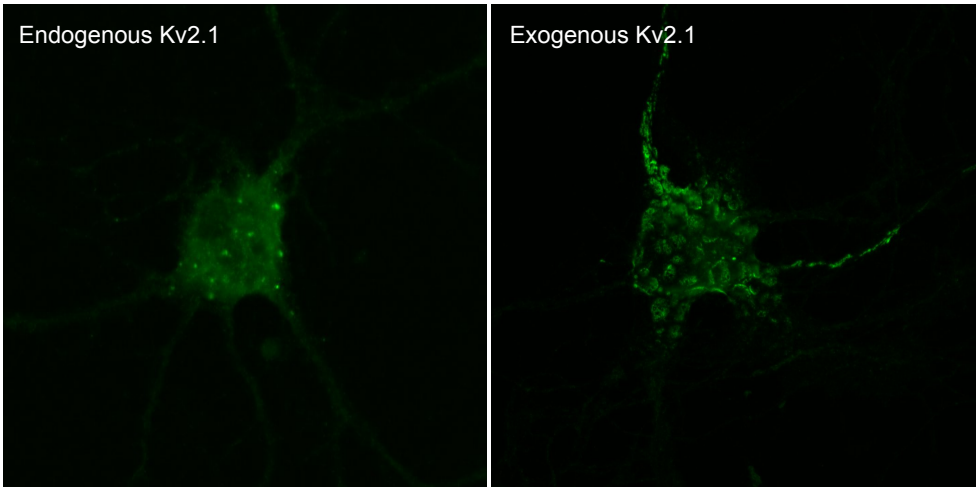

Figure 15: Kv2.1 in primary mouse hippocampal neurons. *Left*) Attempt to visualize endogenous Kv2.1 in mouse hippocampal neurons. Notice how the Kv2.1 distribution is very diffuse with only few larger clusters. *Right*) Overexpression of Kv2.1 in hippocampal neurons led to unnatural donut-shaped Kv2.1 clusters with uneven fluorescence. Images were kindly provided by Camilla Stampe Jensen (Section of Heart and Circulatory Research, University of Copenhagen).

We are in the process of complementing the presented work with electrophysiological measurements of Kv2.1 ion channel properties in HEK cells upon SL manipulations through a collaboration with the laboratory of Professor Michael Tamkun, Department of Biomedical Sciences, Colorado State University, USA. As mentioned, disturbance of membrane microdomain integrity by cholesterol depletion as well as hydrolysis of SM has been associated with changes in Kv2.1 properties [189, 190, 192]. Moreover, cholesterol depletion and inhibition of ceramide synthesis by FB1 have been shown to have similar effects on Kv1.5 properties with hyperpolarization shifts of both the activation and inactivation curve [188]. Opposed to Kv2.1, Kv1.5 localizes to caveolin-rich microdomains [188], and therefore it can only be speculated that inhibition of ceramide synthesis has a corresponding effect on Kv2.1 properties. However, as the FB1 treatment of HEK presented here results in a clear reduction in the level of SM, it is possible that FB1 treatment will affect Kv2.1 properties as observed for SM hydrolysis. Hopefully in the near future, we will be able to assess the importance of SLs in Kv2.1 function, which will be most valuable for the understanding of the potential role of Kv2.1 in SL-related neurological disorders.

It is becoming evident that the Kv2.1 ion channel has an additional function besides regulating excitability during high frequency firing. Kv2.1 is not exclusively located in clusters neither in hippocampal neurons nor

when being overexpressed in HEK cells [202, 212]. A portion of Kv2.1 remains unclustered, and it has been shown that only a fraction of these are actually conducting [202, 212]. Moreover, it has been suggested that the Kv2.1 channels in clusters do not serve as a reservoir of nonconducting channels that are activated upon release, as declustering by dephosphorylation was found not to increase whole-cell currents in HEK cells [212]. This points towards a secondary function of Kv2.1, which is not directly involved in controlling the membrane potential. It has been suggested that Kv2.1 clusters may act as specialized platforms involved in membrane protein trafficking as the clusters have proven to be sites for delivery of Kv channels [213]. In addition, Kv2.1 has been associated with SNARE protein-mediated vesicular trafficking, indicating that Kv2.1 is involved in exocytosis as well [214]. To which extent the SL metabolism is involved in regulating these non-channel functions of Kv2.1 still needs to be elucidated.

Besides functioning as a membrane-trafficking hub, a recent study has shown that Kv2.1 clusters have a structural role in the formation of stable ER-plasma membrane junctions in both HEK cells and in hippocampal neurons [215, 216]. The ER is a known Ca^{2+} store, and interestingly Kv2.1 co-localizes with several proteins involved in Ca^{2+} homeostasis in neurons, including the ryanodine receptor, the Ca^{2+} sensor stromal interaction molecule 1, and the plasma membrane Ca^{2+} ion channel ORAII [215]. Dispersion of Kv2.1 channels upon glutamate treatment has been shown to induce retraction of ER from the plasma membrane [215]. This could suggest that phosphorylation of Kv2.1 mediates binding to an ER component preventing translocation of Kv2.1, as seen upon glutamate-mediated dephosphorylation of Kv2.1. Overall, this suggests that Kv2.1 has a significant role in regulating the Ca^{2+} homeostasis in neurons. If changes in the SL metabolism indeed affect Kv2.1 clustering both in an “inactive” and in an “active” state, this in turn could lead to disturbances in the Ca^{2+} homeostasis, which would be damaging for neuronal functions [217]. Future experiments are needed on order to enlighten this aspect of SL metabolism.

3.2.2. Sphingolipids in Kv2.1 Phosphorylation

The phosphorylation state of Kv2.1 is tightly coupled to its localization in the plasma membrane. Multiple kinases and phosphatases are thought to orchestrate the phosphorylation of Kv2.1, including the kinases protein kinase C (PKC), casein kinase II, Ca^{2+}-calmodulin kinase II, and AMP-activated protein kinase, as well as the phosphatases protein phosphatase 1 (PP1), protein phosphatase 2A (PP2A), calcineurin (also known as PP2B) [218, 219]. Ceramide and sphingosine have been associated with modulation of several of these kinases and phosphatases [220-222], thereby making it relevant to investigate the role of altered SL metabolism in Kv2.1 phosphorylation. It has been suggested that the phosphatases PP1 and PP2A are involved in constitutive regulation of Kv2.1 phosphorylation, as inhibition of these increases Kv2.1 phosphorylation in resting rat hippocampal neurons [186]. In this study, glutamate-mediated dephosphorylation of Kv2.1 through NMDA and AMPA receptors was not affected by okadiac acid, an inhibitor of PP1 and PP2A, indicating that PP1 and PP2A are not involved in the activity-dependent

regulation of Kv2.1 phosphorylation. Instead, calcineurin has been shown to be pivotal in the glutamate-induced, Ca^{2+}-dependent dephosphorylation of Kv2.1 leading to a hyperpolarized shift in its voltage-dependence of activation [186]. In other studies, synaptic stimulation through the NMDA glutamate receptor has been found to activate PP1 in primary mouse neurons [223, 224], which occurs in a manner independent of calcineurin [223]. Furthermore, the activation of PP1 was found to led to dephosphorylation of Kv2.1 and a hyperpolarizing shift in its inactivation kinetics [224]. Thus, regulation of Kv2.1 phosphorylation upon synaptic activity in neurons is not straightforward.

We set out to investigate if changes in the SL metabolism was involved in the regulation of constitutive Kv2.1 phosphorylation. Initially, HEK cells overexpressing Kv2.1 (*HEK293 cells overexpressing Kv2.1 was kindly provided by Professor James Trimmer (University of Southern California, USA*)) was treated with either 20 µM FB1, 50 mU/mL SMase, 1 µM Sa, or 0.01 µM deoxySa. Kv2.1 phosphorylation was evaluated by monitoring mobility of Kv2.1 by Western Blotting. *In vitro* phosphatase treatment by alkaline phosphatase (AP) was included as a control for Kv2.1 mobility shift. As seen in Figure 16, treatment with either FB1, SMase, Sa, or deoxySa did not induce a higher phosphorylation state or dephosphorylation of Kv2.1. As expected, treatment with AP led to Kv2.1 dephosphorylation seen as increased mobility (Figure 16). The experiment indicates that the constitutive phosphorylation of Kv2.1 is not sensitive towards changes in the SL metabolism in HEK cells.

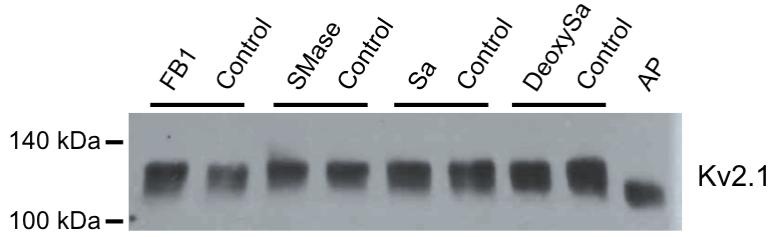

Figure 16: Modulation of sphingolipid metabolism does not appear to affect the constitutive phosphorylation of Kv2.1. HEK293 cells overexpressing Kv2.1 were treated with 20 µM fumonisin B1 (FB1) (48 hr), 50 mU/mL SMase for 10 min, 1 µM sphinganine (Sa) complexed with bovine serum albumin (BSA) (24 hr), or 0.01 µM 1-deoxysphinganine (deoxySa) complexed with BSA (24 hr). *In vitro* alkaline phosphatase (AP) treatment (1 U/µg protein) of a non-treated sample was applied as positive control for Kv2.1 dephosphorylation. Kv2.1 detection was performed by Western Blotting using a 7.5% SDS-PAGE gel and an antibody against full Kv2.1. Mobility of molecular weight standards is shown on the left.

It can be speculated that the described increase in Kv2.1 cluster size upon modulation of the SL metabolism can inhibit translocation of the ion channel upon "activation", which in turn also can affect the Kv2.1 phosphorylation state. It is possible that the regulation of Kv2.1 localization is a matter of regulating the accessibility of kinases to phosphorylate Kv2.1. In line with this, SL-mediated predisposition of Kv2.1 ion channels to remain in clusters would lead to an increase in Kv2.1 phosphorylation. Thus, we wanted to investigate if altered SL metabolism would affect Kv2.1 phosphorylation after "activation". In order to do

this, HEK cells overexpressing Kv2.1 were treated with 20 µM FB1, 1 µM Sa, or 0.01 µM deoxy Sa after which the cells were incubated with 1 µM ionomycin, a Ca^{2+} ionophore, which has been shown to induce dephosphorylation of Kv2.1 in HEK cells [194]. AP treatment was used as a positive control for Kv2.1 dephosphorylation. No obvious changes in Kv2.1 phosphorylation were observed upon incubation with ionomycin (Figure 17), indicating that the treatment was not sufficient to increase the intracellular level of Ca^{2+} to the extent of activating phosphatases, such as calcineurin, which could dephosphorylate Kv2.1. Overall, the mobility of the samples corresponds to the mobility in Figure 16, yet including a sample treated with an inhibitor of calcineurin would have been decisive for whether or not the ionomycin treatment had worked or not. Nonetheless, optimization of the ionomycin-mediated elevation of intracellular Ca^{2+} is necessary in order to evaluate the role of SLs in regulating the "activated" phosphorylation state of Kv2.1. Other Ca^{2+} ionophores, such as A23187, could also be applied to increase intracellular Ca^{2+}, or alternatively glutamate receptors could be expressed in the cells allowing for glutamate-induced elevation of Ca^{2+}. Optimization of the intracellular Ca^{2+} level was unfortunately not possible within the timeframe of this project, but it will be pivotal in future research of how SL metabolism might be involved in the regulation of activity-induced dephosphorylation of Kv2.1.

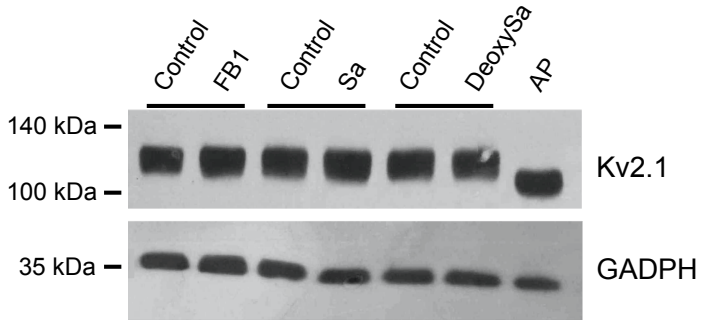

Figure 17: Modulation of sphingolipid metabolism does not appear to affect the phosphorylation of Kv2.1 upon treatment with ionomycin. HEK293 cells overexpressing Kv2.1 were treated with 20 µM fumonisin B1 (FB1) (48 hr), 1 µM sphinganine (Sa) complexed with bovine serum albumin (BSA) (24 hr), or 0.01 µM 1-deoxysphinganine (deoxySa) complexed with BSA (24 hr). The cells were treated with 1 µM ionomycin for 5 hr, 37 °C, prior to harvesting of cells. *In vitro* alkaline phosphatase (AP) treatment (1 U/µg protein) of a non-treated sample was applied as positive control for Kv2.1 dephosphorylation. Kv2.1 detection was performed by Western Blotting using a 7.5% SDS-PAGE gel and an antibody against full Kv2.1. GADPH was used as a loading control. Mobility of molecular weight standards is shown on the left. Results were kindly provided by Cathrine Høyer Christensen (Dept. Biochemistry and Molecular Biology, University of Southern Denmark).

In Figure 16 and Figure 17 the Kv2.1 band is very broad indicating that there are several phosphorylation states of Kv2.1. It is possible that changes in the SL metabolism only affect a subset of these states. It proved difficult to separate the phosphorylation states of Kv2.1 using regular SDS-PAGE, and therefore we attempted to set up Phos-Tag SDS-PAGE, which is an improved method for the separation and detection of large phosphoproteins [225]. The Phos-Tag interacts with phosphorylated proteins slowing down their migration and hence induces a mobility-shift compared to the less phosphorylated proteins. This method

requires careful optimization of gel pore size, Phos-Tag concentration, and electrophoresis timing, which unfortunately was not achieved within the timeframe of this project (optimizations tests not shown). Yet, Phos-Tag SDS-PAGE combined with phosphoproteomics will be valuable tools in the investigation of SL-mediated regulation of Kv2.1 phosphorylation. Phos-Tag SDS-PAGE will provide information of the overall phosphorylation state of Kv2.1, while phosphoproteomics will reveal regulation of specific phosphorylation sites on Kv2.1.

3.2.3. Summary and Comments

Collectively, the presented results show that disturbed SL metabolism leads to increase in Kv2.1 cluster size in HEK cells. Particularly reduction of SM in the plasma membrane as well as increasing the concentrations of Sa and deoxySa induce accumulation of Kv2.1 into larger patches compared to smaller assemblies under control conditions. Furthermore, our intention was to investigate if disturbed SL metabolism would affect the phosphorylation state of Kv2.1. Our results indicate that the SL profile is not important for constitutive Kv2.1 phosphorylation during a "resting" state. It was not possible to evaluate the role of SLs in regulation of Kv2.1 phosphorylation during an "active" state, however this information will be essential for the understanding of how SL metabolism might be involved in the regulation of activity-induced dephosphorylation of Kv2.1 and ultimately regulation of neuronal excitability.

As mentioned, we are in the process of complementing our observations with functional studies of Kv2.1 kinetics. The ongoing electrophysiological measurements of Kv2.1 kinetics are performed at room temperature, as many electrophysiological experiments are. In order to provide a standard of comparison, the Kv2.1 localization experiments were performed at room temperature. It is known that membrane fluidity is heavily dependent on temperature, which should be kept in mind when interoperating the results as membrane fluidity can impact internal dynamics of proteins as well as protein movement potentially affecting protein-protein interactions [226]. Thus, it would be highly relevant to perform equivalent studies under more physiological relevant settings with regards to both Kv2.1 localization and electrophysiological experiments if possible.

Chapter 4

CONCLUDING REMARKS

SLs constitute a multifaceted metabolic network, which is involved in the regulation of a vast array of cellular functions. SLs are highly expressed in the nervous system where they are pivotal both for the developing and mature brain. Indeed, perturbation of SL network has been implicated in range of human diseases, including many neurological disorders. As SLs are involved in many aspects of cell physiology, it is challenging to pinpoint the specific causes behind the pathophysiology of each disease as it is most likely to the combination of several factors. Understanding the interchangeable nature of SLs and how they are involved in modulating cellular processes are fundamental for delineating how disturbances in the SL homeostasis lead to the development of diseases. The review, research paper, manuscript, and unpublished data included in my PhD thesis all contribute this delineation.

Several defects along the SL pathways have been associated with the development of epilepsy. The overall aim of the thesis was to investigate how perturbation of the SL metabolism can contribute to the development of epilepsy or associated phenotypes. We have for the first time described a patient diagnosed with PME linked to a heterozygous deletion the gene encoding CERS2. Characterization of patient skin fibroblasts shows that the patient indeed has only one functional *CERS2* allele, which leads to subtle alterations of the SL as well as glycerophospholipid profile. These changes are likely to disturb processes relying on plasma membrane compartmentalization and the dynamics hereof, as indicated by preliminary data suggesting that patient fibroblasts are more insulin sensitive. This hypothesis is strengthened by the observation that heterozygous *CerS2* mice are also more sensitive towards insulin, and the fact that processes relying on membrane microdomains are perturbed in *CerS2*$^{-/-}$ *mice*. Thus, disturbances in the regulation of plasma membrane compartmentalization probably contribute to the pathogenesis of the PME. We have addressed the importance of SL-mediated plasma membrane organization in a more neurological relevant setting through investigation of the role of SL metabolism on properties of the Kv2.1 ion channel. Kv2.1 is, by its dynamic modulation of phosphorylation and localization in clusters in the plasma membrane, involved in regulating the intrinsic excitability of neurons. We demonstrate that SL homeostasis is important for

Kv2.1 cluster size restriction, but not constitutive phosphorylation state, during a “resting” state. Future research is needed to determine if similar SL-mediated restriction of Kv2.1 clustering is present during an “active” state and to which extend SL homeostasis affects the activity-induced dephosphorylation of Kv2.1. Moreover, functional studies are pivotal for determining if disturbances of the SL metabolism affect Kv2.1 kinetics and thereby the regulation of neuronal excitability.

Although membrane compartmentalization via microdomains has been studied for years, we are at the infancy of understanding the variety in SL composition in these compartments and subsequently their functions. The major diversity of SLs is reflected in their expression patterns and chemical properties, which is crucial for determining protein interaction partners and hence functions. The development of advanced imaging techniques and high-resolution secondary ion mass spectrometry (SIMS) has paved the way direct imaging of the SL distribution in the plasma membrane [227, 228]. Interestingly, super-resolution fluorescence techniques have recently shown that cholesterol analogs diffuses unhindered in the membrane of living cells, and that cholesterol, in contrast to SLs, is evenly distributed in the plasma membrane [229, 230]. These observations indicate that SLs indeed are key actors in the organization of the plasma membrane. Furthermore, it is now possible to globally identify SL-protein interactions using chemical proteomics combined with a recently developed bifunctional sphingosine, which can be cross-linked to neighboring proteins [36]. Using this technique in neurological systems will significantly contribute to the understanding of the interplay between SLs and proteins in neurophysiological functions. Thus, with these tools we are at the beginning of a new era of elucidating how SLs modulate cellular processes, which is pivotal for future research unraveling how disturbances in the SL metabolism is involved in the development of human diseases, including neurological disorders.

References

1. van Echten-Deckert, G., and Herget, T. (2006). Sphingolipid metabolism in neural cells. Biochimica et biophysica acta *1758*, 1978-1994.
2. Marin, R., Rojo, J.A., Fabelo, N., Fernandez, C.E., and Diaz, M. (2013). Lipid raft disarrangement as a result of neuropathological progresses: a novel strategy for early diagnosis? Neuroscience *245*, 26-39.
3. Piccinini, M., Scandroglio, F., Prioni, S., Buccinna, B., Loberto, N., Aureli, M., Chigorno, V., Lupino, E., DeMarco, G., Lomartire, A., et al. (2010). Deregulated sphingolipid metabolism and membrane organization in neurodegenerative disorders. Molecular neurobiology *41*, 314-340.
4. Aureli, M., Grassi, S., Prioni, S., Sonnino, S., and Prinetti, A. (2015). Lipid membrane domains in the brain. Biochimica et biophysica acta *1851*, 1006-1016.
5. Ohmi, Y., Ohkawa, Y., Yamauchi, Y., Tajima, O., Furukawa, K., and Furukawa, K. (2012). Essential roles of gangliosides in the formation and maintenance of membrane microdomains in brain tissues. Neurochemical research *37*, 1185-1191.
6. Gault, C.R., Obeid, L.M., and Hannun, Y.A. (2010). An overview of sphingolipid metabolism: from synthesis to breakdown. Advances in experimental medicine and biology *688*, 1-23.
7. Mullen, T.D., Hannun, Y.A., and Obeid, L.M. (2012). Ceramide synthases at the centre of sphingolipid metabolism and biology. The Biochemical journal *441*, 789-802.
8. Hannun, Y.A., and Obeid, L.M. (2011). Many ceramides. The Journal of biological chemistry *286*, 27855-27862.
9. Hanada, K. (2003). Serine palmitoyltransferase, a key enzyme of sphingolipid metabolism. Biochimica et biophysica acta *1632*, 16-30.
10. Duan, J., and Merrill, A.H., Jr. (2015). 1-Deoxysphingolipids Encountered Exogenously and Made de Novo: Dangerous Mysteries inside an Enigma. The Journal of biological chemistry *290*, 15380-15389.
11. Pruett, S.T., Bushnev, A., Hagedorn, K., Adiga, M., Haynes, C.A., Sullards, M.C., Liotta, D.C., and Merrill, A.H., Jr. (2008). Biodiversity of sphingoid bases ("sphingosines") and related amino alcohols. Journal of lipid research *49*, 1621-1639.
12. Lahiri, S., and Futerman, A.H. (2007). The metabolism and function of sphingolipids and glycosphingolipids. Cellular and molecular life sciences : CMLS *64*, 2270-2284.
13. Zheng, W., Kollmeyer, J., Symolon, H., Momin, A., Munter, E., Wang, E., Kelly, S., Allegood, J.C., Liu, Y., Peng, Q., et al. (2006). Ceramides and other bioactive sphingolipid backbones in health and disease: lipidomic analysis, metabolism and roles in membrane structure, dynamics, signaling and autophagy. Biochimica et biophysica acta *1758*, 1864-1884.
14. Hirschberg, K., Rodger, J., and Futerman, A.H. (1993). The long-chain sphingoid base of sphingolipids is acylated at the cytosolic surface of the endoplasmic reticulum in rat liver. The Biochemical journal *290 (Pt 3)*, 751-757.
15. Mandon, E.C., Ehses, I., Rother, J., van Echten, G., and Sandhoff, K. (1992). Subcellular localization and membrane topology of serine palmitoyltransferase, 3-dehydrosphinganine reductase, and sphinganine N-acyltransferase in mouse liver. The Journal of biological chemistry *267*, 11144-11148.
16. Michel, C., and van Echten-Deckert, G. (1997). Conversion of dihydroceramide to ceramide occurs at the cytosolic face of the endoplasmic reticulum. FEBS letters *416*, 153-155.
17. Michel, C., van Echten-Deckert, G., Rother, J., Sandhoff, K., Wang, E., and Merrill, A.H., Jr. (1997). Characterization of ceramide synthesis. A dihydroceramide desaturase introduces the 4,5-trans-

double bond of sphingosine at the level of dihydroceramide. The Journal of biological chemistry *272*, 22432-22437.

18. Kruse, V., Neess, D., and Faergeman, N.J. (2017). The Significance of Epidermal Lipid Metabolism in Whole-Body Physiology. Trends in endocrinology and metabolism: TEM.
19. Sprong, H., Kruithof, B., Leijendekker, R., Slot, J.W., van Meer, G., and van der Sluijs, P. (1998). UDP-galactose:ceramide galactosyltransferase is a class I integral membrane protein of the endoplasmic reticulum. The Journal of biological chemistry *273*, 25880-25888.
20. Vacaru, A.M., Tafesse, F.G., Ternes, P., Kondylis, V., Hermansson, M., Brouwers, J.F., Somerharju, P., Rabouille, C., and Holthuis, J.C. (2009). Sphingomyelin synthase-related protein SMSr controls ceramide homeostasis in the ER. The Journal of cell biology *185*, 1013-1027.
21. Hanada, K., Kumagai, K., Tomishige, N., and Yamaji, T. (2009). CERT-mediated trafficking of ceramide. Biochimica et biophysica acta *1791*, 684-691.
22. Pagano, R.E. (1988). What is the fate of diacylglycerol produced at the Golgi apparatus? Trends in biochemical sciences *13*, 202-205.
23. Yamaoka, S., Miyaji, M., Kitano, T., Umehara, H., and Okazaki, T. (2004). Expression cloning of a human cDNA restoring sphingomyelin synthesis and cell growth in sphingomyelin synthase-defective lymphoid cells. The Journal of biological chemistry *279*, 18688-18693.
24. Jeckel, D., Karrenbauer, A., Burger, K.N., van Meer, G., and Wieland, F. (1992). Glucosylceramide is synthesized at the cytosolic surface of various Golgi subfractions. The Journal of cell biology *117*, 259-267.
25. D'Angelo, G., Uemura, T., Chuang, C.C., Polishchuk, E., Santoro, M., Ohvo-Rekila, H., Sato, T., Di Tullio, G., Varriale, A., D'Auria, S., et al. (2013). Vesicular and non-vesicular transport feed distinct glycosylation pathways in the Golgi. Nature *501*, 116-120.
26. Yaghootfam, A., Sorkalla, T., Haberlein, H., Gieselmann, V., Kappler, J., and Eckhardt, M. (2007). Cerebroside sulfotransferase forms homodimers in living cells. Biochemistry *46*, 9260-9269.
27. Boath, A., Graf, C., Lidome, E., Ullrich, T., Nussbaumer, P., and Bornancin, F. (2008). Regulation and traffic of ceramide 1-phosphate produced by ceramide kinase: comparative analysis to glucosylceramide and sphingomyelin. The Journal of biological chemistry *283*, 8517-8526.
28. Lamour, N.F., Stahelin, R.V., Wijesinghe, D.S., Maceyka, M., Wang, E., Allegood, J.C., Merrill, A.H., Jr., Cho, W., and Chalfant, C.E. (2007). Ceramide kinase uses ceramide provided by ceramide transport protein: localization to organelles of eicosanoid synthesis. Journal of lipid research *48*, 1293-1304.
29. Arana, L., Gangoiti, P., Ouro, A., Trueba, M., and Gomez-Munoz, A. (2010). Ceramide and ceramide 1-phosphate in health and disease. Lipids in health and disease *9*, 15.
30. Bienias, K., Fiedorowicz, A., Sadowska, A., Prokopiuk, S., and Car, H. (2016). Regulation of sphingomyelin metabolism. Pharmacological reports : PR *68*, 570-581.
31. Jenkins, R.W., Canals, D., and Hannun, Y.A. (2009). Roles and regulation of secretory and lysosomal acid sphingomyelinase. Cellular signalling *21*, 836-846.
32. Rother, J., van Echten, G., Schwarzmann, G., and Sandhoff, K. (1992). Biosynthesis of sphingolipids: dihydroceramide and not sphinganine is desaturated by cultured cells. Biochemical and biophysical research communications *189*, 14-20.
33. Wattenberg, B.W., Pitson, S.M., and Raben, D.M. (2006). The sphingosine and diacylglycerol kinase superfamily of signaling kinases: localization as a key to signaling function. Journal of lipid research *47*, 1128-1139.
34. Valaperta, R., Chigorno, V., Basso, L., Prinetti, A., Bresciani, R., Preti, A., Miyagi, T., and Sonnino, S. (2006). Plasma membrane production of ceramide from ganglioside GM3 in human fibroblasts. FASEB journal : official publication of the Federation of American Societies for Experimental Biology *20*, 1227-1229.

35. Kihara, A., Mitsutake, S., Mizutani, Y., and Igarashi, Y. (2007). Metabolism and biological functions of two phosphorylated sphingolipids, sphingosine 1-phosphate and ceramide 1-phosphate. Progress in lipid research *46*, 126-144.
36. Haberkant, P., Stein, F., Hoglinger, D., Gerl, M.J., Brugger, B., Van Veldhoven, P.P., Krijgsveld, J., Gavin, A.C., and Schultz, C. (2016). Bifunctional Sphingosine for Cell-Based Analysis of Protein-Sphingolipid Interactions. ACS chemical biology *11*, 222-230.
37. D'Mello N, P., Childress, A.M., Franklin, D.S., Kale, S.P., Pinswasdi, C., and Jazwinski, S.M. (1994). Cloning and characterization of LAG1, a longevity-assurance gene in yeast. The Journal of biological chemistry *269*, 15451-15459.
38. Schorling, S., Vallee, B., Barz, W.P., Riezman, H., and Oesterhelt, D. (2001). Lag1p and Lac1p are essential for the Acyl-CoA-dependent ceramide synthase reaction in Saccharomyces cerevisae. Molecular biology of the cell *12*, 3417-3427.
39. Guillas, I., Kirchman, P.A., Chuard, R., Pfefferli, M., Jiang, J.C., Jazwinski, S.M., and Conzelmann, A. (2001). C26-CoA-dependent ceramide synthesis of Saccharomyces cerevisiae is operated by Lag1p and Lac1p. The EMBO journal *20*, 2655-2665.
40. Jiang, J.C., Kirchman, P.A., Zagulski, M., Hunt, J., and Jazwinski, S.M. (1998). Homologs of the yeast longevity gene LAG1 in Caenorhabditis elegans and human. Genome research *8*, 1259-1272.
41. Venkataraman, K., Riebeling, C., Bodennec, J., Riezman, H., Allegood, J.C., Sullards, M.C., Merrill, A.H., Jr., and Futerman, A.H. (2002). Upstream of growth and differentiation factor 1 (uog1), a mammalian homolog of the yeast longevity assurance gene 1 (LAG1), regulates N-stearoyl-sphinganine (C18-(dihydro)ceramide) synthesis in a fumonisin B1-independent manner in mammalian cells. The Journal of biological chemistry *277*, 35642-35649.
42. Pewzner-Jung, Y., Ben-Dor, S., and Futerman, A.H. (2006). When do Lasses (longevity assurance genes) become CerS (ceramide synthases)?: Insights into the regulation of ceramide synthesis. The Journal of biological chemistry *281*, 25001-25005.
43. Spassieva, S., Seo, J.G., Jiang, J.C., Bielawski, J., Alvarez-Vasquez, F., Jazwinski, S.M., Hannun, Y.A., and Obeid, L.M. (2006). Necessary role for the Lag1p motif in (dihydro)ceramide synthase activity. The Journal of biological chemistry *281*, 33931-33938.
44. Levy, M., and Futerman, A.H. (2010). Mammalian ceramide synthases. IUBMB life *62*, 347-356.
45. Park, W.J., and Park, J.W. (2015). The effect of altered sphingolipid acyl chain length on various disease models. Biological chemistry *396*, 693-705.
46. Laviad, E.L., Albee, L., Pankova-Kholmyansky, I., Epstein, S., Park, H., Merrill, A.H., Jr., and Futerman, A.H. (2008). Characterization of ceramide synthase 2: tissue distribution, substrate specificity, and inhibition by sphingosine 1-phosphate. The Journal of biological chemistry *283*, 5677-5684.
47. Mizutani, Y., Kihara, A., and Igarashi, Y. (2006). LASS3 (longevity assurance homologue 3) is a mainly testis-specific (dihydro)ceramide synthase with relatively broad substrate specificity. The Biochemical journal *398*, 531-538.
48. Eckl, K.M., Tidhar, R., Thiele, H., Oji, V., Hausser, I., Brodesser, S., Preil, M.L., Onal-Akan, A., Stock, F., Muller, D., et al. (2013). Impaired epidermal ceramide synthesis causes autosomal recessive congenital ichthyosis and reveals the importance of ceramide acyl chain length. The Journal of investigative dermatology *133*, 2202-2211.
49. Riebeling, C., Allegood, J.C., Wang, E., Merrill, A.H., Jr., and Futerman, A.H. (2003). Two mammalian longevity assurance gene (LAG1) family members, trh1 and trh4, regulate dihydroceramide synthesis using different fatty acyl-CoA donors. The Journal of biological chemistry *278*, 43452-43459.
50. Lahiri, S., and Futerman, A.H. (2005). LASS5 is a bona fide dihydroceramide synthase that selectively utilizes palmitoyl-CoA as acyl donor. The Journal of biological chemistry *280*, 33735-33738.
51. Mizutani, Y., Kihara, A., and Igarashi, Y. (2005). Mammalian Lass6 and its related family members regulate synthesis of specific ceramides. The Biochemical journal *390*, 263-271.

52. Tidhar, R., Ben-Dor, S., Wang, E., Kelly, S., Merrill, A.H., Jr., and Futerman, A.H. (2012). Acyl chain specificity of ceramide synthases is determined within a region of 150 residues in the Tram-Lag-CLN8 (TLC) domain. The Journal of biological chemistry *287*, 3197-3206.
53. Becker, I., Wang-Eckhardt, L., Yaghootfam, A., Gieselmann, V., and Eckhardt, M. (2008). Differential expression of (dihydro)ceramide synthases in mouse brain: oligodendrocyte-specific expression of CerS2/Lass2. Histochemistry and cell biology *129*, 233-241.
54. Wegner, M.S., Schiffmann, S., Parnham, M.J., Geisslinger, G., and Grosch, S. (2016). The enigma of ceramide synthase regulation in mammalian cells. Progress in lipid research *63*, 93-119.
55. Gencer, E.B., Ural, A.U., Avcu, F., and Baran, Y. (2011). A novel mechanism of dasatinib-induced apoptosis in chronic myeloid leukemia; ceramide synthase and ceramide clearance genes. Annals of hematology *90*, 1265-1275.
56. Separovic, D., Breen, P., Boppana, N.B., Van Buren, E., Joseph, N., Kraveka, J.M., Rahmaniyan, M., Li, L., Gudz, T.I., Bielawska, A., et al. (2013). Increased killing of SCCVII squamous cell carcinoma cells after the combination of Pc 4 photodynamic therapy and dasatinib is associated with enhanced caspase-3 activity and ceramide synthase 1 upregulation. International journal of oncology *43*, 2064-2072.
57. Pewzner-Jung, Y., Park, H., Laviad, E.L., Silva, L.C., Lahiri, S., Stiban, J., Erez-Roman, R., Brugger, B., Sachsenheimer, T., Wieland, F., et al. (2010). A critical role for ceramide synthase 2 in liver homeostasis: I. alterations in lipid metabolic pathways. The Journal of biological chemistry *285*, 10902-10910.
58. Mullen, T.D., Spassieva, S., Jenkins, R.W., Kitatani, K., Bielawski, J., Hannun, Y.A., and Obeid, L.M. (2011). Selective knockdown of ceramide synthases reveals complex interregulation of sphingolipid metabolism. Journal of lipid research *52*, 68-77.
59. Villen, J., Beausoleil, S.A., Gerber, S.A., and Gygi, S.P. (2007). Large-scale phosphorylation analysis of mouse liver. Proceedings of the National Academy of Sciences of the United States of America *104*, 1488-1493.
60. Sassa, T., Hirayama, T., and Kihara, A. (2016). Enzyme Activities of the Ceramide Synthases CERS2-6 Are Regulated by Phosphorylation in the C-terminal Region. The Journal of biological chemistry *291*, 7477-7487.
61. Sridevi, P., Alexander, H., Laviad, E.L., Pewzner-Jung, Y., Hannink, M., Futerman, A.H., and Alexander, S. (2009). Ceramide synthase 1 is regulated by proteasomal mediated turnover. Biochimica et biophysica acta *1793*, 1218-1227.
62. Sridevi, P., Alexander, H., Laviad, E.L., Min, J., Mesika, A., Hannink, M., Futerman, A.H., and Alexander, S. (2010). Stress-induced ER to Golgi translocation of ceramide synthase 1 is dependent on proteasomal processing. Experimental cell research *316*, 78-91.
63. Ohno, Y., Suto, S., Yamanaka, M., Mizutani, Y., Mitsutake, S., Igarashi, Y., Sassa, T., and Kihara, A. (2010). ELOVL1 production of C24 acyl-CoAs is linked to C24 sphingolipid synthesis. Proceedings of the National Academy of Sciences of the United States of America *107*, 18439-18444.
64. Ferreira, N.S., Engelsby, H., Neess, D., Kelly, S.L., Volpert, G., Merrill, A.H., Futerman, A.H., and Faergeman, N.J. (2017). Regulation of very-long acyl chain ceramide synthesis by acyl-CoA-binding protein. The Journal of biological chemistry *292*, 7588-7597.
65. Laviad, E.L., Kelly, S., Merrill, A.H., Jr., and Futerman, A.H. (2012). Modulation of ceramide synthase activity via dimerization. The Journal of biological chemistry *287*, 21025-21033.
66. Posse de Chaves, E., and Sipione, S. (2010). Sphingolipids and gangliosides of the nervous system in membrane function and dysfunction. FEBS letters *584*, 1748-1759.
67. Palmano, K., Rowan, A., Guillermo, R., Guan, J., and McJarrow, P. (2015). The role of gangliosides in neurodevelopment. Nutrients *7*, 3891-3913.
68. Olsen, A.S.B., and Faergeman, N.J. (2017). Sphingolipids: membrane microdomains in brain development, function and neurological diseases. Open biology *7*.

69. College, O. Neurons and Glial Cells, Biology (CC BY 3.0). (https://cnx.org/contents/GFy_h8cu@9.87:c9j4p0aj@3/Neurons-and-Glial-Cells - fig-ch35_01_03: OpenStax).
70. Xu, Y.H., Barnes, S., Sun, Y., and Grabowski, G.A. (2010). Multi-system disorders of glycosphingolipid and ganglioside metabolism. Journal of lipid research *51*, 1643-1675.
71. Bejaoui, K., Wu, C., Scheffler, M.D., Haan, G., Ashby, P., Wu, L., de Jong, P., and Brown, R.H., Jr. (2001). SPTLC1 is mutated in hereditary sensory neuropathy, type 1. Nature genetics *27*, 261-262.
72. Dawkins, J.L., Hulme, D.J., Brahmbhatt, S.B., Auer-Grumbach, M., and Nicholson, G.A. (2001). Mutations in SPTLC1, encoding serine palmitoyltransferase, long chain base subunit-1, cause hereditary sensory neuropathy type I. Nature genetics *27*, 309-312.
73. Rotthier, A., Baets, J., De Vriendt, E., Jacobs, A., Auer-Grumbach, M., Levy, N., Bonello-Palot, N., Kilic, S.S., Weis, J., Nascimento, A., et al. (2009). Genes for hereditary sensory and autonomic neuropathies: a genotype-phenotype correlation. Brain : a journal of neurology *132*, 2699-2711.
74. Rotthier, A., Auer-Grumbach, M., Janssens, K., Baets, J., Penno, A., Almeida-Souza, L., Van Hoof, K., Jacobs, A., De Vriendt, E., Schlotter-Weigel, B., et al. (2010). Mutations in the SPTLC2 subunit of serine palmitoyltransferase cause hereditary sensory and autonomic neuropathy type I. American journal of human genetics *87*, 513-522.
75. Rotthier, A., Penno, A., Rautenstrauss, B., Auer-Grumbach, M., Stettner, G.M., Asselbergh, B., Van Hoof, K., Sticht, H., Levy, N., Timmerman, V., et al. (2011). Characterization of two mutations in the SPTLC1 subunit of serine palmitoyltransferase associated with hereditary sensory and autonomic neuropathy type I. Human mutation *32*, E2211-2225.
76. Auer-Grumbach, M., Bode, H., Pieber, T.R., Schabhuttl, M., Fischer, D., Seidl, R., Graf, E., Wieland, T., Schuh, R., Vacariu, G., et al. (2013). Mutations at Ser331 in the HSN type I gene SPTLC1 are associated with a distinct syndromic phenotype. European journal of medical genetics *56*, 266-269.
77. Penno, A., Reilly, M.M., Houlden, H., Laura, M., Rentsch, K., Niederkofler, V., Stoeckli, E.T., Nicholson, G., Eichler, F., Brown, R.H., Jr., et al. (2010). Hereditary sensory neuropathy type 1 is caused by the accumulation of two neurotoxic sphingolipids. The Journal of biological chemistry *285*, 11178-11187.
78. Bode, H., Bourquin, F., Suriyanarayanan, S., Wei, Y., Alecu, I., Othman, A., Von Eckardstein, A., and Hornemann, T. (2016). HSAN1 mutations in serine palmitoyltransferase reveal a close structure-function-phenotype relationship. Human molecular genetics *25*, 853-865.
79. Ginkel, C., Hartmann, D., vom Dorp, K., Zlomuzica, A., Farwanah, H., Eckhardt, M., Sandhoff, R., Degen, J., Rabionet, M., Dere, E., et al. (2012). Ablation of neuronal ceramide synthase 1 in mice decreases ganglioside levels and expression of myelin-associated glycoprotein in oligodendrocytes. The Journal of biological chemistry *287*, 41888-41902.
80. Vanni, N., Fruscione, F., Ferlazzo, E., Striano, P., Robbiano, A., Traverso, M., Sander, T., Falace, A., Gazzerro, E., Bramanti, P., et al. (2014). Impairment of ceramide synthesis causes a novel progressive myoclonus epilepsy. Annals of neurology *76*, 206-212.
81. Ferlazzo, E., Striano, P., Italiano, D., Calarese, T., Gasparini, S., Vanni, N., Fruscione, F., Genton, P., and Zara, F. (2016). Autosomal recessive progressive myoclonus epilepsy due to impaired ceramide synthesis. Epileptic disorders : international epilepsy journal with videotape *18*, 120-127.
82. Mosbech, M.B., Olsen, A.S., Neess, D., Ben-David, O., Klitten, L.L., Larsen, J., Sabers, A., Vissing, J., Nielsen, J.E., Hasholt, L., et al. (2014). Reduced ceramide synthase 2 activity causes progressive myoclonic epilepsy. Annals of clinical and translational neurology *1*, 88-98.
83. Simpson, M.A., Cross, H., Proukakis, C., Priestman, D.A., Neville, D.C., Reinkensmeier, G., Wang, H., Wiznitzer, M., Gurtz, K., Verganelaki, A., et al. (2004). Infantile-onset symptomatic epilepsy syndrome caused by a homozygous loss-of-function mutation of GM3 synthase. Nature genetics *36*, 1225-1229.
84. Fragaki, K., Ait-El-Mkadem, S., Chaussenot, A., Gire, C., Mengual, R., Bonesso, L., Beneteau, M., Ricci, J.E., Desquiret-Dumas, V., Procaccio, V., et al. (2013). Refractory epilepsy and mitochondrial

dysfunction due to GM3 synthase deficiency. European journal of human genetics : EJHG *21*, 528-534.

85. Harlalka, G.V., Lehman, A., Chioza, B., Baple, E.L., Maroofian, R., Cross, H., Sreekantan-Nair, A., Priestman, D.A., Al-Turki, S., McEntagart, M.E., et al. (2013). Mutations in B4GALNT1 (GM2 synthase) underlie a new disorder of ganglioside biosynthesis. Brain : a journal of neurology *136*, 3618-3624.
86. Fishman, P.H., Max, S.R., Tallman, J.F., Brady, R.O., Maclaren, N.K., and Cornblath, M. (1975). Deficient Ganglioside Biosynthesis: a novel human sphingolipidosis. Science (New York, N.Y.) *187*, 68-70.
87. Spassieva, S.D., Ji, X., Liu, Y., Gable, K., Bielawski, J., Dunn, T.M., Bieberich, E., and Zhao, L. (2016). Ectopic expression of ceramide synthase 2 in neurons suppresses neurodegeneration induced by ceramide synthase 1 deficiency. Proceedings of the National Academy of Sciences of the United States of America *113*, 5928-5933.
88. Cuadros, R., Montejo de Garcini, E., Wandosell, F., Faircloth, G., Fernandez-Sousa, J.M., and Avila, J. (2000). The marine compound spisulosine, an inhibitor of cell proliferation, promotes the disassembly of actin stress fibers. Cancer letters *152*, 23-29.
89. Takamiya, K., Yamamoto, A., Furukawa, K., Yamashiro, S., Shin, M., Okada, M., Fukumoto, S., Haraguchi, M., Takeda, N., Fujimura, K., et al. (1996). Mice with disrupted GM2/GD2 synthase gene lack complex gangliosides but exhibit only subtle defects in their nervous system. Proceedings of the National Academy of Sciences of the United States of America *93*, 10662-10667.
90. Sheikh, K.A., Sun, J., Liu, Y., Kawai, H., Crawford, T.O., Proia, R.L., Griffin, J.W., and Schnaar, R.L. (1999). Mice lacking complex gangliosides develop Wallerian degeneration and myelination defects. Proceedings of the National Academy of Sciences of the United States of America *96*, 7532-7537.
91. Susuki, K., Baba, H., Tohyama, K., Kanai, K., Kuwabara, S., Hirata, K., Furukawa, K., Furukawa, K., Rasband, M.N., and Yuki, N. (2007). Gangliosides contribute to stability of paranodal junctions and ion channel clusters in myelinated nerve fibers. Glia *55*, 746-757.
92. Vyas, A.A., Patel, H.V., Fromholt, S.E., Heffer-Lauc, M., Vyas, K.A., Dang, J., Schachner, M., and Schnaar, R.L. (2002). Gangliosides are functional nerve cell ligands for myelin-associated glycoprotein (MAG), an inhibitor of nerve regeneration. Proceedings of the National Academy of Sciences of the United States of America *99*, 8412-8417.
93. Schnaar, R.L., and Lopez, P.H. (2009). Myelin-associated glycoprotein and its axonal receptors. Journal of neuroscience research *87*, 3267-3276.
94. McGovern, M.M., Avetisyan, R., Sanson, B.J., and Lidove, O. (2017). Disease manifestations and burden of illness in patients with acid sphingomyelinase deficiency (ASMD). Orphanet journal of rare diseases *12*, 41.
95. Schuchman, E.H. (2016). Acid ceramidase and the treatment of ceramide diseases: The expanding role of enzyme replacement therapy. Biochimica et biophysica acta *1862*, 1459-1471.
96. Zhou, J., Tawk, M., Tiziano, F.D., Veillet, J., Bayes, M., Nolent, F., Garcia, V., Servidei, S., Bertini, E., Castro-Giner, F., et al. (2012). Spinal muscular atrophy associated with progressive myoclonic epilepsy is caused by mutations in ASAH1. American journal of human genetics *91*, 5-14.
97. Rubboli, G., Veggiotti, P., Pini, A., Berardinelli, A., Cantalupo, G., Bertini, E., Tiziano, F.D., D'Amico, A., Piazza, E., Abiusi, E., et al. (2015). Spinal muscular atrophy associated with progressive myoclonic epilepsy: A rare condition caused by mutations in ASAH1. Epilepsia *56*, 692-698.
98. Gan, J.J., Garcia, V., Tian, J., Tagliati, M., Parisi, J.E., Chung, J.M., Lewis, R., Baloh, R., Levade, T., and Pierson, T.M. (2015). Acid ceramidase deficiency associated with spinal muscular atrophy with progressive myoclonic epilepsy. Neuromuscular disorders : NMD *25*, 959-963.
99. Dyment, D.A., Sell, E., Vanstone, M.R., Smith, A.C., Garandeau, D., Garcia, V., Carpentier, S., Le Trionnaire, E., Sabourdy, F., Beaulieu, C.L., et al. (2014). Evidence for clinical, genetic and

biochemical variability in spinal muscular atrophy with progressive myoclonic epilepsy. Clinical genetics *86*, 558-563.

100. Koch, J., Gartner, S., Li, C.M., Quintern, L.E., Bernardo, K., Levran, O., Schnabel, D., Desnick, R.J., Schuchman, E.H., and Sandhoff, K. (1996). Molecular cloning and characterization of a full-length complementary DNA encoding human acid ceramidase. Identification Of the first molecular lesion causing Farber disease. The Journal of biological chemistry *271*, 33110-33115.
101. Li, C.M., Park, J.H., He, X., Levy, B., Chen, F., Arai, K., Adler, D.A., Disteche, C.M., Koch, J., Sandhoff, K., et al. (1999). The human acid ceramidase gene (ASAH): structure, chromosomal location, mutation analysis, and expression. Genomics *62*, 223-231.
102. Levade, T., Moser, H.W., Fensom, A.H., Harzer, K., Moser, A.B., and Salvayre, R. (1995). Neurodegenerative course in ceramidase deficiency (Farber disease) correlates with the residual lysosomal ceramide turnover in cultured living patient cells. Journal of the neurological sciences *134*, 108-114.
103. Sugita, M., Dulaney, J.T., and Moser, H.W. (1972). Ceramidase deficiency in Farber's disease (lipogranulomatosis). Science (New York, N.Y.) *178*, 1100-1102.
104. Bar, J., Linke, T., Ferlinz, K., Neumann, U., Schuchman, E.H., and Sandhoff, K. (2001). Molecular analysis of acid ceramidase deficiency in patients with Farber disease. Human mutation *17*, 199-209.
105. Zhang, Z., Mandal, A.K., Mital, A., Popescu, N., Zimonjic, D., Moser, A., Moser, H., and Mukherjee, A.B. (2000). Human acid ceramidase gene: novel mutations in Farber disease. Molecular genetics and metabolism *70*, 301-309.
106. Wolfe, H.J., and Pietra, G.G. (1964). THE VISCERAL LESIONS OF METACHROMATIC LEUKODYSTROPHY. The American journal of pathology *44*, 921-930.
107. Phelan, M.C., Thomas, G.R., Saul, R.A., Rogers, R.C., Taylor, H.A., Wenger, D.A., and McDermid, H.E. (1992). Cytogenetic, biochemical, and molecular analyses of a 22q13 deletion. American journal of medical genetics *43*, 872-876.
108. Gieselmann, V., Polten, A., Kreysing, J., and von Figura, K. (1989). Arylsulfatase A pseudodeficiency: loss of a polyadenylylation signal and N-glycosylation site. Proceedings of the National Academy of Sciences of the United States of America *86*, 9436-9440.
109. Wang, Z., Lin, Y., Zheng, D., Yan, A., Tu, X., Lin, J., and Lan, F. (2016). Whole-exome sequencing identifies compound heterozygous mutations in ARSA of two siblings presented with atypical onset of metachromatic leukodystrophy from a Chinese pedigree. Clinica chimica acta; international journal of clinical chemistry *460*, 135-137.
110. Xu, C., Sakai, N., Taniike, M., Inui, K., and Ozono, K. (2006). Six novel mutations detected in the GALC gene in 17 Japanese patients with Krabbe disease, and new genotype-phenotype correlation. Journal of human genetics *51*, 548-554.
111. Lissens, W., Arena, A., Seneca, S., Rafi, M., Sorge, G., Liebaers, I., Wenger, D., and Fiumara, A. (2007). A single mutation in the GALC gene is responsible for the majority of late onset Krabbe disease patients in the Catania (Sicily, Italy) region. Human mutation *28*, 742.
112. Dai, L., Han, T., Yang, X., Wang, X., Li, J., Lu, J., Zhang, W., Ren, X., and Fang, F. (2017). Clinical and molecular analysis of six novel GALC mutations identified in 7 Chinese children with Krabbe disease. Brain & development.
113. Wenger, D.A., Rafi, M.A., and Luzi, P. (2016). Krabbe disease: One Hundred years from the bedside to the bench to the bedside. Journal of neuroscience research *94*, 982-989.
114. Stirnemann, J., Belmatoug, N., Camou, F., Serratrice, C., Froissart, R., Caillaud, C., Levade, T., Astudillo, L., Serratrice, J., Brassier, A., et al. (2017). A Review of Gaucher Disease Pathophysiology, Clinical Presentation and Treatments. International journal of molecular sciences *18*.
115. Hruska, K.S., LaMarca, M.E., Scott, C.R., and Sidransky, E. (2008). Gaucher disease: mutation and polymorphism spectrum in the glucocerebrosidase gene (GBA). Human mutation *29*, 567-583.

116. Brunetti-Pierri, N., and Scaglia, F. (2008). GM1 gangliosidosis: review of clinical, molecular, and therapeutic aspects. Molecular genetics and metabolism *94*, 391-396.
117. Sandhoff, K., and Harzer, K. (2013). Gangliosides and gangliosidoses: principles of molecular and metabolic pathogenesis. The Journal of neuroscience : the official journal of the Society for Neuroscience *33*, 10195-10208.
118. Bley, A.E., Giannikopoulos, O.A., Hayden, D., Kubilus, K., Tifft, C.J., and Eichler, F.S. (2011). Natural history of infantile G(M2) gangliosidosis. Pediatrics *128*, e1233-1241.
119. Hendriksz, C.J., Corry, P.C., Wraith, J.E., Besley, G.T., Cooper, A., and Ferrie, C.D. (2004). Juvenile Sandhoff disease--nine new cases and a review of the literature. Journal of inherited metabolic disease *27*, 241-249.
120. Levran, O., Desnick, R.J., and Schuchman, E.H. (1991). Niemann-Pick disease: a frequent missense mutation in the acid sphingomyelinase gene of Ashkenazi Jewish type A and B patients. Proceedings of the National Academy of Sciences of the United States of America *88*, 3748-3752.
121. Levran, O., Desnick, R.J., and Schuchman, E.H. (1992). Identification and expression of a common missense mutation (L302P) in the acid sphingomyelinase gene of Ashkenazi Jewish type A Niemann-Pick disease patients. Blood *80*, 2081-2087.
122. Schuchman, E.H. (2009). The pathogenesis and treatment of acid sphingomyelinase-deficient Niemann-Pick disease. International journal of clinical pharmacology and therapeutics *47 Suppl 1*, S48-57.
123. Ricci, V., Stroppiano, M., Corsolini, F., Di Rocco, M., Parenti, G., Regis, S., Grossi, S., Biancheri, R., Mazzotti, R., and Filocamo, M. (2004). Screening of 25 Italian patients with Niemann-Pick A reveals fourteen new mutations, one common and thirteen private, in SMPD1. Human mutation *24*, 105.
124. Cesani, M., Lorioli, L., Grossi, S., Amico, G., Fumagalli, F., Spiga, I., Filocamo, M., and Biffi, A. (2016). Mutation Update of ARSA and PSAP Genes Causing Metachromatic Leukodystrophy. Human mutation *37*, 16-27.
125. Platt, F.M. (2014). Sphingolipid lysosomal storage disorders. Nature *510*, 68-75.
126. Garofalo, K., Penno, A., Schmidt, B.P., Lee, H.J., Frosch, M.P., von Eckardstein, A., Brown, R.H., Hornemann, T., and Eichler, F.S. (2011). Oral L-serine supplementation reduces production of neurotoxic deoxysphingolipids in mice and humans with hereditary sensory autonomic neuropathy type 1. The Journal of clinical investigation *121*, 4735-4745.
127. Eichler, F. L-Serine Supplementation in Hereditary Sensory Neuropathy Type 1, ClinicalTrials.gov Identifier: NCT01733407. Last updated: June 27, 2016. Avaliable from: https://clinicaltrials.gov/ct2/show/NCT01733407. (Massachusetts General Hospital).
128. Chien, Y.H., Peng, S.F., Yang, C.C., Lee, N.C., Tsai, L.K., Huang, A.C., Su, S.C., Tseng, C.C., and Hwu, W.L. (2013). Long-term efficacy of miglustat in paediatric patients with Niemann-Pick disease type C. Journal of inherited metabolic disease *36*, 129-137.
129. Dodge, J.E., Kang, Y.K., Beppu, H., Lei, H., and Li, E. (2004). Histone H3-K9 methyltransferase ESET is essential for early development. Molecular and cellular biology *24*, 2478-2486.
130. Tan, S.L., Nishi, M., Ohtsuka, T., Matsui, T., Takemoto, K., Kamio-Miura, A., Aburatani, H., Shinkai, Y., and Kageyama, R. (2012). Essential roles of the histone methyltransferase ESET in the epigenetic control of neural progenitor cells during development. Development (Cambridge, England) *139*, 3806-3816.
131. Jiang, Y., Jakovcevski, M., Bharadwaj, R., Connor, C., Schroeder, F.A., Lin, C.L., Straubhaar, J., Martin, G., and Akbarian, S. (2010). Setdb1 histone methyltransferase regulates mood-related behaviors and expression of the NMDA receptor subunit NR2B. The Journal of neuroscience : the official journal of the Society for Neuroscience *30*, 7152-7167.
132. Cukier, H.N., Lee, J.M., Ma, D., Young, J.I., Mayo, V., Butler, B.L., Ramsook, S.S., Rantus, J.A., Abrams, A.J., Whitehead, P.L., et al. (2012). The expanding role of MBD genes in autism: identification of a MECP2 duplication and novel alterations in MBD5, MBD6, and SETDB1. Autism research : official journal of the International Society for Autism Research *5*, 385-397.

133. Kremser, C., Klemm, A.L., van Uelft, M., Imgrund, S., Ginkel, C., Hartmann, D., and Willecke, K. (2013). Cell-type-specific expression pattern of ceramide synthase 2 protein in mouse tissues. Histochemistry and cell biology *140*, 533-547.
134. Imgrund, S., Hartmann, D., Farwanah, H., Eckhardt, M., Sandhoff, R., Degen, J., Gieselmann, V., Sandhoff, K., and Willecke, K. (2009). Adult ceramide synthase 2 (CERS2)-deficient mice exhibit myelin sheath defects, cerebellar degeneration, and hepatocarcinomas. The Journal of biological chemistry *284*, 33549-33560.
135. Ben-David, O., Pewzner-Jung, Y., Brenner, O., Laviad, E.L., Kogot-Levin, A., Weissberg, I., Biton, I.E., Pienik, R., Wang, E., Kelly, S., et al. (2011). Encephalopathy caused by ablation of very long acyl chain ceramide synthesis may be largely due to reduced galactosylceramide levels. The Journal of biological chemistry *286*, 30022-30033.
136. Baumann, N., and Pham-Dinh, D. (2001). Biology of oligodendrocyte and myelin in the mammalian central nervous system. Physiological reviews *81*, 871-927.
137. Zama, K., Hayashi, Y., Ito, S., Hirabayashi, Y., Inoue, T., Ohno, K., Okino, N., and Ito, M. (2009). Simultaneous quantification of glucosylceramide and galactosylceramide by normal-phase HPLC using O-phtalaldehyde derivatives prepared with sphingolipid ceramide N-deacylase. Glycobiology *19*, 767-775.
138. Shiffman, D., Pare, G., Oberbauer, R., Louie, J.Z., Rowland, C.M., Devlin, J.J., Mann, J.F., and McQueen, M.J. (2014). A gene variant in CERS2 is associated with rate of increase in albuminuria in patients with diabetes from ONTARGET and TRANSCEND. PloS one *9*, e106631.
139. Pewzner-Jung, Y., Brenner, O., Braun, S., Laviad, E.L., Ben-Dor, S., Feldmesser, E., Horn-Saban, S., Amann-Zalcenstein, D., Raanan, C., Berkutzki, T., et al. (2010). A critical role for ceramide synthase 2 in liver homeostasis: II. insights into molecular changes leading to hepatopathy. The Journal of biological chemistry *285*, 10911-10923.
140. Zupanc, M.L., and Legros, B. (2004). Progressive myoclonic epilepsy. Cerebellum (London, England) *3*, 156-171.
141. Zhao, L., Spassieva, S.D., Jucius, T.J., Shultz, L.D., Shick, H.E., Macklin, W.B., Hannun, Y.A., Obeid, L.M., and Ackerman, S.L. (2011). A deficiency of ceramide biosynthesis causes cerebellar purkinje cell neurodegeneration and lipofuscin accumulation. PLoS genetics *7*, e1002063.
142. Liu, Y., Su, Y., Wiznitzer, M., Epifano, O., and Ladisch, S. (2008). Ganglioside depletion and EGF responses of human GM3 synthase-deficient fibroblasts. Glycobiology *18*, 593-601.
143. Yoshikawa, M., Go, S., Takasaki, K., Kakazu, Y., Ohashi, M., Nagafuku, M., Kabayama, K., Sekimoto, J., Suzuki, S., Takaiwa, K., et al. (2009). Mice lacking ganglioside GM3 synthase exhibit complete hearing loss due to selective degeneration of the organ of Corti. Proceedings of the National Academy of Sciences of the United States of America *106*, 9483-9488.
144. Giraldez, B.G., Guerrero-Lopez, R., Ortega-Moreno, L., Verdu, A., Carrascosa-Romero, M.C., Garcia-Campos, O., Garcia-Munozguren, S., Pardal-Fernandez, J.M., and Serratosa, J.M. (2015). Uniparental disomy as a cause of spinal muscular atrophy and progressive myoclonic epilepsy: phenotypic homogeneity due to the homozygous c.125C>T mutation in ASAH1. Neuromuscular disorders : NMD *25*, 222-224.
145. Sikora, J., Dworski, S., Jones, E.E., Kamani, M.A., Micsenyi, M.C., Sawada, T., Le Faouder, P., Bertrand-Michel, J., Dupuy, A., Dunn, C.K., et al. (2017). Acid Ceramidase Deficiency in Mice Results in a Broad Range of Central Nervous System Abnormalities. The American journal of pathology *187*, 864-883.
146. Stewart, R.J., and Boggs, J.M. (1993). A carbohydrate-carbohydrate interaction between galactosylceramide-containing liposomes and cerebroside sulfate-containing liposomes: dependence on the glycolipid ceramide composition. Biochemistry *32*, 10666-10674.
147. Boggs, J.M., Gao, W., Zhao, J., Park, H.J., Liu, Y., and Basu, A. (2010). Participation of galactosylceramide and sulfatide in glycosynapses between oligodendrocyte or myelin membranes. FEBS letters *584*, 1771-1778.

148. DeBruin, L.S., Haines, J.D., Wellhauser, L.A., Radeva, G., Schonmann, V., Bienzle, D., and Harauz, G. (2005). Developmental partitioning of myelin basic protein into membrane microdomains. Journal of neuroscience research *80*, 211-225.
149. Pan, B., Fromholt, S.E., Hess, E.J., Crawford, T.O., Griffin, J.W., Sheikh, K.A., and Schnaar, R.L. (2005). Myelin-associated glycoprotein and complementary axonal ligands, gangliosides, mediate axon stability in the CNS and PNS: neuropathology and behavioral deficits in single- and double-null mice. Experimental neurology *195*, 208-217.
150. Dupree, J.L., Coetzee, T., Blight, A., Suzuki, K., and Popko, B. (1998). Myelin galactolipids are essential for proper node of Ranvier formation in the CNS. The Journal of neuroscience : the official journal of the Society for Neuroscience *18*, 1642-1649.
151. Ishibashi, T., Dupree, J.L., Ikenaka, K., Hirahara, Y., Honke, K., Peles, E., Popko, B., Suzuki, K., Nishino, H., and Baba, H. (2002). A myelin galactolipid, sulfatide, is essential for maintenance of ion channels on myelinated axon but not essential for initial cluster formation. The Journal of neuroscience : the official journal of the Society for Neuroscience *22*, 6507-6514.
152. Dupree, J.L., Girault, J.A., and Popko, B. (1999). Axo-glial interactions regulate the localization of axonal paranodal proteins. The Journal of cell biology *147*, 1145-1152.
153. Nave, K.A. (2010). Myelination and the trophic support of long axons. Nature reviews. Neuroscience *11*, 275-283.
154. Dutta, R., and Trapp, B.D. (2011). Mechanisms of neuronal dysfunction and degeneration in multiple sclerosis. Progress in neurobiology *93*, 1-12.
155. Zigdon, H., Kogot-Levin, A., Park, J.W., Goldschmidt, R., Kelly, S., Merrill, A.H., Jr., Scherz, A., Pewzner-Jung, Y., Saada, A., and Futerman, A.H. (2013). Ablation of ceramide synthase 2 causes chronic oxidative stress due to disruption of the mitochondrial respiratory chain. The Journal of biological chemistry *288*, 4947-4956.
156. Dong, X.X., Wang, Y., and Qin, Z.H. (2009). Molecular mechanisms of excitotoxicity and their relevance to pathogenesis of neurodegenerative diseases. Acta pharmacologica Sinica *30*, 379-387.
157. Thorburne, S.K., and Juurlink, B.H. (1996). Low glutathione and high iron govern the susceptibility of oligodendroglial precursors to oxidative stress. Journal of neurochemistry *67*, 1014-1022.
158. Roth, A.D., and Nunez, M.T. (2016). Oligodendrocytes: Functioning in a Delicate Balance Between High Metabolic Requirements and Oxidative Damage. Advances in experimental medicine and biology *949*, 167-181.
159. Jana, A., and Pahan, K. (2007). Oxidative stress kills human primary oligodendrocytes via neutral sphingomyelinase: implications for multiple sclerosis. Journal of neuroimmune pharmacology : the official journal of the Society on NeuroImmune Pharmacology *2*, 184-193.
160. Venable, M.E., Lee, J.Y., Smyth, M.J., Bielawska, A., and Obeid, L.M. (1995). Role of ceramide in cellular senescence. The Journal of biological chemistry *270*, 30701-30708.
161. Cutler, R.G., Kelly, J., Storie, K., Pedersen, W.A., Tammara, A., Hatanpaa, K., Troncoso, J.C., and Mattson, M.P. (2004). Involvement of oxidative stress-induced abnormalities in ceramide and cholesterol metabolism in brain aging and Alzheimer's disease. Proceedings of the National Academy of Sciences of the United States of America *101*, 2070-2075.
162. Fujita, A., Cheng, J., Hirakawa, M., Furukawa, K., Kusunoki, S., and Fujimoto, T. (2007). Gangliosides GM1 and GM3 in the living cell membrane form clusters susceptible to cholesterol depletion and chilling. Molecular biology of the cell *18*, 2112-2122.
163. Yim, S.H., Farrer, R.G., Hammer, J.A., Yavin, E., and Quarles, R.H. (1994). Differentiation of oligodendrocytes cultured from developing rat brain is enhanced by exogenous GM3 ganglioside. Journal of neuroscience research *38*, 268-281.
164. Yim, S.H., Farrer, R.G., and Quarles, R.H. (1995). Expression of glycolipids and myelin-associated glycoprotein during the differentiation of oligodendrocytes: comparison of the CG-4 glial cell line to primary cultures. Developmental neuroscience *17*, 171-180.

165. Svennerholm, L., and Vanier, M.T. (1973). The distribution of lipids in the human nervous system. IV. Fatty acid composition of major sphingolipids of human infant brain. Brain research *55*, 413-423.
166. Petrache, I., Kamocki, K., Poirier, C., Pewzner-Jung, Y., Laviad, E.L., Schweitzer, K.S., Van Demark, M., Justice, M.J., Hubbard, W.C., and Futerman, A.H. (2013). Ceramide synthases expression and role of ceramide synthase-2 in the lung: insight from human lung cells and mouse models. PloS one *8*, e62968.
167. Raichur, S., Wang, S.T., Chan, P.W., Li, Y., Ching, J., Chaurasia, B., Dogra, S., Ohman, M.K., Takeda, K., Sugii, S., et al. (2014). CerS2 haploinsufficiency inhibits beta-oxidation and confers susceptibility to diet-induced steatohepatitis and insulin resistance. Cell metabolism *20*, 687-695.
168. Arthur, J.R., Heinecke, K.A., and Seyfried, T.N. (2011). Filipin recognizes both GM1 and cholesterol in GM1 gangliosidosis mouse brain. Journal of lipid research *52*, 1345-1351.
169. Ishitsuka, R., Hirabayashi, Y., and Kobayashi, T. (2009). Glycosphingolipid deficiency increases the sterol regulatory element-mediated gene transcription. Biochemical and biophysical research communications *378*, 240-243.
170. Worgall, T.S. (2011). Sphingolipid synthetic pathways are major regulators of lipid homeostasis. Advances in experimental medicine and biology *721*, 139-148.
171. Brown, M.S., and Goldstein, J.L. (1986). A receptor-mediated pathway for cholesterol homeostasis. Science (New York, N.Y.) *232*, 34-47.
172. Eckhardt, E.R., Cai, L., Shetty, S., Zhao, Z., Szanto, A., Webb, N.R., and Van der Westhuyzen, D.R. (2006). High density lipoprotein endocytosis by scavenger receptor SR-BII is clathrin-dependent and requires a carboxyl-terminal dileucine motif. The Journal of biological chemistry *281*, 4348-4353.
173. Ali, M., Fritsch, J., Zigdon, H., Pewzner-Jung, Y., Schutze, S., and Futerman, A.H. (2013). Altering the sphingolipid acyl chain composition prevents LPS/GLN-mediated hepatic failure in mice by disrupting TNFR1 internalization. Cell death & disease *4*, e929.
174. Volpert, G., Ben-Dor, S., Tarcic, O., Duan, J., Saada, A., Merrill, A.H., Jr., Pewzner-Jung, Y., and Futerman, A.H. (2017). Oxidative stress elicited by modifying the ceramide acyl chain length reduces the rate of clathrin-mediated endocytosis. Journal of cell science *130*, 1486-1493.
175. Glade, M.J., and Smith, K. (2015). Phosphatidylserine and the human brain. Nutrition (Burbank, Los Angeles County, Calif.) *31*, 781-786.
176. Parpal, S., Karlsson, M., Thorn, H., and Stralfors, P. (2001). Cholesterol depletion disrupts caveolae and insulin receptor signaling for metabolic control via insulin receptor substrate-1, but not for mitogen-activated protein kinase control. The Journal of biological chemistry *276*, 9670-9678.
177. Kabayama, K., Sato, T., Saito, K., Loberto, N., Prinetti, A., Sonnino, S., Kinjo, M., Igarashi, Y., and Inokuchi, J. (2007). Dissociation of the insulin receptor and caveolin-1 complex by ganglioside GM3 in the state of insulin resistance. Proceedings of the National Academy of Sciences of the United States of America *104*, 13678-13683.
178. Kabayama, K., Sato, T., Kitamura, F., Uemura, S., Kang, B.W., Igarashi, Y., and Inokuchi, J. (2005). TNFalpha-induced insulin resistance in adipocytes as a membrane microdomain disorder: involvement of ganglioside GM3. Glycobiology *15*, 21-29.
179. Park, J.W., Park, W.J., Kuperman, Y., Boura-Halfon, S., Pewzner-Jung, Y., and Futerman, A.H. (2013). Ablation of very long acyl chain sphingolipids causes hepatic insulin resistance in mice due to altered detergent-resistant membranes. Hepatology (Baltimore, Md.) *57*, 525-532.
180. Yamashita, T., Hashiramoto, A., Haluzik, M., Mizukami, H., Beck, S., Norton, A., Kono, M., Tsuji, S., Daniotti, J.L., Werth, N., et al. (2003). Enhanced insulin sensitivity in mice lacking ganglioside GM3. Proceedings of the National Academy of Sciences of the United States of America *100*, 3445-3449.
181. Du, J., Tao-Cheng, J.H., Zerfas, P., and McBain, C.J. (1998). The K+ channel, Kv2.1, is apposed to astrocytic processes and is associated with inhibitory postsynaptic membranes in hippocampal and cortical principal neurons and inhibitory interneurons. Neuroscience *84*, 37-48.
182. Bishop, H.I., Guan, D., Bocksteins, E., Parajuli, L.K., Murray, K.D., Cobb, M.M., Misonou, H., Zito, K., Foehring, R.C., and Trimmer, J.S. (2015). Distinct Cell- and Layer-Specific Expression Patterns and

Independent Regulation of Kv2 Channel Subtypes in Cortical Pyramidal Neurons. The Journal of neuroscience : the official journal of the Society for Neuroscience *35*, 14922-14942.

183. Martens, J.R., Navarro-Polanco, R., Coppock, E.A., Nishiyama, A., Parshley, L., Grobaski, T.D., and Tamkun, M.M. (2000). Differential targeting of Shaker-like potassium channels to lipid rafts. The Journal of biological chemistry *275*, 7443-7446.
184. Du, J., Haak, L.L., Phillips-Tansey, E., Russell, J.T., and McBain, C.J. (2000). Frequency-dependent regulation of rat hippocampal somato-dendritic excitability by the K+ channel subunit Kv2.1. The Journal of physiology *522 Pt 1*, 19-31.
185. Mohapatra, D.P., Misonou, H., Pan, S.J., Held, J.E., Surmeier, D.J., and Trimmer, J.S. (2009). Regulation of intrinsic excitability in hippocampal neurons by activity-dependent modulation of the KV2.1 potassium channel. Channels (Austin, Tex.) *3*, 46-56.
186. Misonou, H., Mohapatra, D.P., Park, E.W., Leung, V., Zhen, D., Misonou, K., Anderson, A.E., and Trimmer, J.S. (2004). Regulation of ion channel localization and phosphorylation by neuronal activity. Nature neuroscience *7*, 711-718.
187. Sarmiere, P.D., Weigle, C.M., and Tamkun, M.M. (2008). The Kv2.1 K+ channel targets to the axon initial segment of hippocampal and cortical neurons in culture and in situ. BMC neuroscience *9*, 112.
188. Martens, J.R., Sakamoto, N., Sullivan, S.A., Grobaski, T.D., and Tamkun, M.M. (2001). Isoform-specific localization of voltage-gated K+ channels to distinct lipid raft populations. Targeting of Kv1.5 to caveolae. The Journal of biological chemistry *276*, 8409-8414.
189. O'Connell, K.M., and Tamkun, M.M. (2005). Targeting of voltage-gated potassium channel isoforms to distinct cell surface microdomains. Journal of cell science *118*, 2155-2166.
190. Ramu, Y., Xu, Y., and Lu, Z. (2006). Enzymatic activation of voltage-gated potassium channels. Nature *442*, 696-699.
191. Milescu, M., Bosmans, F., Lee, S., Alabi, A.A., Kim, J.I., and Swartz, K.J. (2009). Interactions between lipids and voltage sensor paddles detected with tarantula toxins. Nature structural & molecular biology *16*, 1080-1085.
192. Xu, Y., Ramu, Y., and Lu, Z. (2008). Removal of phospho-head groups of membrane lipids immobilizes voltage sensors of K+ channels. Nature *451*, 826-829.
193. Park, K.S., Mohapatra, D.P., Misonou, H., and Trimmer, J.S. (2006). Graded regulation of the Kv2.1 potassium channel by variable phosphorylation. Science (New York, N.Y.) *313*, 976-979.
194. Mohapatra, D.P., and Trimmer, J.S. (2006). The Kv2.1 C terminus can autonomously transfer Kv2.1-like phosphorylation-dependent localization, voltage-dependent gating, and muscarinic modulation to diverse Kv channels. The Journal of neuroscience : the official journal of the Society for Neuroscience *26*, 685-695.
195. Misonou, H., Mohapatra, D.P., and Trimmer, J.S. (2005). Kv2.1: a voltage-gated k+ channel critical to dynamic control of neuronal excitability. Neurotoxicology *26*, 743-752.
196. Lim, S.T., Antonucci, D.E., Scannevin, R.H., and Trimmer, J.S. (2000). A novel targeting signal for proximal clustering of the Kv2.1 K+ channel in hippocampal neurons. Neuron *25*, 385-397.
197. Saitsu, H., Akita, T., Tohyama, J., Goldberg-Stern, H., Kobayashi, Y., Cohen, R., Kato, M., Ohba, C., Miyatake, S., Tsurusaki, Y., et al. (2015). De novo KCNB1 mutations in infantile epilepsy inhibit repetitive neuronal firing. Scientific reports *5*, 15199.
198. Thiffault, I., Speca, D.J., Austin, D.C., Cobb, M.M., Eum, K.S., Safina, N.P., Grote, L., Farrow, E.G., Miller, N., Soden, S., et al. (2015). A novel epileptic encephalopathy mutation in KCNB1 disrupts Kv2.1 ion selectivity, expression, and localization. The Journal of general physiology *146*, 399-410.
199. Torkamani, A., Bersell, K., Jorge, B.S., Bjork, R.L., Jr., Friedman, J.R., Bloss, C.S., Cohen, J., Gupta, S., Naidu, S., Vanoye, C.G., et al. (2014). De novo KCNB1 mutations in epileptic encephalopathy. Annals of neurology *76*, 529-540.

200. Speca, D.J., Ogata, G., Mandikian, D., Bishop, H.I., Wiler, S.W., Eum, K., Wenzel, H.J., Doisy, E.T., Matt, L., Campi, K.L., et al. (2014). Deletion of the Kv2.1 delayed rectifier potassium channel leads to neuronal and behavioral hyperexcitability. Genes, brain, and behavior *13*, 394-408.
201. Thomas, P., and Smart, T.G. (2005). HEK293 cell line: a vehicle for the expression of recombinant proteins. Journal of pharmacological and toxicological methods *51*, 187-200.
202. Fox, P.D., Loftus, R.J., and Tamkun, M.M. (2013). Regulation of Kv2.1 K(+) conductance by cell surface channel density. The Journal of neuroscience : the official journal of the Society for Neuroscience *33*, 1259-1270.
203. Gelderblom, W.C., Smuts, C.M., Abel, S., Snyman, S.D., Cawood, M.E., van der Westhuizen, L., and Swanevelder, S. (1996). Effect of fumonisin B1 on protein and lipid synthesis in primary rat hepatocytes. Food and chemical toxicology : an international journal published for the British Industrial Biological Research Association *34*, 361-369.
204. Zitomer, N.C., Mitchell, T., Voss, K.A., Bondy, G.S., Pruett, S.T., Garnier-Amblard, E.C., Liebeskind, L.S., Park, H., Wang, E., Sullards, M.C., et al. (2009). Ceramide synthase inhibition by fumonisin B1 causes accumulation of 1-deoxysphinganine: a novel category of bioactive 1-deoxysphingoid bases and 1-deoxydihydroceramides biosynthesized by mammalian cell lines and animals. The Journal of biological chemistry *284*, 4786-4795.
205. Merrill, A.H., Jr., van Echten, G., Wang, E., and Sandhoff, K. (1993). Fumonisin B1 inhibits sphingosine (sphinganine) N-acyltransferase and de novo sphingolipid biosynthesis in cultured neurons in situ. The Journal of biological chemistry *268*, 27299-27306.
206. Riley, R.T., Enongene, E., Voss, K.A., Norred, W.P., Meredith, F.I., Sharma, R.P., Spitsbergen, J., Williams, D.E., Carlson, D.B., and Merrill, A.H., Jr. (2001). Sphingolipid perturbations as mechanisms for fumonisin carcinogenesis. Environmental health perspectives *109 Suppl 2*, 301-308.
207. Genin, M.J., Gonzalez Valcarcel, I.C., Holloway, W.G., Lamar, J., Mosior, M., Hawkins, E., Estridge, T., Weidner, J., Seng, T., Yurek, D., et al. (2016). Imidazopyridine and Pyrazolopiperidine Derivatives as Novel Inhibitors of Serine Palmitoyl Transferase. Journal of medicinal chemistry *59*, 5904-5910.
208. Silva, L.C., Ben David, O., Pewzner-Jung, Y., Laviad, E.L., Stiban, J., Bandyopadhyay, S., Merrill, A.H., Jr., Prieto, M., and Futerman, A.H. (2012). Ablation of ceramide synthase 2 strongly affects biophysical properties of membranes. Journal of lipid research *53*, 430-436.
209. Miyaji, M., Jin, Z.X., Yamaoka, S., Amakawa, R., Fukuhara, S., Sato, S.B., Kobayashi, T., Domae, N., Mimori, T., Bloom, E.T., et al. (2005). Role of membrane sphingomyelin and ceramide in platform formation for Fas-mediated apoptosis. The Journal of experimental medicine *202*, 249-259.
210. Siskind, L.J., Kolesnick, R.N., and Colombini, M. (2006). Ceramide forms channels in mitochondrial outer membranes at physiologically relevant concentrations. Mitochondrion *6*, 118-125.
211. Alecu, I., Tedeschi, A., Behler, N., Wunderling, K., Lamberz, C., Lauterbach, M.A., Gaebler, A., Ernst, D., Van Veldhoven, P.P., Al-Amoudi, A., et al. (2017). Localization of 1-deoxysphingolipids to mitochondria induces mitochondrial dysfunction. Journal of lipid research *58*, 42-59.
212. O'Connell, K.M., Loftus, R., and Tamkun, M.M. (2010). Localization-dependent activity of the Kv2.1 delayed-rectifier K+ channel. Proceedings of the National Academy of Sciences of the United States of America *107*, 12351-12356.
213. Deutsch, E., Weigel, A.V., Akin, E.J., Fox, P., Hansen, G., Haberkorn, C.J., Loftus, R., Krapf, D., and Tamkun, M.M. (2012). Kv2.1 cell surface clusters are insertion platforms for ion channel delivery to the plasma membrane. Molecular biology of the cell *23*, 2917-2929.
214. Feinshreiber, L., Singer-Lahat, D., Friedrich, R., Matti, U., Sheinin, A., Yizhar, O., Nachman, R., Chikvashvili, D., Rettig, J., Ashery, U., et al. (2010). Non-conducting function of the Kv2.1 channel enables it to recruit vesicles for release in neuroendocrine and nerve cells. Journal of cell science *123*, 1940-1947.
215. Fox, P.D., Haberkorn, C.J., Akin, E.J., Seel, P.J., Krapf, D., and Tamkun, M.M. (2015). Induction of stable ER-plasma-membrane junctions by Kv2.1 potassium channels. Journal of cell science *128*, 2096-2105.

216. Mandikian, D., Bocksteins, E., Parajuli, L.K., Bishop, H.I., Cerda, O., Shigemoto, R., and Trimmer, J.S. (2014). Cell type-specific spatial and functional coupling between mammalian brain Kv2.1 K+ channels and ryanodine receptors. The Journal of comparative neurology *522*, 3555-3574.
217. Gleichmann, M., and Mattson, M.P. (2011). Neuronal calcium homeostasis and dysregulation. Antioxidants & redox signaling *14*, 1261-1273.
218. Salinas, M., Duprat, F., Heurteaux, C., Hugnot, J.P., and Lazdunski, M. (1997). New modulatory alpha subunits for mammalian Shab K+ channels. The Journal of biological chemistry *272*, 24371-24379.
219. Ikematsu, N., Dallas, M.L., Ross, F.A., Lewis, R.W., Rafferty, J.N., David, J.A., Suman, R., Peers, C., Hardie, D.G., and Evans, A.M. (2011). Phosphorylation of the voltage-gated potassium channel Kv2.1 by AMP-activated protein kinase regulates membrane excitability. Proceedings of the National Academy of Sciences of the United States of America *108*, 18132-18137.
220. Mao, C., and Obeid, L.M. (2008). Ceramidases: regulators of cellular responses mediated by ceramide, sphingosine, and sphingosine-1-phosphate. Biochimica et biophysica acta *1781*, 424-434.
221. Oaks, J., and Ogretmen, B. (2014). Regulation of PP2A by Sphingolipid Metabolism and Signaling. Frontiers in oncology *4*, 388.
222. Chalfant, C.E., Kishikawa, K., Mumby, M.C., Kamibayashi, C., Bielawska, A., and Hannun, Y.A. (1999). Long chain ceramides activate protein phosphatase-1 and protein phosphatase-2A. Activation is stereospecific and regulated by phosphatidic acid. The Journal of biological chemistry *274*, 20313-20317.
223. Hou, H., Sun, L., Siddoway, B.A., Petralia, R.S., Yang, H., Gu, H., Nairn, A.C., and Xia, H. (2013). Synaptic NMDA receptor stimulation activates PP1 by inhibiting its phosphorylation by Cdk5. The Journal of cell biology *203*, 521-535.
224. Siddoway, B., Hou, H., Yang, J., Sun, L., Yang, H., Wang, G.Y., and Xia, H. (2014). Potassium channel Kv2.1 is regulated through protein phosphatase-1 in response to increases in synaptic activity. Neuroscience letters *583*, 142-147.
225. Kinoshita, E., Kinoshita-Kikuta, E., and Koike, T. (2009). Separation and detection of large phosphoproteins using Phos-tag SDS-PAGE. Nature protocols *4*, 1513-1521.
226. Tillman, T.S., and Cascio, M. (2003). Effects of membrane lipids on ion channel structure and function. Cell biochemistry and biophysics *38*, 161-190.
227. Owen, D.M., Magenau, A., Williamson, D., and Gaus, K. (2012). The lipid raft hypothesis revisited--new insights on raft composition and function from super-resolution fluorescence microscopy. BioEssays : news and reviews in molecular, cellular and developmental biology *34*, 739-747.
228. Kraft, M.L., and Klitzing, H.A. (2014). Imaging lipids with secondary ion mass spectrometry. Biochimica et biophysica acta *1841*, 1108-1119.
229. Hiramoto-Yamaki, N., Tanaka, K.A., Suzuki, K.G., Hirosawa, K.M., Miyahara, M.S., Kalay, Z., Tanaka, K., Kasai, R.S., Kusumi, A., and Fujiwara, T.K. (2014). Ultrafast diffusion of a fluorescent cholesterol analog in compartmentalized plasma membranes. Traffic (Copenhagen, Denmark) *15*, 583-612.
230. Frisz, J.F., Klitzing, H.A., Lou, K., Hutcheon, I.D., Weber, P.K., Zimmerberg, J., and Kraft, M.L. (2013). Sphingolipid domains in the plasma membranes of fibroblasts are not enriched with cholesterol. The Journal of biological chemistry *288*, 16855-16861.

Appendix

Appendix I – Insulin Stimulation of Primary Skin Fibroblasts

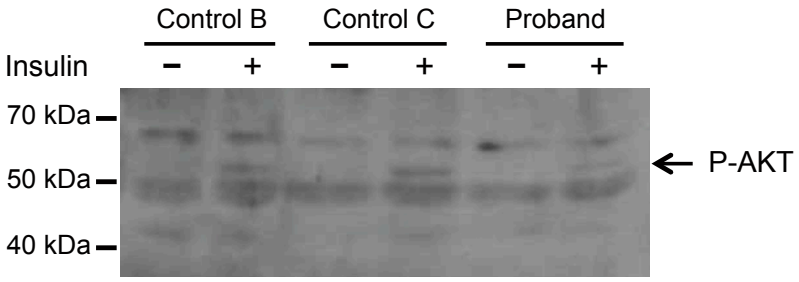

Figure 18: Primary skin fibroblasts from patient and gender- and age-matched controls are not responding to stimulation with insulin. Primary skin fibroblasts isolated from patient and gender- and age-matched controls were serum starved for 16 hours and stimulated with 10 nM insulin for 10 min. Cell extracts were harvested and used for detection of phosphorylated Akt (Ser473) (60 kDa) by Western Blotting as a measure for insulin sensitivity. Equal amount of protein (35 µg) was loaded in each lane. Only a faint band around 60 kDa is observed, indicating that the fibroblasts did not respond to the insulin treatment.

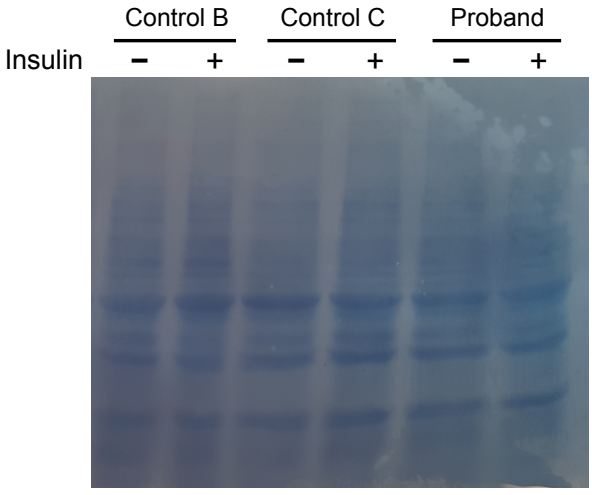

Figure 19: Amido Black staining. Amido Black staining was performed on the membrane used in the experiment described in Figure 15 in order to assess the protein amount being blotted onto the membrane. As seen on the figure, the reduced signal for phosphorylated AKT was not due to problems with blotting.

Appendix II – Kv2.1 Clustering in HEK Cells

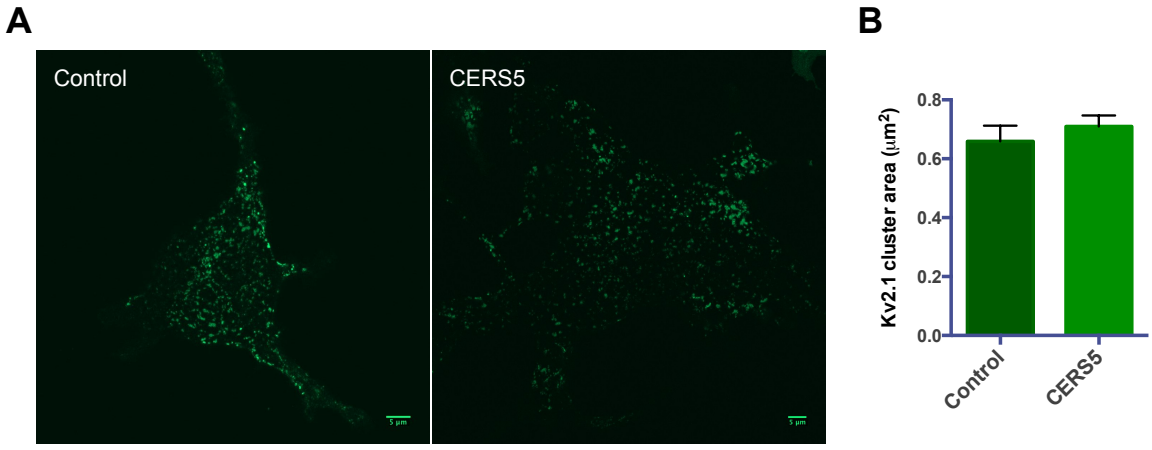

Figure 20: Overexpression of CERS5 does not affect Kv2.1 cluster size in HEK293 cells. HEK293 stably transfected with CERS5 transfected with EGFP-tagged Kv2.1. Within 1 hour, confocal imaging of the basal surface of the cells was performed in order to evaluate Kv2.1 cluster size. The laser power was adjusted manually for each image in order to avoid signal saturation. Cluster size analysis was performed using FIJI software with the LSM Toolbox plugin. Six representative clusters were measured per cell. A) Representative fluorescent images. *Scale bar*: 5 μm. B) Kv2.1 cluster area is shown as mean ±SEM. The average cluster area for control cells was 0.66 ± 0.05 μm^2 (n = 42) and 0.71 ± 0.04 μm^2 (n = 36) for CERS5 cells. Statistical analysis was performed by unpaired t-test with Welch's correction using the GraphPad Prism software. No significant difference was found on Kv2.1 cluster area upon overexpression of CERS5. The data represent one of three independent replicates.

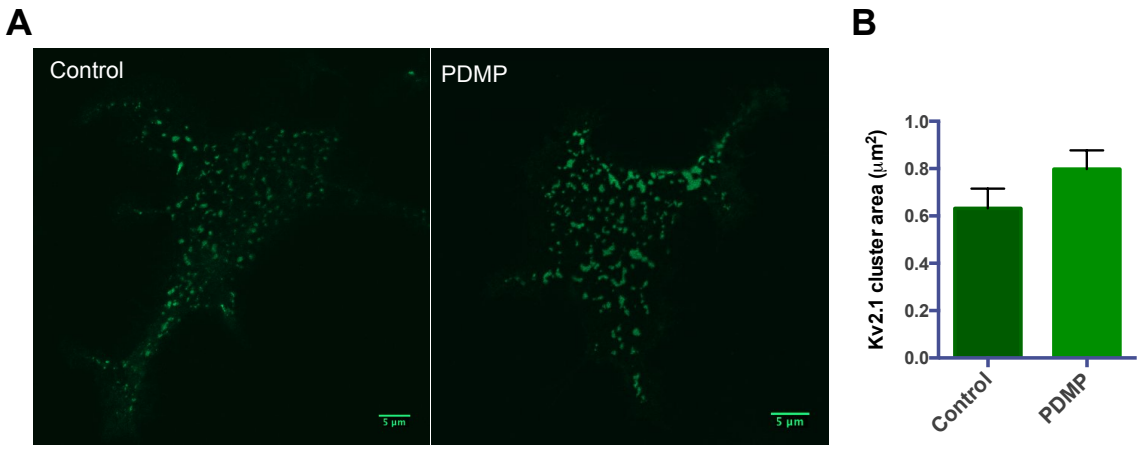

Figure 21: Inhibition of glycosphingolipid synthesis does not affect Kv2.1 cluster size in HEK293 cells. HEK293 cells transfected with EGFP-tagged Kv2.1 were treated with 10 uM D-*threo*-1-phenyl-2-decanoylamino-3-morpholino-1-propanol (PDMP) for 48 hours at 5% CO_2, 37°C in order to inhibit the synthesis of glucosylceramide and downstream glycosphingolipids. Within 1 hour, confocal imaging of the basal surface of the cells was performed in order to evaluate Kv2.1 cluster size. The laser power was adjusted manually for each image in order to avoid signal saturation. Cluster size analysis was performed using FIJI software with the LSM Toolbox plugin. Six representative clusters were measured per cell. A) Representative fluorescent images. *Scale bar*: 5 μm. B) Kv2.1 cluster area is shown as mean ±SEM. The average cluster area for control cells was 0.53 ± 0.04 μm^2 (n = 42) and 0.67 ± 0.10 μm^2 (n = 36) for PDMP treated cells. Statistical analysis was performed by unpaired t-test with Welch's correction using the GraphPad Prism software. No significant difference was found on Kv2.1 cluster area upon PDMP treatment. The data represent one of two independent replicates.

Appendix III – Lipidomics Data for PDMP Treatment of HEK Cells

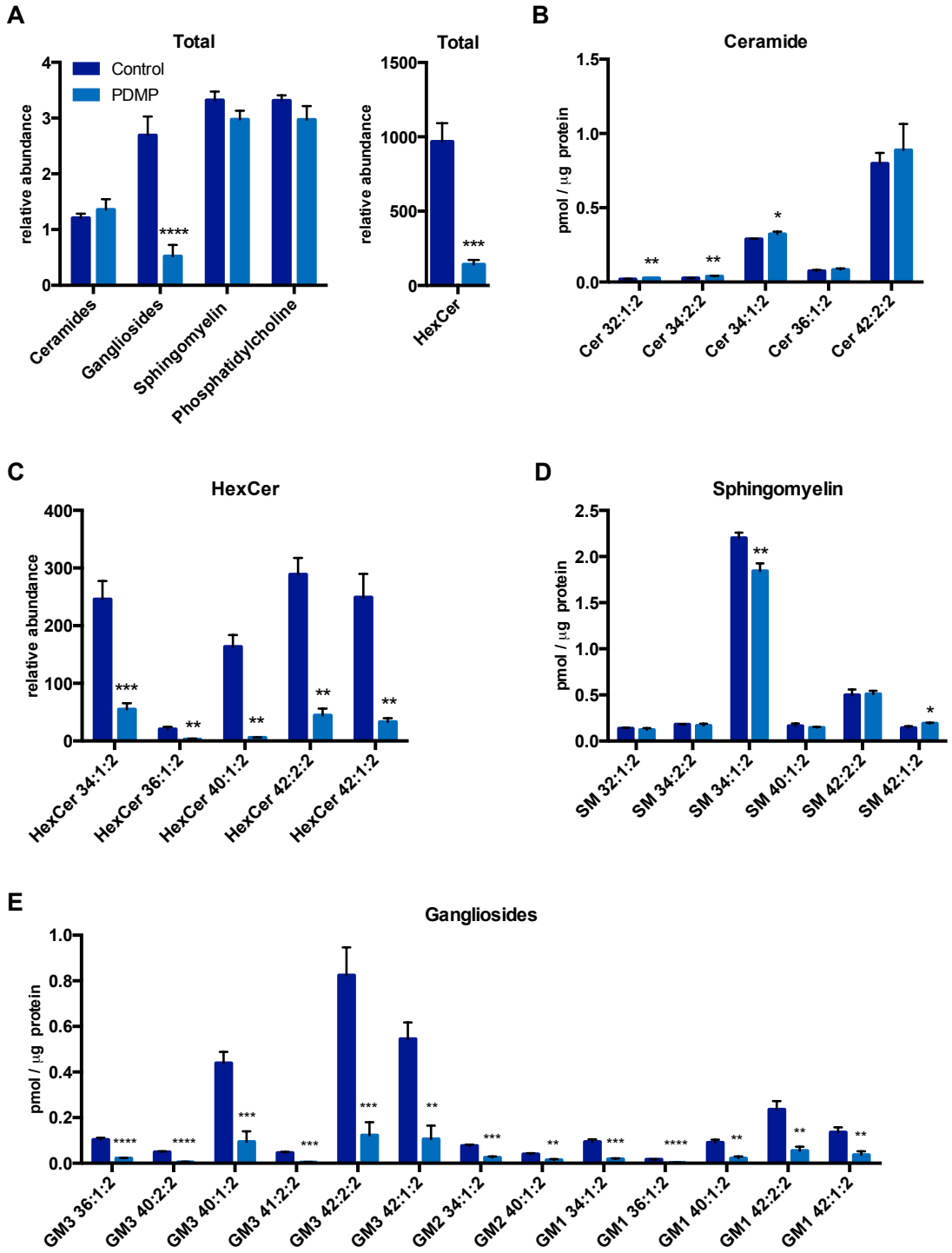

Figure 22: Major changes in the sphingolipid profile upon inhibition of ceramide synthesis. Lipid extracts prepared from three independent HEK293 cell control cultures and cultures treated with 20 µM FB1 for 48 hours at 5% CO_2, 37 °C were analyzed by LC-MS using appropriate internal standards. All lipid species besides hexosylceramides (HexCer) are presented as pmol/µg protein. Due to lack of internal standards, HexCer species are presented as relative abundance. Mean ± SD of n = 3 HEK293 cell cultures per group is shown. A) Total levels of analyzed lipid species. B) Ceramide, C) HexCer species. D) Sphingomyelin species E) Ganglioside species. F) Phosphatidylcholine species. Statistical analysis was performed by multiple t-test using GraphPad Prism software. Lipid extraction and analysis were kindly performed by Marta Moreno Torres (Dept. Biochemistry and Molecular Biology, University of Southern Denmark)

Appendix IV – Lipidomics Data for Sphinganine and 1-deoxysphinganine Treatments of HEK Cells

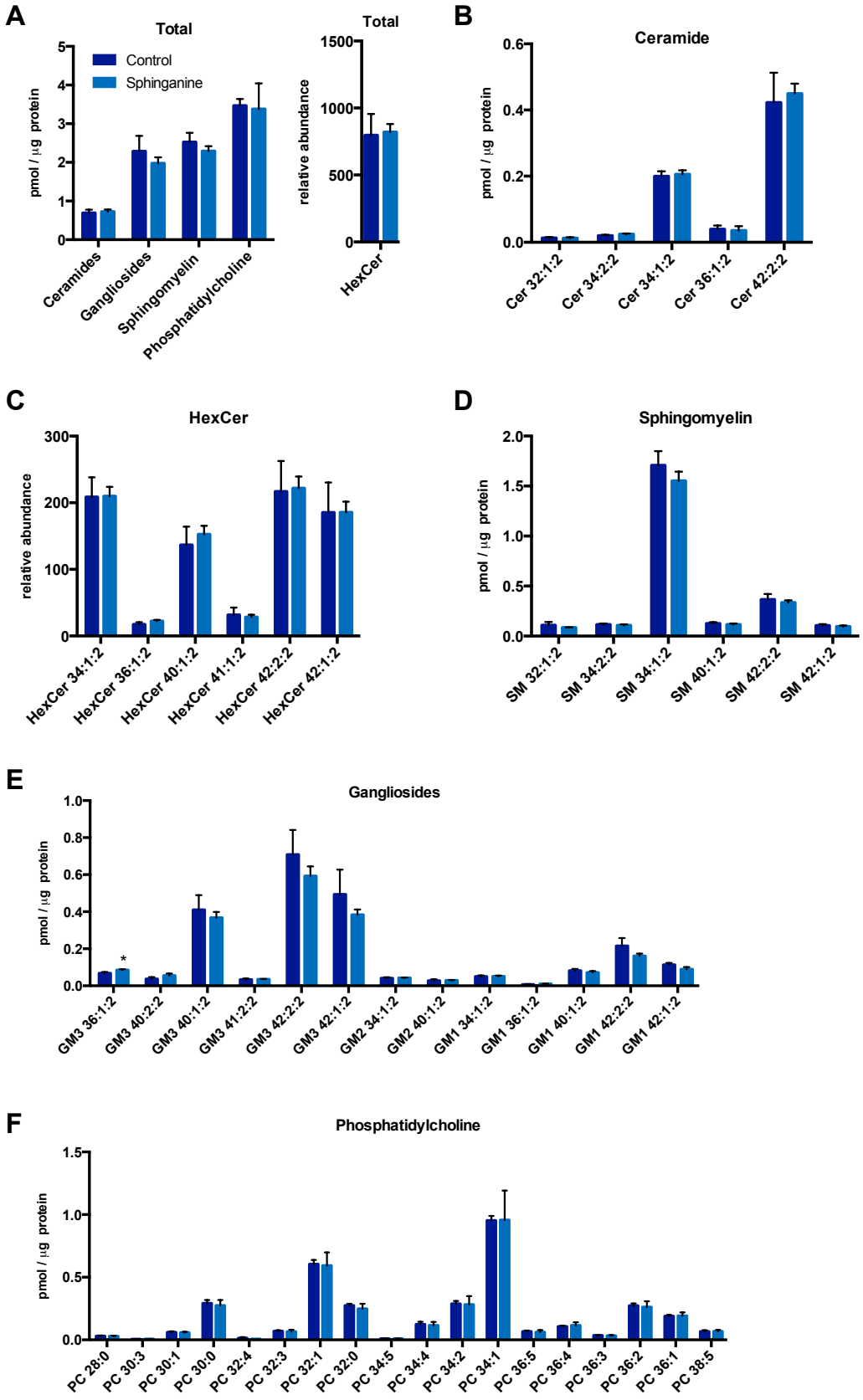

Figure 23: Treatment with deoxysphinganine does not change the levels of canonical sphingolipids. Lipid extracts prepared from three independent HEK293 cell control cultures and cultures treated with 0.01 μM deoxysphinganine (deoxySa) complexed with bovine serum albumin (mol 1:1) for 24 hours at 5% CO_2, 37 °C were analyzed by LC-MS using appropriate internal standards. All lipid species besides hexosylceramides (HexCer) are presented as pmol/μg protein. Due to lack of internal standards, HexCer species are presented as relative abundance. Mean ± SD of n = 3 HEK293 cell cultures per group is shown. A) Total levels of analyzed lipid species. B) Ceramide, C) Sphingomyelin species. D) HexCer species. E) Ganglioside species. Statistical analysis was performed by multiple t-test using GraphPad Prism software. Lipid extraction and analysis were kindly performed by Marta Moreno Torres (Dept. Biochemistry and Molecular Biology, University of Southern Denmark).

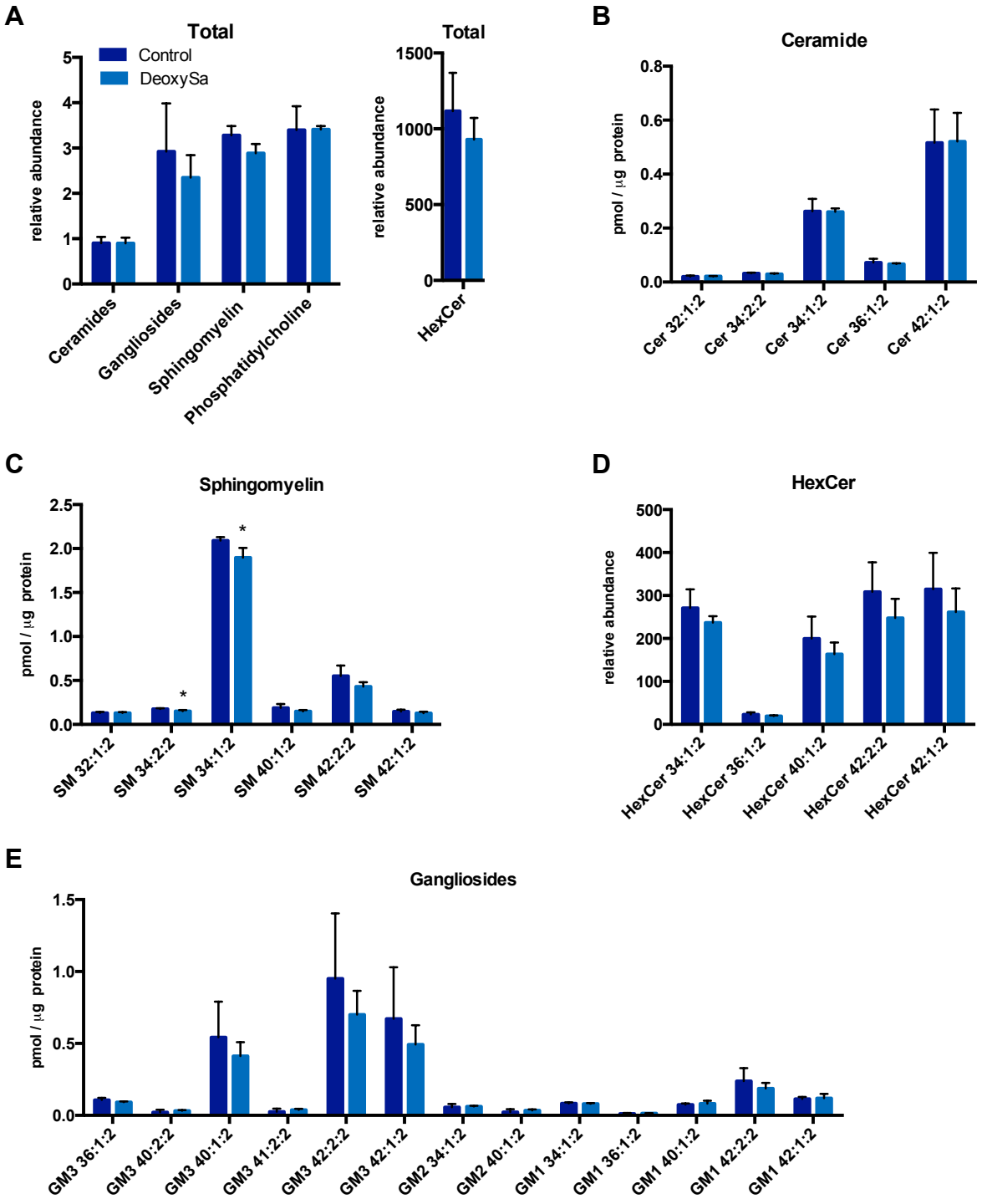

Figure 24: Treatment with deoxysphinganine does not change the levels of canonical sphingolipids. Lipid extracts prepared from three independent HEK293 cell control cultures and cultures treated with 0.01 µM deoxysphinganine (deoxySa) complexed with bovine serum albumin (mol 1:1) for 24 hours at 5% CO_2, 37 °C were analyzed by LC-MS using appropriate internal standards. All lipid species besides hexosylceramides (HexCer) are presented as pmol/µg protein. Due to lack of internal standards, HexCer species are presented as relative abundance. Mean ± SD of n = 3 HEK293 cell cultures per group is shown. A) Total levels of analyzed lipid species. B) Ceramide, C) Sphingomyelin species. D) HexCer species. E) Ganglioside species. Statistical analysis was performed by multiple t-test using GraphPad Prism software. Lipid extraction and analysis were kindly performed by Marta Moreno Torres (Dept. Biochemistry and Molecular Biology, University of Southern Denmark).

Supplement I

Published in OPEN BIOLOGY, May 2017

Sphingolipids: membrane microdomains in brain development, function and neurological diseases

Olsen ASB & Færgeman NJ

OPEN BIOLOGY

rsob.royalsocietypublishing.org

Review

Cite this article: Olsen ASB, Færgeman NJ. 2017 Sphingolipids: membrane microdomains in brain development, function and neurological diseases. *Open Biol.* **7**: 170069. http://dx.doi.org/10.1098/rsob.170069

Received: 21 March 2017
Accepted: 30 April 2017

Subject Area:
biochemistry/cellular biology/molecular biology/neuroscience

Keywords:
sphingolipid, ganglioside, membrane microdomain, raft, brain, neurological disease

Author for correspondence:
Nils J. Færgeman
e-mail: nils.f@bmb.sdu.dk

THE ROYAL SOCIETY PUBLISHING

Sphingolipids: membrane microdomains in brain development, function and neurological diseases

Anne S. B. Olsen and Nils J. Færgeman

Villum Center for Bioanalytical Sciences, Department of Biochemistry and Molecular Biology, University of Southern Denmark, 5230 Odense M, Denmark

ASBO, 0000-0003-0431-5723; NJF, 0000-0002-9281-5287

Sphingolipids are highly enriched in the nervous system where they are pivotal constituents of the plasma membranes and are important for proper brain development and functions. Sphingolipids are not merely structural elements, but are also recognized as regulators of cellular events by their ability to form microdomains in the plasma membrane. The significance of such compartmentalization spans broadly from being involved in differentiation of neurons and synaptic transmission to neuronal–glial interactions and myelin stability. Thus, perturbations of the sphingolipid metabolism can lead to rearrangements in the plasma membrane, which has been linked to the development of various neurological diseases. Studying microdomains and their functions has for a long time been synonymous with studying the role of cholesterol. However, it is becoming increasingly clear that microdomains are very heterogeneous, which among others can be ascribed to the vast number of sphingolipids. In this review, we discuss the importance of microdomains with emphasis on sphingolipids in brain development and function as well as how disruption of the sphingolipid metabolism (and hence microdomains) contributes to the pathogenesis of several neurological diseases.

1. Introduction

The nervous system is among the tissues in the mammalian body that has the highest lipid content as well as the highest lipid complexity. This complexity can be ascribed to the lipid class of sphingolipids. Sphingolipids are particularly abundant in the brain and are essential for the development and maintenance of the functional integrity of the nervous system [1,2]. The grey matter and neurons are highly enriched in the glycosphingolipid (GSL) subgroup gangliosides, while the sphingolipid species sphingomyelin (SM), galactosylceramide (GalCer) and sulfatide are enriched in oligodendrocytes and myelin [3,4]. However, the sphingolipid profile of the brain is far from static as it continuously changes as the brain develops and ages [4–6].

The plasma membrane is a very heterogeneous environment composed of several hundreds of different lipid species [7]. Yet the movement of lipids and proteins has been shown to be more or less restricted due compartmentalization of the membrane as a consequence of lipid–lipid, lipid–protein and membrane–cytoskeletal interactions [8]. The compartmentalization is a consequence of the generation of microdomains that can be described as dynamic assemblies enriched in cholesterol and/or sphingolipids, which are located in the outer leaflet of the plasma membrane [9]. The saturated acyl chains of the sphingolipids allow these to pack more readily against cholesterol, which leads to the formation of highly packed liquid-ordered phases that are distinct from the bulk liquid-disordered phase of the plasma membrane [10]. Indeed, the plasma membrane of cells in the nervous system is highly enriched in

both cholesterol and sphingolipids, especially GSLs [11–13]. The existence of microdomains has been highly debated, as they have proven difficult to define experimentally and thus study. Recent studies indicate that this may very well be attributed to the heterogeneity of microdomain composition, which is reflected in the numerous combinations of lipids as well as proteins [14]. Morphologically only one type of microdomain has been defined, namely the caveolar microdomain. Caveolae are small 50–100 nm invaginations of the plasma membrane where the protein caveolin associates with membrane enriched in cholesterol and sphingolipids [15]. However, sphingolipid- and cholesterol-dependent microdomains with a diameter less than 20 nm and an average lifespan of 10–20 ms have been identified in living cells [16,17].

Neurons and oligodendrocytes are highly polarized cells, and compartmentalization of signalling events is required in order to maintain normal neuronal physiology, including neuronal differentiation, polarization, synapse formation, synaptic transmission and glial–neural interactions [18]. Studies show the involvement of sphingolipids in all these processes (reviewed in [2,3,18,19]). Dysregulation of the sphingolipid metabolism has been associated with a vast number of neurological diseases via disturbances of membrane organization [2,20,21]. The list of ion channels and signalling receptors that localize to and are regulated by sphingolipid microdomains in the brain is expanding, but for a long time cholesterol has been the pivot when studying the formation of membrane microdomains. In the present review, we discuss the connection between sphingolipids and their involvement in membrane microdomains, brain development as well as neurological diseases.

2. Biosynthesis and metabolism of sphingolipids

Numerous studies during the past decades have led to significant advances in our understanding of the biosynthesis and degradation of the sphingolipid pathway [22–24]. Ceramide constitutes the basal building block for the more complex sphingolipids and consists of a long-chain sphingoid base (LCB), sphinganine or sphingosine, with a fatty acid attached via an amide bond at the C2 position [25]. More complex sphingolipids are generated by attaching various head groups in the C1 position of ceramide [26]. Sphingolipids constitute a very diverse group of lipids, which counts several hundred different species. The vast number of species originates from the structural diversity and combinations within LCBs, fatty acids and head group variants [27–30].

Figure 1 outlines the synthesis and major parts of the metabolism of sphingolipids. The de novo synthesis of ceramide is initiated at the cytosolic leaflet of the endoplasmic reticulum (ER) where it is generated in a four-step process [31–33]. Briefly, serine and palmitoyl-CoA are condensed to 3-ketodihydrosphingosine by the serine palmitoyltransferase (SPT). 3-ketodihydrosphingosine is rapidly reduced to sphinganine before a ceramide synthase (CERS) converts sphinganine to dihydroceramide. Lastly, dihydroceramide is desaturated resulting in the formation of ceramide [34]. Six different mammalian CERSs have been identified. They all display unique expression profiles as well as fatty acyl-CoA specificity ranging from C14 to C26 carbon atoms [35]. For instance CERS1, which mainly uses C18 CoAs, is highly expressed in the brain and skeletal muscles, while CERS2 is more ubiquitously expressed, but with a high expression in oligodendrocytes and generates mainly C20–C26 ceramides.

Once formed, ceramide can be converted into more complex sphingolipids through different pathways. In the ER lumen, ceramide can either be turned into ceramide phosphoethanolamine or be glycosylated to GalCer [36,37]. GalCer is a precursor for sulfatides that along with GalCer are important components in myelin that insulates neurons in the central nervous system (CNS) [22]. Ceramide can also be delivered to the Golgi apparatus where it is converted into SM or glucosylceramide (GluCer). GluCer can then be converted into lactosylceramide (LacCer) by addition of galactose [22]. LacCer serves as an intermediate in the synthesis of more complex GSLs, which is conducted by sequential transfer of sugars and other chemical groups by galactosyltransferases, sialyltransferases, N-acetylgalactosamine transferases and GalCer sulfotransferases all residing in the Golgi apparatus [24]. Gangliosides constitute a rather large GSLs subgroup, which is particularly abundant in the grey matter of the brain. Combinations of glucose, galactose and N-acetylgalactosamine constitute the head groups of gangliosides and give rise to a highly structural diversity [38].

Once synthesis is complete, SM and GSLs are relocated to the plasma membrane where they are known to participate in microdomain formation [24]. The fact that complex GSL synthesis occurs on the luminal side of Golgi apparatus renders that GSLs are oriented towards the extracellular matrix after trafficking to the plasma membrane. The plasma membrane is very dynamic in the sense that microdomains form and disperse in response to cellular signals. Sphingolipids in the plasma membrane can undergo remodelling, which allows for fast modulation of membrane composition in response to stimuli. For instance, ceramide can be generated from both SM and GM3 by the action of sphingomyelinases (SMases) and N-acetyl-α-neuraminidase 3 (Neu3) in combination with glycosylhydrolases, respectively [39,40], and SM can be re-synthesized by the action of SM synthase 2 [41].

Removal of sphingolipids from the plasma membrane occurs through the endolysosomal pathway where SM and GSLs are degraded to ceramide by the action of acid sphingomyelinase (aSMase) and glycosidases, respectively [42]. Here ceramide is further deacylated to sphingosine by the acid ceramidase (aCDase). Sphingosine can either be re-acylated by CERSs, allowing sphingosine to enter the recycling pathway and be used as a precursor for complex sphingolipids, or alternatively be broken down.

As the function of each sphingolipid species depends on their specific structure, pathway and subcellular localization [43], tight regulation of the sphingolipid network is necessary in order to ensure proper brain functions, as discussed below.

3. Sphingolipid composition during brain development and ageing

The sphingolipid composition of the human brain has been studied in detail since the 1960s [4,5,44–48]. Numerous studies have shown that sphingolipids are found in high concentrations in nervous system and that the distribution and composition of sphingolipids are distinct in different regions as well as cell types of the CNS. The grey matter and neurons are particularly enriched in gangliosides, while

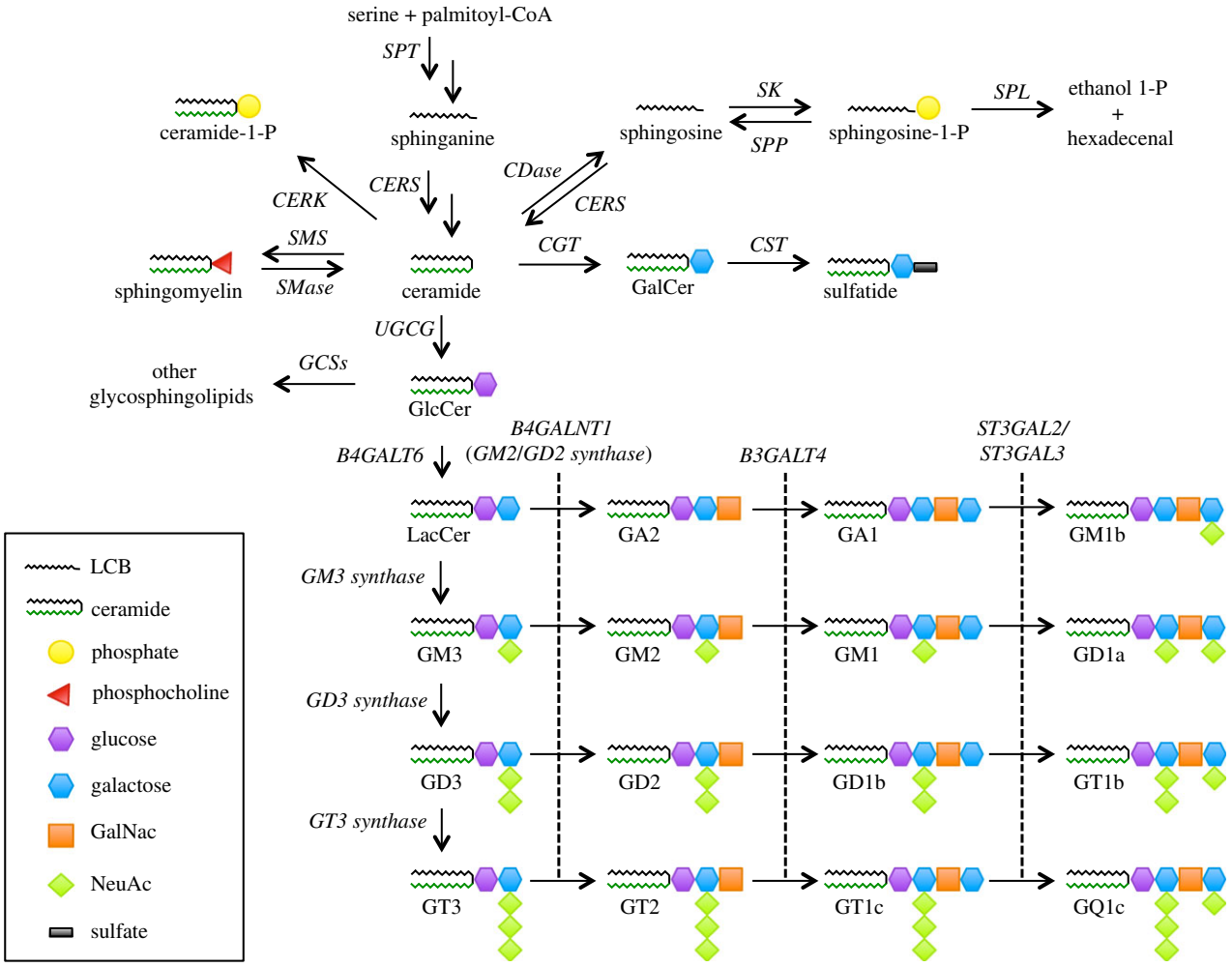

Figure 1. Overview of the sphingolipid metabolism. Sphingolipids encompass a broad spectrum of lipids. Ceramide is central in the sphingolipid metabolism as it serves as a precursor for the synthesis of more complex sphingolipids. Ceramide is synthesized de novo from serine and palmitoyl-CoA. Subsequently, complex sphingolipids are synthesized by attachment of different head groups to ceramide as indicated in the figure. In particular, ganglioside biosynthesis has been highlighted. Gangliosides are mono- or multi-sialosylated glycosphingolipids, which are highly abundant in the nervous system. Their synthesis is a multistep process of addition of sugars and sialic acids. Degradation of complex sphingolipids contributes to the pool of ceramide that can either be re-used for complex sphingolipid synthesis or alternatively be broken down. Degradation of glycosphingolipids by glycosidases and sialidases is not indicated in the figure. Abbreviations: beta-1,4-N-acetyl-galactosaminyl transferase 1 (B4GALNT1), beta-1,3-galactosyltransferase 4 (B3GALT4), beta-1,4-galactosyltransferase 6 (B4GALT6), ceramidase (CDase), ceramide galactosyltransferase (CGT), ceramide kinase (CERK), ceramide synthase (CERS), galactosylceramide sulfotransferase (CST), glycosphingolipid synthases (GCSs), serine palmitoyltransferase (SPT), sphingomyelin synthase (SMS), sphingomyelinase (SMase), sphingosine kinase (SK), sphingosine 1-phosphate phosphatase (SPP), sphingosine 1-phosphate lyase (SPL), ST3 beta-galactoside alpha-2,3-sialyltransferase 2 (ST3GAL2), ST3 beta-galactoside alpha-2,3-sialyltransferase 3 (ST3GAL3).

oligodendrocytes and myelin are highly enriched in galactolipids GalCer and its sulfated derivate sulfatide [48]. Furthermore, the sphingolipid profile changes continuously as the brain develops and ages (figure 2), indicating that sphingolipids are involved in the differentiation and maintenance of neural functions [4–6]. Consistently, expression of enzymes involved in sphingolipid biosynthesis follows brain development [3].

Gangliosides are major components of the neuronal membranes as they account for 10–12% of the lipid content [49]. They are located on the external leaflet of the plasma membrane from where they participate in key processes maintaining neuronal functions such as neuronal development and myelin stability [13,38,49]. In the adult mammalian brain, the four major brain gangliosides are GM1, GD1a, GD1b and GT1b [46,50]. It is well known that the ganglioside profile changes remarkably during development of the nervous system as well as throughout life, and these changes are region-specific [46,51]. The tight regulation of ganglioside expression is thought to instruct brain maturation processes, which as the brain ages are being reversed [52]. The importance of the ganglioside changes in brain maturation is highlighted by the fact that they correlate with several neurodevelopmental milestones including neural tube formation, neuronal differentiation, axongenesis, outgrowth of dendrites and synaptogenesis. During embryogenesis in mice, there is a marked shift from the simplest gangliosides, GM3 and GD3, to the more complex gangliosides [53]. There is a rapid increase in GD1a in human cortical layers between weeks 16 and 30 of gestation, coinciding with a rapid cortical synaptogenesis [51]. Increase of GM1 and GD1a in the human frontal cortex correlates with neuronal differentiation, outgrowth of dendrites and axons, as well as synaptogenesis [46]. Furthermore, the four major brain gangliosides GM1, GD1a, GD1b and GT1b all increase significantly from 5 months of gestation to 5 years of age, which is coinciding with the most active

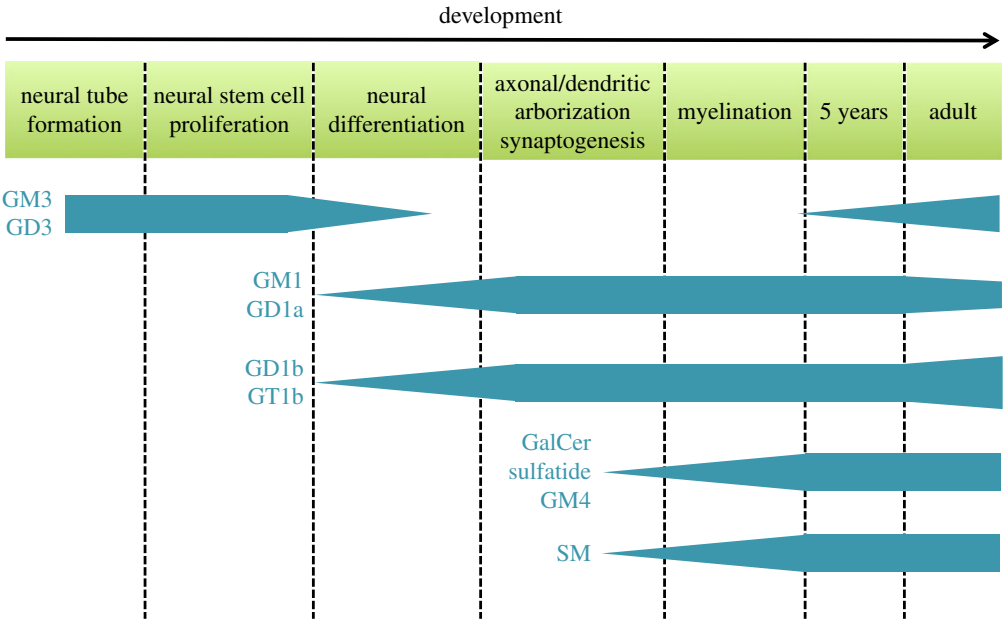

Figure 2. Outline of how key sphingolipids change during neurodevelopment and ageing. During development of the nervous system the ganglioside profile changes from the simple species (GM3 and GD3) early in embryogenesis to the more complex gangliosides (GM1, GD1a, GD1b and GT1b) later in embryogenesis. Concurrent with myelination, the levels of the myelin sphingolipids sphingomyelin (SM), galactosylceramide (GalCer), sulfatide and GM4 increase. In adulthood, the ganglioside profile changes again with increasing levels of GM3, GD3, GD1b and GT1b, while the levels of GM1 and GD1a decrease.

period of myelination [46]. After 5 years of age, the proportion of GM1 and GD1a decreases, while the levels of GM3, GD3, GT1b and GD1b increase with age [6,46]. It is not only the ganglioside head group that changes with age. The length of LCB and the fatty acid attached to the LCB also changes [45]. The most common ganglioside chain lengths of both LCBs and fatty acids in the human brain are C18, but C20 species increase from birth [30,45,49].

SM and the galactolipids are major lipids in myelin and their concentrations increase proportionally during the development of myelin [44]. GalCer and sulfatide comprise 23 wt% and 4 wt% of the total lipid of myelin, respectively [54]. During the first 2 years of post-natal life, there is a marked shift in the type of SM in the white matter [5]. C18 SM decreases from 82% to 33%, while C24:0 SM and C24:1 SM increases from 4% to 33% and 2% to 11%, respectively. This pronounced shift from medium-long-chain to very-long-chain SMs is not observed in the cerebral cortex. Here, the SM pattern remains fairly constant from birth to 2 years of age with C18:0 SM constituting more than 85% [5]. GalCer in myelin is enriched in very-long-chain fatty acids (C22–C26) [55]. Thus, overall the dominating fatty acid in ceramide found in the grey matter of the brain is C18, while C24 dominates the white matter. This is in line with a high expression of CERS1 and CERS2 in the grey and white matter, respectively.

It is important to keep in mind that the changes in sphingolipid composition can be highly regional. For instance, there is an age-dependent increase in SM and GM1 in synaptosomes isolated from mice brains [56,57]. Enrichment of GM1 occurs in microdomains isolated from synaptosomes that are resistant to cholesterol depletion indicating the presence of GSL microdomains at synaptic terminals [57]. Thus local changes in the sphingolipid profile, which might be hidden in the overall level of brain sphingolipids, can be functionally important.

4. Microdomains in brain development and maintenance

Neurons and oligodendrocytes are highly polarized cells with morphological differences that allow them to carry out specialized functions. This is attributed to the organization of their membranes in specific sub compartments of which sphingolipids play an important role. During neuronal development, the composition and organization of synaptic membranes are being remodelled. Establishment and maintenance of membrane organization is crucial in order to maintain neuronal physiology including neuronal differentiation, polarization, synapse formation and glial–neural interactions. Hence, perturbations of the sphingolipid network, and thus membrane microdomains, have been implicated in multiple dysfunctions affecting neuronal physiology. The diverse roles of sphingolipids in brain development and maintenance are described below and outlined in figure 3.

4.1. Neural differentiation, polarization and synapse formation

As discussed above, the ganglioside profile changes during embryonic development with simple gangliosides dominating the early phases. The simple ganglioside GD3 may have a central role in early neurogenesis as the activity of the GD3 synthase increases during this period, where it also constitutes the major ganglioside [58]. This is supported by studies showing GD3 being crucial for sustaining the self-renewal capability and neurogenesis of mice neural stem cells [59,60]. Sorting of the epidermal growth factor receptor (EGFR) has proven to be essential for the regulation of stem cell renewal, and it has been shown that EGFR co-localizes with GD3 in membrane microdomains in mice neural stem cells [59]. Furthermore, neural stem cells from GD3

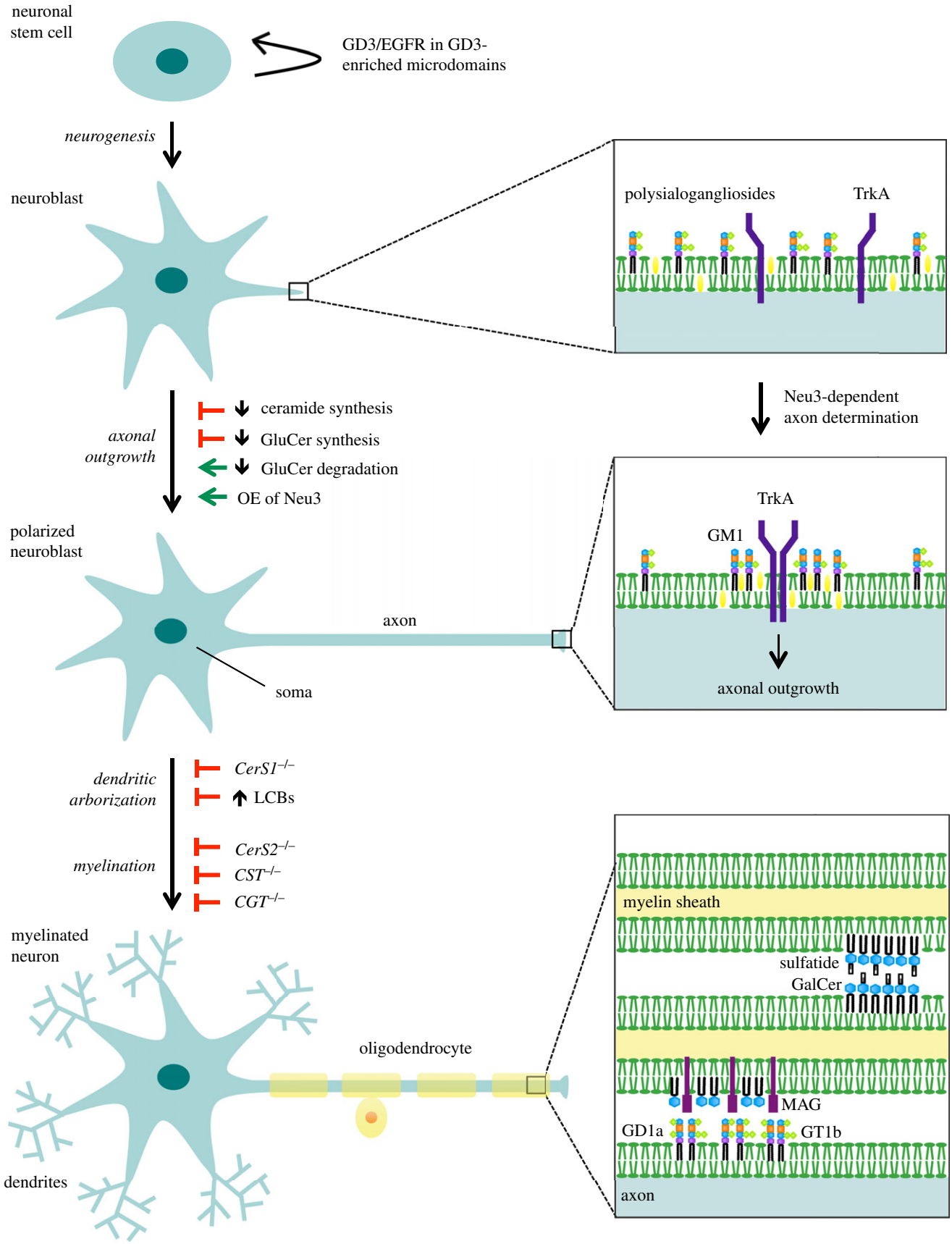

Figure 3. Roles of sphingolipids in neuronal and glial development and interaction. Sphingolipids are involved in multiple steps of the development of the nervous system. Ganglioside GD3 is important for neuronal stem cell proliferation during which it is found co-localizing with the epidermal growth factor receptor (EGFR) in microdomains. Inhibition of ceramide and glucosylceramide (GluCer) synthesis both inhibit axonal outgrowth, while inhibition of GluCer degradation and overexpression (OE) of the sialidase Neu3 stimulate axonal outgrowth. Neu3 stimulates breakdown of polysialogangliosides to GM1, which recruits the nerve growth factor receptor TrkA into microdomains thereby promoting axonal outgrowth. Dendritic arborization is reduced in *CerS1*$^{-/-}$ mice, which is likely to be caused by increase of long-chain bases (LCBs). Myelination defects have been found in mice deficient in ceramide synthase 2 (CERS2), GalCer sulfotransferase (CST) as well as UDP-galactose:ceramide galactosyltransferase (CGT). Sphingolipids are important for myelin stability. Galactosylceramide (GalCer) and sulfatide in microdomains in opposing membranes of the myelin sheath form glycosynapses important for long-term myelin stability. GD1a and GT1b in axonal membrane microdomains contribute to myelin stability by interacting with myelin-associated glycoprotein (MAG) residing in the myelin sheath.

synthase-deficient mice have reduced level of EGFR expression and accelerated EGF-induced EGFR degradation consistent with decreased self-renewal capacity [59].

Early studies have shown that exogenously supplemented gangliosides promote neurite outgrowth in neuroblastoma cell lines, primary neurons and sensory ganglia [61–64]. The nerve growth factor (NGF) induces neurite extension through binding to and activation of the tropomyosin receptor kinase A (TrkA) receptor leading to the activation of the Ras/Raf/MEK/Erk pathway [65]. Accordingly, exogenous GM1 binds to the TrkA receptor in membrane microdomains augmenting NGF-induced activation in the rat pheochromocytoma cell line PC12 and in rat primary hippocampal neurons [66–69]. Interestingly, overexpression of the GD3 synthase in PC12 cells leads to continuous activation of TrkA signalling through the Ras/Raf/MEK/Erk pathway [70]. Overexpression of the GD3 synthase also leads to an increase in GD1b and GT1b, while the level of GM1 decreases indicating that GD1b and GT1b might also be involved in regulating TrkA signalling. Surprisingly, overexpression of the GM1 synthase (B3GALT4) in PC12 cells prevents NGF-induced activation of TrkA, which is probably due to significant changes in the intracellular localization of the receptor [71]. Thus, balancing the level of GM1, as well as GD1b and GT1b, is important in controlling the TrkA signalling response in neuronal polarization.

Axonal outgrowth, projection of the axon from the soma of a neuron towards a target cell, is an essential process in the wiring of the neural network. It has been shown that inhibition of CERS activity leading to depletion of ceramide, SM and GSLs significantly reduces axonal outgrowth in cultured hippocampal neurons [72]. The depletion of GSLs might be the primary effector responsible for this phenotype as inhibition of GluCer synthesis decreases axonal outgrowth as well as axonal branching in cultured hippocampal neurons [73], whereas the opposite effect is observed when GluCer degradation is inhibited. As inhibition of ceramide synthesis leads to build-up of the ceramide precursors, sphingosine and sphinganine, it is possible that these precursors contribute to the decrease in axonal growth as treating distal neuritis of cultured rat sympathetic neurons with exogenous sphingosine causes neurites to retract and/or degenerate [74]. GM1 may very well be a central player in determining axonal fate, as Neu3, which converts more complex gangliosides to GM1, is essential for determining which growth cone of unpolarized neurons will become the axon (axon specification) in rat primary embryonic hippocampal neurons [69]. Consistently, overexpression of Neu3 accelerates the axon specification as well as axonal growth, while suppressing Neu3 activity blocks axonal generation [69]. Furthermore, NGF-induced polarization is significantly enhanced by Neu3 overexpression, which is in line with a pronounced increase in TrkA phosphorylation, indicating Neu3 induces axon specification through enhancing TrkA signalling [69].

Purkinje cells are some of the largest neurons in the human brain and are characterized by their extensive dendritic arborization. It has been shown that inhibition of CERS activity compromises dendrite genesis by decreasing length, expanse and arborization of dendrites along with reduced survival of rat Purkinje cells [75]. Consistent with the fact that CERS1 is the primary neuronal CERS, loss of CERS1 function in mice leads to shortening of dendritic arbours and degeneration of Purkinje cells [76]. Similar phenotypes have been observed for inhibition of SPT in Purkinje neurons, indicating that the de novo sphingolipid synthesis is pivotal for dendritic development and survival [77]. Pinpointing the sphingolipid species responsible for these phenotypes is highly challenging. Purkinje cell-specific knockout (KO) of the glucosyltransferase has little effect on dendrites, but leads to axonal degeneration and disrupted myelin sheath, which suggests that GSLs are not responsible for the dendritic phenotypes [78]. Inhibition of CERS activity and loss of CERS1 in Purkinje cells result in accumulation of the ceramide precursors sphinganine, sphingosine and 1-deoxysphinganine [76,79]. Ectopic expression of CERS2 in neurons suppresses Purkinje cell death in *CerS1*$^{-/-}$ mice through restoration of LCBs to wild-type levels indicating that elevation of LCBs is the primary cause of neuronal death in CERS1-deficient mice [79]. This is supported by the observation that treatment of cultured neurons with LCB levels corresponding to the levels found in the brain of *CerS1*$^{-/-}$ mice causes neurite fragmentation [79]. Thus, LCBs may be a central player of neurodegeneration upon disruption of the sphingolipid metabolism.

During brain development neurons migrate to a final localization where they interact with their appropriate signalling partners ensuring correct formation of pre- and post-synaptic elements at the right time and place. Early in the developing rat nervous system the expression of a variant of GD3, 9-O-acetyl GD3, appears to be involved in glial-guided neuronal migration and neurite outgrowth [80]. A similar role might be performed by GM1 in the early stages of the human brain development as GM1 has been implicated in glial-neuronal contacts during the migration of neuroblasts [81].

Synapses are key sites of communication between neuronal cells where the presynaptic cell propagates a response to the postsynaptic cell through either a chemical or electrical signal. Compartmentalization is pivotal at synapses in order to transmit the signal as efficiently as possible. In rat hippocampal neurons disruption of microdomains by simultaneous cholesterol depletion and CERS inhibition leads to fewer, but larger clusters of both the excitatory AMPA receptor and the inhibitory $GABA_A$ receptor [82]. Structurally the microdomain disruption means loss of inhibitory and excitatory synapses as well as reduction in the number of dendritic spines [82]. As excitatory synapses are usually located on spines in hippocampal neurons the morphological consequences caused by microdomain disruption most probably also have functional consequences. This is in line with the fact that gradual loss of synapses and spines are characteristic for neurodegenerative diseases [83].

4.2. Sphingolipids mediating axon-glial architecture

Myelination of axons is crucial in order to provide electrical insulation of axons ensuring rapid and efficient action potential propagation. Proper myelination in the CNS requires oligodendrocytes to form multilayered myelin membranes wrapped around axons, the myelin sheaths, which involves precise sorting and compartmentalization of myelin proteins as well as GSLs and galactosphingolipids into microdomains (reviewed in [3,55,84]). Disruption hereof leads to deterioration of myelin, resulting in axon degeneration, which contributes to the pathogenesis of demyelinating diseases [14]. Indeed, myelin defects have been associated with several enzymes of the sphingolipid pathway including the GM2/

GD2 synthase, UDP-galactose:ceramide galactosyltransferase (CGT) and GalCer sulfotransferase (CST) [85–89].

Formation and stability of the myelin sheath depends on protein–lipid interaction between the sheath and axon, but it also depends on lipid–lipid interactions between myelin sheath layers. Gangliosides GD1a and GT1b localized in microdomains in the axonal membrane interact and regulate the myelin protein myelin-associated glycoprotein (MAG) [87,90,91], which itself is located in GalCer-enriched microdomains in mature myelin [92]. Disturbance of GD1a and GT1b in neurons by either neuramidase treatment, blockage of ganglioside biosynthesis or blockage of access by specific IgG-class anti-ganglioside antibodies all prevent MAG-mediated inhibition of neurite outgrowth [90]. Other major myelin proteins found within GalCer-enriched microdomains in mature myelin are myelin basic protein (MBP), 2′,3′-cyclic-nucleotide 3′-phosphodiesterase (CNP), myelin/oligodendrocyte glycoprotein (MOG) and proteolipid protein (PLP) [92]. Sorting of the myelin proteins into the GalCer-enriched microdomains may already occur in the Golgi apparatus as it has been shown that PLP association with GalCer- and cholesterol-enriched microdomains in the Golgi is necessary for correct localization in the membrane of oligodendrocytes [93]. Besides controlling the localization of the major myelin proteins, GalCer contributes to the long-term stability of myelin by interacting with sulfatide located in the membrane of opposing layers in the myelin sheath forming what is known as a glycosynapse [94,95].

Between myelin sheaths there are regularly spaced unmyelinated regions of the axon, also known as nodes of Ranvier, where ion channels driving the action potential propagation are highly enriched. The structural stability of the nodes and their neighbouring functional regions (paranodal, juxtaparanodal and internode region) depends on cell adhesion molecules (CAMs) in the axonal and glial membranes, as well as oligodendrial GalCer and sulfatide [85,86,96,97]. Disturbances of the nodes of Ranvier have been observed in CGT-deficient mice lacking the ability to synthesize both GalCer as well as sulfatide, and in CST-deficient mice, which are unable to synthesize sulfatide from GalCer [96,98]. Both mice strains have disrupted axo–glial interactions, which in turn lead to dislocation of axolemma proteins including juxtaparanodal K^+ channels transcending into the paranodal region and diffuse distribution of the axonal CAMs contactin-associated protein (Caspr) and paranodin [86,96,98]. These disturbances result in conduction deficits and pronounced tremor combined with progressive ataxia [86,89]. Similar ultrastructural dysfunctions may very well be present in the *CerS2*$^{-/-}$ mouse. As mentioned, CERS2 is responsible for the synthesis of very-long-chain ceramides including C22 and C24 ceramide. The lipid composition of myelin in CERS2-deficient mice is significantly changed on the level of ceramide, SM, and in particular GalCer [99]. As WT mice age from birth to 1 month, the acyl chain length of GalCer changes from C18 to C22/C24 coinciding with active myelination. As *CerS2*$^{-/-}$ mice are not able to compensate for the loss of C22 and C24 GalCer, these mice develop unstable myelin including degeneration and detachment [99]. This is consistent with myelin degeneration after the age of 1.5 months as seen in CGT-deficient mice [86]. Not only galactolipids have proven to be important for maintaining the structure of the nodes of Ranvier; imbalance in the ganglioside profile has been shown to challenge their stability. Mice deficient in the GM2/GD2 synthase have normal levels of ganglioside, but express only the simple gangliosides GM3 and GD3, yet no major abnormalities have been observed in the gross development of their nervous system [100]. However, ultrastructural defects have been detected, including axon degeneration and demyelination resulting in progressive behavioural neuropathies as deficits in strength, coordination and balance as well as development of tremor and catalepsy [88,100]. GM2/GD2 synthase-deficient mice have abnormal microdomain composition at the nodes of Ranvier affecting the myelination, which might be explained by attenuated expression of the axonal CAM Caspr and the glial CAM neurofascin 155 (NF155) [85]. Furthermore, in these mice the microdomain disturbance leads to mislocalization of K^+ channels and Na^+ channels that in turn results in ion channel dysfunction and reduced motor nerve conduction [85]. These effects only get more prominent with age.

4.3. Neuronal plasticity

The brain is far from being static after development has completed. Throughout life the brain adapts to stimuli, which underlie functions of learning, behaviour and memory, and it is this ability that helps the brain to overcome brain damage. Neuronal plasticity is evident as modulation of synapse efficacy, which is controlled by organization and composition of the synapse structure. As sphingolipids play an important role in organizing neuronal membranes, it is not surprising that alterations in the sphingolipid pathway have been associated with disturbances in neuronal plasticity.

Several lines of evidence point towards the neutral sphingomyelinase-2 (nSMase) being able to modulate postsynaptic function. nSMase is enriched in the hippocampus, where it quickly can hydrolyse SM to ceramide [101]. It has been shown that nSMase regulates excitatory postsynaptic currents by controlling membrane insertion and clustering of NMDA receptors [102]. Not surprisingly, mice deficient in nSMase show compromised plasticity by having impaired spatial and episodic-like memory [103]. It is becoming evident that the balance between SM and ceramide is important in order to maintain a normal state of mind as increased level of ceramide has been associated with major depression [104,105]. Several anti-depressant drugs have been shown to inhibit the aSMase thereby lowering the concentration of ceramide in the hippocampus resulting in increased neuronal proliferation, maturation and survival as well as improving stress-induced depression in mice [104]. Similar effects are seen in mice deficient in aSMase activity, while the reverse is observed in mice accumulating ceramide by either overexpression of aSMase, heterozygous loss of acid ceramidase, pharmalogic inhibition of ceramide metabolism or direct injections of C16 ceramide into the hippocampus [104]. Thus the concentration of ceramide appears to determine the behaviour mediated through hippocampal functions.

Synaptic plasticity covers several phenomena including long-term potentiation (LTP), the strengthening of synapse signalling through repeated presynaptic stimulation. LTP is one of the major mechanisms constituting the basis for memory and learning. The molecular mechanisms governing LTP are diverse, and are neuronal and region-specific [106]. In the hippocampus, regulation of the glutamate receptor NMDA in number and localization in postsynaptic

membranes is one of these mechanisms. NMDA receptors localize to membrane microdomains enriched in sphingolipids [102,107], indicating that the sphingolipids may very well be involved in NMDA-mediated LTP. Indeed, several studies have associated exogenous gangliosides with regulation of LTP in hippocampal neurons [108,109]. Both exogenous GQ1b and stimulation of ganglioside synthesis enhance ATP-induced LTP in hippocampal CA1 neurons, which can be blocked by NMDA antagonists [109]. Furthermore, GQ1b has been found to increase brain-derived neurotrophic factor (BDNF), an important protein in synaptic plasticity, through regulation of the NMDA receptor in rat cortical neurons [110]. Understanding the mechanisms behind sphingolipid modulation of neural plasticity will be a valuable tool in treatment of disabilities of learning, behaviour and memory as well as brain injury.

5. Brain ion channels and receptors in microdomains

A vast number of ion channels and receptors have been reported to localize to brain membrane microdomains (reviewed in [7] and [111]). However, the focus has primarily been on microdomains defined by detergent methods and cholesterol depletion and less on the role of sphingolipids. Table 1 gives an overview of neuronal ion channels and receptors that have been shown to be affected by sphingolipids. When interpreting the effect of changed sphingolipid metabolism on ion channel/receptor function, it should be kept in mind that table 1 includes findings in neuronal cells as well as in non-neuronal model cells. Future research will help determine whether or not the findings in the non-neuronal cells can be equated with neurons.

The multifaceted nature of membrane microdomains is reflected in the way they regulate ion channel and receptor functions. The effect can be direct through protein–lipid interactions, but also more indirect by influencing the physical properties of the membrane. The consequence of the effect is highly dependent on the ion channel/receptor in question, and can include alterations in kinetics, membrane localization and trafficking. Yet some overall regulation strategies can be deduced, which are described in the following sections.

The list of sphingolipid-binding proteins is expanding, but only relatively few sphingolipid-binding motifs have been identified [129–131]. SM has been shown to regulate the activity of the Kv2.1 channel by interacting with the helix-turn-helix motif found in the S3b and S4 voltage-sensing domains of the channel in oocytes [113,116]. Hydrolysis of SM into ceramide profoundly inhibits K^+ conductance along with ionic and gating currents [113]. The latter was also observed for the Kv1.3 channel pointing towards a general regulation mechanism of the channel's voltage sensor by SM. Furthermore, hydrolysis of SM into ceramide-1-phosphate causes a hyperpolarization shift in the conductance–voltage relation along with slowing of the deactivation, which overall leads to a stabilization of the open state of Kv2.1 [113,116,117]. However, removal of SM phosphoheads also inhibits K^+ conductance of the Kir1.1 channel, which contains no voltage sensor, indicating that SM has several modes of ion channel regulation [113].

The major feature of microdomains is their ability to include or exclude proteins and thereby dictate which proteins are in close proximity to each other. The tightly packed microdomains favour incorporation of molecules with saturated and unbranched side chains, and thus many of the proteins that reside in the microdomains are often acylated, primarily palmitoylated and/or myristoylated [132,133]. Acylated proteins include postsynaptic density protein 95 (PSD-95), caveolin, GPI-anchored proteins, Src-family of tyrosine kinases and the neural protein GAP-43 [132,134]. As several ion channels are regulated by phosphorylation, co-localization of ion channels with kinases provides a convenient mode of ion channel modulation. It has been shown that Kv1.5 associates with the Src kinase Fyn in mammalian hippocampus through Kv1.5's Src homology 3 (SH3) domain [135]. This association facilitates phosphorylation of Kv1.2 and Kv1.4 subunits, which both lack the SH3 domain, but reside in a heteromultimeric complex with the Kv1.5 subunit. The phosphorylation of Kv1.2 and Kv1.4 leads to suppression of depolarization-evoked currents [135]. Kv1.5 is also an example of an ion channel that localizes to caveolin-rich microdomains. Interestingly, disruption of the microdomains by cholesterol depletion and hindering of ceramide synthesis by inhibition of CERS activity cause hyperpolarizing shifts in both the voltage-dependent activation and inactivation of Kv1.5 in Ltk cells [115].

The strategy of targeting ion channels/receptors to microdomains varies depending on the specific ion channel/receptor. Protein acylation is one strategy, as mentioned above, while recruitment to microdomains through binding to an acylated microdomain-residing protein has proven to be another strategy. PSD-95, a major synaptic scaffolding-protein, is an example of such a protein in the postsynaptic membrane. Palmitoylation of PSD-95, a PSD-95/Dlg/ZO-1 (PDZ) domain protein, localizes it to microdomains to which it has been shown to recruit the Kv1.4 ion channel and NMDA receptor subunits through interaction with the PDZ domain [134,136]. The recruitment of Kv1.4 is eliminated when palmitoylation of PSD-95 is prevented [134,137]. Interestingly, disturbance of the SM/ceramide balance by inhibition of nSMase results in increased level of PSD-95 in mice brain, which further leads to changes in NMDA subunit composition and an increase in AMPA receptors [103]. This illustrates the ripple effect that can occur when alterations in synaptic sphingolipids affect central synapse functions.

Sphingolipids have also proven to be important for the ability of receptors to bind and respond to ligands. Blockage of ceramide synthesis resulting in SM depletion leads to loss of agonist binding to the serotonin$_{1A}$ and serotonin$_7$ receptors in CHO cells and HeLa cells, respectively [122,123]. Furthermore, disturbance of microdomains has been shown to regulate initiation of signal transduction through nicotinic acetylcholine receptors (nAChRs). Simultaneous cholesterol removal and hydrolysis of SM into ceramide in rat hippocampal neurons increased the rate of recovery from desensitization and agonist affinity of the neuronal α7 nAChR, which overall led to slowing of the desensitization kinetics [112]. However, the same treatment gave an opposite effect for the α3β2 nAChR where the desensitization half-time was decreased [112]. This underlines the very individual nature of how ion channels are being regulated by microdomains.

Collectively, the mechanism by which ion channel/receptor functions is altered, and as a consequence of changes, microdomain composition remains elusive in most cases. There are

Table 1. Examples of neuronal ion channels and receptors being affected by sphingolipid metabolism.

	tissue/cell line	functional effects/comments	references
ion channels			
$\alpha3\beta2$ nicotinic acetylcholine receptor	rat hippocampal neurons	removal of cholesterol and hydrolysis of SM into ceramide decreases desensitization half-time	[112]
$\alpha7$ nicotinic acetylcholine receptor	rat hippocampal neurons	removal of cholesterol and hydrolysis of SM into ceramide slows down the desensitization kinetics including increased agonist affinity	[112]
Kir1.1	oocytes	hydrolysis of SM into ceramide inhibits K^+ conductance and decreases ionic and gating currents	[113]
Kv1.3	jurkat T-lymphocytes	constitutively localized in sphingolipid-rich microdomains; generation of ceramide mediates formation of large ceramide-enriched domains and inhibits channel activity	[114]
	oocytes	hydrolysis of SM into ceramide decreases ionic and gating currents	[113]
Kv1.5	Ltk cells	Co-localizes with caveolin; inhibition of CERS activity induces hyperpolarization shift of the activation and inactivation curve	[115]
Kv2.1	oocytes	hydrolysis of SM into ceramide-1-phosphate induces hyperpolarization shift in the conductance–voltage relation	[113,116,117]
	oocytes	interaction with SM. Hydrolysis of SM into ceramide-1-phosphate induces hyperpolarization shift in the conductance–voltage relation; hydrolysis of SM into ceramide decreases current to 90% and reduces gating currents	[113]
	oocytes	interacts with SM probably through the S3b and S4 voltage-sensing domains	[116]
TRPA1	rat trigeminal neurons	SM hydrolysis and inhibition of de novo synthesis of ceramide decrease AITC-induced Ca^{2+} uptake, which is not due to an increase in ceramide or sphingosine	[118]
	rat peripheral sensory nerve terminals	SM hydrolysis inhibits AITC-induced release of CGRP, which is not due to an increase in ceramide or sphingosine	[118]
TRPM8	rat trigeminal neurons	SM hydrolysis and inhibition of de novo synthesis of ceramide decrease icilin-induced Ca^{2+} uptake	[118]
TRPV1	rat trigeminal neurons	SM hydrolysis as well as inhibition of the synthesis of GSLs and de novo ceramide decrease both capsaicin- and resiniferatoxin-evoked Ca^{2+} uptake	[119]
	rat trigeminal neurons	SM hydrolysis and inhibition of de novo synthesis of ceramide decrease capsaicin-induced Ca^{2+} uptake, which is not due to an increase in ceramide or sphingosine	[118]
	rat peripheral sensory nerve terminals	SM hydrolysis inhibits capsaicin-induced release of CGRP, which is not due to an increase in ceramide or sphingosine	[118]
GPCRs			
AMPA receptor	rat hippocampal neurons	disruption of microdomains by simultaneous cholesterol depletion and CERS inhibition results in fewer, but larger receptor clusters; loss of synapses and dendritic spines	[82]
$GABA_A$	rat hippocampal neurons	disruption of microdomains by simultaneous cholesterol depletion and CERS inhibition result in fewer, but larger receptor clusters, meaning reduced synapse number; loss of synapses and dendritic spines	[82]

(*Continued*.)

Table 1. (*Continued.*)

	tissue/cell line	functional effects/comments	references
NMDA receptor	rat forebrain	localized into PSD-95-rich microdomains and synaptic microdomains	[107]
	rat hippocampal neurons	generation of ceramide by TNFα-induced activation of nSMase2 stimulate NMDA receptor clustering	[102]
	CA1 pyramidal cells in rat hippocampal slices	C_2-ceramide induces a sustained synaptic current depression probably mediated through the activation of protein phosphatases 1 and/or 2A	[120]
	rat hippocampal slices	long-term treatment with S1P agonist increases phosphorylation and membrane level of NMDA receptor subunit GluN2B probably through activation of the microdomain-associated Src kinase Fyn	[121]
serotonin$_{1A}$ receptor	CHO cells	inhibition of ceramide synthesis leads to impaired function of the serotonin$_{1A}$ receptor due to reduced ligand binding	[122]
serotonin$_7$ receptor	HeLa cells	inhibition of ceramide and GSL synthesis reduces maximum agonist binding	[123]
other receptors			
Trk A	PC12 cells	GM1 directly associates with Trk and enhances neurite outgrowth and neurofilament expression induced by nerve growth factor (NGF)	[66]
		GM1 enhances NGF-dependent homodimerization of Trk	[68]
		GM1 depletion by inhibition of GluCer synthase inhibits NGF-induced neurite outgrowth, which is abolished by co-treatment with GM1	[67]
EGFR	mouse neural stem cells	GD3 mediates membrane microdomain localization of EGFR; ablation of GD3 results in reduced level of EGFR expression and accelerates EGF-induced EGFR degradation leading to decreased self-renewal capability	[59]
insulin receptor	*CerS2*$^{-/-}$ mouse liver	lack of C22–C24 ceramides inhibits phosphorylation and translocation of the insulin receptor into microdomains upon insulin stimulation	[124]
	Huh7 cells	clustering of GM2 inhibits signalling through the insulin receptor by excluding the receptor from non-caveolar membrane microdomains	[125]
	3T3-L1 adipocytes	TNFα-induced accumulation of GM3 eliminates insulin receptor from microdomains and inhibits insulin signalling	[126]
		GM3 disturbs interaction between the insulin receptor and caveola protein Cav-1 resulting in exclusion of the receptor from caveola and impairs insulin signalling	[127]
		inhibition of GluCer synthase counteracts TNFα-induced abnormalities in insulin signalling by normalizing GM2 and GM3 levels	[128]

many possible scenarios of how changes in the sphingolipid metabolism may affect the synaptic structure and hence function: lack of lipid–protein interaction, mislocalization, incorrect assembly of ion channel/receptor subunits, hindering of activity-regulating proteins/factors, changes in trafficking, altered agonist affinity and so on. Extensive research is needed in order to decipher the role of sphingolipids in regulation synaptic function through microdomains.

6. Sphingolipids and microdomains in neurological diseases

In the previous sections, we have discussed how alterations in sphingolipid metabolism can lead to abnormal organization and functions of membrane microdomains, and how functions of many neuronal ion channels and receptors depend on proper microdomain composition and integrity. Not surprisingly, defects in the sphingolipid metabolism have been linked to numerous neurological diseases, including Alzheimer's disease (AD), Parkinson's disease (PD), several types of epilepsy, Huntington's disease, Krabbe's disease, Gaucher's disease, inherited sensory and autonomic neuropathy, and dementia. This section outlines examples of how sphingolipids and microdomains are involved in the development of neurological diseases.

6.1. Alzheimer's disease

One of the major characteristics of AD is accumulation of the amyloid beta-peptide (Aβ), which ultimately leads to

formation of plaques linked to disease progression. Several key enzymes associated with AD have been shown to localize to membrane microdomains including amyloid precursor protein (APP), β-site APP cleaving enzyme (BACE-1), γ-secretase complex and neprilysin (an Aβ-degrading enzyme) (reviewed in [2,18,138]). Co-localization of APP and secretases in microdomains promotes APP processing leading to accumulation of Aβ, which is abolished upon microdomain disturbance by cholesterol depletion [139]. An SM-binding motif has been identified in Aβ, and *in vitro* studies have shown that SM promotes aggregation of Aβ [130,140]. Accumulation of Aβ leads to SM depletion by activation of SMase, which is thought to disrupt a range of protein–lipid interactions and hence downstream signalling pathways [141]. Furthermore, activation of aSMase correlates with reported elevated levels of ceramide in the brain and cerebrospinal fluid of AD patients, which possibly is a result of increased expression of CERS1, CERS2, aSMase, nSMase and galactosylceramidase [142–146]. Spreading of plaque formation in the brain is thought to involve ceramide-enriched exosomes of Aβ and phosphorylated Tau [147]. A recent study has shown that ablation of nSMase in the AD mouse model 5xFAD improves AD pathology by reducing brain exosomes, ceramide levels, Aβ, phosphorylated Tau and plaques [148]. Thus, tilting the SM/ceramide balance towards ceramide contributes to the development of AD.

Evidence points towards gangliosides contributing to the initiation and progression of AD. Using model membranes, it has been shown that Aβ can bind to GM1 and that GM1 facilitates Aβ aggregation in membrane microdomains [149,150]. Consistently, increased levels of GM1 and GM2 have been found in microdomains isolated from the frontal and temporal cortex of AD patients and in brains of AD mice models, which correlate with accelerating plaque formation [151–153]. Recently, GM1 has been proposed to have a protective role towards Aβ aggregation rather than contributing to it. Using physiological concentrations of GM1 and Aβ in model membranes, it has been shown that GM1 in nanodomains does not induce Aβ oligomerization, but rather prevents SM-induced aggregation [140]. Thus, as the overall level of GM1 decreases during ageing [154], the protective role of GM1 decreases, thereby contributing to the onset of AD. However, it has been shown that GM1 is enriched in microdomains isolated from mice synaptosomes in an age-dependent manner despite an overall reduction of GM1 with age [57], indicating that regionally GM1 might facilitate plaque formation. The latter is supported by enrichment of GM1 and GM2 found in microdomains isolated from AD patients [151]. Additional studies are necessary in order to elucidate the role of GM1 in plaque formation in AD, which probably depends on the timing of disease onset [152].

It is evident that AD is accompanied by deregulated sphingolipid metabolism, yet the precise mechanisms behind AD pathogenesis need to be clarified. Meanwhile, a sphingolipid profile and microdomain composition might function as a diagnostic tool in the development of AD.

6.2. Parkinson's disease

The cause of PD is generally not known, but it is characterized by accumulation and fibrillation of α-synuclein in neurons leading to neurodegeneration. An increasing number of studies report that mutations in the glucocerebrosidase (GCase) gene confer increased susceptibility to the development of PD [155–158]. A reduced activity of GCase has been found in the brain of PD patients [159,160]. In line with this, GCase deficiency promotes accumulation of α-synuclein in cultured neurons [161]. GCase is located in lysosomes where it cleaves GluCer into ceramide and glucose. α-synuclein has been shown to bind to gangliosides, sharing the GluCer core structure, derived from the human brain [162]. GCase deficiency leading to increase in GluCer has been shown to control intracellular accumulation of α-synuclein in mice and human brains as well as in cultured neurons [161]. Additionally, the assemblies of α-synuclein were shown to inhibit normal activity of GCase and maturation of lysosomes, thereby contributing to pathology [161].

Other studies show no changes in the level of GluCer in human PD brains [163,164], indicating that GluCer is not pivotal to PD development. The attention has turned to membrane microdomains as α-synuclein has been observed to bind to lipids within these microdomains [165]. Indeed, membrane microdomains isolated from the frontal cortex of patients with incidental PD display profound alterations in lipid composition with a higher content of saturated lipids and lower content of unsaturated lipids as well as a reduction in cerebrosides and sulfatide, which overall indicates an increase in microdomain order [166]. GM1 has been of great interest as it binds α-synuclein, thereby promoting oligomerization. [167]. However, treatment of primate PD models with GM1 has shown beneficial effects including restoring neurochemical and physiological parameters [168–170]. Additionally, a study has shown that a consistent portion of PD patients have increased anti-GM1 antibodies [171]. The positive effect of GM1 may be explained by its ability to stabilize α-synuclein in an α-helix structure, thereby preventing fibrillation [167]. This effect is abolished in the familial PD mutant A30P of α-synuclein. Further studies are necessary in order to elucidate the role of membrane microdomains and sphingolipids in PD development.

6.3. Epilepsy

An increasing number of studies implicate defects in the sphingolipid metabolism, both in the biosynthesis and degradation pathway, with the development of epilepsy. Although our knowledge of how these defects affect membrane microdomains in the epileptic brains is limited, it can be speculated that the changed sphingolipid profiles perturb microdomain functions.

Recently, a homozygous mutation in the *CERS1* gene and a heterozygous deletion of the *CERS2* gene have been associated with the development of progressive myoclonic epilepsy [172,173]. CERS1 is the primary CERS in neurons responsible for synthesis of C18 ceramide. Downregulation of CERS1 in a neuroblastoma cell line induces ER stress and proapoptotic pathways, which points towards a role of CERS1 in neurodegeneration [172]. CERS1 deficiency in mice results in a pronounced decrease in brain gangliosides, along with diminution and neuronal apoptosis in the cerebellum [76,174]. Moreover, loss of CERS1 also causes impaired lysosomal degradation leading to accumulation of lipofuscin, which is a common mechanism observed in ageing and neurodegenerative diseases [76]. CERS1 deficiency in mice also leads to a reduction in MAG in oligodendrocytes, indicating how the lipid composition of neuronal membranes can affect the

protein expression in oligodendrocytes [174]. CERS2 is the major CERS in oligodendrocytes, and lipidomic analysis of skin fibroblasts from the *CERS2*$^{+/-}$ patient shows that the SM profile resembles the changes in SM observed in the *CerS2*$^{-/-}$ mice [99,173,175,176]. CERS2 is important for maintaining membrane integrity shown by severely altered biophysical properties of membranes isolated from the brain of *CerS2*$^{-/-}$ mice [177]. Ablation of CERS2 in mice results in degeneration and detachment of myelin as well as cerebellar degeneration [99,175]. The latter again pinpoints the functional relationship between neurons and oligodendrocytes as insufficient myelination of neurons leads to their degeneration.

There have been multiple reports associating mutations in the gene encoding the aCDase with spinal muscular atrophy with progressive myoclonic epilepsy (SMA-PME) [178–181], although initially the interest of aCDase was on its involvement in the lysosomal storage disease Farber's disease [182]. Loss of aCDase in mice is embryonically lethal due to early apoptotic cell death [183]. It has been speculated that the development of SMA-PME instead of Farber's disease is a result of different residual activities of aCDase in the two diseases [182]. Knockdown of the aCDase orthologue in zebrafish compromises motor neuron axonal branching and increases apoptosis in the spinal cord [178]. It is known that increased levels of ceramide rearrange microdomains into larger membrane domains of which one of the possible outcomes is apoptosis [182,184]. Thus, control of ceramide levels is crucial in order to prevent neuronal loss.

Defect ganglioside biosynthesis has been associated with the development of epilepsy through the discovery of a homozygous loss-of-function mutation of the GM3 synthase gene linked to infantile-onset symptomatic epilepsy syndrome and refractory epilepsy [185,186]. Loss of GM3 synthase activity in the affected children was accompanied by complete lack of GM3 and its downstream biosynthetic derivatives in plasma with evidence of increased flux through the remaining functional ganglioside synthesis pathways [185]. However, a compensatory effect is not observed in patient-derived GM3 synthase-deficient skin fibroblasts, which have a 93% reduction in ganglioside content compared with control skin fibroblasts [187]. This leads to a decrease in EGF-induced proliferation as well as migration of the patient skin fibroblasts caused by lack of GM3 facilitation of EGF binding to the EGFR receptor, which is known to localize to membrane microdomains [187,188]. GM3 synthase-deficient mice show no obvious neurological defects [189], and thus an alternative model system must be employed in order to evaluate the role of GM3 synthase in brain membrane microdomains.

7. Concluding remarks

Genetically engineered mice models with defective sphingolipid metabolism at various stages of the sphingolipid pathway have paved the way for understanding how sphingolipids are involved in regulating the nervous system. The phenotypes observed in KO mice deficient in ganglioside synthases have often been milder than expected, pointing towards a redundancy in the functions of gangliosides. Yet some ganglioside functions are highly specific and cannot be substituted for by others. It is important to take into account that what we see in mice models might not be representative for humans. For instance, KO of the GM3 synthase in mice does not show any major abnormalities [190], while the human equivalent has been diagnosed with infantile-onset symptomatic epilepsy [185,186]. Thus, even though our knowledge of how the brain functions has expanded substantially through animal models, we must always keep in mind the limitations of these models.

Membrane microdomains play a central role in brain development and maintenance. The existence of membrane microdomains has been highly debated, but accumulating evidence indicates that the lipid composition of the plasma membrane is very heterogeneous and laterally organized into microdomains [191]. Technological advances such as stimulated emission depletion (STED) microscopy now allow us to visualize these former enigmatic compartments in living cells [16,17]. Perturbations of the sphingolipid metabolism affect dynamics, integrity and functions of the microdomains. Disarrangement of sphingolipid microdomains has been associated with numerous neurological diseases, and it has been proposed that analysis of membrane microdomain disorder can function as a diagnostic tool in the early diagnosis of neuropathological development [18]. The challenge is how to take advantage of this early diagnosis in the treatment of patients as it can be challenging to distinguish between primary and secondary effects. Future research will help clarify the role of sphingolipids in neurological disorders, and further reveal whether individual sphingolipid species or collective changes in the sphingolipid profile are primary effectors. This will be pivotal in the development of therapeutic strategies in treatment of sphingolipid related neurological diseases.

Authors' contributions. A.S.B.O. wrote the first draft of manuscript; A.S.B.O. and N.J.F. completed the manuscript

Competing interests. We declare we have no competing interests.

Funding. This work was supported by the Lundbeck Foundation (12097) and the Danish Council for Independent Research, Natural Sciences (23459).

Acknowledgements. We thank Louise Cathrine Braun Elmelund-Præstekær for proofreading and discussion of the manuscript.

References

1. van Echten-Deckert G, Herget T. 2006 Sphingolipid metabolism in neural cells. *Biochim. Biophys. Acta* **1758**, 1978–1994. (doi:10.1016/j.bbamem.2006.06.009)
2. Piccinini M *et al.* 2010 Deregulated sphingolipid metabolism and membrane organization in neurodegenerative disorders. *Mol. Neurobiol.* **41**, 314–340. (doi:10.1007/s12035-009-8096-6)
3. Aureli M, Grassi S, Prioni S, Sonnino S, Prinetti A. 2015 Lipid membrane domains in the brain. *Biochim. Biophys. Acta* **1851**, 1006–1016. (doi:10.1016/j.bbalip.2015.02.001)
4. O'Brien JS, Sampson EL. 1965 Lipid composition of the normal human brain: gray matter, white matter, and myelin. *J. Lipid Res.* **6**, 537–544.
5. Svennerholm L, Vanier MT. 1973 The distribution of lipids in the human nervous system. IV. Fatty acid composition of major sphingolipids of human infant

brain. *Brain Res.* **55**, 413–423. (doi:10.1016/0006-8993(73)90306-5)

6. Svennerholm L, Bostrom K, Jungbjer B, Olsson L. 1994 Membrane lipids of adult human brain: lipid composition of frontal and temporal lobe in subjects of age 20 to 100 years. *J. Neurochem.* **63**, 1802–1811. (doi:10.1046/j.1471-4159.1994.63051802.x)
7. Dart C. 2010 Lipid microdomains and the regulation of ion channel function. *J. Physiol.* **588**, 3169–3178. (doi:10.1113/jphysiol.2010.191585)
8. Nicolau Jr DV, Burrage K, Parton RG, Hancock JF. 2006 Identifying optimal lipid raft characteristics required to promote nanoscale protein–protein interactions on the plasma membrane. *Mol. Cell. Biol.* **26**, 313–323. (doi:10.1128/mcb.26.1.313-323.2006)
9. Simons K, Ikonen E. 1997 Functional rafts in cell membranes. *Nature* **387**, 569–572. (doi:10.1038/42408)
10. Lingwood D, Simons K. 2010 Lipid rafts as a membrane-organizing principle. *Science* **327**, 46–50. (doi:10.1126/science.1174621)
11. Saher G, Quintes S, Nave KA. 2011 Cholesterol: a novel regulatory role in myelin formation. *The Neuroscientist* **17**, 79–93. (doi:10.1177/1073858410373835)
12. Pfrieger FW, Ungerer N. 2011 Cholesterol metabolism in neurons and astrocytes. *Progr. Lipid Res.* **50**, 357–371. (doi:10.1016/j.plipres.2011.06.002)
13. Schengrund CL. 2015 Gangliosides: glycosphingolipids essential for normal neural development and function. *Trends Biochem. Sci.* **40**, 397–406. (doi:10.1016/j.tibs.2015.03.007)
14. Pike LJ. 2004 Lipid rafts: heterogeneity on the high seas. *Biochem. J.* **378**, 281–292. (doi:10.1042/bj20031672)
15. Razani B, Woodman SE, Lisanti MP. 2002 Caveolae: from cell biology to animal physiology. *Pharmacol. Rev.* **54**, 431–467. (doi:10.1124/pr.54.3.431)
16. Eggeling C *et al.* 2009 Direct observation of the nanoscale dynamics of membrane lipids in a living cell. *Nature* **457**, 1159–1162. (doi:10.1038/nature07596)
17. Ekyalongo RC, Nakayama H, Kina K, Kaga N, Iwabuchi K. 2015 Organization and functions of glycolipid-enriched microdomains in phagocytes. *Biochim. Biophys. Acta* **1851**, 90–97. (doi:10.1016/j.bbalip.2014.06.009)
18. Marin R, Rojo JA, Fabelo N, Fernandez CE, Diaz M. 2013 Lipid raft disarrangement as a result of neuropathological progresses: a novel strategy for early diagnosis? *Neuroscience* **245**, 26–39. (doi:10.1016/j.neuroscience.2013.04.025)
19. Ohmi Y, Ohkawa Y, Yamauchi Y, Tajima O, Furukawa K, Furukawa K. 2012 Essential roles of gangliosides in the formation and maintenance of membrane microdomains in brain tissues. *Neurochem. Res.* **37**, 1185–1191. (doi:10.1007/s11064-012-0764-7)
20. Astudillo L, Sabourdy F, Therville N, Bode H, Segui B, Andrieu-Abadie N, Hornemann T, Levade T. 2015 Human genetic disorders of sphingolipid biosynthesis. *J. Inherit. Metab. Dis.* **38**, 65–76. (doi:10.1007/s10545-014-9736-1)
21. Ong WY, Herr DR, Farooqui T, Ling EA, Farooqui AA. 2015 Role of sphingomyelinases in neurological disorders. *Expert Opin. Therapeutic Targets* **19**, 1725–1742. (doi:10.1517/14728222.2015.1071794)
22. Gault CR, Obeid LM, Hannun YA. 2010 An overview of sphingolipid metabolism: from synthesis to breakdown. *Adv. Exp. Med. Biol.* **688**, 1–23. (doi:10.1007/978-1-4419-6741-1_1)
23. Zheng W *et al.* 2006 Ceramides and other bioactive sphingolipid backbones in health and disease: lipidomic analysis, metabolism and roles in membrane structure, dynamics, signaling and autophagy. *Biochim. Biophys. Acta* **1758**, 1864–1884. (doi:10.1016/j.bbamem.2006.08.009)
24. Lahiri S, Futerman AH. 2007 The metabolism and function of sphingolipids and glycosphingolipids. *Cell. Mol. Life Sci.* **64**, 2270–2284. (doi:10.1007/s00018-007-7076-0)
25. Karlsson KA. 1970 Sphingolipid long chain bases. *Lipids* **5**, 878–891. (doi:10.1007/BF02531119)
26. Sullards MC, Allegood JC, Kelly S, Wang E, Haynes CA, Park H, Chen Y, Merrill Jr AH. 2007 Structure-specific, quantitative methods for analysis of sphingolipids by liquid chromatography-tandem mass spectrometry: 'inside-out' sphingolipidomics. *Methods Enzymol.* **432**, 83–115. (doi:10.1016/s0076-6879(07)32004-1)
27. Merrill Jr AH. 2011 Sphingolipid and glycosphingolipid metabolic pathways in the era of sphingolipidomics. *Chem. Rev.* **111**, 6387–6422. (doi:10.1021/cr2002917)
28. Sandhoff R. 2010 Very long chain sphingolipids: tissue expression, function and synthesis. *FEBS Lett.* **584**, 1907–1913. (doi:10.1016/j.febslet.2009.12.032)
29. Pruett ST, Bushnev A, Hagedorn K, Adiga M, Haynes CA, Sullards MC, Liotta DC, Merrill Jr AH. 2008 Biodiversity of sphingoid bases ('sphingosines') and related amino alcohols. *J. Lipid Res.* **49**, 1621–1639. (doi:10.1194/jlr.R800012-JLR200)
30. Sonnino S, Chigorno V. 2000 Ganglioside molecular species containing C18- and C20-sphingosine in mammalian nervous tissues and neuronal cell cultures. *Biochim. Biophys. Acta* **1469**, 63–77. (doi:10.1016/S0005-2736(00)00210-8)
31. Hirschberg K, Rodger J, Futerman AH. 1993 The long-chain sphingoid base of sphingolipids is acylated at the cytosolic surface of the endoplasmic reticulum in rat liver. *Biochem. J.* **290**, 751–757. (doi:10.1042/bj2900751)
32. Mandon EC, Ehses I, Rother J, van Echten G, Sandhoff K. 1992 Subcellular localization and membrane topology of serine palmitoyltransferase, 3-dehydrosphinganine reductase, and sphinganine N-acyltransferase in mouse liver. *J. Biol. Chem.* **267**, 11 144–11 148.
33. Michel C, van Echten-Deckert G. 1997 Conversion of dihydroceramide to ceramide occurs at the cytosolic face of the endoplasmic reticulum. *FEBS letters.* **416**, 153–155. (doi:10.1016/S0014-5793(97)01187-3)
34. Michel C, van Echten-Deckert G, Rother J, Sandhoff K, Wang E, Merrill Jr AH. 1997 Characterization of ceramide synthesis: a dihydroceramide desaturase introduces the 4,5-trans-double bond of sphingosine at the level of dihydroceramide. *J. Biol. Chem.* **272**, 22 432–22 437. (doi:10.1074/jbc.272.36.22432)
35. Levy M, Futerman AH. 2010 Mammalian ceramide synthases. *IUBMB Life* **62**, 347–356. (doi:10.1002/iub.319)
36. Vacaru AM, Tafesse FG, Ternes P, Kondylis V, Hermansson M, Brouwers JF, Somerharju P, Rabouille C, Holthuis JC. 2009 Sphingomyelin synthase-related protein SMSr controls ceramide homeostasis in the ER. *J. Cell Biol.* **185**, 1013–1027. (doi:10.1083/jcb.200903152)
37. Sprong H, Kruithof B, Leijendekker R, Slot JW, van Meer G, van der Sluijs P. 1998 UDP-galactose:ceramide galactosyltransferase is a class I integral membrane protein of the endoplasmic reticulum. *J. Biol. Chem.* **273**, 25 880–25 888. (doi:10.1074/jbc.273.40.25880)
38. Palmano K, Rowan A, Guillermo R, Guan J, McJarrow P. 2015 The role of gangliosides in neurodevelopment. *Nutrients* **7**, 3891–3913. (doi:10.3390/nu7053891)
39. Valaperta R, Chigorno V, Basso L, Prinetti A, Bresciani R, Preti A, Miyagi T, Sonnino S. 2006 Plasma membrane production of ceramide from ganglioside GM3 in human fibroblasts. *FASEB J.* **20**, 1227–1229. (doi:10.1096/fj.05-5077fje)
40. Jenkins RW, Canals D, Hannun YA. 2009 Roles and regulation of secretory and lysosomal acid sphingomyelinase. *Cell. Signall.* **21**, 836–846. (doi:10.1016/j.cellsig.2009.01.026)
41. Tani M, Kuge O. 2009 Sphingomyelin synthase 2 is palmitoylated at the COOH-terminal tail, which is involved in its localization in plasma membranes. *Biochem. Biophys. Res. Commun.* **381**, 328–332. (doi:10.1016/j.bbrc.2009.02.063)
42. Mullen TD, Hannun YA, Obeid LM. 2012 Ceramide synthases at the centre of sphingolipid metabolism and biology. *Biochem. J.* **441**, 789–802. (doi:10.1042/bj20111626)
43. Hannun YA, Obeid LM. 2011 Many ceramides. *J. Biol. Chem.* **286**, 27 855–27 862. (doi:10.1074/jbc.R111.254359)
44. Norton WT, Poduslo SE. 1973 Myelination in rat brain: changes in myelin composition during brain maturation. *J. Neurochem.* **21**, 759–773. (doi:10.1111/j.1471-4159.1973.tb07520.x)
45. Mansson JE, Vanier MT, Svennerholm L. 1978 Changes in the fatty acid and sphingosine composition of the major gangliosides of human brain with age. *J. Neurochem.* **30**, 273–275. (doi:10.1111/j.1471-4159.1978.tb07064.x)
46. Svennerholm L, Bostrom K, Fredman P, Mansson JE, Rosengren B, Rynmark BM. 1989 Human brain gangliosides: developmental changes from early fetal stage to advanced age. *Biochim. Biophys. Acta* **1005**, 109–117. (doi:10.1016/0005-2760(89)90175-6)
47. Sastry PS. 1985 Lipids of nervous tissue: composition and metabolism. *Progr. Lipid Res.* **24**, 69–176. (doi:10.1016/0163-7827(85)90011-6)

48. Norton WT, Autilio LA. 1966 The lipid composition of purified bovine brain myelin. *J. Neurochem.* **13**, 213–222. (doi:10.1111/j.1471-4159.1966.tb06794.x)
49. Posse de Chaves E, Sipione S. 2010 Sphingolipids and gangliosides of the nervous system in membrane function and dysfunction. *FEBS Lett.* **584**, 1748–1759. (doi:10.1016/j.febslet.2009.12.010)
50. Tettamanti G. 2004 Ganglioside/glycosphingolipid turnover: new concepts. *Glycoconjugate J.* **20**, 301–317. (doi:10.1023/B:GLYC.0000033627.02765.cc)
51. Kracun I, Rosner H, Drnovsek V, Heffer-Lauc M, Cosovic C, Lauc G. 1991 Human brain gangliosides in development, aging and disease. *Inter. J. Dev. Biol.* **35**, 289–295.
52. Segler-Stahl K, Webster JC, Brunngraber EG. 1983 Changes in the concentration and composition of human brain gangliosides with aging. *Gerontology* **29**, 161–168. (doi:10.1159/000213109)
53. Ngamukote S, Yanagisawa M, Ariga T, Ando S, Yu RK. 2007 Developmental changes of glycosphingolipids and expression of glycogenes in mouse brains. *J. Neurochem.* **103**, 2327–2341. (doi:10.1111/j.1471-4159.2007.04910.x)
54. Norton WT, Cammer W. 1977 *Isolation and characterization of myelin*. New York, NY: Springer.
55. Baumann N, Pham-Dinh D. 2001 Biology of oligodendrocyte and myelin in the mammalian central nervous system. *Physiol. Rev.* **81**, 871–927.
56. Yamamoto N, Matsubara T, Sato T, Yanagisawa K. 2008 Age-dependent high-density clustering of GM1 ganglioside at presynaptic neuritic terminals promotes amyloid β-protein fibrillogenesis. *Biochim. Biophys. Acta* **1778**, 2717–2726. (doi:10.1016/j.bbamem.2008.07.028)
57. Yamamoto N, Igbabvoa U, Shimada Y, Ohno-Iwashita Y, Kobayashi M, Wood WG, Fujita SC, Yanagisawa K. 2004 Accelerated Aβ aggregation in the presence of GM1-ganglioside-accumulated synaptosomes of aged apoE4-knock-in mouse brain. *FEBS Lett.* **569**, 135–139. (doi:10.1016/j.febslet.2004.05.037)
58. Yu RK, Macala LJ, Taki T, Weinfield HM, Yu FS. 1988 Developmental changes in ganglioside composition and synthesis in embryonic rat brain. *J. Neurochem.* **50**, 1825–1829. (doi:10.1111/j.1471-4159.1988.tb02484.x)
59. Wang J, Yu RK. 2013 Interaction of ganglioside GD3 with an EGF receptor sustains the self-renewal ability of mouse neural stem cells in vitro. *Proc. Natl Acad. Sci. USA* **110**, 19 137–19 142. (doi:10.1073/pnas.1307224110)
60. Wang J, Cheng A, Wakade C, Yu RK. 2014 Ganglioside GD3 is required for neurogenesis and long-term maintenance of neural stem cells in the postnatal mouse brain. *J. Neurosci.* **34**, 13 790–13 800. (doi:10.1523/jneurosci.2275-14.2014)
61. Roisen FJ, Bartfeld H, Nagele R, Yorke G. 1981 Ganglioside stimulation of axonal sprouting *in vitro*. *Science* **214**, 577–578. (doi:10.1126/science.7291999)
62. Byrne MC, Ledeen RW, Roisen FJ, Yorke G, Sclafani JR. 1983 Ganglioside-induced neuritogenesis: verification that gangliosides are the active agents, and comparison of molecular species. *J. Neurochem.* **41**, 1214–1222. (doi:10.1111/j.1471-4159.1983.tb00814.x)
63. Wu G, Fang Y, Lu ZH, Ledeen RW. 1998 Induction of axon-like and dendrite-like processes in neuroblastoma cells. *J. Neurocytol.* **27**, 1–14. (doi:10.1023/A:1006910001869)
64. Ferreira A, Busciglio J, Landa C, Caceres A. 1990 Ganglioside-enhanced neurite growth: evidence for a selective induction of high-molecular-weight MAP-2. *J. Neurosci.* **10**, 293–302.
65. Vaudry D, Stork PJ, Lazarovici P, Eiden LE. 2002 Signaling pathways for PC12 cell differentiation: making the right connections. *Science* **296**, 1648–1649. (doi:10.1126/science.1071552)
66. Mutoh T, Tokuda A, Miyadai T, Hamaguchi M, Fujiki N. 1995 Ganglioside GM1 binds to the Trk protein and regulates receptor function. *Proc. Natl Acad. Sci. USA* **92**, 5087–5091. (doi:10.1073/pnas.92.11.5087)
67. Mutoh T, Tokuda A, Inokuchi J, Kuriyama M. 1998 Glucosylceramide synthase inhibitor inhibits the action of nerve growth factor in PC12 cells. *J. Biol. Chem.* **273**, 26 001–26 007. (doi:10.1074/jbc.273.40.26001)
68. Farooqui T, Franklin T, Pearl DK, Yates AJ. 1997 Ganglioside GM1 enhances induction by nerve growth factor of a putative dimer of TrkA. *J. Neurochem.* **68**, 2348–2355. (doi:10.1046/j.1471-4159.1997.68062348.x)
69. Da Silva JS, Hasegawa T, Miyagi T, Dotti CG, Abad-Rodriguez J. 2005 Asymmetric membrane ganglioside sialidase activity specifies axonal fate. *Nat. Neurosci.* **8**, 606–615. (doi:10.1038/nn1442)
70. Fukumoto S, Mutoh T, Hasegawa T, Miyazaki H, Okada M, Goto G, Furukawa K, Urano T. 2000 GD3 synthase gene expression in PC12 cells results in the continuous activation of TrkA and ERK1/2 and enhanced proliferation. *J. Biol. Chem.* **275**, 5832–5838. (doi:10.1074/jbc.275.8.5832)
71. Furukawa K, Ohmi Y, Ohkawa Y, Tajima O, Furukawa K. 2014 Glycosphingolipids in the regulation of the nervous system. *Adv. Neurobiol.* **9**, 307–320. (doi:10.1007/978-1-4939-1154-7_14)
72. Harel R, Futerman AH. 1993 Inhibition of sphingolipid synthesis affects axonal outgrowth in cultured hippocampal neurons. *J. Biol. Chem.* **268**, 14 476–14 481.
73. Schwarz A, Rapaport E, Hirschberg K, Futerman AH. 1995 A regulatory role for sphingolipids in neuronal growth: inhibition of sphingolipid synthesis and degradation have opposite effects on axonal branching. *J. Biol. Chem.* **270**, 10 990–10 998. (doi:10.1074/jbc.270.18.10990)
74. Campenot RB, Walji AH, Draker DD. 1991 Effects of sphingosine, staurosporine, and phorbol ester on neurites of rat sympathetic neurons growing in compartmented cultures. *J. Neurosci.* **11**, 1126–1139.
75. Furuya S, Ono K, Hirabayashi Y. 1995 Sphingolipid biosynthesis is necessary for dendrite growth and survival of cerebellar Purkinje cells in culture. *J. Neurochem.* **65**, 1551–1561. (doi:10.1046/j.1471-4159.1995.65041551.x)
76. Zhao L, Spassieva SD, Jucius TJ, Shultz LD, Shick HE, Macklin WB, Hannun YA, Obeid LM, Ackerman SL. 2011 A deficiency of ceramide biosynthesis causes cerebellar purkinje cell neurodegeneration and lipofuscin accumulation. *PLoS Genetics.* **7**, e1002063. (doi:10.1371/journal.pgen.1002063)
77. Furuya S, Mitoma J, Makino A, Hirabayashi Y. 1998 Ceramide and its interconvertible metabolite sphingosine function as indispensable lipid factors involved in survival and dendritic differentiation of cerebellar Purkinje cells. *J. Neurochem.* **71**, 366–377. (doi:10.1046/j.1471-4159.1998.71010366.x)
78. Watanabe S, Endo S, Oshima E, Hoshi T, Higashi H, Yamada K, Tohyama K, Yamashita T, Hirabayashi Y. 2010 Glycosphingolipid synthesis in cerebellar Purkinje neurons: roles in myelin formation and axonal homeostasis. *Glia* **58**, 1197–1207. (doi:10.1002/glia.20999)
79. Spassieva SD, Ji X, Liu Y, Gable K, Bielawski J, Dunn TM, Bieberich E, Zhao L. 2016 Ectopic expression of ceramide synthase 2 in neurons suppresses neurodegeneration induced by ceramide synthase 1 deficiency. *Proc. Natl Acad. Sci. USA* **113**, 5928–5933. (doi:10.1073/pnas.1522071113)
80. Mendez-Otero R, Santiago MF. 2003 Functional role of a specific ganglioside in neuronal migration and neurite outgrowth. *Brazilian J. Med. Biol. Res.* **36**, 1003–1013.
81. Stojiljkovic M, Blagojevic T, Vukosavic S, Zvezdina ND, Pekovic S, Nikezic G, Rakic L. 1996 Ganglioside GM1 and GM3 in early human brain development: an immunocytochemical study. *Int. J. Dev. Neurosci.* **14**, 35–44. (doi:10.1016/0736-5748(95)00078-X)
82. Hering H, Lin CC, Sheng M. 2003 Lipid rafts in the maintenance of synapses, dendritic spines, and surface AMPA receptor stability. *J. Neurosci.* **23**, 3262–3271.
83. van Spronsen M, Hoogenraad CC. 2010 Synapse pathology in psychiatric and neurologic disease. *Curr. Neurol. Neurosci. Rep.* **10**, 207–214. (doi:10.1007/s11910-010-0104-8)
84. Gielen E, Baron W, Vandeven M, Steels P, Hoekstra D, Ameloot M. 2006 Rafts in oligodendrocytes: evidence and structure–function relationship. *Glia* **54**, 499–512. (doi:10.1002/glia.20406)
85. Susuki K *et al.* 2007 Gangliosides contribute to stability of paranodal junctions and ion channel clusters in myelinated nerve fibers. *Glia* **55**, 746–757. (doi:10.1002/glia.20503)
86. Dupree JL, Coetzee T, Blight A, Suzuki K, Popko B. 1998 Myelin galactolipids are essential for proper node of Ranvier formation in the CNS. *J. Neurosci.* **18**, 1642–1649.
87. Pan B, Fromholt SE, Hess EJ, Crawford TO, Griffin JW, Sheikh KA, Schnaar RL. 2005 Myelin-associated glycoprotein and complementary axonal ligands, gangliosides, mediate axon stability in the CNS and PNS: neuropathology and behavioral deficits in single- and double-null mice. *Exp. Neurol.* **195**, 208–217. (doi:10.1016/j.expneurol.2005.04.017)
88. Sheikh KA, Sun J, Liu Y, Kawai H, Crawford TO, Proia RL, Griffin JW, Schnaar RL. 1999 Mice lacking complex gangliosides develop Wallerian

degeneration and myelination defects. *Proc. Natl Acad. Sci. USA* **96**, 7532–7537. (doi:10.1073/pnas.96.13.7532)

89. Honke K *et al.* 2002 Paranodal junction formation and spermatogenesis require sulfoglycolipids. *Proc. Natl Acad. Sci. USA* **99**, 4227–4232. (doi:10.1073/pnas.032068299)
90. Vyas AA, Patel HV, Fromholt SE, Heffer-Lauc M, Vyas KA, Dang J, Schachner M, Schnaar RL. 2002 Gangliosides are functional nerve cell ligands for myelin-associated glycoprotein (MAG), an inhibitor of nerve regeneration. *Proc. Natl Acad. Sci. USA* **99**, 8412–8417. (doi:10.1073/pnas.072211699)
91. Schnaar RL, Lopez PH. 2009 Myelin-associated glycoprotein and its axonal receptors. *J. Neurosci. Res.* **87**, 3267–3276. (doi:10.1002/jnr.21992)
92. DeBruin LS, Haines JD, Wellhauser LA, Radeva G, Schonmann V, Bienzle D, Harauz G. 2005 Developmental partitioning of myelin basic protein into membrane microdomains. *J. Neurosci. Res.* **80**, 211–225. (doi:10.1002/jnr.20452)
93. Simons M, Kramer EM, Thiele C, Stoffel W, Trotter J. 2000 Assembly of myelin by association of proteolipid protein with cholesterol- and galactosylceramide-rich membrane domains. *J. Cell Biol.* **151**, 143–154. (doi:10.1083/jcb.151.1.143)
94. Stewart RJ, Boggs JM. 1993 A carbohydrate-carbohydrate interaction between galactosylceramide-containing liposomes and cerebroside sulfate-containing liposomes: dependence on the glycolipid ceramide composition. *Biochemistry* **32**, 10 666–10 674. (doi:10.1021/bi00091a017)
95. Boggs JM, Gao W, Zhao J, Park HJ, Liu Y, Basu A. 2010 Participation of galactosylceramide and sulfatide in glycosynapses between oligodendrocyte or myelin membranes. *FEBS Lett.* **584**, 1771–1778. (doi:10.1016/j.febslet.2009.11.074)
96. Ishibashi T *et al.* 2002 A myelin galactolipid, sulfatide, is essential for maintenance of ion channels on myelinated axon but not essential for initial cluster formation. *J. Neurosci.* **22**, 6507–6514. (20026705)
97. Schafer DP, Bansal R, Hedstrom KL, Pfeiffer SE, Rasband MN. 2004 Does paranode formation and maintenance require partitioning of neurofascin 155 into lipid rafts? *J. Neurosc.* **24**, 3176–3185. (doi:10.1523/jneurosci.5427-03.2004)
98. Dupree JL, Girault JA, Popko B. 1999 Axo-glial interactions regulate the localization of axonal paranodal proteins. *J. Cell Biol.* **147**, 1145–1152. (doi:10.1083/jcb.147.6.1145)
99. Ben-David O *et al.* 2011 Encephalopathy caused by ablation of very long acyl chain ceramide synthesis may be largely due to reduced galactosylceramide levels. *J. Biol. Chem.* **286**, 30 022–30 033. (doi:10.1074/jbc.M111.261206)
100. Chiavegatto S, Sun J, Nelson RJ, Schnaar RL. 2000 A functional role for complex gangliosides: motor deficits in GM2/GD2 synthase knockout mice. *Exp. Neurol.* **166**, 227–234. (doi:10.1006/exnr.2000.7504)
101. Dotti CG, Esteban JA, Ledesma MD. 2014 Lipid dynamics at dendritic spines. *Front. Neuroanat.* **8**, 76. (doi:10.3389/fnana.2014.00076)
102. Wheeler D, Knapp E, Bandaru VV, Wang Y, Knorr D, Poirier C, Mattson MP, Geiger JD, Haughey NJ. 2009 Tumor necrosis factor-α-induced neutral sphingomyelinase-2 modulates synaptic plasticity by controlling the membrane insertion of NMDA receptors. *J. Neurochem.* **109**, 1237–1249. (doi:10.1111/j.1471-4159.2009.06038.x)
103. Tabatadze N, Savonenko A, Song H, Bandaru VV, Chu M, Haughey NJ. 2010 Inhibition of neutral sphingomyelinase-2 perturbs brain sphingolipid balance and spatial memory in mice. *J. Neurosci. Res.* **88**, 2940–2951. (doi:10.1002/jnr.22438)
104. Gulbins E *et al.* 2013 Acid sphingomyelinase-ceramide system mediates effects of antidepressant drugs. *Nat. Med.* **19**, 934–938. (doi:10.1038/nm.3214)
105. Gulbins E *et al.* 2015 A central role for the acid sphingomyelinase/ceramide system in neurogenesis and major depression. *J. Neurochem.* **134**, 183–192. (doi:10.1111/jnc.13145)
106. Sonnino S, Prinetti A. 2016 The role of sphingolipids in neuronal plasticity of the brain. *J. Neurochem.* **137**, 485–488. (doi:10.1111/jnc.13589)
107. Besshoh S, Bawa D, Teves L, Wallace MC, Gurd JW. 2005 Increased phosphorylation and redistribution of NMDA receptors between synaptic lipid rafts and post-synaptic densities following transient global ischemia in the rat brain. *J. Neurochem.* **93**, 186–194. (doi:10.1111/j.1471-4159.2004.03009.x)
108. Okada Y, Rahmann H, Hirai H, Terashima A. 1994 Exogenously applied gangliosides (GM1, GD1a and Gmix) fail to facilitate the induction of long-term potentiation (LTP) in the slices of hippocampus and superior colliculus of the guinea pig. *Neurosci. Lett.* **170**, 269–272. (doi:10.1016/0304-3940(94)90335-2)
109. Fujii S *et al.* 2002 Effects of the mono- and tetrasialogangliosides GM1 and GQ1b on ATP-induced long-term potentiation in hippocampal CA1 neurons. *Glycobiology* **12**, 339–344. (doi:10.1093/glycob/12.5.339)
110. Shin MK, Jung WR, Kim HG, Roh SE, Kwak CH, Kim CH, Kim SJ, Kim KL. 2014 The ganglioside GQ1b regulates BDNF expression via the NMDA receptor signaling pathway. *Neuropharmacology* **77**, 414–421. (doi:10.1016/j.neuropharm.2013.10.022)
111. Allen JA, Halverson-Tamboli RA, Rasenick MM. 2007 Lipid raft microdomains and neurotransmitter signalling. *Nat. Rev. Neurosci.* **8**, 128–140. (doi:10.1038/nrn2059)
112. Colon-Saez JO, Yakel JL. 2011 The α7 nicotinic acetylcholine receptor function in hippocampal neurons is regulated by the lipid composition of the plasma membrane. *J. Physiol.* **589**, 3163–3174. (doi:10.1113/jphysiol.2011.209494)
113. Xu Y, Ramu Y, Lu Z. 2008 Removal of phospho-head groups of membrane lipids immobilizes voltage sensors of K^+ channels. *Nature* **451**, 826–829. (doi:10.1038/nature06618)
114. Bock J, Szabo I, Gamper N, Adams C, Gulbins E. 2003 Ceramide inhibits the potassium channel Kv1.3 by the formation of membrane platforms. *Biochem. Biophys. Res. Commun.* **305**, 890–897. (doi:10.1016/S0006-291X(03)00763-0)
115. Martens JR, Sakamoto N, Sullivan SA, Grobaski TD, Tamkun MM. 2001 Isoform-specific localization of voltage-gated K^+ channels to distinct lipid raft populations: targeting of Kv1.5 to caveolae. *J. Biol. Chem.* **276**, 8409–8414. (doi:10.1074/jbc.M009948200)
116. Milescu M, Bosmans F, Lee S, Alabi AA, Kim JI, Swartz KJ. 2009 Interactions between lipids and voltage sensor paddles detected with tarantula toxins. *Nat. Struct. Mol. Biol.* **16**, 1080–1085. (doi:10.1038/nsmb.1679)
117. Ramu Y, Xu Y, Lu Z. 2006 Enzymatic activation of voltage-gated potassium channels. *Nature* **442**, 696–699. (doi:10.1038/nature04880)
118. Saghy E, Szoke E, Payrits M, Helyes Z, Borzsei R, Erostyak J, Janosi TZ, Setalo Jr G, Szolcsanyi J. 2015 Evidence for the role of lipid rafts and sphingomyelin in $Ca2^+$-gating of Transient Receptor Potential channels in trigeminal sensory neurons and peripheral nerve terminals. *Pharmacol. Res.* **100**, 101–116. (doi:10.1016/j.phrs.2015.07.028)
119. Szoke E, Borzsei R, Toth DM, Lengl O, Helyes Z, Sandor Z, Szolcsanyi J. 2010 Effect of lipid raft disruption on TRPV1 receptor activation of trigeminal sensory neurons and transfected cell line. *Eur. J. Pharmacol.* **628**, 67–74. (doi:10.1016/j.ejphar.2009.11.052)
120. Yang SN. 2000 Ceramide-induced sustained depression of synaptic currents mediated by ionotropic glutamate receptors in the hippocampus: an essential role of postsynaptic protein phosphatases. *Neuroscience* **96**, 253–258. (doi:10.1016/S0306-4522(99)00582-5)
121. Attiori Essis S, Laurier-Laurin ME, Pepin E, Cyr M, Massicotte G. 2015 GluN2B-containing NMDA receptors are upregulated in plasma membranes by the sphingosine-1-phosphate analog FTY720P. *Brain Res.* **1624**, 349–358. (doi:10.1016/j.brainres.2015.07.055)
122. Paila YD, Ganguly S, Chattopadhyay A. 2010 Metabolic depletion of sphingolipids impairs ligand binding and signaling of human serotonin1A receptors. *Biochemistry* **49**, 2389–2397. (doi:10.1021/bi1001536)
123. Sjogren B, Svenningsson P. 2007 Depletion of the lipid raft constituents, sphingomyelin and ganglioside, decreases serotonin binding at human 5-HT7(a) receptors in HeLa cells. *Acta Physiol.* **190**, 47–53. (doi:10.1111/j.1365-201X.2007.01687.x)
124. Park JW, Park WJ, Kuperman Y, Boura-Halfon S, Pewzner-Jung Y, Futerman AH. 2013 Ablation of very long acyl chain sphingolipids causes hepatic insulin resistance in mice due to altered detergent-resistant membranes. *Hepatology* **57**, 525–532. (doi:10.1002/hep.26015)
125. Vainio S, Heino S, Mansson JE, Fredman P, Kuismanen E, Vaarala O, Ikonen E. 2002 Dynamic association of human insulin receptor with lipid rafts in cells lacking caveolae. *EMBO Rep.* **3**, 95–100. (doi:10.1093/embo-reports/kvf010)
126. Kabayama K, Sato T, Kitamura F, Uemura S, Kang BW, Igarashi Y, Inokuchi J. 2005 TNFα-induced insulin resistance in adipocytes as a membrane

microdomain disorder: involvement of ganglioside GM3. *Glycobiology* **15**, 21–29. (doi:10.1093/glycob/cwh135)

127. Kabayama K, Sato T, Saito K, Loberto N, Prinetti A, Sonnino S, Kinjo M, Igarashi Y, Inokuchi J. 2007 Dissociation of the insulin receptor and caveolin-1 complex by ganglioside GM3 in the state of insulin resistance. *Proc. Natl Acad. Sci. USA* **104**, 13 678–13 683. (doi:10.1073/pnas.0703650104)
128. Aerts JM *et al.* 2007 Pharmacological inhibition of glucosylceramide synthase enhances insulin sensitivity. *Diabetes* **56**, 1341–1349. (doi:10.2337/db06-1619)
129. Snook CF, Jones JA, Hannun YA. 2006 Sphingolipid-binding proteins. *Biochim. Biophys. Acta* **1761**, 927–946. (doi:10.1016/j.bbalip.2006.06.004)
130. Mahfoud R, Garmy N, Maresca M, Yahi N, Puigserver A, Fantini J. 2002 Identification of a common sphingolipid-binding domain in Alzheimer, prion, and HIV-1 proteins. *J. Biol. Chem.* **277**, 11 292–11 296. (doi:10.1074/jbc.M111679200)
131. Bjorkholm P, Ernst AM, Hacke M, Wieland F, Brugger B, von Heijne G. 2014 Identification of novel sphingolipid-binding motifs in mammalian membrane proteins. *Biochim. Biophys. Acta* **1838**, 2066–2070. (doi:10.1016/j.bbamem.2014.04.026)
132. Melkonian KA, Ostermeyer AG, Chen JZ, Roth MG, Brown DA. 1999 Role of lipid modifications in targeting proteins to detergent-resistant membrane rafts. Many raft proteins are acylated, while few are prenylated. *J. Biol. Chem.* **274**, 3910–3917. (doi:10.1074/jbc.274.6.3910)
133. Yang W, Di Vizio D, Kirchner M, Steen H, Freeman MR. 2010 Proteome scale characterization of human S-acylated proteins in lipid raft-enriched and non-raft membranes. *Mol. Cell. Proteomics* **9**, 54–70. (doi:10.1074/mcp.M800448-MCP200)
134. Wong W, Schlichter LC. 2004 Differential recruitment of Kv1.4 and Kv4.2 to lipid rafts by PSD-95. *J. Biol. Chem.* **279**, 444–452. (doi:10.1074/jbc.M304675200)
135. Nitabach MN, Llamas DA, Araneda RC, Intile JL, Thompson IJ, Zhou YI, Holmes TC. 2001 A mechanism for combinatorial regulation of electrical activity: potassium channel subunits capable of functioning as Src homology 3-dependent adaptors. *Proc. Natl Acad. Sci. USA* **98**, 705–710. (doi:10.1073/pnas.031446198)
136. Brenman JE *et al.* 1996 Interaction of nitric oxide synthase with the postsynaptic density protein PSD-95 and α1-syntrophin mediated by PDZ domains. *Cell* **84**, 757–767. (doi:10.1016/S0092-8674(00)81053-3)
137. Topinka JR, Bredt DS. 1998 N-terminal palmitoylation of PSD-95 regulates association with cell membranes and interaction with K^+ channel Kv1.4. *Neuron* **20**, 125–134. (doi:10.1016/S0896-6273(00)80440-7)
138. Hicks DA, Nalivaeva NN, Turner AJ. 2012 Lipid rafts and Alzheimer's disease: protein-lipid interactions and perturbation of signaling. *Front. Physiol.* **3**, 189. (doi:10.3389/fphys.2012.00189)
139. Simons M, Keller P, De Strooper B, Beyreuther K, Dotti CG, Simons K. 1998 Cholesterol depletion inhibits the generation of β-amyloid in hippocampal neurons. *Proc. Natl Acad. Sci. USA* **95**, 6460–6464. (doi:10.1073/pnas.95.11.6460)
140. Amaro M, Sachl R, Aydogan G, Mikhalyov II, Vacha R, Hof M. 2016 GM1 Ganglioside inhibits β-amyloid oligomerization induced by sphingomyelin. *Angew. Chem.* **55**, 9411–9415. (doi:10.1002/anie.201603178)
141. Horres CR, Hannun YA. 2012 The roles of neutral sphingomyelinases in neurological pathologies. *Neurochem. Res.* **37**, 1137–1149. (doi:10.1007/s11064-011-0692-y)
142. He X, Huang Y, Li B, Gong CX, Schuchman EH. 2010 Deregulation of sphingolipid metabolism in Alzheimer's disease. *Neurobiol. Aging* **31**, 398–408. (doi:10.1016/j.neurobiolaging.2008.05.010)
143. Cutler RG, Kelly J, Storie K, Pedersen WA, Tammara A, Hatanpaa K, Troncoso JC, Mattson MP. 2004 Involvement of oxidative stress-induced abnormalities in ceramide and cholesterol metabolism in brain aging and Alzheimer's disease. *Proc. Natl Acad. Sci. USA* **101**, 2070–2075. (doi:10.1073/pnas.0305799101)
144. Han X, Rozen S, Boyle SH, Hellegers C, Cheng H, Burke JR, Welsh-Bohmer KA, Doraiswamy PM, Kaddurah-Daouk R. 2011 Metabolomics in early Alzheimer's disease: identification of altered plasma sphingolipidome using shotgun lipidomics. *PLoS ONE* **6**, e21643. (doi:10.1371/journal.pone.0021643)
145. Filippov V, Song MA, Zhang K, Vinters HV, Tung S, Kirsch WM, Yang J, Duerksen-Hughes PJ. 2012 Increased ceramide in brains with Alzheimer's and other neurodegenerative diseases. *J. Alzheimer's Dis.* **29**, 537–547. (doi:10.3233/jad-2011-111202)
146. Katsel P, Li C, Haroutunian V. 2007 Gene expression alterations in the sphingolipid metabolism pathways during progression of dementia and Alzheimer's disease: a shift toward ceramide accumulation at the earliest recognizable stages of Alzheimer's disease? *Neurochem. Res.* **32**, 845–856. (doi:10.1007/s11064-007-9297-x)
147. Malm T, Loppi S, Kanninen KM. 2016 Exosomes in Alzheimer's disease. *Neurochem. Int.* **97**, 193–199. (doi:10.1016/j.neuint.2016.04.011)
148. Dinkins MB, Enasko J, Hernandez C, Wang G, Kong J, Helwa I, Liu Y, Terry Jr AV, Bieberich E. 2016 Neutral sphingomyelinase-2 deficiency ameliorates Alzheimer's disease pathology and improves cognition in the 5XFAD mouse. *J. Neurosci.* **36**, 8653–8667. (doi:10.1523/jneurosci.1429-16.2016)
149. McLaurin J, Chakrabartty A. 1996 Membrane disruption by Alzheimer β-amyloid peptides mediated through specific binding to either phospholipids or gangliosides: implications for neurotoxicity. *J. Biol. Chem.* **271**, 26 482–26 489. (doi:10.1074/jbc.271.43.26482)
150. Kakio A, Nishimoto S, Kozutsumi Y, Matsuzaki K. 2003 Formation of a membrane-active form of amyloid β-protein in raft-like model membranes. *Biochem. Biophys. Res. Commun.* **303**, 514–518. (doi:10.1016/S0006-291X(03)00386-3)
151. Molander-Melin M, Blennow K, Bogdanovic N, Dellheden B, Mansson JE, Fredman P. 2005 Structural membrane alterations in Alzheimer brains found to be associated with regional disease development: increased density of gangliosides GM1 and GM2 and loss of cholesterol in detergent-resistant membrane domains. *J. Neurochem.* **92**, 171–182. (doi:10.1111/j.1471-4159.2004.02849.x)
152. Ariga T, McDonald MP, Yu RK. 2008 Role of ganglioside metabolism in the pathogenesis of Alzheimer's disease: a review. *J. Lipid Res.* **49**, 1157–1175. (doi:10.1194/jlr.R800007-JLR200)
153. Chan RB, Oliveira TG, Cortes EP, Honig LS, Duff KE, Small SA, Wenk MR, Shui G, Di Paolo G. 2012 Comparative lipidomic analysis of mouse and human brain with Alzheimer disease. *J. Biol. Chem.* **287**, 2678–2688. (doi:10.1074/jbc.M111.274142)
154. Fukami Y, Ariga T, Yamada M, Yuki N. 2017 Brain gangliosides in Alzheimer's disease: increased expression of cholinergic neuron-specific gangliosides. *Curr. Alzheimer Res.* **3**, 145.
155. Aharon-Peretz J, Rosenbaum H, Gershoni-Baruch R. 2004 Mutations in the glucocerebrosidase gene and Parkinson's disease in Ashkenazi Jews. *N. Engl. J. Med.* **351**, 1972–1977. (doi:10.1056/NEJMoa033277)
156. Sidransky E *et al.* 2009 Multicenter analysis of glucocerebrosidase mutations in Parkinson's disease. *N. Engl. J. Med.* **361**, 1651–1661. (doi:10.1056/NEJMoa0901281)
157. Wu YR, Chen CM, Chao CY, Ro LS, Lyu RK, Chang KH, Lee-Chen GJ. 2007 Glucocerebrosidase gene mutation is a risk factor for early onset of Parkinson disease among Taiwanese. *J. Neurol. Neurosurg. Psychiatry* **78**, 977–979. (doi:10.1136/jnnp.2006.105940)
158. Kumar KR *et al.* 2013 Glucocerebrosidase mutations in a Serbian Parkinson's disease population. *Eur. J. Neurol.* **20**, 402–405. (doi:10.1111/j.1468-1331.2012.03817.x)
159. Gegg ME, Burke D, Heales SJ, Cooper JM, Hardy J, Wood NW, Schapira AH. 2012 Glucocerebrosidase deficiency in substantia nigra of Parkinson disease brains. *Ann. Neurol.* **72**, 455–463. (doi:10.1002/ana.23614)
160. Murphy KE, Gysbers AM, Abbott SK, Tayebi N, Kim WS, Sidransky E, Cooper A, Garner B, Halliday GM. 2014 Reduced glucocerebrosidase is associated with increased α-synuclein in sporadic Parkinson's disease. *Brain J. Neurol.* **137**, 834–848. (doi:10.1093/brain/awt367)
161. Mazzulli JR, Xu YH, Sun Y, Knight AL, McLean PJ, Caldwell GA, Sidransky E, Grabowski GA, Krainc D. 2011 Gaucher disease glucocerebrosidase and α-synuclein form a bidirectional pathogenic loop in synucleinopathies. *Cell* **146**, 37–52. (doi:10.1016/j.cell.2011.06.001)
162. Schlossmacher MG, Cullen V, Muthing J. 2005 The glucocerebrosidase gene and Parkinson's disease in Ashkenazi Jews. *N. Engl. J. Med.* **352**, 728–731; author reply 728-731. (doi:10.1056/NEJM200502173520719)

163. Gegg ME, Sweet L, Wang BH, Shihabuddin LS, Sardi SP, Schapira AH. 2015 No evidence for substrate accumulation in Parkinson brains with GBA mutations. *Movement Disorders* **30**, 1085–1089. (doi:10.1002/mds.26278)
164. Boutin M, Sun Y, Shacka JJ, Auray-Blais C. 2016 Tandem mass spectrometry multiplex analysis of glucosylceramide and galactosylceramide isoforms in brain tissues at different stages of Parkinson disease. *Anal. Chem.* **88**, 1856–1863. (doi:10.1021/acs.analchem.5b04227)
165. Kubo S, Nemani VM, Chalkley RJ, Anthony MD, Hattori N, Mizuno Y, Edwards RH, Fortin DL. 2005 A combinatorial code for the interaction of α-synuclein with membranes. *J. Biol. Chem.* **280**, 31 664–31 672. (doi:10.1074/jbc.M504894200)
166. Fabelo N, Martin V, Santpere G, Marin R, Torrent L, Ferrer I, Diaz M. 2011 Severe alterations in lipid composition of frontal cortex lipid rafts from Parkinson's disease and incidental Parkinson's disease. *Mol. Med.* **17**, 1107–1118. (doi:10.2119/molmed.2011.00119)
167. Martinez Z, Zhu M, Han S, Fink AL. 2007 GM1 specifically interacts with α-synuclein and inhibits fibrillation. *Biochemistry* **46**, 1868–1877. (doi:10.1021/bi061749a)
168. Schneider JS, Pope A, Simpson K, Taggart J, Smith MG, DiStefano L. 1992 Recovery from experimental parkinsonism in primates with GM1 ganglioside treatment. *Science* **256**, 843–846. (doi:10.1126/science.1350379)
169. Pope-Coleman A, Tinker JP, Schneider JS. 2000 Effects of GM1 ganglioside treatment on pre- and postsynaptic dopaminergic markers in the striatum of Parkinsonian monkeys. *Synapse* **36**, 120–128. (doi:10.1002/(sici)1098-2396(200005)36:2<120::aid-syn5>3.0.co;2-y)
170. Herrero MT, Perez-Otano I, Oset C, Kastner A, Hirsch EC, Agid Y, Luquin MR, Obeso JA, Del Rio J. 1993 GM-1 ganglioside promotes the recovery of surviving midbrain dopaminergic neurons in MPTP-treated monkeys. *Neuroscience* **56**, 965–972. (doi:10.1016/0306-4522(93)90142-3)
171. Zappia M *et al.* 2002 Anti-GM1 ganglioside antibodies in Parkinson's disease. *Acta Neurol. Scandinavica* **106**, 54–57. (doi:10.1034/j.1600-0404.2002.01240.x)
172. Ferlazzo E, Striano P, Italiano D, Calarese T, Gasparini S, Vanni N, Fruscione F, Genton P, Zara F. 2016 Autosomal recessive progressive myoclonus epilepsy due to impaired ceramide synthesis. *Epileptic Disorders* **18**, 120–127. (doi:10.1684/epd.2016.0857)
173. Mosbech MB *et al.* 2014 Reduced ceramide synthase 2 activity causes progressive myoclonic epilepsy. *Ann. Clin. Transl. Neurol.* **1**, 88–98. (doi:10.1002/acn3.28)
174. Ginkel C *et al.* 2012 Ablation of neuronal ceramide synthase 1 in mice decreases ganglioside levels and expression of myelin-associated glycoprotein in oligodendrocytes. *J. Biol. Chem.* **287**, 41 888–41 902. (doi:10.1074/jbc.M112.413500)
175. Imgrund S, Hartmann D, Farwanah H, Eckhardt M, Sandhoff R, Degen J, Gieselmann V, Sandhoff K, Willecke K. 2009 Adult ceramide synthase 2 (CERS2)-deficient mice exhibit myelin sheath defects, cerebellar degeneration, and hepatocarcinomas. *J. Biol. Chem.* **284**, 33 549–33 560. (doi:10.1074/jbc.M109.031971)
176. Pewzner-Jung Y *et al.* 2010 A critical role for ceramide synthase 2 in liver homeostasis: I. alterations in lipid metabolic pathways. *J. Biol. Chem.* **285**, 10 902–10 910. (doi:10.1074/jbc.M109.077594)
177. Silva LC, Ben David O, Pewzner-Jung Y, Laviad EL, Stiban J, Bandyopadhyay S, Merrill Jr AH, Prieto M, Futerman AH. 2012 Ablation of ceramide synthase 2 strongly affects biophysical properties of membranes. *J. Lipid Res.* **53**, 430–436. (doi:10.1194/jlr.M022715)
178. Zhou J *et al.* 2012 Spinal muscular atrophy associated with progressive myoclonic epilepsy is caused by mutations in ASAH1. *Am. J. Human Genetics* **91**, 5–14. (doi:10.1016/j.ajhg.2012.05.001)
179. Rubboli G *et al.* 2015 Spinal muscular atrophy associated with progressive myoclonic epilepsy: a rare condition caused by mutations in ASAH1. *Epilepsia* **56**, 692–698. (doi:10.1111/epi.12977)
180. Gan JJ *et al.* 2015 Acid ceramidase deficiency associated with spinal muscular atrophy with progressive myoclonic epilepsy. *NMD* **25**, 959–963. (doi:10.1016/j.nmd.2015.09.007)
181. Dyment DA *et al.* 2014 Evidence for clinical, genetic and biochemical variability in spinal muscular atrophy with progressive myoclonic epilepsy. *Clin. Genetics* **86**, 558–563. (doi:10.1111/cge.12307)
182. Schuchman EH. 2016 Acid ceramidase and the treatment of ceramide diseases: the expanding role of enzyme replacement therapy. *Biochim. Biophys. Acta* **1862**, 1459–1471. (doi:10.1016/j.bbadis.2016.05.001)
183. Li CM *et al.* 2002 Insertional mutagenesis of the mouse acid ceramidase gene leads to early embryonic lethality in homozygotes and progressive lipid storage disease in heterozygotes. *Genomics* **79**, 218–224. (doi:10.1006/geno.2002.6686)
184. Young MM, Kester M, Wang HG. 2013 Sphingolipids: regulators of crosstalk between apoptosis and autophagy. *J. Lipid Res.* **54**, 5–19. (doi:10.1194/jlr.R031278)
185. Simpson MA *et al.* 2004 Infantile-onset symptomatic epilepsy syndrome caused by a homozygous loss-of-function mutation of GM3 synthase. *Nature genetics.* **36**, 1225–1229. (doi:10.1038/ng1460)
186. Fragaki K *et al.* 2013 Refractory epilepsy and mitochondrial dysfunction due to GM3 synthase deficiency. *EJHG* **21**, 528–534. (doi:10.1038/ejhg.2012.202)
187. Liu Y, Su Y, Wiznitzer M, Epifano O, Ladisch S. 2008 Ganglioside depletion and EGF responses of human GM3 synthase-deficient fibroblasts. *Glycobiology* **18**, 593–601. (doi:10.1093/glycob/cwn039)
188. Pike LJ, Han X, Gross RW. 2005 Epidermal growth factor receptors are localized to lipid rafts that contain a balance of inner and outer leaflet lipids: a shotgun lipidomics study. *J. Biol. Chem.* **280**, 26 796–26 804. (doi:10.1074/jbc.M503805200)
189. Yamashita T *et al.* 2005 Interruption of ganglioside synthesis produces central nervous system degeneration and altered axon-glial interactions. *Proc. Natl Acad. Sci. USA* **102**, 2725–2730. (doi:10.1073/pnas.0407785102)
190. Yamashita T *et al.* 2003 Enhanced insulin sensitivity in mice lacking ganglioside GM3. *Proc. Natl Acad. Sci. USA* **100**, 3445–3449. (doi:10.1073/pnas.0635898100)
191. Sezgin E, Levental I, Mayor S, Eggeling C. In press. The mystery of membrane organization: composition, regulation and roles of lipid rafts. *Nat. Rev. Mol. Cell Biol.* (doi:10.1038/nrm.2017.16)

Supplement II

Published in Annals of Clinical and Translational Neurology, February 2014

Reduced ceramide synthase 2 activity causes progressive myoclonic epilepsy

Mosbech MB[a], **Olsen AS[a]**, Neess D, Ben-David O, Klitten LL, Larsen J, Sabers A, Vissing J, Nielsen JE, Hasholt L, Klein AD, Tsoory MM, Hjalgrim H, Tommerup, N, Futerman AH, Møller RS, Færgeman NJ

[a]Shared 1st author.

ANNALS of Clinical and Translational Neurology
Open Access
ANA American Neurological Association since 1875

RESEARCH PAPER

Reduced ceramide synthase 2 activity causes progressive myoclonic epilepsy

Mai-Britt Mosbech[1,a], Anne S. B. Olsen[1,a], Ditte Neess[1], Oshrit Ben-David[2], Laura L. Klitten[3], Jan Larsen[3,4], Anne Sabers[5], John Vissing[5], Jørgen E. Nielsen[6], Lis Hasholt[4], Andres D. Klein[2], Michael M. Tsoory[7], Helle Hjalgrim[3,8], Niels Tommerup[4], Anthony H. Futerman[2], Rikke S. Møller[3,8] & Nils J. Færgeman[1]

[1]Department of Biochemistry and Molecular Biology, University of Southern Denmark, Odense M, DK-5230, Denmark
[2]Department of Biological Chemistry, Weizmann Institute of Science, Rehovot, 76100, Israel
[3]The Danish Epilepsy Centre, Filadelfia, Dianalund, DK-4293, Denmark
[4]Department of Cellular and Molecular Medicine, The Panum Institute, University of Copenhagen, Copenhagen, DK-2100, Denmark
[5]Department of Neurology, Rigshospitalet, University of Copenhagen, Copenhagen, DK-2100, Denmark
[6]Neurogenetics Clinic, Danish Dementia Research Centre, Department of Neurology, Rigshospitalet, Copenhagen University Hospital, Copenhagen, DK-2100, Denmark
[7]Behavioral and Physiological Phenotyping Unit, Department of Veterinary Resources, Weizmann Institute of Science, Rehovot, 76100, Israel
[8]Institute for Regional Health Services, University of Southern Denmark, Odense, Denmark

Correspondence
Nils Joakim Færgeman, Department of Biochemistry and Molecular Biology, University of Southern Denmark, Campusvej 55, Odense M DK-5230, Denmark.
Tel: +45 65502453; Fax: +45 65502467;
E-mail: nils.f@bmb.sdu.dk

Rikke Steensbjerre Møller,
Danish Epilepsy Center,
Filadelfia, Kolonivej 1,
Dianalund DK-4293, Denmark.
Tel: +45 61208636; Fax: +45 58271050
E-mail: rimo@filadelfia.dk

Funding Information
This study has been supported by The Lundbeck Foundation and The Danish Council for Independent Research, Natural Sciences.

Received: 4 December 2013;
Accepted: 4 December 2013

doi: 10.1002/acn3.28

[a]Equally contributing authors.

Abstract

Objective: Ceramides are precursors of complex sphingolipids (SLs), which are important for normal functioning of both the developing and mature brain. Altered SL levels have been associated with many neurodegenerative disorders, including epilepsy, although few direct links have been identified between genes involved in SL metabolism and epilepsy. **Methods**: We used quantitative real-time PCR, Western blotting, and enzymatic assays to determine the mRNA, protein, and activity levels of ceramide synthase 2 (CERS2) in fiibroblasts isolated from parental control subjects and from a patient diagnosed with progressive myoclonic epilepsy (PME). Mass spectrometry and fluorescence microscopy were used to examine the effects of reduced CERS2 activity on cellular lipid composition and plasma membrane functions. **Results**: We identify a novel 27 kb heterozygous deletion including the *CERS2* gene in a proband diagnosed with PME. Compared to parental controls, levels of *CERS2* mRNA, protein, and activity were reduced by ~50% in fibroblasts isolated from this proband, resulting in significantly reduced levels of ceramides and sphingomyelins containing the very long-chain fatty acids C24:0 and C26:0. The change in SL composition was also reflected in a reduction in cholera toxin B immunofluorescence, indicating that membrane composition and function are altered. **Interpretation**: We propose that reduced levels of CERS2, and consequently diminished levels of ceramides and SLs containing very long-chain fatty acids, lead to development of PME.

Introduction

Progressive myoclonic epilepsy (PME) is a heterogeneous group of disorders characterized by myoclonus, tonic-clonic seizures, and progressive neurological dysfunction, including cognitive impairment and ataxia. Disease onset and symptoms vary greatly among these disorders. A greater understanding of the underlying pathophysiological processes would help both diagnosis and treatment.[1–3]

Sphingolipids (SLs) are abundant in nervous tissue and are especially enriched in myelin. Most typical myelin lipids are cerebrosides (glucosylceramide [GlcCer] and galactosylceramide [GalCer]), which are approximately 10-fold more abundant in white compared to gray matter.[4]

GalCer is the most abundant cerebroside in the brain, and is especially enriched in C22-24-fatty acids (FAs).[4,5] Sphingomyelin (SM) is another major myelin lipid and is highly enriched in C18- and C24-SLs. During development, C18-SM decreases from 80% to 30% of the total SM content in myelin, while C24-SM increases from 4% to 33%. Oligodendrocytes show a SL composition similar to myelin and are also enriched in C24-SLs.[4,5] Gangliosides, acidic glycosphingolipids, are predominantly comprised of C18-SLs, and are especially enriched in gray matter.[6]

Ceramides are the building blocks of all complex SLs (Fig. 1). In mammals, Ceramides are synthesized by a family of six enzymes (CERS1-6), which all display distinct tissue expression levels and utilize acyl-CoAs of defined chain length (reviewed in[7,8]). Ceramide synthase 2 (*CERS2*) is the most widely expressed and is especially abundant in liver and kidney, and primarily uses C22-C24-acyl-CoAs for ceramide synthesis.[9] CERS1 predominantly uses C18:0- and C18:1-acyl-CoAs is the most abundant ceramide synthase in the central nervous system, and more abundant in gray matter than in white matter; however, *CERS2* is also highly expressed in white matter.[10] Knockout of *CerS2* in mice results in decreased levels of C22-24-ceramides and -SLs in the brain, whereas long-chain ceramides, for example, C18-ceramide and sphinganine, increase. In addition to impaired liver function,[11] *CerS2* null mice exhibit a number of nervous system dysfunctions, including myelin sheath defects and cerebellar degeneration, which consequently results in abnormal motor function, including generalized and symmetrical myoclonic jerks and sensitivity to auditory stimuli.[9,12,13] *CerS2* null mice also have altered biophysical membrane properties and show elevated levels of reactive oxygen species in the liver due to impaired activity of mitochondrial complex IV.[14–16]

Previously, homozygous loss of GM3 synthase (also known as lactosylceramide α-2,3 sialyltransferase) has been linked to infantile-onset, symptomatic epilepsy syndrome,[17] and more recently two *CerS1* knockout mice strains have been shown to display degeneration of cerebellar Purkinje neurons and accumulation of lipofuscin.[18] As altered SL levels are found in many neurodegenerative disorders and in a variety of other diseases,[19] understanding the consequences of these alterations and deciphering SL regulation, as well as its impact on cellular properties, may provide novel therapeutic targets.

Case Report

The proband is a 30-year-old man born to unrelated Caucasian parents with no family history of known chromosomal abnormalities, epilepsy, or developmental

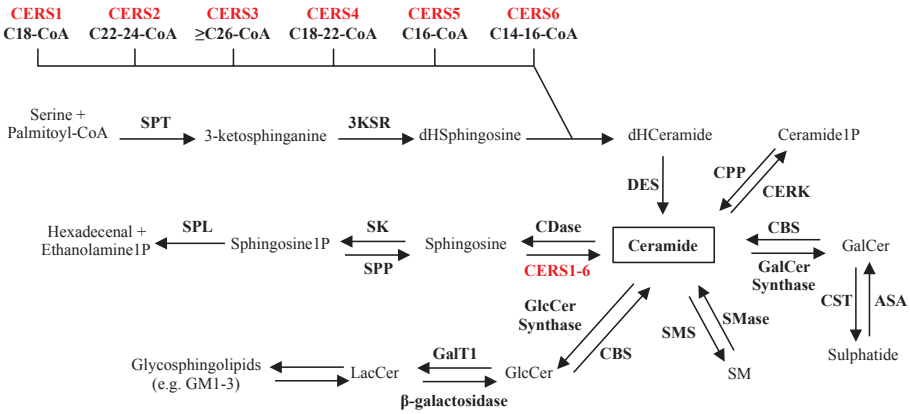

Figure 1. Overview of sphingolipid metabolism. Ceramide is at the central hub of sphingolipid metabolism and is synthesized de novo from serine and palmitoyl-CoA. In the third step of this four-step process, ceramide synthases acylate dihydro-sphingosine (dHSphingosine) to form dihydro-ceramide (dHCeramide). Six mammalian ceramide synthases (CERS1-6) (shown in red) have been identified and each of these utilizes a unique subset of acyl-CoAs (indicated beneath each CERS). Once formed, ceramide can be metabolized in five different ways: (1) Ceramide can be phosphorylated by ceramide kinase (CERK). (2) Ceramide can be glycosylated by galactosylceramide (GalCer) synthase producing GalCer which can be further metabolized into sulfatides. (3) Attachment of phosphocholine to ceramide yields sphingomyelin (SM) in a reaction catalyzed by SM synthase (SMS). (4) Glycosylation of ceramide by glucosylceramide (GlcCer) synthase followed by galactosyltransferase I (GalTI) produces GlcCer and lactosylceramide (LacCer), respectively. LacCer constitute the foundation for the synthesis of more complex glycosphingolipids including gangliosides GM1 and GM3. (5) Ceramide can be degraded to sphingosine, which in turn can be phosphorylated to sphingosine 1-phosphate (sphingosine1P) and further degraded into hexadecanal and ethanolamine 1-phosphate (ethanolamine1P). The last step is the only known exit route from the sphingolipid pathway. SPT, serine palmitoyltransferase; 3KSR, 3-ketosphinganine reductase; DES, dihydroceramide desaturase; CPP, ceramide phosphatase; CBS, cerebrosidase; ASA, arylsulfatase A; CST, cerebroside sulfotransferase; SMase, sphingomyelinase; SK, sphingosine kinase; SPP, sphingosine phosphate phosphatase; SPL, sphingosine1P lyase.

delay. Pregnancy and delivery were normal. He had no neonatal problems, weighed 2.9 kg, and had a length of 50 cm at birth. Before the age of 2 years, he had three febrile seizures (FS) and two afebrile seizures, presumably generalized tonic-clonic seizures (GTCS). Initial electroencephalography (EEG) recordings and computerized tomography (CT) scans were normal. To prevent seizures, he was treated with valproic acid (VPA), which rendered him seizure-free. When he was 6 years old, VPA was withdrawn and he remained seizure-free without antiepileptic treatment until the age of 10 years, when VPA was reintroduced due to recurrence of GTCS. He attended a regular school until he was 12 years old, at which time he was diagnosed with learning disabilities and therefore moved to a special class. At the age of 13 years, developmental delay was noticed along with tremor of the hands, and gait disturbances were observed but regarded as side effects of VPA. At the age of 14, he was diagnosed with severe myoclonus. When VPA was substituted by Lamotrigine, cognitive function appeared to improve, but due to unacceptable myoclonia, VPA was reintroduced at the proband's demand. A combination of high dose VPA and oxcarbazepine kept him seizure-free with almost no myoclonia for nearly 2 years. At the age of 20, the frequency of GTCS (predominantly during sleep) and myoclonia increased, and despite administration of several antiepileptic drugs, such as clonazepam, clobazam, levetiracetam, piracetam, and zonisamide, his seizures could not be controlled. Furthermore, withdrawal of oxcarbazepine severely increased the frequency of tonic-clonic seizures. For a period of time, he was is reluctant to go outside due to extreme photosensitivity, which caused frequent falls.

Laboratory investigations revealed normal hematological indices as well as normal liver and kidney function. Prior to Simvastatin treatment, the plasma level of cholesterol was >10 mmol/L (normal level <5.2 mmol/L) and after treatment, high-density lipoprotein, low-density lipoprotein, and triglyceride levels were 6.6, 1.4, and 1.5 mmol/L, respectively. Hematoxylin and eosin staining of a muscle biopsy demonstrated discrete myopathic abnormalities with increased fiber variability and an increased number of central nuclei. The inherited mitochondrial disorders, Mitochondrial encephalomyopathy, lactic acidosis, and stroke-like episodes (MELAS), Myoclonic Epilepsy with Ragged Red Fibers (MERRF), and Neuropathy, ataxia, and retinitis pigmentosa (NARP) were excluded, and genetic tests for the lipid storage disease, Niemann Pick Type C (sequencing of *NPC1* and *NPC2*), were normal. In addition, whole exome sequencing was performed without detecting any disease-causing mutations. A variety of other tests were performed, and the only abnormality detected was a small reduction in the respiratory chain complex I/citrate synthase ratio (0.18 compared to the normal range of 0.19–0.54) (Table 1).

Table 1. Case report: list of test values

Test	Value	Normal range
Hemoglobin	>10	10–11.1
Lactate	1.2	0.7–2.1
Alkaline phosphatase	117–125	35–105
Glut1 deficiency	4.3	–
β-Galactosidase	201	130–340
Arylsulfatase A	8.0	3.5–15
Hexosaminidase A + B	2225	1200–3500
Hexosaminase A	211	140–410
Galactocerebrosidase	1.01	0.5–3.4
α-Fucosidase	59	20–110
Palmitoyl-protein thioesterase	22	15–90
Hexosaminidase A + B (plasma)	596	400–1800
Chitotriosidase I (plasma)	13	0–115
Cerotic acid	98	40–115
Complex I	63	25–164
Complex II	130	39–171
Complex II + III	134	33–216
Complex III	467	117–794
Complex IV	1225	286–1852
Citrate synthase (CS)	351	127–477
Complex I/CS ratio	0.18	0.19–0.54
Complex II/CS ratio	0.37	0.24–0.50
Complex II + III/CS ratio	0.38	0.19–0.72
Complex III/CS ratio	1.33	0.82–2.14
Complex IV/CS ratio	3.5	2.2–5.0
Complex I/II ratio	0.48	0.45–1.33
Complex II + III/II ratio	1.03	0.48–1.71
Complex III/II ratio	3.6	1.6–5.8
Complex IV/II ratio	9.4	7.3–13.6
PCR analysis of whole mitochondria gene on DNA isolated from muscle biopsy is normal		
MELAS (3243A G)	Not detected	–
MERRF (8834A G)	Not detected	–
NARP (993T G)	Not detected	–

EEG recordings at disease onset did not reveal any abnormalities. When the proband was 19 years of age, alpha background activity was preserved, with intermittent and irregular beta and theta activity without an altered pattern during intermittent photic stimulation. Over the years, the EEG background activity was slightly reduced to an activity of 7½–8 Hz, with sharp waves followed by 2–3 Hz slow waves in the left temporal region. During photostimulation and during sleep, myoclonic jerks without EEG correlation were seen, predominantly in the upper limbs and on the left side of the body. EEG-EMG polygraphic recordings were not performed.

Sensory evoked potentials (SEP) analysis showed a cortical response with increased amplitude. Moreover, visual evoked potentials (VEP) showed abnormal cortical potentials and high amplitude spikes in the mid-occipital region. Magnetic resonance imaging (MRI) of the brain

at the age of 15 years indicated no abnormalities. However, at 27 years of age, an MRI scan showed a minor lesion, probably a minimal heterotropia in the left temporal lobe, and discrete atrophy bilaterally of the frontoparietal lobes and cerebellum.

Upon neurological examination at 30 years of age, the proband appeared moderately intellectually disabled with dysarthria and ataxia. He was slim (weight 62 kg, height 167 cm), myopic, and had normal hearing. He now lives in residential care, cohousing with younger mentally disabled persons. Within the last year, his condition has worsened and he has been compelled to give up his sheltered employment at the local supermarket. At present he is having 4–8 GTCS per month and consistently experiences myoclonus. He is treated with 2300 mg VPA, 900 mg oxcarbazepine, and 4800 mg piracetam per day.

Subjects/Material and Methods

Study oversight

This study was approved by the Ethics Committee at Western Sealand and written informed consent was obtained from the patient and his parents.

Genetic studies

DNA samples were typed for 1.8 million probe sets on the Affymetrix Genome-Wide Human SNP Array 6.0 (Affymetrix, Santa Clara, CA). CNV (copy number variation) analysis was performed by the algorithm implemented in the Affymetrix Genotyping Console version 4.0. (Affymetrix, Santa Clara, CA). The presumed pathogenic CNV was verified in the index patient, and also tested in the parents with TaqMan qPCR (Life Technologies, Carlsbad, CA) according to manufacturer's instructions. Seven specific primer pairs were designed to amplify the 10 coding exons of *CERS2* and the adjacent intron-exon boundaries. PCR amplicons were sequenced using Applied BiosystemsTM according to the supplier's recommendations. Paternity was confirmed by genotyping 15 short tandem repeat (STR) markers located on 10 different chromosomes.

Control cohort

The control cohort comprised 1075 unselected individuals provided by the PopGen biobank.

Cell culture

A skin biopsy excised from the upper arm was transferred to a tissue culture flask. The biopsy was cultured in Roswell Park Memorial Institute media-1640, 20% Fetal calf serum (supplemented with 4 mmol/L L-glutamine, 0.017 mg/mL benzylpenicillin) and grown at 37°C, with 5% CO_2. Primary fibroblasts were grown in Dulbecco's modified Eagle's medium supplemented with high glucose, 1 mmol/L sodium pyruvate (Invitrogen, Carlsbad, CA), 44.04 mmol/L sodium hydrogen carbonate, 33 μmol/L biotin, 34 μmol/L pantothenic acid, 20% fetal bovine serum (Sigma-Aldrich, St. Louis, MO), 100 units penicillin/0.1 mg streptomycin per liter (Sigma-Aldrich), and GlutaMAX supplement (Invitrogen) at 37°C, with 5% CO_2.

Quantitative real-time PCR

Total RNA was harvested from muscle biopsies and human primary fibroblasts using ice-cold Trizol (Invitrogen) according to manufacturer's instructions. cDNA and quantitative real-time PCR were performed as described.[20] Expressions were normalized to TATA-binding protein (TBP) and/or β-actin. Statistical analyses were performed in GraphPad Prism version 6 (GraphPad Software, La Jolla, CA).

Western blotting

Total cell extracts were prepared from cultured fibroblasts, and proteins were separated by sodium dodecyl sulfate (SDS) polyacrylamide gel electrophoresis and subsequently transferred to a Polyvinylidene Difluoride membrane by electroblotting. CERS2 was probed using a rabbit anti-human CERS2 antibody (Abcam, Cambridge, England). TBP was probed using a rabbit anti-human TFIIB antibody (Santa Cruz Biotechnology, Inc., Dallas, TX), which served as loading control. All immunoprobed proteins were detected by enhanced chemiluminescence.

Ceramide synthase activity

Ceramide synthase activities were determined in cell extracts as previously described.[21]

Lipid analysis by mass spectrometry

Analysis of ceramides and SLs in isolated fibroblasts were carried out by Avanti Polar Lipids, Inc., Alabama, AL. Results were normalized to cell number.

GM1 staining

Fibroblasts were washed three times in M1 medium (150 mmol/L NaCl, 5 mmol/L KCl, 1 mmol/L $CaCl_2$, 1 mmol/L $MgCl_2$, 5 mmol/L glucose, 20 mmol/L Hepes,

pH 7.3) and stained with Cholera Toxin B-Alexa488 (10 μg/mL in M1 medium) (Invitrogen) for 20 min at 37°C. Wide-field fluorescence microscopy and digital image acquisition were performed using a Leica DMIRBE microscope with a 63×, 1.4 NA oil immersion objective (Leica Lasertechnik GmbH, Wetzlar, Germany). All pictures were taken within 20 min after CTxB staining using a standard fluorescein filter set (470-nm, [20-nm bandpass] excitation filter, 510-nm longpass dichromatic filter, and 537-nm [23-nm] bandpass emission filter). All images were acquired using identical settings. Images were analyzed using the freeware ImageJ [National Institute of Health (NIH), Bethesda, MD].

Light sensitivity of *CerS2* null mice

Mice were maintained in a specific pathogen-free and temperature-controlled (22 ± 1°C) mouse facility on a reverse 12 h light/dark cycle (lights on at 20:00) according to institutional guidelines. Food and water were given ad libitum. All experimental protocols were approved by the Institutional Animal Care and Use Committee of The Weizmann Institute of Science. Light sensitivity was assessed by measuring freezing behavior in a circular open field (Ø = 56.5 cm) under two illumination conditions, dark (10 lux, 5 min) and light (120 lux, 5 min). An overhead camera (Sony DCR-SR30E HANDYCAM, Tokyo, Japan) recorded mouse behavior. Freezing was determined by off-line analyses of the video tracks using an automated tracking system (Ethovision, Noldus, Wageningen, the Netherlands).

Results

Genetic analysis

We performed genome-wide SNP 6.0 array analysis on DNA isolated from the proband and identified a heterozygous 27 kb de novo deletion on chromosome 1q21 containing the entire *CERS2* gene (Fig. 2A). To exclude a recessive condition, we sequenced the remaining allele of *CERS2*, but no further mutations were identified. The

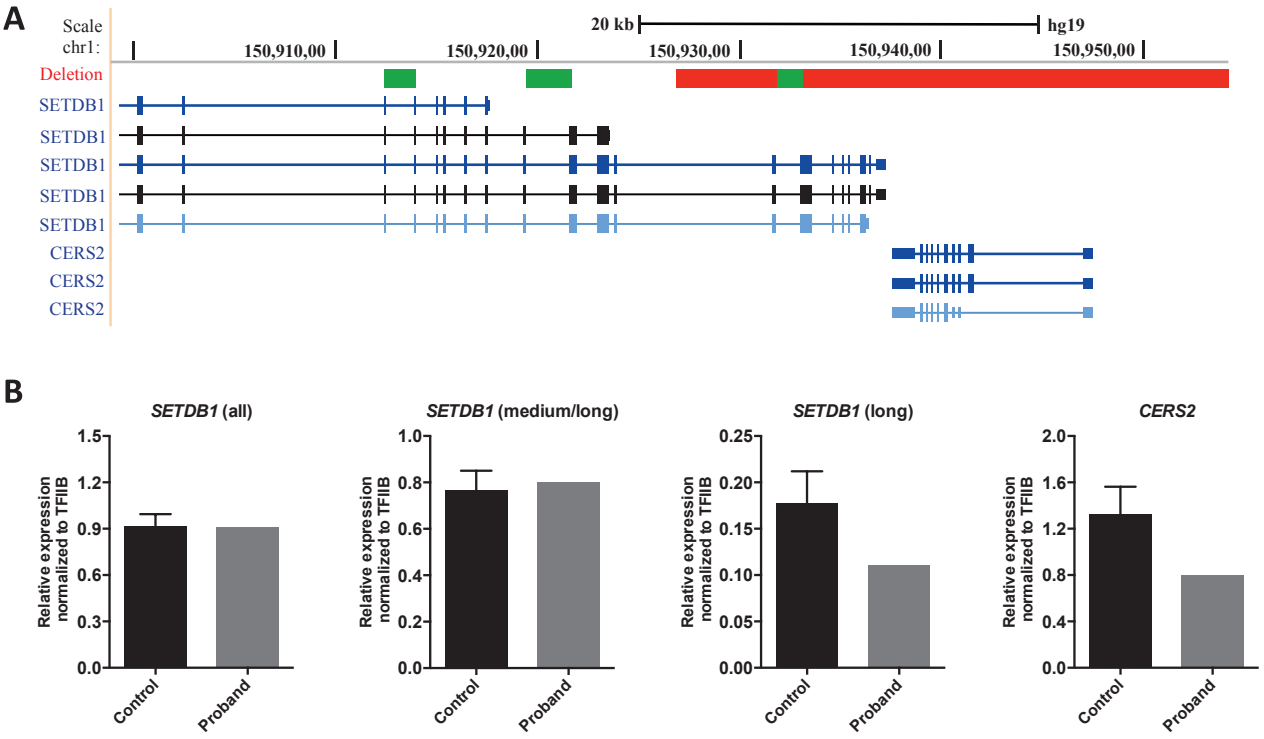

Figure 2. Genomic location of the *CERS2* deletion. (A) The deletion is indicated by the red bar. The figure is based on the UCSC Genome Browser (http://www.genome.ucsc.edu, assembly hg19) showing the genomic positions from the Affymetrix Genome-Wide Human SNP Array 6.0. The deletion is a heterozygous 27 kb deletion of 1q21 containing the entire *CERS2* gene and part of the *SETDB1* gene (exon 15–22). Regions of *SETDB1* amplified by quantitative real-time PCR are indicated by the green bars. (B) Total RNA was isolated from muscle biopsies from the proband and six unrelated controls as described in the experimental section and expression levels of *CERS2* and *SETDB1* isoforms were determined by quantitative real-time PCR. Three primer sets were used for the detection of *SETDB1*; all detects all isoforms, medium/long detects the medium to long isoforms, and long detects the three long isoforms. Mean ± SD is shown, N (control) = 6, N (proband) = 1.

deletion also included the distal part of *SETDB1* (exon 15–22), a histone methyltransferase. To examine the expression levels of both genes, we performed quantitative PCR on total RNA isolated from muscle biopsies from the proband and six unrelated controls. As predicted, the level of *CERS2* mRNA was reduced to ~50% in the proband (Fig. 2B). Moreover, expression of the longest predicted transcripts of *SETDB1* was reduced, while expression of shorter transcripts was unaffected (Fig. 2B), consistent with the identified deletion. To obtain further genetic evidence for *CERS2* pathogenicity, we performed SNP 6.0 array analysis on 1075 healthy controls, and no deletions or duplications involving *CERS2* were detected. In addition, we performed a mutation analysis of all 10 coding exons and intron-exon boundaries of *CERS2* using bidirectional sequencing in a cohort of 100 probands with progressive ataxia and/or epilepsy. No *CERS2* mutations were detected in this cohort.

Biochemical analysis of primary fibroblasts isolated from proband

In order to characterize the biochemical phenotypes associated with the heterozygous deletion of *CERS2*, we characterized primary fibroblasts generated from skin biopsies from the proband and the healthy parents. Parental fibroblasts were used as controls, and after establishing paternal consanguinity, we confirmed that both parents carry two functional *CERS2* alleles (results not shown). Compared to parental cells, expression levels of *CERS2* and the long *SETDB1* transcripts were reduced by more than 50% in proband cells (Fig. 3A; data not shown). We observed similar decreases in protein levels of CERS2 and high molecular weight isoforms of SETDB1 (Fig. 3B; data not shown). The mRNA expression levels of *CERS1*, *CERS4*, and *CERS6* varied between proband and parents, with no obvious tendency to be either increased or decreased in proband fibroblasts compared to parental fibroblasts (Fig. 3A). Analysis of CERS2 activity using C22-CoA as a substrate showed a 50% reduction compared to control fibroblasts (Fig. 3C). However, no changes in ceramide synthase activity were observed in proband cells using C24- or C24:1-CoAs as substrate. We next examined ceramide and SL composition by mass spectrometry (Figs. 4, 5); ceramides containing very long-chain FAs (i.e., C24–C26) were significantly reduced in proband cells compared to controls, while long-chain ceramides (i.e., C16–C18) increased (Fig. 4A and B). Additionally, the abundance of SMs containing very long-chain FAs was significantly reduced in proband fibroblasts compared to parental control cells, while the abundance of SMs with long-chain FAs was unchanged (Fig. 4C and D). Despite these changes in ceramide and SM composition and levels, levels of the very long-chain glycosylated ceramides lactosylceramide (LacCer) and GlcCer were not reduced (Fig. 5).

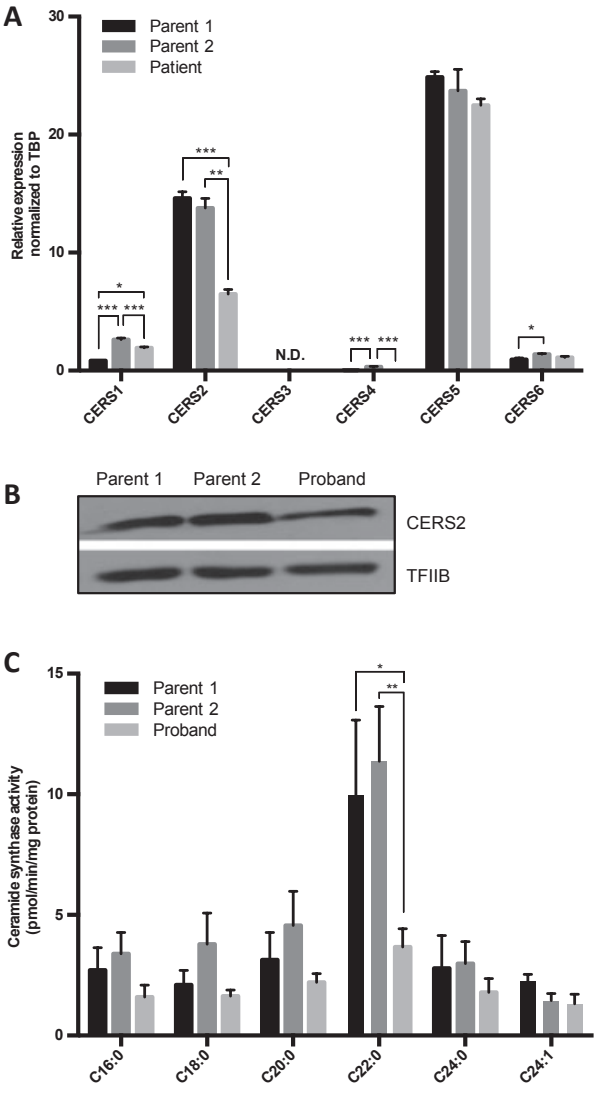

Figure 3. Heterozygous deletion of *CERS2* reduces *CERS2* expression, CERS2 protein level, and activity in fibroblasts. (A) Total RNA was isolated from cultured fibroblasts from the proband and controls and expression levels of *CERS1-6* were determined by quantitative real-time PCR. Mean ± SD is shown, $N = 3$. Statistical analyses were performed using a multiple *t*-test with significance levels: *($P < 0.05$), **($P < 0.01$), and ***($P < 0.001$). (B) Total cell extracts were prepared from cultured fibroblasts and CERS2 levels were determined by Western blotting. TFIIB served as loading control. (C) Ceramide synthase activities were determined in whole cell extracts using the indicated acyl-CoAs as substrates. Mean ± SEM is shown, $N = 6–9$. Statistical analyses were performed using multiple *t*-test with significance levels: *($P < 0.05$) and **($P < 0.01$).

SLs play important roles in the formation of membrane microdomains, which are lipid domains enriched in cho-

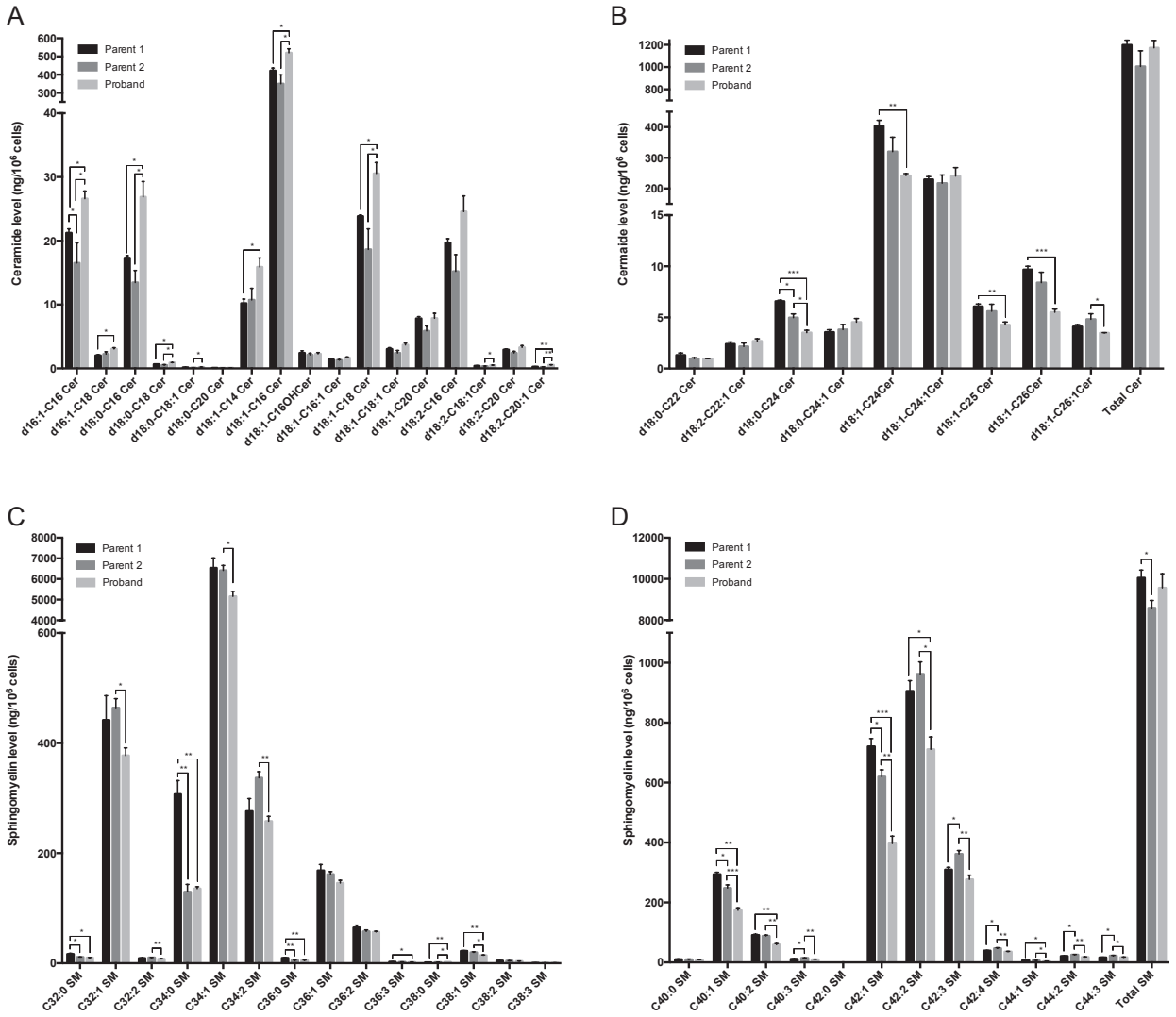

Figure 4. Ceramides and sphingomyelin species containing very long-chain fatty acids are reduced in proband fibroblasts. Lipid extracts prepared from cultured fibroblasts were analyzed using LC-MS. Ceramides containing long-chain fatty acids are shown in (A), while ceramides with very long-chain fatty acids are shown in (B). (C) Sphingomyelins containing long-chain fatty acids and (D) sphingomyelins containing very long-chain fatty acids from proband and parental control fibroblasts. Assuming that all ceramide and sphingomyelin species contain a C18-sphingoid base, sphingolipids were categorized into long-chain or very long-chain species. Levels of lipid species have been normalized to total cell number and internal standards. Three independent cultures of fibroblasts from the proband and controls were analyzed. Mean ± SD is shown, $N = 3$. Statistical analyses were performed using multiple *t*-test with significance levels: *($P < 0.05$), **($P < 0.01$), and ***($P < 0.001$).

lesterol and SLs. These domains orchestrate assembly of membrane proteins and ensure proper signal transduction (reviewed in[22]). Staining cells with cholera toxin B, a marker of membrane microdomains which binds to ganglioside GM1, revealed significantly reduced labeling in fibroblasts derived from the proband compared to both parental cell lines (Fig. 6), indicating that membrane lipid composition, and possibly formation of microdomains, are altered when CERS2 activity is reduced.

Photosensitivity in *CerS2* null mice

Finally, as the proband is photosensitive, we examined whether *CerS2* null mice are sensitized to light, using freezing behavior, a well-known index of fear,[23,24] under dim and bright illumination conditions. Although *CerS2* heterozygosity in mice did not sensitize mice to light, *CerS2* null mice were significantly more sensitive to light than $CerS2^{+/+}$ mice (Fig. 7).

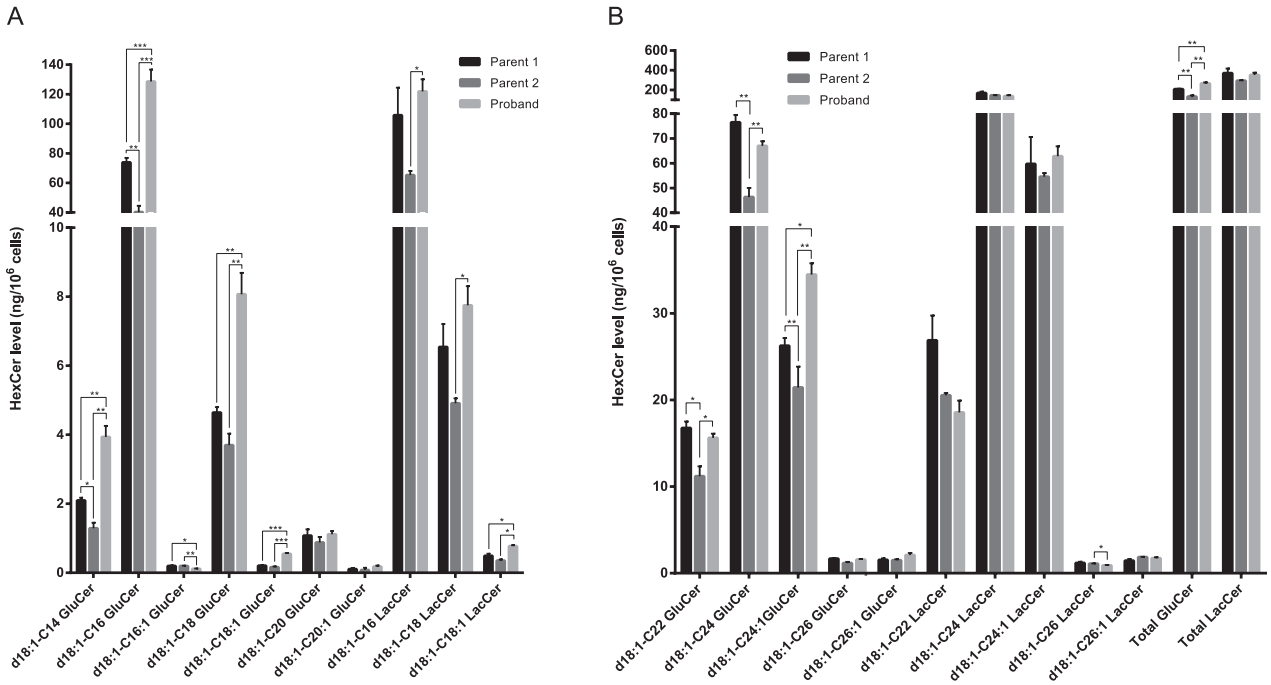

Figure 5. Lipid profile of glycosylceramide species in proband fibroblasts. Lipid extracts, prepared from cultured fibroblasts were analyzed using LC-MS. Glycosylceramide species containing long-chain fatty acids are shown in (A), while glycosylceramide species with very long-chain fatty acids are shown in (B). Lipids levels were normalized to total cell number and internal standards. Three independent cultures of fibroblasts from the proband and controls were analyzed. Mean ± SD is shown, $N = 3$. Statistical analyses were performed using multiple *t*-test with significance levels: *($P < 0.05$) and **($P < 0.01$).

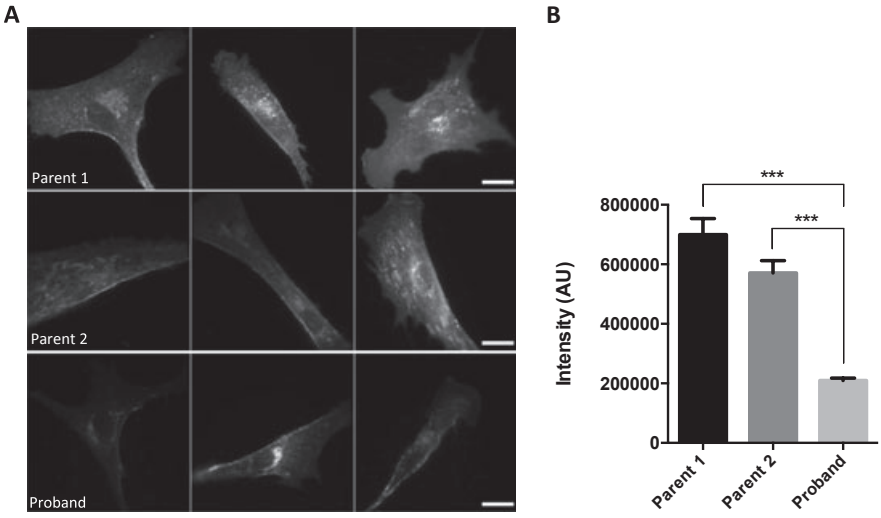

Figure 6. Cholera toxin B labeling of fibroblasts from proband and parental controls. (A) Fibroblasts from proband and controls were stained with Alexa488-labeled cholera toxin B for 20 min., and subsequently examined by fluorescence microscopy. (B) Images and fluorescence intensities were analyzed using ImageJ. Mean ± SEM is shown, N (parent 2) = 38 and N (proband) = 49. Statistical analyses were performed using unpaired two-tailed *t*-test with Welch's correction with significance level: ***($P = 0.0004$).

Discussion

In this study, we identified a *de novo* 27 kb heterozygous deletion of 1q21, including *CERS2* and the distal part of *SETDB1*, in a male proband diagnosed with PME. In the brain, *CERS2* is highly expressed in white matter tracts including the corpus callosum, striatum, and white matter of the cerebellum and brainstem, which is consistent with

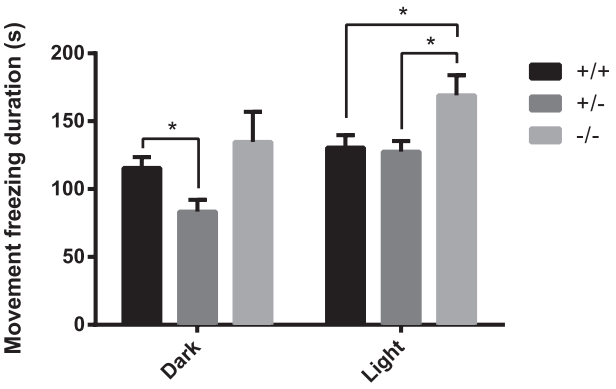

Figure 7. CERS2 KO mice exhibit increased sensitivity to light. Sensitivity to light was assessed by measuring freezing behavior, an index of fear, in a circular open field under two illumination conditions, dark (10 lux, 5 min) and light (120 lux, 5 min). ANOVA for GENE (KO/HT/WT) indicated no difference in freezing duration in the DARK ($F_{(2,15)} = 3.185$; n.s.), but a statistically longer duration of freezing in CerS2 null mice than in both WT and heterozygote mice under light. $N = 6$. (ANOVA for GENE: $F_{(2,15)} = 4.42$; $P < 0.05$; Dunnet post-hoc test: KO>het $P < 0.05$, KO>WT $P < 0.05$).

CERS2 expression in mature myelin-producing oligodendrocytes. Schwann cells of the peripheral nervous system display high *CERS2* expression as well.[4,10] *SETDB1* is also expressed in the nervous system, and removal of *Setdb1* in mice results in peri-implantation lethality.[25] Studies of the forebrain of transgenic *Setdb1* mice demonstrated that it targets ionotropic glutamatergic NMDA receptors.[26] Recently, mutations and intragenic deletions of *SETDB1* have been associated with Autism Spectrum Disorder (ASD) although all the detected *SETDB1* variants were inherited from healthy parents.[27] As our proband was not diagnosed with ASD, and heterozygous mutations and intragenetic deletions of *SETDB1* have been identified in healthy individuals, we do not believe that the partial *SETDB1* deletion causes the currently described phenotype.

Besides a recent genome-wide association study, which identified a *CERS2* mutation to be associated with primary rhegmatogenous retinal detachment,[28] *CERS2* mutations causing human disorders have, until now, not been reported. This study suggests that *CERS2* haploinsufficiency may cause PME. PMEs are a group of rare and devastating genetic disorders, which are often refractory to conventional treatment. Almost all PMEs reported so far have been associated with recessive inheritance. In the present report, we have confirmed that both parents have two functional *CERS2* alleles, thus the *CERS2* haploinsufficiency must have arisen due to a spontaneous deletion of one of the *CERS2* alleles. Accordingly, fibroblasts isolated from the proband display reduced levels of *CERS2* mRNA, protein, and activity, which cause reduced levels of very long-chain ceramides and SMs.

Little is known about how CERS2 deficiency might affect cellular functions in humans. In mice, total loss of *CerS2* expression significantly diminishes levels of ceramides and more complex SLs such as C22-24 GalCer, which results in myelin instability and in degeneration of both white and gray matter in the cerebellum.[12,13] This suggests that CERS2 activity is important in both neurons and formation of myelin sheath.[12,13] *CerS2* null mice also display astrogliosis and microglial activation in both white and gray matter, which may be related to the motor initiation difficulties and myoclonic jerks observed in these mice.[13,29] EEG revealed abnormal fast rhythmic activity (>40 Hz) and, similar to that found in the proband, the null mice display no changes in EEG during myoclonic events.[13] To this end, our present studies suggest that *CerS2* null mice also are significantly more sensitive to light than wild-type mice (Fig. 6), implying that the light sensitivity in the proband may be caused by impaired CERS2 function.

Disruption of CERS2 activity in mice not only causes neurological phenotypes but also results in impaired hepatic and lung functions.[11,29–31] In the present proband, *CERS2* haploinsufficiency does not appear to impair liver and kidney function (Table 1). Although *CERS2* is ubiquitously expressed, it is abundantly expressed in both liver and kidney, and found at significantly lower levels in the brain. We therefore propose that *CERS2* haploinsufficiency in humans only has detrimental effects in tissues containing low levels of CERS2, such as the brain, while the remaining CERS2 activity in the liver and kidney may synthesize sufficient amounts of very long-chain SLs to sustain central cellular functions. Alternatively, compensatory mechanisms by other ceramide synthases may exist in vivo, which are not evident in isolated fibroblasts.

Ablation of *CerS2* in mice results in a small and inconsistent reduction in total GM1[13] and in altered biophysical membrane properties.[15] Consistent with this notion, we also found that *CERS2* haploinsufficiency reduced cholera toxin B staining of the plasma membrane, suggesting that the altered SL composition can ultimately impair membrane microdomain formation and hence plasma membrane functions. Interestingly, such membrane microdomains have been shown to modulate neuronal excitability by controlling neurotransmitter receptor sensitivity and functions,[32,33] which could contribute to the phenotypes displayed by the proband.

Collectively, we have identified a proband with PME coupled to altered synthesis and composition of very long-chain ceramides and SM. The proband has only one functional *CERS2* allele, reduced *CERS2* mRNA, protein, and activity levels, resulting in impaired synthesis of cera-

mides and SM containing very long acyl chains, which consequently can affect the formation of membrane microdomains. We foresee that this proband will provide a unique opportunity for addressing the functions of CERS2 and SLs in the development of PME, and lay the foundation for further exploration of the role of SL metabolism in human neurodegenerative disorders.

Acknowledgments

We thank Michael Witting, Andre Franke and Ingo Helbig from the POPGEN database at Christian-Albrechts-University (Kiel, Germany) for help with database analyses. We thank the patients and families for their essential help and support. The authors declare no conflicts of interest. This study was supported by The Lundbeck Foundation and The Danish Research Councils.

Author Contributions

M. B. M., A. S. B. O., D. N., O. B. D., L. H., A. H. F., and N. J. F. were all involved in designing and performing the described biochemical analyses. L. L. K. identified the family, analyzed CNV data, and designed and performed sequencing of CERS2. J. L. sequenced CERS2. H. H., A. S., N. T., and J. E. N. provided and examined the clinical information and discussed the functional effects of the CNV. J. V. provided clinical data and muscle tissue from the patient and parental controls. A. D. K. and M. M. T. performed the light sensitivity experiments in mice. M. B. M., A. S. B. O., A. H. F., R. S. M., and N. J. F. wrote the manuscript.

Conflict of Interest

None declared.

References

1. Shahwan A, Farrell M, Delanty N. Progressive myoclonic epilepsies: a review of genetic and therapeutic aspects. Lancet Neurol 2005;4:239–248.
2. Zupanc ML, Legros B. Progressive myoclonic epilepsy. Cerebellum 2004;3:156–171.
3. Satishchandra P, Sinha S. Progressive myoclonic epilepsy. Neurol India 2010;58:514–522.
4. Ben-David O, Futerman AH. The role of the ceramide acyl chain length in neurodegeneration: involvement of ceramide synthases. Neuromolecular Med 2010;12:341–350.
5. Baumann N, Pham-Dinh D. Biology of oligodendrocyte and myelin in the mammalian central nervous system. Physiol Rev 2001;81:871–927.
6. Sastry PS. Lipids of nervous tissue: composition and metabolism. Prog Lipid Res 1985;24:69–176.
7. Levy M, Futerman AH. Mammalian ceramide synthases. IUBMB Life 2010;62:347–356.
8. Mullen TD, Hannun YA, Obeid LM. Ceramide synthases at the centre of sphingolipid metabolism and biology. Biochem J 2012;441:789–802.
9. Laviad EL, Albee L, Pankova-Kholmyansky I, et al. Characterization of ceramide synthase 2: tissue distribution, substrate specificity, and inhibition by sphingosine 1-phosphate. J Biol Chem 2008;283:5677–5684.
10. Becker I, Wang-Eckhardt L, Yaghootfam A, et al. Differential expression of (dihydro)ceramide synthases in mouse brain: oligodendrocyte-specific expression of CerS2/Lass2. Histochem Cell Biol 2008;129:233–241.
11. Pewzner-Jung Y, Park H, Laviad EL, et al. A critical role for ceramide synthase 2 in liver homeostasis: I. alterations in lipid metabolic pathways. J Biol Chem 2010;285:10902–10910.
12. Imgrund S, Hartmann D, Farwanah H, et al. Adult ceramide synthase 2 (CERS2)-deficient mice exhibit myelin sheath defects, cerebellar degeneration, and hepatocarcinomas. J Biol Chem 2009;284:33549–33560.
13. Ben-David O, Pewzner-Jung Y, Brenner O, et al. Encephalopathy caused by ablation of very long acyl chain ceramide synthesis may be largely due to reduced galactosylceramide levels. J Biol Chem 2011;286:30022–30033.
14. Zigdon H, Kogot-Levin A, Park JW, et al. Ablation of ceramide synthase 2 causes chronic oxidative stress due to disruption of the mitochondrial respiratory chain. J Biol Chem 2013;288:4947–4956.
15. Silva LC, Ben David O, Pewzner-Jung Y, et al. Ablation of ceramide synthase 2 strongly affects biophysical properties of membranes. J Lipid Res 2012;53:430–436.
16. Yurlova L, Kahya N, Aggarwal S, et al. Self-segregation of myelin membrane lipids in model membranes. Biophys J 2011;101:2713–2720.
17. Simpson MA, Cross H, Proukakis C, et al. Infantile-onset symptomatic epilepsy syndrome caused by a homozygous loss-of-function mutation of GM3 synthase. Nat Genet 2004;36:1225–1229.
18. Zhao L, Spassieva SD, Jucius TJ, et al. A deficiency of ceramide biosynthesis causes cerebellar purkinje cell neurodegeneration and lipofuscin accumulation. PLoS Genet 2011;7:e1002063.
19. Lahiri S, Futerman AH. The metabolism and function of sphingolipids and glycosphingolipids. Cell Mol Life Sci 2007;64:2270–2284.
20. Neess D, Bloksgaard M, Bek S, et al. Disruption of the acyl-CoA-binding protein gene delays hepatic adaptation to metabolic changes at weaning. J Biol Chem 2011;286:3460–3472.

21. Eckl KM, Tidhar R, Thiele H, et al. Impaired epidermal ceramide synthesis causes autosomal recessive congenital ichthyosis and reveals the importance of ceramide acyl chain length. J Invest Dermatol 2013;133:2202–2211.
22. Zhang Y, Li X, Becker KA, Gulbins E. Ceramide-enriched membrane domains – structure and function. Biochim Biophys Acta 2009;1788:178–183.
23. Blanchard DC, Griebel G, Blanchard RJ. The mouse defense test battery: pharmacological and behavioral assays for anxiety and panic. Eur J Pharmacol 2003;463:97–116.
24. Crawley JN. Behavioral phenotyping of transgenic and knockout mice: experimental design and evaluation of general health, sensory functions, motor abilities, and specific behavioral tests. Brain Res 1999;835:18–26.
25. Lohmann F, Loureiro J, Su H, et al. KMT1E mediated H3K9 methylation is required for the maintenance of embryonic stem cells by repressing trophectoderm differentiation. Stem Cells 2010;28:201–212.
26. Jiang Y, Jakovcevski M, Bharadwaj R, et al. Setdb1 histone methyltransferase regulates mood-related behaviors and expression of the NMDA receptor subunit NR2B. J Neurosci 2010;30:7152–7167.
27. Cukier HN, Lee JM, Ma D, et al. The expanding role of MBD genes in autism: identification of a MECP2 duplication and novel alterations in MBD5, MBD6, and SETDB1. Autism Res 2012;5:385–397.
28. Kirin M, Chandra A, Charteris DG, et al. Genome-wide association study identifies genetic risk underlying primary rhegmatogenous retinal detachment. Hum Mol Genet 2013;22:3174–3185.
29. Pewzner-Jung Y, Brenner O, Braun S, et al. A critical role for ceramide synthase 2 in liver homeostasis: II. insights into molecular changes leading to hepatopathy. J Biol Chem 2010;285:10911–10923.
30. Park JW, Park WJ, Kuperman Y, et al. Ablation of very long acyl chain sphingolipids causes hepatic insulin resistance in mice due to altered detergent-resistant membranes. Hepatology 2012;57:525–532.
31. Petrache I, Kamocki K, Poirier C, et al. Ceramide synthases expression and role of ceramide synthase-2 in the lung: insight from human lung cells and mouse models. PLoS One 2013;8:e62968.
32. Allen JA, Halverson-Tamboli RA, Rasenick MM. Lipid raft microdomains and neurotransmitter signalling. Nat Rev Neurosci 2007;8:128–140.
33. Zhu D, Xiong WC, Mei L. Lipid rafts serve as a signaling platform for nicotinic acetylcholine receptor clustering. J Neurosci 2006;26:4841–4851.

Supplement III

Manuscript in preparation

Global lipidomics analysis of ceramide synthase 2-deficient fibroblasts reveals alterations in membrane lipid composition

Sandra F. Gallego, **Anne S. B. Olsen**, Christer S. Ejsing, and Nils J. Færgeman

Global lipidomics analysis of ceramide synthase 2-deficient fibroblasts reveals alterations in membrane lipid composition

Sandra F. Gallego, Anne S. B. Olsen, Christer S. Ejsing, and Nils J. Færgeman

Villum Center for Bioanalytical Sciences, Department of Biochemistry and Molecular Biology, University of Southern Denmark, DK-5230 Odense M, Denmark.

Correspondence to:

Nils J. Færgeman, nils.f@bmb.sd.dk

Abstract

Altered lipid metabolism has been associated with many neurological diseases, including epilepsy, Alzheimer's, and Parkinson's disease. Recently, ceramide synthase 2 (CERS2) was linked to progressive myoclonic epilepsy (PME), a group of rare neurological disorders characterized by myoclonus, tonic-clonic seizures, and progressive neurological dysfunction.

Ceramide is a key intermediate in sphingolipid metabolism. In mammals ceramide is synthesized by a family of six ceramide synthases (CERS1-6) that differ in tissue distribution and substrate specificity. Each CERS catalyzes the synthesis of ceramide species of distinct chain length, accounting for the diversity in acyl-chain composition of ceramide species. CERS2, the most ubiquitously expressed CERS, is mainly expressed in kidney and liver, but is also found in oligodendrocytes in the brain. It primarily uses C22-24 acyl-CoAs for ceramide synthesis.

In this study have we applied mass spectrometry-based lipidomics to characterize the cellular lipid composition of primary skin fibroblasts isolated from the patient carrying a heterozygous deletion of the *CERS2* gene and diagnosed with PME. Our results show that *CERS2* haploinsufficiency alters sphingolipid and glycerophospholipid composition, which may affect plasma membrane dynamics and organization, leading to compromised oligodendrocyte function, and ultimately contributing to the development of PME.

Introduction

Lipids are abundant in nervous system, where they perform important functions in both maturing and adult brain. Dysregulation of lipid metabolism contributes to the pathogenesis of neurological disorders, including epilepsy, and in neurodegenerative diseases, such as Alzheimer's, Parkinson's, and Huntington's disease [1]. Therefore understanding the consequences of these alterations at the molecular level and how they impact cellular functions may provide novel therapeutic targets for the treatment of neurological diseases.

All eukaryotic cells are surrounded by a lipid bilayer consisting of three major lipid classes: glycerophospholipids, sphingolipids, and cholesterol [2, 3]. Glycerophospholipids (GPLs) are composed of a glycerol-3-phosphate backbone with a polar head group attached to the *sn-3* position, and two fatty acid (FA) moieties to the *sn-1* (*via* and ester, ether, or vinyl-ether bond) and *sn-2* positions (*via* an ester bond). Phosphatidylcholine (PC) and phosphatidylethanolamine (PE) are the most abundant GPLs in eukaryotic cell membranes. Other GPLs, such as phosphatidylserine (PS) and phosphatidylinositol (PI) are quantitatively minor membrane GPLs accounting for 2-15% of total GPL content. Their relative proportion varies depending on the tissue and cell type [4]. Ceramide constitute a building block for the synthesis of more complex sphingolipid (i.e., sphingomyelin and glycosphingolipids), which are also important components of eukaryotic cell membranes. Ceramide is synthesized *de novo* by acylation of long-chain bases with fatty acyl-CoAs, in a reaction catalyzed by ceramide synthases (CERSs). In mammals, a family of six CERSs (CERS1-6) determines the specific acyl chain length of sphingolipids [5]. CERS5 and CERS6 use primarily 16:0-CoA, CERS4 uses 18:0- and 20:0-CoAs, while CERS3 uses very-long chain acyl-CoAs (≥26:0-CoA). CERS1 predominantly uses C18:0- and C18:1-CoA and is the most abundant CERS in the central nervous system. CERS2 can utilize a wider range of fatty acyl-CoAs, but uses mainly 22:0- to 24:0-CoAs [5]. CERS2 is the most ubiquitously expressed CERS and is especially abundant in liver, kidney, and white matter tracts of the brain [6, 7].

Mosbech, Olsen *et al.* recently described a 27 kb heterozygous deletion including the *CERS2* gene in a patient diagnosed with progressive myoclonic epilepsy (PME) [8]. PME comprises several disorders characterized by myoclonic/tonic-clonic seizures and progressive neurological dysfunction, including cognitive impairment and ataxia [9]. Levels of CERS2 mRNA, protein, and activity were reduced by ~50% in primary skin fibroblasts isolated from this patient, compared to parental controls, resulting in significantly reduced levels of C24:0/C26:0 ceramide and sphingomyelin species [8]. The aim of the present study was to further delineate how reduced CERS2 activity affects the global cellular lipid composition. We have applied mass spectrometry-based lipidomics for a global and comprehensive characterization of skin fibroblasts isolated form the PME patient compared to gender- and age-matched

controls, and show that *CERS2* haploinsufficiency not only alters the sphingolipid composition, but also the GPL composition.

Materials and Methods

Chemicals and lipid standards

Chloroform, methanol, and 2-propanol were from Rathburn Chemical (Walkerburn, Scotland). Ammonium acetate and ammonium formate were from Fluka Analytical (Buchs, Switzerland). All solvents and chemicals were HPLC grade. Lipid standards were purchased from Avanti Polar Lipids (Alabaster, USA), and Larodan Fine Chemicals (Malmö, Sweden).

Cell culture

Primary fibroblasts isolated from skin biopsies from the patient and four healthy gender- and age-matched controls were kindly provided by collaborators from the Filadelfia Epilepsy Hospital, Dianalund, Denmark. Human primary skin fibroblasts were grown in Dulbecco's Modified Eagles Medium (DMEM) supplemented with 44.04 mM $NaHCO_3$, 32.75 μM biotin, 33.58 μM pantothenic acid, 20% fetal bovine serum (FBS, Sigma-Aldrich) (vol/vol), 100 units penicillin/0.1 mg streptomycin per liter (Sigma-Aldrich), and GlutaMAX supplement (Gibco) at 37°C, 5% CO_2. Medium was changed every second day, and cells were trypsinized and sub-cultured when being 90-100% confluent in ratios 1:2 to 1:3. Fibroblasts were harvested by trypsinization and washed with PBS. Cell concentration was measured using a Scepter cell counter (Millipore). Fibroblasts were resuspended in 155 mM ammonium acetate buffer, transferred to eppendorf tubes, snap frozen in liquid nitrogen, and stored at -80°C until further analysis.

Lipid extraction

Fibroblast homogenates were analyzed for total protein concentration using Pierce BCA Protein Assay kit (Thermo Scientific, Rockford, IL, USA). Aliquots of cell homogenates corresponding to $1.5 \cdot 10^5$ cells were subjected to two-step lipid extraction at 4°C as previously described [10, 11]. Briefly, the cell homogenates were diluted with 155 mM ammonium acetate to a final volume of 200 μL and spiked with an internal lipid standard mixture containing cholesterol ester (CE) 19:0, triacylglycerol (TAG) 17:0-17:1-17:0-d5, diacylglycerol (DAG) 1,3-17:0-d5, phosphatidic acid (PA) 17:0/20:4, phosphatidylserine (PS) 17:0/20:4, phosphatidylinositol (PI) 17:0/14:1, phosphatidylethanolamine (PE) O-20:0/O-20:0, phosphatidylcholine (PC) 16:0/16:0-d6, ceramide (Cer) 18:1;2/17:0;0, sphingomyelin (SM) 18:1;2/17:0;0, glucosylceramide (HexCer) 18:1;2/12:0;0, and ganglioside GM3 18:1/18:0-d3. Samples were subsequently added 990 μL of chloroform/methanol (10:1, v/v) and mixed for 120 min at 1400 rpm. Samples were centrifuged for 2 min at 1000 g to facilitate phase separation. The lower organic phase was collected and vacuum evaporated. The remaining aqueous phase was re-extracted with 990 μL of chloroform/methanol (2:1, v/v) and mixed for 90 min at 1400 rpm. Samples were centrifuged for 2 min at 1000 g, and the lower organic phase was collected and vacuum evaporated.

Mass spectrometric lipid analysis

Lipid extracts were dissolved in chloroform/methanol (1:2, v/v) and analyzed by MS^{ALL} [12] using an Orbitrap Fusion Tribrid (Thermo Fisher Scientific, San Jose, CA, USA) equipped with a robotic nanoflow ion source TriVersa NanoMate (Advion Biosciences, Ithaca, NY, USA). Two technical replicates from each sample were analyzed.

In positive ion mode, 10 µL aliquots of 10:1 lipid extracts were mixed with 12.9 µL 13.3 mM ammonium acetate in 2-propanol, and infused using a back pressure of 1.25 psi and ionization voltage of +0.96 kV. In negative ion mode, 10 µL aliquots of 10:1 lipid extracts were mixed with 12.9 µL 1.33 mM ammonium formate in 2-propanol, and infused using a back pressure of 1.25 psi and ionization voltage of -0.96 kV. In an additional negative ion mode, 10 µL aliquots of 2:1 lipid extracts were mixed with 10 µL 0.01% w/v methylamine in methanol, and infused using a back pressure of 0.6 psi and ionization voltage of -0.96 kV [11]. All FTMS data were recorded using a max injection time of 100 ms, automated gain control for an ion target of $1 \cdot 10^5$, three microscans, and a target resolution setting of 450,000 (FWHM at *m/z* 200). All $FTMS^2$ data were acquired using max injection time of 100 ms, automated gain control for an ion target of 50,000, three microscans, and a target resolution setting of 30,000 (FWHM at *m/z* 200). All FTMS data were acquired in profile mode, using an ion transfer tube temperature of 275 °C for both positive and negative ion mode.

Positive ion mode MS^{ALL} analysis was performed using (1) high resolution FTMS analysis of the *m/z* range 375–605 (monitoring LPC and LPC O- species), (2) high resolution FTMS analysis of the *m/z* range 470–1030 (monitoring CE, SM, HexCer, PC, PC O-, and TAG species), and (3) sequential $FTMS^2$ analysis in 1.0008 u steps across the *m/z* range 400.3–1000.8 using a quadrupole ion isolation width of 1.0 u and HCD with normalized collision energy optimized for each lipid class. Negative ion mode MS^{ALL} analysis of 10:1 lipid extracts was performed using (1) high resolution FTMS analysis of the *m/z* range 200-675 (monitoring LPE and LPE O- species), (2) high resolution FTMS analysis of the *m/z* range 500-1080 (monitoring Cer, DAG, PE, and PE O-), (3) sequential $FTMS^2$ analysis in 1.0008 u steps across the *m/z* range 400.2–1000.7 using a quadrupole ion isolation width of 1.0 u and HCD with collision energy optimized for each lipid class. Negative ion mode MS^{ALL} analysis of 2:1 lipid extracts was performed using (1) high resolution FTMS analysis of the *m/z* range 200-675 (monitoring LPA, LPI, and LPS), (2) high resolution FTMS analysis of the *m/z* range 530-1080 (monitoring PA, PI, and PS species), (3) high resolution FTMS analysis of the *m/z* range 1000-1400 (monitoring GM3 species), (4) sequential $FTMS^2$ analysis in 1.0008 u steps across the *m/z* range 400.2–1000.7 using a quadrupole ion isolation width of 1.0 u and HCD with collision energy optimized for each lipid class.

Annotation of lipid species

Lipid species were annotated as previously described [11]. Glycerolipids and GPLs annotated by sum composition are reported as [lipid class] [total number of carbon atoms in FA moieties]:[total number of double bonds in FA moieties] (e.g., TAG 52:3 or PC 36:4). Sphingolipid species annotated by sum composition are reported as [lipid class][total number of carbon atoms in the long-chain base and FA moiety]:[total number of double bonds in the long-chain base and FA moiety];[total number of OH groups in the long-chain base and FA moiety] (e.g. SM 42:1;2). GPLs annotated by molecular species composition are reported as [lipid class][number of carbon atoms in the first FA moiety]:[number of double bonds in the first FA moiety]-[number of carbon atoms in the second FA moiety]:[number of double bonds in the second FA moiety] (e.g., PC 16:0-18:1). Sphingolipid species annotated by molecular species composition are reported as [lipid class][number of carbon atoms in the long-chain base]:[number of double bonds in the long-chain base];[number of OH groups in the long-chain base]/[number of carbon atoms in the FA moiety]:[number of double bonds in the FA moiety] (e.g., Cer 18:1;2/16:0).

Data processing and lipid identification

Lipid species detected by MS^{ALL} using high resolution FTMS analysis were identified using ALEX software and SAS 9.3 [12, 13]. Lipid species detected by FTMS and annotated by sum composition were quantified by normalizing their intensity to the intensity of an internal lipid standard of identical lipid class and multiplying by the spike amount of the internal lipid standard. Background abundances estimated from blank samples were subtracted. The two technical replicates of each sample were averaged and lipid species not detected in the three biological replicates were discarded. Data are presented as means of n=3 biological replicates ± standard deviation (SD) and displayed as mol%, which was calculated by normalizing individual values to the summed abundance of all lipid species.

Results

Lipid class composition of CERS2-deficient fibroblasts

We determined the effects of reduced CERS2 activity on cellular lipid composition by performing an in-depth quantitative lipidomics analysis of *CERS2*$^{+/-}$ primary skin fibroblasts from the PME patient and gender- and age-matched controls. As differences in cell size or protein amount between control and patient samples could affect the total lipid content, the abundance of individual lipids was normalized to the summed abundance of the total lipid species (mol% per all lipid species). We observed no pronounced differences in the lipid class composition when comparing PME patient cells with control samples. PC was the most abundant lipid class found in both control and patient fibroblasts, making up to 50% of all quantified lipid species (Figure 1). The less abundant GPL classes (PE, ether-linked PE, PI, PS, and ether-linked PC) constituted on average 27% and 31% of all quantified lipid species in control and patient samples, respectively (Figure 1). In the control samples PS represented on average 7.3% of total lipid classes, while in the PME patient cells PS was increased to 9.5%. Sphingolipid constituted 7.8% of all quantified lipid species in both control and PME cells (Figure 1).

Changes in sphingolipid molecular species in CERS2-deficient fibroblasts

Our data show that ceramide species are reduced in skin fibroblasts from the PME patient compared to controls. Ceramide accounted for only 0.25% of all lipid molecular species quantified in PME patient fibroblasts and 0.40% in control samples (Figure 1). We combined high resolution Fourier Transform mass spectrometry (FTMS) analysis and high resolution $FTMS^2$ for a more detailed structural characterization of molecular lipid species, which allowed the assignment of fatty acyl chains of the detected lipid species. Ceramide species consisted almost exclusively of species containing 16:0, 24:0, and 24:1 FA moieties (Figure 2A).

Ceramide serves as precursor for sphingomyelin (SM) and ganglioside synthesis; however in contrast to previous observations (Mosbech, Olsen *et al.* 2014) the differences detected in ceramide molecular species were not mirrored in SM species. Analysis of the SM species composition showed that SM 34:1;2 (18:1;2/16:0) was the most abundant SM species in both control and PME patient fibroblasts, accounting for on average 2.9% in control cells and 3.9% in patient cells of all quantified lipid species (Figure 2B). SM species containing very long-chain fatty acyl moieties (i.e., C24:0 and C24:1) showed no difference compared to control samples (Figure 2B). However, analysis of GM3 molecular species showed that GM3 containing very long-chain fatty acyl moieties (i.e., 22:0, 24:0, 24:1) were reduced in PME patient cells compared with control cells (Figure 2C), correlating with the observations on ceramide species.

Changes in glycerophospholipid molecular species in CERS2-deficient fibroblasts

The quantitative analysis of GPLs showed major differences in PS molecular species and to a lesser extent PE (Figure 3) and ether-linked PE (PE O-) species (Figure S1). PS 36:1 (18:0-18:1) was the most abundant PS species found in both control and PME patient samples (Figure 3A). Interestingly, when inspecting differences in the molecular composition of PS species, we observed a 2.5-fold increase in PS 40:4 (18:0-22:4), PS 40:5 (18:0-22:5), and PS 40:6 (18:0-22:6 and 18:1-22:5) molecular species in PME patient cells compared with control samples (Figure 3A). Similarly, levels of PE 40:4 (18:0-22:4), PE 40:5 (18:0-22:5 and 18:1-22:4), PE 40:6 (18:0-22:6 and 18:1-22:5), and PE 40:7 (18:1-22:6) were also increased in PME patient cells compared with control samples (Figure 3B), resembling those changes detected in PS. We did not observe any major differences in the PC species profile (Figure 3C).

Discussion

Here we applied mass spectrometry-based lipidomics to determine the effects of reduced CERS2 activity on the global cellular lipid composition. Our results show that *CERS2* haploinsufficiency alters sphingolipid and GPL composition. Ceramide species containing long and very long-chain fatty acyl moieties (i.e., 16:1, 22:0, 24:0, and 24:1) were reduced in PME patient cells, while the SM34:1;2 species, corresponding to a fatty acyl moiety of C16 when assuming a long chain base of 18 carbons, was increased. Moreover, ganglioside GM3 species containing very long-chain fatty acyl moieties (i.e., 22:0, 24:0, 24:1) were also reduced in PME patient cells compared with control samples. Our results also showed changes in GPL species. We observed a 2.5-fold increase in PS species as well as a slight increase in PE species containing polyunsaturated (PUFA) fatty acyl moieties (i.e., 22:4, 22:5, 22:6) in PME patient cells compared with control samples.

The decrease in C16-ceramide in patient fibroblasts does not correspond to the acyl-CoA specificity of CERS2. However, it correlates with an increase in the level of SM34:1;2, indicating a change in flux of sphingolipids in patient fibroblasts. The change in lipid flux is also evident on the level of GPLs, as several GPL species, particular PS, containing very long-chain fatty acyl moieties are increased in patient cells.

Within the nervous system, CERS2 is particularly expressed the myelinating cells; oligodendrocytes in the central nervous system and Schwann cells in the peripheral nervous system [6]. As CERS2 is not expressed in neurons, the development of PME in the presented patient is likely caused by malfunctioning oligodendrocytes. Ablation of CERS2 in mice leads to the development of several brain phenotypes, including myelin degeneration and detachment, cerebellar degeneration, as well as abnormal motor behavior with generalized and symmetrical myoclonic jerks [14, 15]. Galactosylceramide (GalCer) and its derivative sulfatide are major sphingolipids in myelin. Both lipids

are significantly reduced in the brain of mice lacking CERS2 [15]. Skin fibroblasts do not synthesis GalCer, and hence it has not been possible to evaluate if having reduced CERS2 activity affects the synthesis of GalCer and sulfatide. Yet as being heterozygous for *CERS2* appears to affect the synthesis of GM3, a major sphingolipid of skin fibroblasts (Figure 1, Figure 2C), it is possible that the level of GalCer, and hence sulfatide, is compromised in the oligodendrocytes of the PME patient. GalCer contributes to myelin stability by strengthening the myelin interactions in between myelin sheaths as well as by mediating the myelin-axon interaction [16]. Neurons require correct myelination in order to maintain axonal organization of proteins, including ion channels, and disturbances hereof impair neuronal signal transduction [17]. Moreover, compromised myelin stability can lead to degeneration of axon, which has been observed in mice lacking key myelin proteins [18].

PS is considered to be the major acidic phospholipid in cellular membranes, and is particularly enriched in myelin in human brain [19]. The increase of PS in patient fibroblasts does probably not add to the pathological phenotypes observed in the patient as supplementation of PS has shown positive effects on multiple cognitive functions, including memory, ability to learn, concentration, and ability to communicate, and also leads to beneficial support of locomotor functions [19].

The global lipidomics analysis also revealed a marked decrease in cholesteryl esters (CE) (Figure 1). Blood work performed on the PME patient has shown an increased level of cholesterol in the plasma, which is also seen for heterozygous *CerS2* mice when kept on a high-fat diet and for mice lacking CERS2 [8, 20, 21]. CERS2-derived SLs are emerging players in the regulation of protein trafficking, including endocytosis [22, 23]. In a recent study the rate of LDL internalization was found to be reduced in astrocytes isolated from the brain of mice lacking CERS2 [23]. Thus, the elevated level of plasma cholesterol in the proband might be explained by impaired cellular cholesterol uptake, elevated cholesterol efflux, or a combination of both. More work is necessary in order to understand how CERS2 is involved in regulation cholesterol metabolism.

Collectively, we show that *CERS2* haploinsufficiency alters sphingolipid and GPL composition, which possibly affect plasma membrane dynamics and membrane organization in oligodendrocytes and secondary in neurons, thereby contributing to the development of PME.

Figures

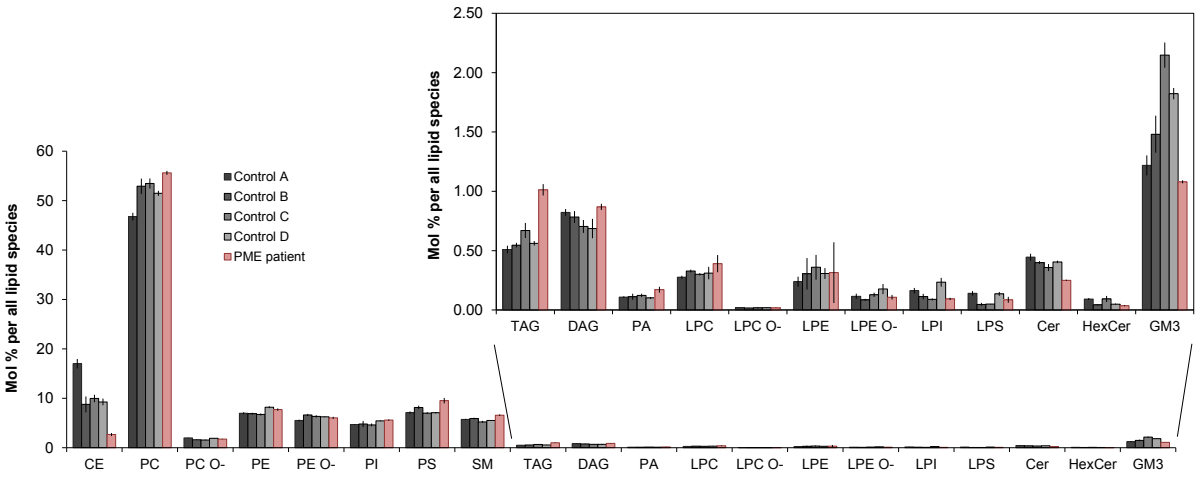

Figure 1. Lipid class composition of controls and PME patient skin fibroblasts. Lipid extracts prepared from three independent skin fibroblast cultures from the PME patient and controls were analyzed as described under "Material and Methods". Mean ± SD of n=3 fibroblast cultures per group is shown. CE, cholesteryl esters; Cer, ceramide; DAG, diacylglycerol; GM3, ganglioside GM3; HexCer, hexosylceramide; LPC O-, ether lysophosphatidylcholine; LPC, lysophosphatidylcholine; LPE O-, ether lysophosphatidylethanolamine; LPE, lysophosphatidylethanolamine; LPI, lysophosphatidylinositol; LPS, lysophosphatidylserine; PA, phosphatidic acid; PC O-, ether phosphatidylcholine; PC, phosphatidylcholine; PE O-, ether phosphatidylethanolamine; PE, phosphatidylethanolamine; PI, phosphatidylinositol; PS, phosphatidylserine; SM, sphingomyelin; TAG, triacylglycerol.

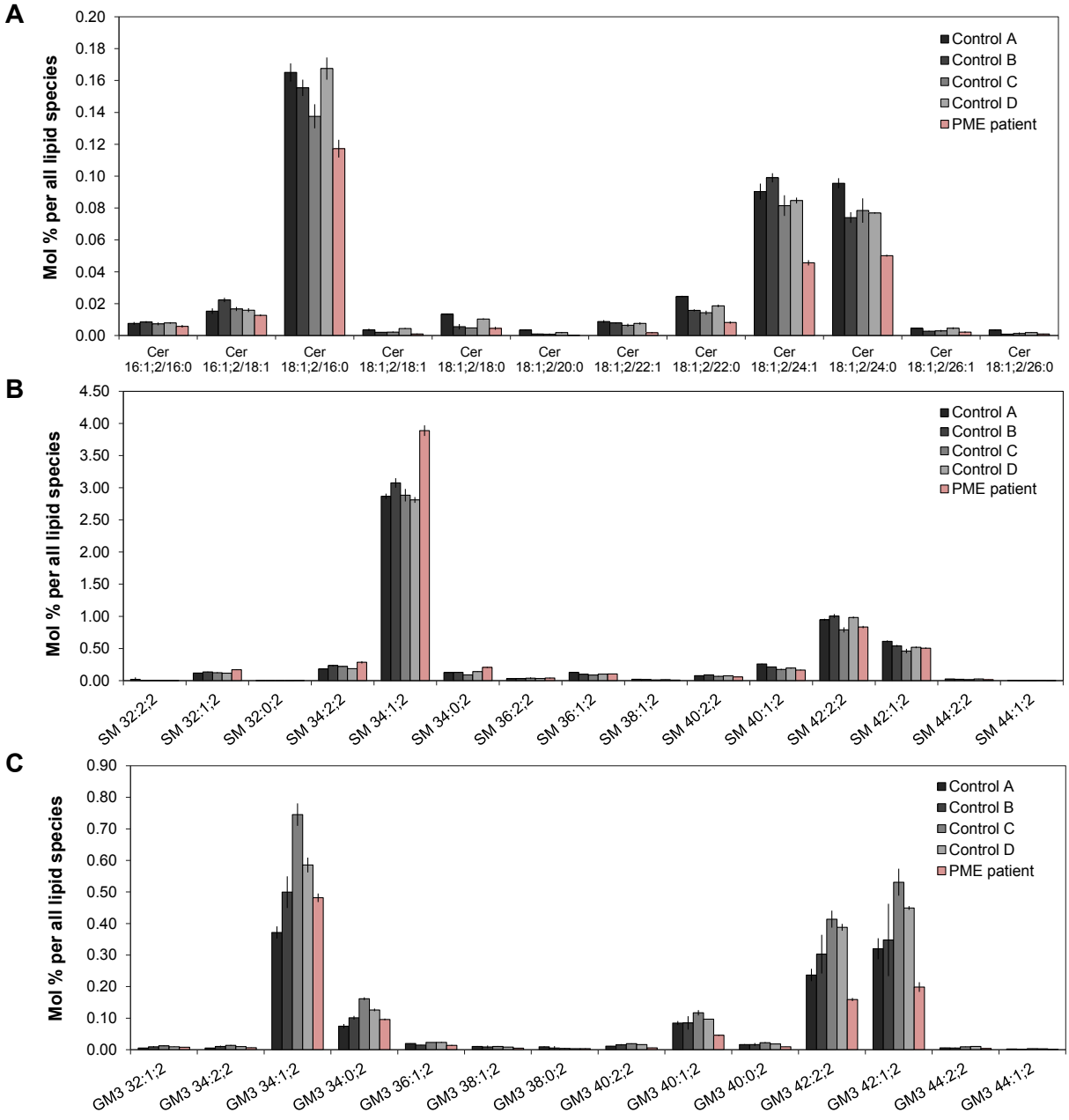

Figure 2. Distribution of (A) ceramide, (B) sphingomyelin, and (C) ganglioside GM3 species in control and PME patient skin fibroblasts. Lipid extracts prepared from three independent skin fibroblast cultures from the PME patient and controls were analyzed as described under "Material and Methods". Only lipid species detected in the three fibroblasts cultures are reported in this graph. Mean ± SD of n=3 fibroblast cultures per group is shown.

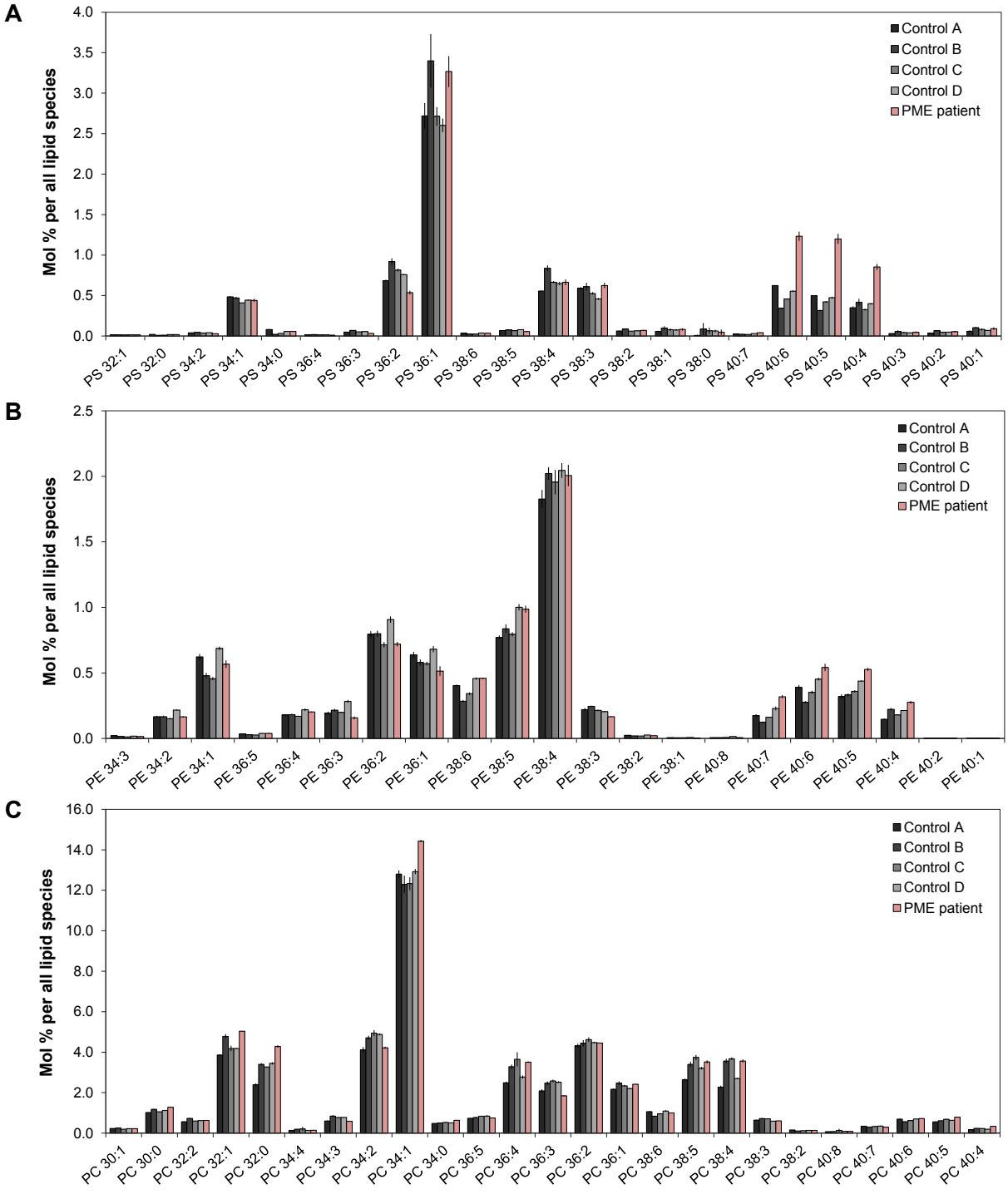

Figure 3. Distribution of (A) phosphatidylserine (PS), (B) phosphatidylethanolamine (PE), and (C) phosphatidylcholine (PC) species in control and PME patient skin fibroblasts. Lipid extracts prepared from three independent skin fibroblast cultures from the PME patient and controls were analyzed as described under "Material and Methods". Only lipid species detected in the three fibroblasts cultures are reported in this graph. Mean ± SD of n=3 fibroblast cultures per group is shown.

Supplementary figures

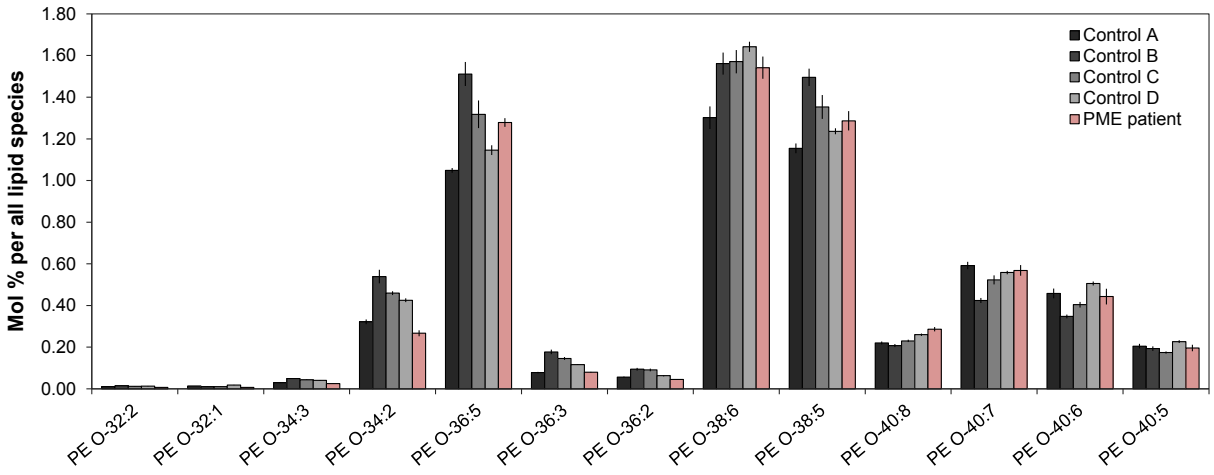

Figure S1. Distribution of ether-linked phosphatidylethanolamine (PE O-) in control and PME patient skin fibroblasts. Lipid extracts prepared from three independent fibroblast cultures from the PME patient and controls were analyzed as described under "Material and Methods". Only lipid species detected in the three fibroblasts cultures are reported in this graph. Mean ± SD of n=3 fibroblast cultures per group is shown.

References

1. Adibhatla, R.M., and Hatcher, J.F. (2008). Altered lipid metabolism in brain injury and disorders. Sub-cellular biochemistry *49*, 241-268.

2. Blom, T., Somerharju, P., and Ikonen, E. (2011). Synthesis and biosynthetic trafficking of membrane lipids. Cold Spring Harbor perspectives in biology *3*, a004713.

3. van Meer, G., Voelker, D.R., and Feigenson, G.W. (2008). Membrane lipids: where they are and how they behave. Nature reviews. Molecular cell biology *9*, 112-124.

4. Vance, J.E. (2015). Phospholipid synthesis and transport in mammalian cells. Traffic (Copenhagen, Denmark) *16*, 1-18.

5. Levy, M., and Futerman, A.H. (2010). Mammalian ceramide synthases. IUBMB life *62*, 347-356.

6. Becker, I., Wang-Eckhardt, L., Yaghootfam, A., Gieselmann, V., and Eckhardt, M. (2008). Differential expression of (dihydro)ceramide synthases in mouse brain: oligodendrocyte-specific expression of CerS2/Lass2. Histochemistry and cell biology *129*, 233-241.

7. Laviad, E.L., Albee, L., Pankova-Kholmyansky, I., Epstein, S., Park, H., Merrill, A.H., Jr., and Futerman, A.H. (2008). Characterization of ceramide synthase 2: tissue distribution, substrate specificity, and inhibition by sphingosine 1-phosphate. The Journal of biological chemistry *283*, 5677-5684.

8. Mosbech, M.B., Olsen, A.S., Neess, D., Ben-David, O., Klitten, L.L., Larsen, J., Sabers, A., Vissing, J., Nielsen, J.E., Hasholt, L., et al. (2014). Reduced ceramide synthase 2 activity causes progressive myoclonic epilepsy. Annals of clinical and translational neurology *1*, 88-98.

9. Zupanc, M.L., and Legros, B. (2004). Progressive myoclonic epilepsy. Cerebellum (London, England) *3*, 156-171.

10. Sampaio, J.L., Gerl, M.J., Klose, C., Ejsing, C.S., Beug, H., Simons, K., and Shevchenko, A. (2011). Membrane lipidome of an epithelial cell line. Proceedings of the National Academy of Sciences of the United States of America *108*, 1903-1907.

11. Ejsing, C.S., Sampaio, J.L., Surendranath, V., Duchoslav, E., Ekroos, K., Klemm, R.W., Simons, K., and Shevchenko, A. (2009). Global analysis of the yeast lipidome by quantitative shotgun mass spectrometry. Proceedings of the National Academy of Sciences of the United States of America *106*, 2136-2141.

12. Almeida, R., Pauling, J.K., Sokol, E., Hannibal-Bach, H., and Ejsing, C. (2015). Comprehensive Lipidome Analysis by Shotgun Lipidomics on a Hybrid Quadrupole-Orbitrap-Linear Ion Trap Mass Spectrometer. J. Am. Soc. Mass Spectrom. *26*, 133-148.

13. Husen, P., Tarasov, K., Katafiasz, M., Sokol, E., Vogt, J., Baumgart, J., Nitsch, R., Ekroos, K., and Ejsing, C.S. (2013). Analysis of lipid experiments (ALEX): a software framework for analysis of high-resolution shotgun lipidomics data. PloS one *8*, e79736.

14. Imgrund, S., Hartmann, D., Farwanah, H., Eckhardt, M., Sandhoff, R., Degen, J., Gieselmann, V., Sandhoff, K., and Willecke, K. (2009). Adult ceramide synthase 2 (CERS2)-deficient mice

exhibit myelin sheath defects, cerebellar degeneration, and hepatocarcinomas. The Journal of biological chemistry *284*, 33549-33560.

15. Ben-David, O., Pewzner-Jung, Y., Brenner, O., Laviad, E.L., Kogot-Levin, A., Weissberg, I., Biton, I.E., Pienik, R., Wang, E., Kelly, S., et al. (2011). Encephalopathy caused by ablation of very long acyl chain ceramide synthesis may be largely due to reduced galactosylceramide levels. The Journal of biological chemistry *286*, 30022-30033.

16. Boggs, J.M., Gao, W., Zhao, J., Park, H.J., Liu, Y., and Basu, A. (2010). Participation of galactosylceramide and sulfatide in glycosynapses between oligodendrocyte or myelin membranes. FEBS letters *584*, 1771-1778.

17. Olsen, A.S.B., and Faergeman, N.J. (2017). Sphingolipids: membrane microdomains in brain development, function and neurological diseases. Open biology *7*.

18. Dutta, R., and Trapp, B.D. (2011). Mechanisms of neuronal dysfunction and degeneration in multiple sclerosis. Progress in neurobiology *93*, 1-12.

19. Glade, M.J., and Smith, K. (2015). Phosphatidylserine and the human brain. Nutrition (Burbank, Los Angeles County, Calif.) *31*, 781-786.

20. Pewzner-Jung, Y., Park, H., Laviad, E.L., Silva, L.C., Lahiri, S., Stiban, J., Erez-Roman, R., Brugger, B., Sachsenheimer, T., Wieland, F., et al. (2010). A critical role for ceramide synthase 2 in liver homeostasis: I. alterations in lipid metabolic pathways. The Journal of biological chemistry *285*, 10902-10910.

21. Raichur, S., Wang, S.T., Chan, P.W., Li, Y., Ching, J., Chaurasia, B., Dogra, S., Ohman, M.K., Takeda, K., Sugii, S., et al. (2014). CerS2 haploinsufficiency inhibits beta-oxidation and confers susceptibility to diet-induced steatohepatitis and insulin resistance. Cell metabolism *20*, 687-695.

22. Ali, M., Fritsch, J., Zigdon, H., Pewzner-Jung, Y., Schutze, S., and Futerman, A.H. (2013). Altering the sphingolipid acyl chain composition prevents LPS/GLN-mediated hepatic failure in mice by disrupting TNFR1 internalization. Cell death & disease *4*, e929.

23. Volpert, G., Ben-Dor, S., Tarcic, O., Duan, J., Saada, A., Merrill, A.H., Jr., Pewzner-Jung, Y., and Futerman, A.H. (2017). Oxidative stress elicited by modifying the ceramide acyl chain length reduces the rate of clathrin-mediated endocytosis. Journal of cell science *130*, 1486-1493.